Novel surfaces to improve oligonucleotide immobilisation and hybridisation for breast cancer assay development

Thesis submitted for the degree of Doctor of Philosophy

By

Milena McKenna B.Sc. (Hons), M.Sc.

School of Electronic Engineering

Dublin City University

Supervised by

Dr. Stephen Daniels

June 2016

Declaration

I hereby certify that this material, which I now submit for assessment on the programme of study leading to the award of Doctor of Philosophy is entirely my own work, that I have exercised reasonable care to ensure that the work is original, and does not to the best of my knowledge breach any law of copyright, and has not been taken from the work of others save and to the extent that such work has been cited and acknowledged within the text of my work.

Signed:_____

Candidate ID No.:_____

Date:_____

Dedication

To my rock, loving mother

Lidia Rowińska;

I could not have done this without her.

Acknowledgements

A dissertation is not solely the efforts of one individual. Many people have contributed to its development. At this time, I take the opportunity to acknowledge those who have made an impact on my doctoral venture and accomplishments.

First and foremost, I would like to express a special thanks and appreciation to my supervisor Dr. Stephen Daniels, it has been an honour to be a PhD student under his guidance for the last 4 years. He has been a tremendous mentor to me, armed with a wealth of knowledge on various topics to help me with my research. Stephen made me believe 'the sky's the limit' until he sent me to NASA, where I now believe that 'Space is my [new found] limit'. His constructive criticism paved the way for my professional development it also helped me shape a broader spectrum of my thesis.

I am extremely indebted to my supervisor and friend Dr. Susan Kelleher. I am very thankful to Susan for being there at a critical stage of my PhD. The determination and enthusiasm she brought was contagious and motivational for me. I am driven by her achievements to date, as a successful female chemist. I appreciate all her contributions of time, appraisal, knowledge and social gatherings to help me on my PhD venture.

I would also like to extend my gratitude to Dr. Tony Ricco. I am extremely humbled by Tony's expertise, valuable guidance and encouragement offered to me. It was a pleasure to have worked with Tony given his academic achievements and stature within the industry.

Thanks to Dr. Vladidmir Gubala for his positive attitude and inspiring ideas at the beginning of my PhD.

I would like to thank all my friends in DCU: Dr. Ruairi Monaghan, Shauna Flynn, Shona O'Brien, Killian Walsh, Dr. Christy O'Mahony and Dr. Robert Nooney whom I worked very closely during my research. Our scientific and not so scientific related chats helped me go through this journey with a big smile on my face.

My sincere thanks to Dr. Ram Prasad Gandhiraman and Dr. Jessica Koehne for welcoming me to their lab in NASA Ames as a visitor researcher. Their friendliness and

outstanding work ethic made my stay unforgetable. Their efforts and warm welcome was extended beyond the working day, which made me feel like I was at home.

I take this opportunity to express gratitude to all of the BDI and DCU faculty members, technical and admin staff for their help and support.

I deeply thank my mother, Lidia Rowińska, for everything she has given me in my life. I would not be here today if it was not for her support. She made a life changing decision to relocate from Poland to Ireland in 2004, which gave me an opportunity to study in Ireland.

I thank my grandparents, who always believed in me and approved my decisions. Their immense love created a positive energy, even though they are almost 2000 km away. I also owe much gratitude to my extended family and my relatives for their unwavering support.

Finally, I cannot begin to express my unfailing gratitude to my husband, Cathal McKenna. He convinced me to take on this momentous challenge all those years ago. His on-going support eased me through this chapter of my life. His boundless energy and capability to see things from a different perspective helped me overcome various tasks that seemed troublesome and overwhelming.

List of abbreviations

A.U.	Arbitrary Units
AA	Acrylic Acid
AFM	Atomic Force Microscopy
APTES	(3-Aminopropyl)triethoxysilane
BC	Breast cancer
BKM	Best Known Method
-COOH	Carboxylic acid groups
Cy3	Cyanine 3 dye
Cy5	Cyanine 5 dye
DiH_2O	Deionized water
DNA	Deoxyribonucleic acid
DPI	Dual Polarization Interferometry
dsDNA	Double stranded Deoxyribonucleic acid
EDC	1-Ethyl-3-(3-dimethylaminopropyl)carbodiimide
EtOH	Ethanol
HMDSO	Hexamethyldisiloxane
LOAC	Lab on a chip
LoB	Limit of blank
LoD	Limit of detection
MUA	11-mercaptoundecanoic acid
NaOH	Sodium hydroxide
NH_2	Primary amino group
NHS	N-Hydroxysuccinimide
NSB	Non-specific binding
Ox. PMMA	Oxidised Poly(methy methacrylate)
PECVD	Plasma Enhanced Chemical Vapour Deposition
POC	Point-of-care
QCM	Quartz Crystal Microbalance
RMS	Root Mean Square
RNA	Ribonucleic Acid
SA	Succinic Anhydride
SAM	Self-Assembled Monolayer
SDS	Sodium Dodecyl Sulphate

SH	Thiol
SSC	Saline-Sodium Citrate
ssDNA	Single stranded Deoxyribonucleic Acid
TB	Toluidine Blue
TEOS	Tetraethyl Orthosilicate
TIRE	Total Internal Reflection Ellipsometry
Tm	Melting temperature
UV/O_3	UV Vis/ozone
W(CA)	Water (Contact Angle)

Table of contents

List of tables and figures

Tables

Figures

Abstract

This thesis mainly focuses on development of suitable films and immobilisation methods for bio conjugation of the biomolecules to solid supports with future application as biosensors for early breast cancer (BC) detection. Point-of-care (POC) device in biosensor format are recognised as a valuable tool in diagnostics field. However there are number of limitations such as non-specific binding, sensitivity, cost, and fabrication challenges. Hence, new formats of POC platforms are required to improve overall performance of the devices. The fabrication and evaluation of surfaces including carboxylic acid and amino deposition by both wet chemistry and Plasma Enhanced Chemical Vapour Depositions (PECVD) are discussed in detail in this thesis. The recipes and production methods as well as morphological, structural and functional characterisation of deposited films are investigated using a panel of different techniques.

This thesis presents that through appropriate surface treatment, poly(methyl methacrylate) (PMMA) can be oxidised using simple methods to form a carboxylic acid surface to enable the covalent attachment of biomolecules for bioassay development. Although spin coating PMMA is a relatively well-known process, to date there has been no direct comparison of the different oxidation methods to activate the surface, nor has oxidised spin coated PMMA been used as a platform for DNA hybridisation or immunoassays. Here, a comparison of the stability, functionality and fabrication process of spin coating and surface activating a thin film of PMMA on a variety of underlying substrates is described.

This research reports on the conditions under which amino-modified ssDNA immobilisation onto carboxylic acid surfaces using 1-ethyl-3-(3 dimethylamino-propyl) carbodiimide hydrochloride (EDC) linkers leads to binding at multiple anchoring sites, i.e. back bone (BB) binding; the effects of such binding on overall hybridisation efficiency are described. An alternative conjugation method, click chemistry (CC), is shown to improve the quantity and quality of target binding by enabling direct covalent attachment of probe oligonucleotides to the surface without BB binding. EDC and CC approaches are compared in terms of hybridisation efficiency in a direct and sandwich DNA hybridisation experiments.

This thesis includes the investigation of the orientation of miR16 DNA probe upon hybridisation with miR16 DNA target and miR195 DNA target on various substrates

Chapter 1

1 Thesis introduction

1.1 Motivation

Breast cancer (BC) occurs in both men and women, however it is more common in females and accounts as second the most common tumour in woman worldwide [1,2]. The main reason of such a high degree of mortality is limitations in early diagnosis of the disease. Currently diagnosis of BC involves: integration of clinical and physical examination, which may not be sensitive enough to detect early stages of the disease.

There is a great need for a non-invasive and cost effective test in aid to decrease mortality. A specific biomarker of panel of biomarkers obtainable from body fluids, such as blood, would be highly desirable and better than current methods such as mammography. MiRNA expression is frequently deregulated in cancer; hence they have a great potential as novel biomarkers and therapeutic targets in cancer. Researchers have been working on exploiting the unique characteristics of these molecules in order to achieve the goal of individualised cancer treatment [1,2]. MiRNAs are a class of very short, non coding RNAs that control gene expression by targeting messenger RNA [1,2]. MiRNA-195 was observed to be significantly overexpressed in blood from BC patients, as reported by research in H. Heneghan et al [1,2].

In this work DNA analogues of this particular miRNA were used, due to its robustness while compared to miRNA. During this study the aim was to develop and optimise a novel surface for DNA bio-conjugation, which can be applied in biosensor development for breast cancer diagnosis. Followed the development of a novel surface design, an investigation of improving DNA immobilisation will be carried out. Furthermore, a full DNA assay with combination of the surface and immobilisation technique will be investigated and tested to detect low levels (less than µM) of BC specific biomarker (DNA - MiRNA 195). Additionally a label free method for detection of DNA target will be suggested and tested.

Future work would involve substituting DNA analogues for miRNA and applying the DNA assay into a biosensor and use of clinical samples.

1.2 Breast cancer and current diagnosis techniques

Early diagnosis of cancer remains a compelling challenge for clinicians; it is the ultimate goal in order to minimize treatment-associated morbidity and mortality and achieve maximal long-term survival [4].

BC forms in tissues of the breast, see figure 1.1. Ductal carcinoma is the most common type of BC, which begins in the lining of the milk ducts, which are thin tubes that carry milk from the lobules of the breast to the nipple. Lobular carcinoma is another type of BC, which begins in the lobules (milk glands) of the breast. Invasive BC refers to a cancer that has spread from where it began in the breast ducts or lobules to surrounding normal tissue [5].
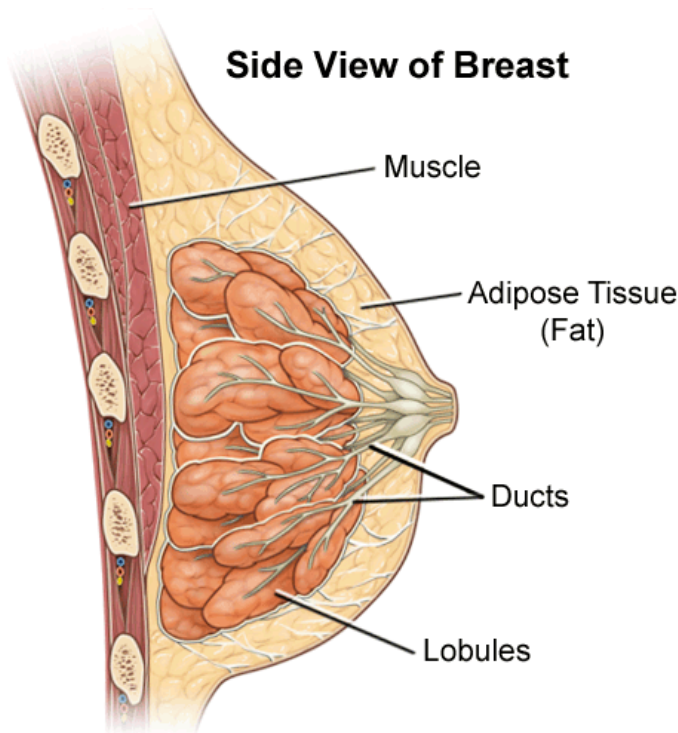
Figure 1.1 Female breast cross-section. The ducts and lobules are primary location of BC

Image taken from http://latebloomer1945.blog.com/files/2013/01/ei_0385.gif

BC occurs in both men and women, although male BC is rare [2]. It is the most common tumour diagnosed in women and it is the second leading cause of cancer death. It is estimated that worldwide over 500 000 women died in 2011 due to BC, which is equivalent to population of whole Co. Cork [1]. In Ireland, BC accounts for 16 % of female cancer deaths during the period 2007-2009 as reported in the most recent report released by the National Cancer Registry of Ireland [5].

There are number of risk factors for BC which have been well described and documented, see figure 1.2. However, for the majority of women presenting with BC it is not possible to identify specific risk factors [6,7]. A familial history of BC increases the risk by a factor of two or three. A very high risk for BC is caused by some mutations, particularly in BRCA1, BRCA2 and p53. However, these mutations are rare and account for a small portion of the total BC causes [1].

Reproductive factors associated with prolonged exposure to endogenous estrogens, such as, late menopause and late age for first childbirth is among the most important risk factors for BC. Exogenous hormones also exert a higher risk. Oral contraceptive and hormone replacement therapy users are at higher risk than non-users [1,6,7]. Danaei et al. calculated the contribution of various modifiable risk factors, excluding reproductive factors, to the overall BC burden. They conclude that 21 % of all BC deaths worldwide are attributable to alcohol use, overweight and obesity, and physical inactivity [8].

Direct factors
+Inherited mutations
+Radiation

Contributing factors
+excess of alcohol
+physical inactivity
+harmful xenohormones (some plastics, fuels, pesticides)

Vulnerability factors
+ early menses
+Late menopause
+No pregnancy or lactation

Breast Cancer
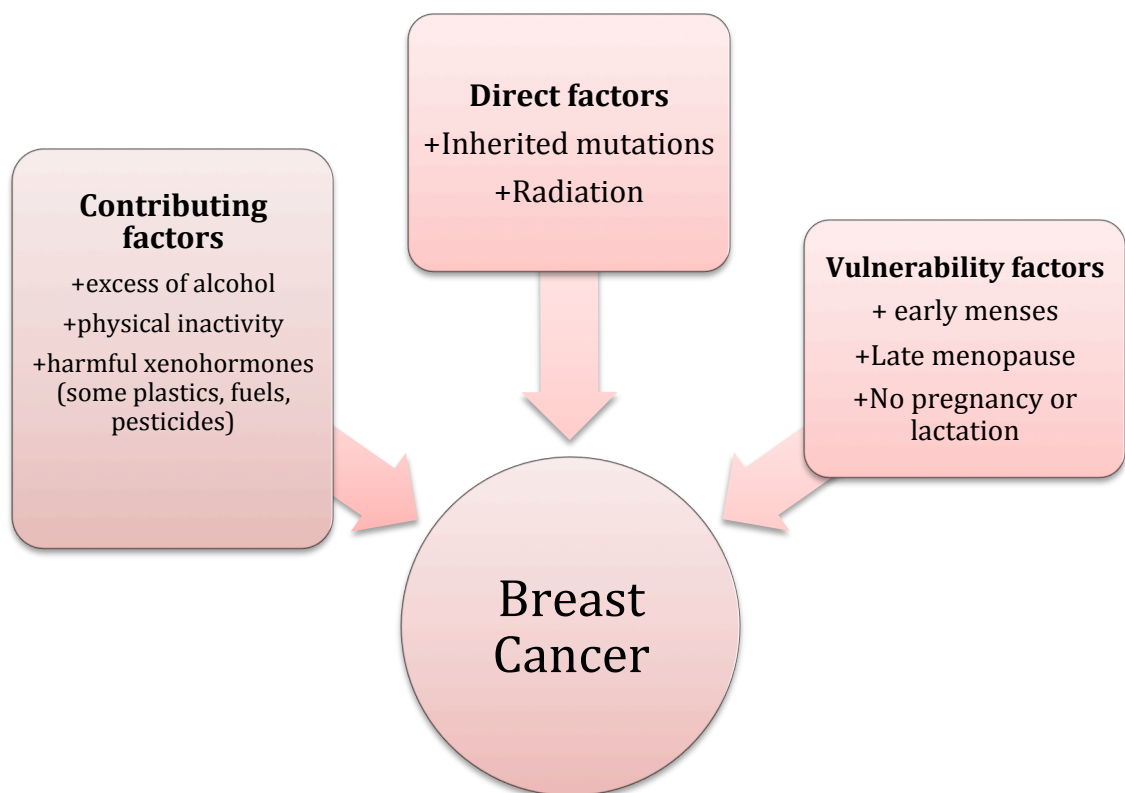
Figure 1.2 Summary of BC risk factors

Cancers are a result of the disruption of normal cell signalling pathways, which can produce cells, commonly referred as cancer cells, which exhibit a decisive growth advantage compared to their neighbours. These growth advantages are typically produced from a number of different genetic changes, which result in the activation of oncogenes and the inactivation of tumour suppressor genes. Unfortunately in terms of diagnosis, no single oncogene or tumour suppressor gene has been discovered to be universally present in all adult cancers. Still, the most common methods for cancer diagnosis and prognosis rely heavily on technologies that are over 100 years old including paraffin fixation of tissues and visual inspection of cell morphology by a pathologist [9].

Currently, research on POC devices is of major importance as it has the potential to make a significant impact on early cancer diagnosis. In vitro diagnostic (IVD) tests performed by a non-experienced individual without laboratory facilities to provide results, could revolutionize the medical devices market [10–15].

There are a significant number of research groups trying to identify sensitive and specific biomarkers that can be exploited to detect BC before any visible symptoms occur [16–20]. Existing diagnostic tools and biomarkers for BC have many inherent deficiencies. Mammography, specialised medical imaging that uses a low – dose x-ray system to see inside the breasts, is currently the gold standard diagnostic tool for BC screening; however, it is not without limitations, including its use of ionizing radiation and a false positive rate of 8 % to 10 % [21,22], figure 1.3.
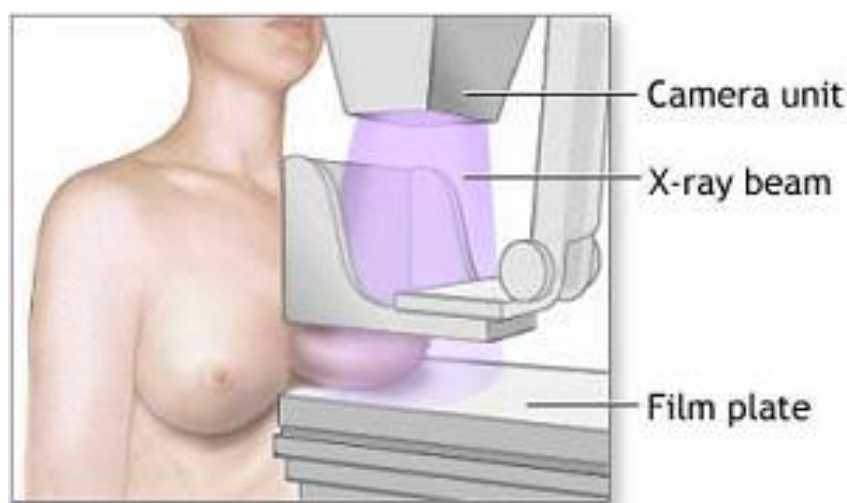
Figure 1.3 Mammogram - gold standard diagnostic tool for BC screening

4

Tomosynthesis is a revolutionary technology that provides the ability to identify and characterise individual breast structures without the confusion of overlapping tissue. During a tomosynthesis scan, multiple, low-dose images of the breast are acquired at different angles [23], see figure 1.4. Unfortunately this technique is not as accessible as mammography.
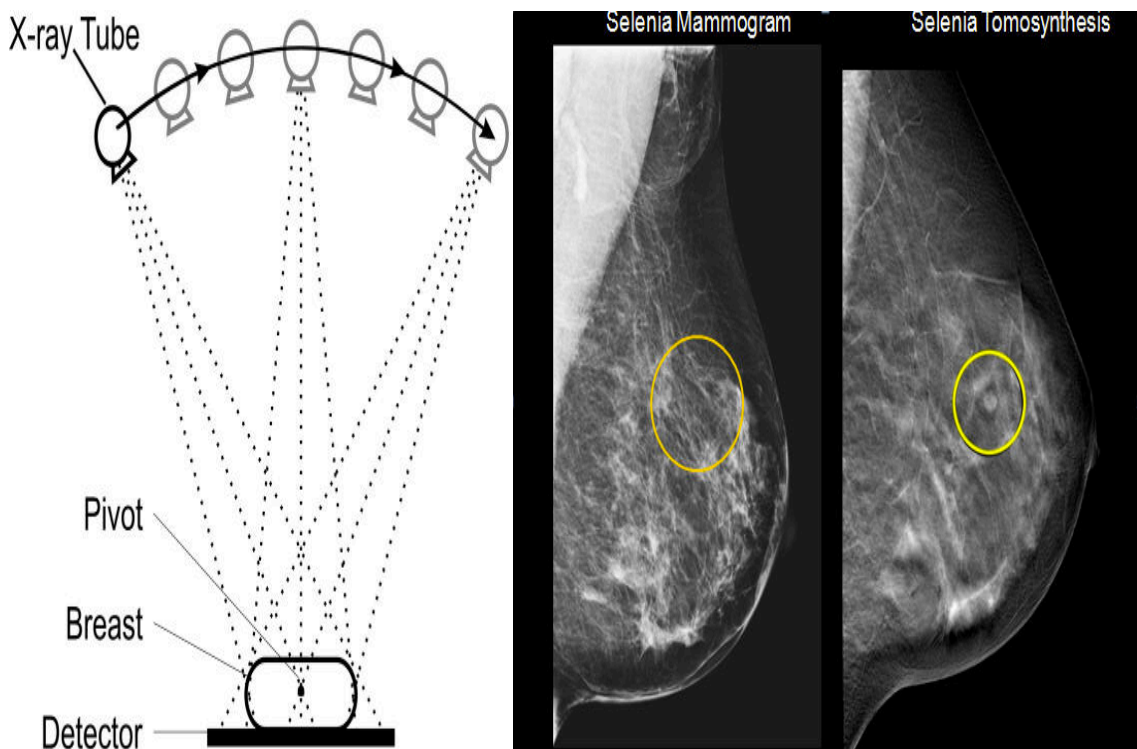
Figure 1.4 *(from left)* Tomosynthesis set up [23]. Lesion not detected by mammogram (left image), however visible with tomosythesis (right image) [23].

The images are used to produce a series of one-millimetre thick slices that can be viewed as a three dimensional reconstruction of the breast. Instead of viewing all tissue complexities superimposed as they are on a traditional 2D mammogram, figure 1.4, the scan scrolls through the layers of the breast in one-millimetre thick slices. Reviewing breast tissue slice-by-slice removes the confusion of superimposed tissue, allowing the radiologist to view a mammogram in a way never before possible. The technology results in fewer "call backs" generated by screening mammography exams.

1.3 Current state of the art in detection of circulating tumour DNA

The early diagnosis of BC is still a challenge involving integration of clinical and physical examinations, ultrasound and mammography imaging and histopathology. A specific panel of biomarkers obtained from blood would be a beneficial and minimally invasive supplement to other clinical and pathological approaches [24,25]. A non-invasive and more accessible test could be more time and cost efficient than currently available methods. The most ideal sample to be collected would be serum or plasma as an accessible bodily fluid and it provides a dynamic representation of the most extensive biological source for cancer biomarkers, see figure 1.5.
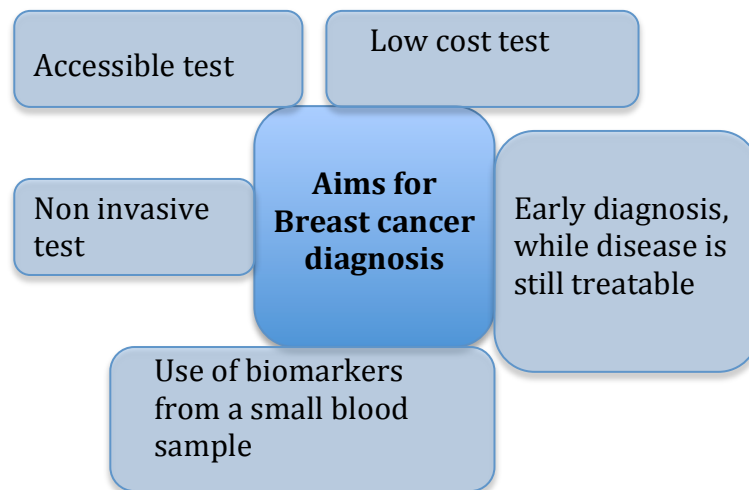
Figure 1.5 Schematic of biggest challenges in breast cancer diagnosis.

There are a number of research groups exploring an area of BC specific biomarkers for the development of diagnosis tests [17,26–30]. New biomarker discoveries as well as improvements in existing technologies are crucial to provide assays, which are more:

- robust,
- reproducible,
- quantitative,
- sensitive,
- and specific.

Hannes M. Muller *et al* use MethyLight assay [31], which is a high throughput assay analysing multiple genes. In the gene evaluation set they have identified five genes (*ESR1, APC, HSD17B4, HIC1*, and *RASSF1A*). They aim to develop a prognostic test, rather than diagnostic, sensitive enough to test for haematogenous metastases, which can be described as the life threatening event in breast cancer affecting mainly bone, liver, lung and brain. This research shows a great demonstration of an useful and simple approach for the risk assessment of breast cancer patients [31]. The more recent research published by Fackler MJ *et al* shows a newly developed cMethDNA, a quantitative multiplexed methylation-specific PCR assay for a panel of ten genes, consisting of novel and known breast cancer markers [32]. The above researchers claim that their assays have applications as a non-invasive indicator for detecting tutor-specific cell free circulating DNA. In the future it could be used to monitor response to therapy and could also serve as an early indicator of tumour recurrence [32]. However both assays are useful for BC patients, they are not suitable to early diagnose the BC, but rather to prognosis or monitor of the disease.

The main cause of death among BC patients is cancer being disseminated through the blood stream into distant organs [33–35]. This has led to a significant interest in identifying markers for early detection of circulating tumour cells. MicroRNAs (miRNAs) have high potential as novel tumour markers due to their tissue specificity, stability and association with clinic-pathological parameters. Biomarkers may facilitate accurate tumour stratification (location), predict response to treatments, predict the risk for disease recurrence or progression, or even represent novel therapeutic targets [34]. MicroRNAs (miRNAs) are described as highly maintained, small endogenous single-strand non-coding RNAs. MicroRNAs are sequentially processed from longer precursor molecules that are encoded by the miRNA genes. MiRNA genes are referred to by the same name (termed *mir*) written in italics to distinguish them from the corresponding mature mRNA (termed miR) followed by a number, e.g., mir-1 or miR-1. They are expressed in the circulation and tissue of patients with cancer. Therefore, it has been suggested that they may act as key regulators of carcinogenesis [27]. The potential of microRNAs (miRNAs) as novel tumour markers has been the focus of recent scrutiny because of their tissue specificity, stability, and association with clinic-pathological parameters. Data has emerged documenting altered systemic miRNA expression across a spectrum of cancers [36,37].

A recent study by Luo *et al*. [27] suggests that *miR-195-5p* may act as a tumour suppressor in BC. Consequently, targeting of this miRNA may provide a novel strategy for the diagnosis and treatment of patients with this lethal disease. Data published by Li *et al*. [28] implies that both *miR-195* and *miR-497* play important inhibitory roles in BC malignancy and may be the potential therapeutic and diagnostic targets.

Research by Heneghan *et al* demonstrates that elevated levels of circulating *miR-195* are specific for BC, as can be seen in figure 1.6. They also describe remarkably high sensitivity of *miR-195* in combination with the general oncomirs such as *let-7a* and *miR-155* for discriminating BC cases from controls. In their opinion, miR-195 biomarker has a potential utility as a unique, non-invasive breast tumour marker [30].
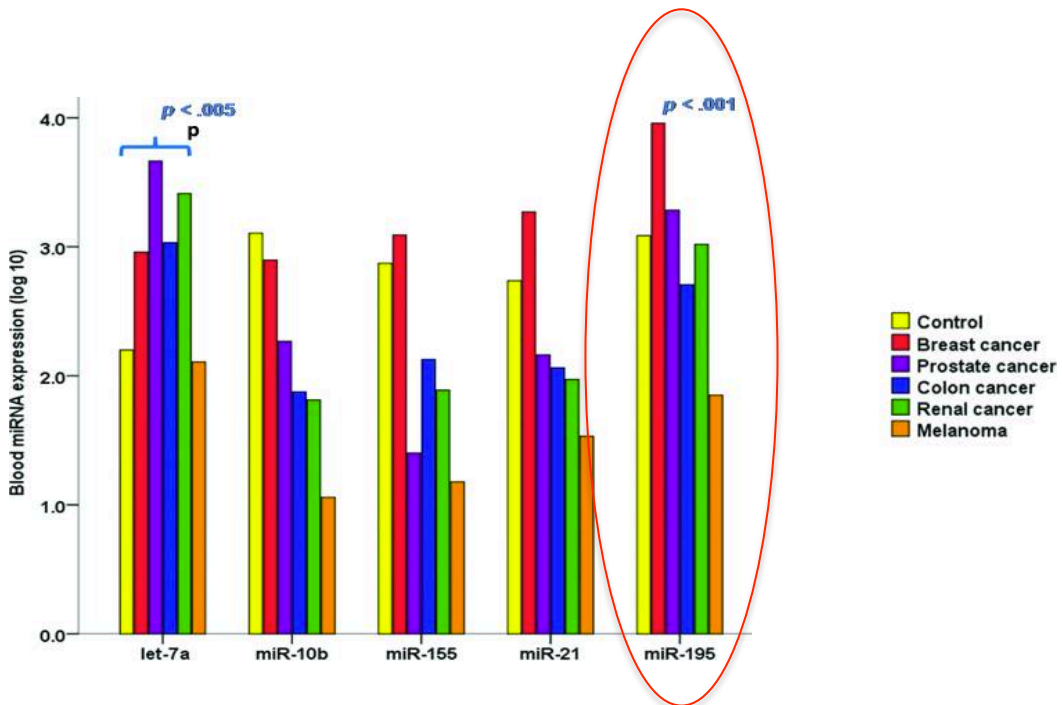
Figure 1.6 Circulating micro-RNA (miRNA) expression in early-stage cancers. Comparing early-stage cancers (TNM stages, in situ, I, and II; *n* = 110) with controls (*n* = 63), *miR-195* expression was observed to be significantly elevated only in breast cancer patients (*p* < .001) [4].

All the findings of several different research groups listed previously provide strong evidence to suggest the suitability of circulating *miR-195* as a BC–specific tumour marker. To conclude, *miR-195* expression is higher in breast tumours than in normal breast tissue, a finding mirrored in blood circulation, wherein *miR-195* levels are considerably higher (19-fold) in BC patients than in healthy controls [30].

Based on the information mentioned previously, micro *RNA 195 (DNA analogue)* was used in this study as a BC specific biomarker. Since micro RNA molecules are very sensitive to RNase, which is a type of enzyme that catalyses the degradation of RNA into smaller components, DNA analogues were used instead due to their robustness. A development of a DNA assay for BC diagnosis is a novel approach investigated in this work. The research done here was mainly focused on the development of an appropriate solid platform for biomolecules attachment, which then can be applied in an assay for DNA detection. The format of the assay could be adapted and optimised to other biomarkers if required. The most important factors in surface development were:

- its robustness,
- low yield of non-specific binding and
- high level of control.

The surface should not interfere with targets or biomolecules other than capture probes. This could potentially decrease the overall hybridisation efficiency and would have a negative effect on overall hybridisation performance and accuracy. If the above milestones are achieved, this test could serve as an early breast cancer (or other cancer, if different cancer specific biomarkers used) tool. It could be adapted to a portable device (point-of-care).

Next paragraphs give an overview of biosensors, which are the potential outcome and application of this study.

1.4 Biosensors

The term "biosensor" stands for "biological sensor" [38] and is described as analytical devices incorporating a biological sensing element and a transducer, figure 1.7. They harness an outstanding sensitivity and specificity of biology in conjunction with physicochemical transducers to deliver complex bio analytical measurements with simple, easy-to-use formats [39,40]. The usual aim of a biosensor is to produce either discrete or continuous digital electronic signals, which are proportional to a single analyte or a related group of analytes. Every biosensor has a biological component, which plays role of a sensor and an electronic component, which detects and transmits the signal.
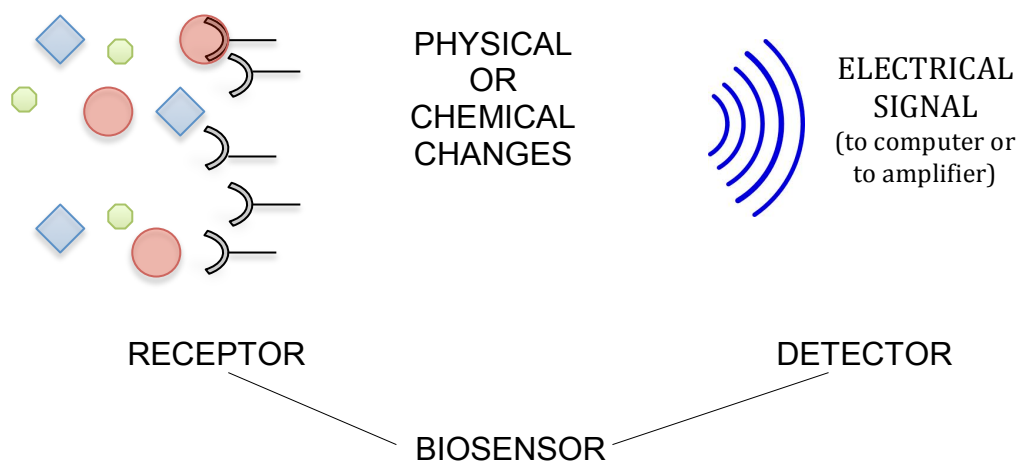
Figure 1.7 Schematic of a biosensor.

Type of biosensors depends on the type of biological element and transducer they contain. Table 1.1 shows the list of the biological elements in biosensors and different types of transducers are discussed in table 1.2.

Table 1.1 List of the biological elements in biosensors [38,40,41].
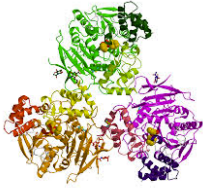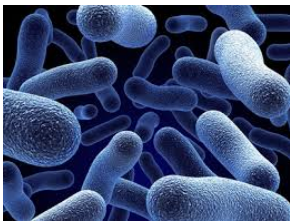
Biological element	Application
Enzymes 	Enzymes are proteins with a high selectivity for a particular substrate, which it binds to, bringing about a catalytic change. Enzymes are useful in the large scale production of sensors as they are avaulable commercially in highly purified states. They can be attached onto the of a transducer through: • adsorption, • covalent attachment, • entrapment in a gel or an electrochemically generated polymer.
Antibodies 	B-lymphocytes in response to antigenic stimuli such as foreign invaders or microbes produce antibodies. Antibodies molecules are anchored or immobilised on the surface of a transducer through covalent attachment by conjugation of: • amino, • carboxyl, • aldehyde or • sulfhydryl groups. Antibodies are sensitive to changes in pH, ionic strength, chemical inhibitors and temperature. Immune sensors usually employ optical, fluorescence or acoustic transducers.
Micro-organism 	Microbes found applications in detection of oxygen or carbon dioxide consumption in an environment using electrochemical techniques. The main advantage of microbe biosensors over the enzymes and antibodies ones is its cheaper price. However the main downfall is it's sensitivity while compared with enzymes or antibodies.
DNA 	Biosensors used for DNA detection are also known as biodetectors. Thet are mainly used to isolate and measure the strength of single DNA–DNA bonds, which in turn helps in detecting and characterizing single molecules of DNA and diseases. Biodetectors are useful in detecting small concentrations of DNA in large samples.

Table 1.1 Types of transducers used in biosensors.

Transducer	Description
Electrochemical transducer	• amperometric – based on detection changes in current occurring due to reduction or oxidation. The reaction is measured based on current difference between the analyte and the bio-element. • potentiometric – measure the charge accumulation or potential of an electrochemical cell.
Optical transducers	For enzymes and antibodies, fluorescence is the most common signal transducer. Fibre optic probes consist of at least two fibres: • One is connected to a light source of a given wavelength range and produces the excitation wave • The other is linked to the photodiode that detects the change in optical density at a selected wavelength. Plasmon resonance is based on measurements of refractive index at and close to the sensing element's surface.
Acoustic transducers	The transduction system in this type of transducers is mechanical acoustic wave. The membrane is build with chemically interactive materials in contact with a piezoelectric material. Most commonly used devices: • bulk acoustic wave (BAW) • surface acoustic wave (SAW). •
Calorimetric transduction	This type of transducer is based on measurements of the heat from the reaction between the analyte and the sensing element.

Biosensors as any other sensors available have number of technical difficulties, which require more research to overcome them. Issues include [42]:

- **contamination** – huge challenge for non disposable biosensors. All bio-elements require to be kept clean and leak prevention is of a paramount importance,

- **biomolecules immobilisation** – molecules may behave differently while covalently attached to the surface rather than free in a solution,

- **sterilisation** – big issue for non disposable biosensors; sterilisation techniques may interact with biomolecules attached to the surface,

- **uniformity of anchored biomolecules** – issues with reproducibility,

- **selectivity and detection range (LOD)** – ideally high selectivity and low LOD,

- **cost** – disposable and low cost biosensors.

1.5 DNA testing and microarray technology

DNA testing, also referred as a genetic testing, has its applications in non-diagnosis testing including determination of a child's parentage. Moreover, a person's ancestry or biological relationship between people can be determined. Nucleic acid testing found its use in the food sector to monitor the exposure to pathogenic microorganisms, to minimize a substantial health risk to consumers, for example research done at National University of Ireland, Galway [43]. DNA diagnosis testing can also involve the analysis of DNA (chromosomes) to detect vulnerabilities or heritable diseases. This type of diagnosis testing provides information about a person's gene and chromosomes throughout life.

A microarray is also called a multiplex lab-on-a-chip (LOAC), see figure 1.8. It is a solid substrate that can assay large amounts of biological material by using high – throughput screening processing and detection methods [44].

The ability to perform laboratory operations on a small scale using miniaturized (lab-on-a-chip) devices is very appealing. Small volumes reduce the time taken to synthesize and analyse a product; the unique behaviour of liquids at the microscale allows greater control of molecular concentrations and interactions; and reagent costs and the amount of chemical waste can be much reduced. Compact devices also allow samples to be analysed at the point of need rather than a centralized laboratory [44].
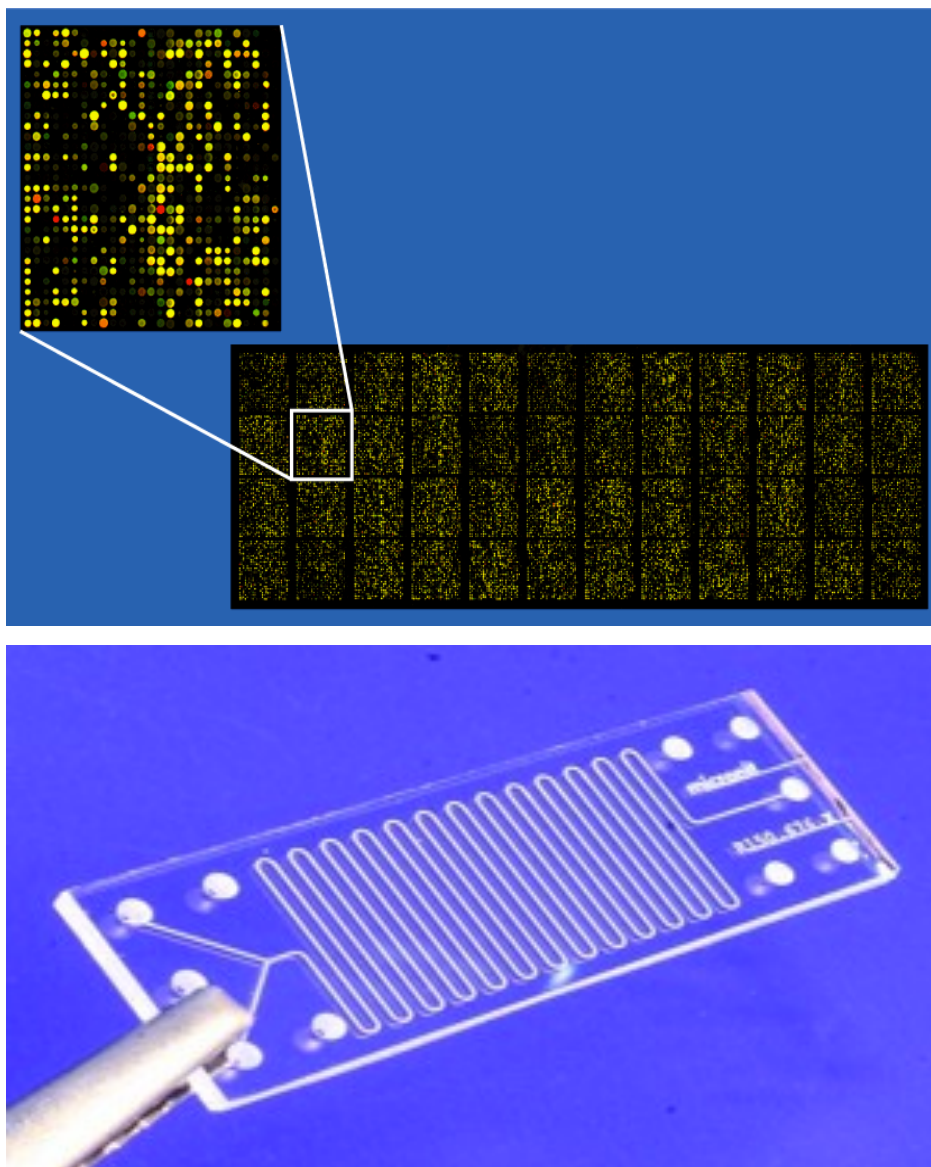
Figure 1.8 (from left) Microarray format; Lab-on-a-chip format [44]

Microarray technology is used for the detection and discrimination of number of different pathogens and it also has applications in monitoring the antimicrobial resistant bacterial and viral strains [45,46].

There are few different characteristics, which distinguish DNA microarrays, including:

- Nature of the probe

- The solid-surface support used

- Specific method used for probe and/or target detection [45] .

The probe refers to the DNA strand anchored to the solid support, whereas the target is the "unknown" strand of DNA of interest. Table 1.3 lists three main requirements for DNA microarrays [47].

Table 1.2 Three main requirements for DNA microarrays

• the immobilisation chemistry needs to be stable
• the probes have to remain functional after attachment
• the DNAs have to be immobilized with an appropriate orientation and configuration

Table 1.4 respresents some of the applications of DNA testing and microarray biosensors for the detection of DNA and protein biomarkers for disease analysis. Point of care diagnostics and nucleic acid diagnostics are explained in more details in the following paragraph.

Table 1.3 Examples of applications of DNA testing and microarray biosensors for the detection of DNA and protein biomarkers for disease analysis

Application	How is it used
New born screening	24 to 48 hours of a child's birth, new-born screening is performed by collecting few drops of blood from a heel stick. The collected sample is then analysed for biomarkers that may reveal hidden congenital disorders (present at birth). If such markers are found, parents are informed and they can avail of follow up program, which involves further diagnostic tests as a confirmation. This testing provides early diagnosis of a disorder and minimizes the effects of it [48].
Prenatal diagnosis	This type of testing involves testing the foetus's genes or chromosomes before birth. This is an invasive test and is provided for couples with a high risk of having a baby with a genetic disorder. However not all the possible inherited disorders can be ruled out using this method. The genetic disorders that can be detected with prenatal testing include: cystic fibrosis, Duchene muscular dystrophy, Polycystic kidney disease or sickle cell anaemia [48].
Carrier testing – cystic fibrosis	The above type of testing is utilized to determine if one carries one or two copy/ies of gene mutation. The test is carried out by direct gene analysis for mutations; the sample is collected from blood. If two copies are present, this potentially can cause a genetic disorder. Individuals with family history of a genetic disorder usually avail of this testing. If both parents are being tested, the outcome can provide a vital information involving the risk of having a child with a genetic condition, such as cystic fibrosis [49].
DNA paternity testing	DNA profiling known as genetic fingerprinting to determine whether two individuals are biologically parent and child. A paternity test establishes genetic proof whether a man is the biological father of an individual, and a maternity test establishes whether a woman is the biological mother of an individual.
Diagnosis of Viral/Bacterial Infections	Detection of infectious diseases such as: • human papillomavirus (HPV), • human influenza virus (H1N1), • pneumonia and • tuberculosis [50].
(DNA)Biomarker Detection	Enzyme-linked Immunosorbent Assays (ELISAs) are one of the earliest techniques employed for the detection of the biomarkers, [46].

1.6 Point-of-care devices and nucleic acid diagnostics

Tools providing extensive molecular profiles of patients to guide the clinician in making viable diagnosis and prognosis are required to tackle the growing number of fatalities resulting from over 100 cancer-related diseases [41]. Unfortunately, there is no one universal molecular marker that can provide sufficient information to assist the clinician in making effective prognoses or even diagnoses. Therefore large panels of markers must typically be scanned and examined before a correct conclusion about an individual's diagnosis can be made. The classical biosensor format, point-of-care (POC) device, is recognised as a valuable tool in diagnostics environment. However they do possess a number of limitations due to the single element nature of these sensing platforms. New formats of POC devices are required in order to improve the overall ability of the clinician to manage cancer patients [41].

Immunoassay technology is utilised in POC devices; this includes antigen-antibody binding, whether the antibody is the assay target or the means to capture it. These assays target disease-specific protein markers such as:

- glycated haemoglobin (HbA1c) for diabetics,

- D-dimer for thrombosis,

- troponin I or T for cardiac damage,

- prostate-specific antigen (PSA) for this common cancer, and

- bacterial and viral infection-related markers such as human immunodeficiency

- virus (HIV), influenza, chlamydia, and hepatitis to name a few.

Figure 1.9 represents the best-known home POC protein-detection device, the pregnancy test kit, which measures the pregnancy hormone human chorionic gonadotropin (hCG) [11].
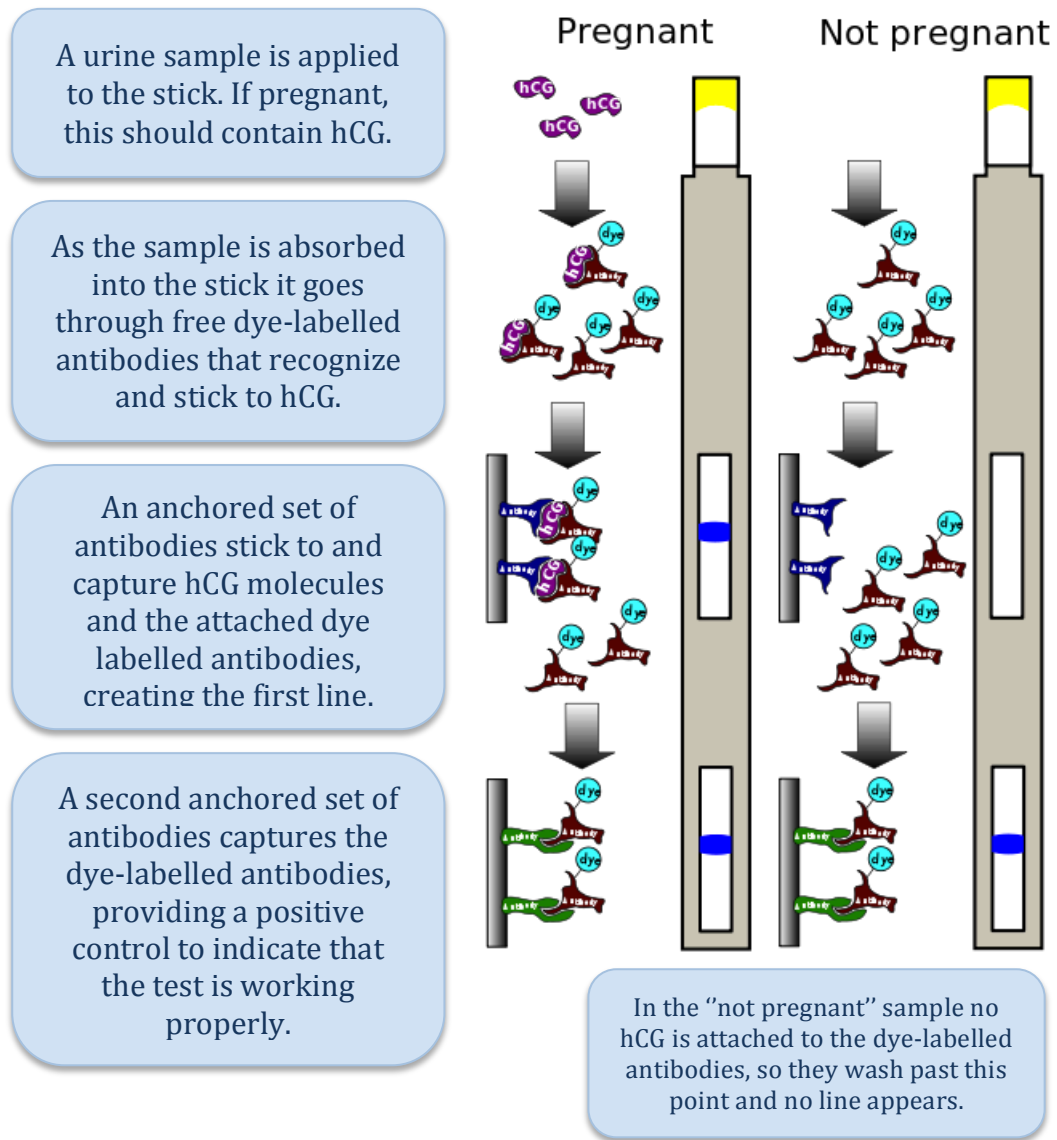
Figure 1.9 Diagram of typical immunoassay home pregnancy test, which detects human chorionic gonadotropin (hCG)

Image taken from https://en.wikibooks.org/wiki/Methods_and_Concepts_in_the_Life_Sciences/Immunoassays

POC technologies offer platforms for complex testing by non-specialists and the benefit of increased robustness and reliability due to fewer world-to-device interfaces. They are viewed as integrated systems that can process clinical samples for a number of different types of biomarkers in a variety of settings, such as clinical laboratories, doctors' offices and eventually, at home. Basically, POC systems make state-of-the-art technology platforms accessible to a large population pool.

From a diagnostic or prognostic perspective, POC systems provide the clinician with the ability to have access to a wealth of molecular information for providing profiles of cancers using platforms that were previously only accessible to major cancer centres. The development of POC technologies provides opportunities for better screening of at-risk patients, tighter surveillance of disease recurrence, and better monitoring of treatment. These technologies can contribute to the realization of personalised medicine by creating a link between the diagnosis of disease and the ability to tailor therapeutics to the individual.

As biomarkers of disease are discovered and validated through genomics and proteomics research, the development of new technology platforms can enable rapid introduction of these discoveries into clinical practice as well as aiding in biomarker discovery efforts [11,41].

Nucleic acid diagnostics or "molecular diagnostics" measures DNA or various types of RNA in order to examine particular genomic or genetic details of a patient or to investigate nucleic acid sequences unique to invading pathogens. In POC diagnostics devices, volumes of the sample are measured in very small quantities, such as microliters and the minimal user manipulation is required. Therefore, the assay design is more challenging than standard microarray based assay [51].

An ideal nucleic acid assay involves just two specific binding events: target nucleic acid from the sample should be specifically captured on a substrate surface via hybridisation with complimentary, surface-immobilised probe DNA and then the capture target is detected in a second hybridisation event between it's free end and a complimentary, free dye-labelled short oligonucleotide (c. 10-15 bases), see figure 1.10.
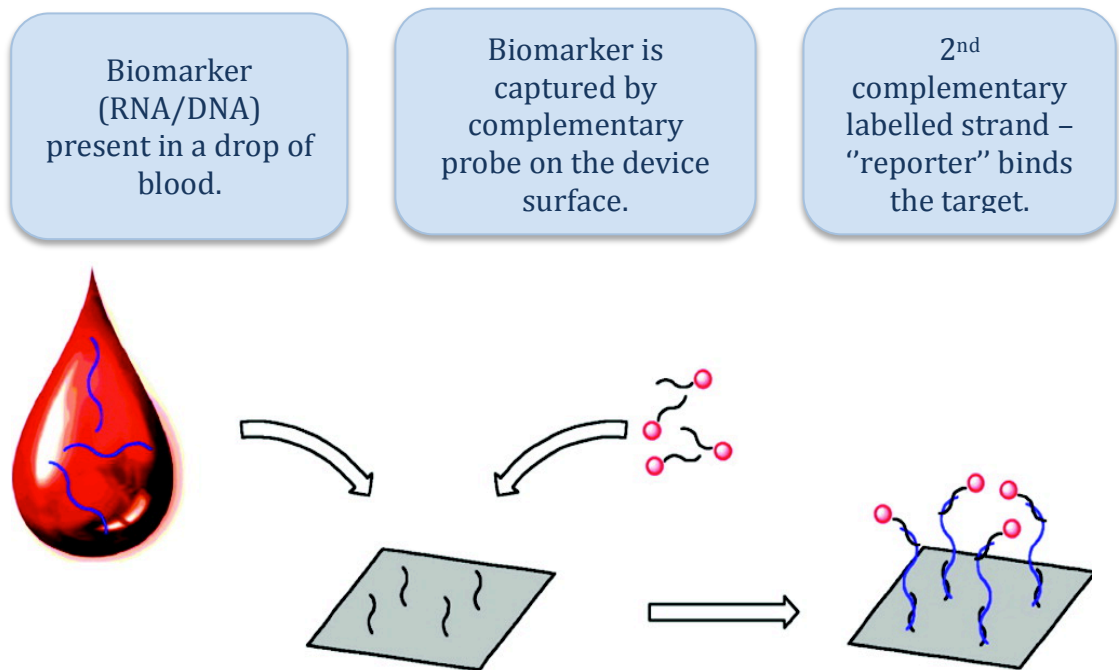
Figure 1.10 Diagram of nucleic acid assay [11].

Sensitivity of nucleic acid assays can often be controlled by factors such as:

- the hybridisation efficiency and

- the level of background signal in the absence of target.

Ionic strength, reaction temperature and probe density are the factors, which have an effect on binding kinetics and target specificity. For instance, recent work has shown that low probe densities can lead to higher hybridisation efficiencies and more binding kinetics [52]. Advantages and disadvantages of POC testing are listed in table 1.5.

Section 1.7 describes two main DNA assay concepts used in this work.

Table 1.4 Advantages and disadvantages of point-of-care testing [53]

Advantages	Disadvantages
Reduced therapeutic turnaround time of diagnostic testing	Concerns about inaccuracy, imprecision, and performance (ie, potential interfering substances)
Reduced preanalytic and postanalytic testing errors	Bedside laboratory tests performed by poorly trained nonlaboratorians
Rapid data availability	Quality management/assurance issues and responsibilities not defined
Self-contained and user-friendly instruments	Cost of point-of-care testing compared with traditional laboratory testing
Small sample volume for a large test menu	Quality of testing is operator-dependent
Shorter patient length of stay	Difficulty in integrating test results with hospital information system (HIS) or laboratory information system (LIS)— lack of connectivity
Convenience for clinicians	Narrower measuring range for some analytes
Ability to test many types of samples	I.e: capillary, saliva, urine

1.7 Nucleic acid assay concept

Nucleic acid assays or DNA assays are a molecular technique used to detect DNA or RNA at low levels. Benefits of DNA assays include:

- Ability to detect low levels of viral RNA or DNA
- High sensitivity and specificity for viral nucleic acid
- Ability to detect viral mutants and occult infections
- Additional layer of safety to the blood supply - allows the detection of infectious agents during their incubation period [54,55].

Immunoassays are used to quantify molecules of biological interest based on the specificity and selectivity of antibody reagents generated. In this research study, two different types of hybridisation assay methods were used:

- **Direct assay**, figure 1.11,

In this type of an assay, a full-length labeled specific target DNA is identified by a complimentary DNA unlabeled probe. The DNA probe is covalently immobilised to the solid supports via chemistry linkage, such as EDC or click chemistry method. DNA target is synthesized with a fluorophore at 5' end, which transduces the binding event into fluorescence signal. The intensity of fluorescence signal is directly proportional to the amount of target hybridised.

- **Sandwich assay**, figure 1.12.

In this type of an assay, a full-length specific unlabeled target DNA is identified by a half-length complimentary unlabeled DNA probe and half-length complimentary labeled detection (secondary) probe. Half-length DNA probe is covalently immobilised to the solid supports via chemistry linkage, such as EDC or click chemistry method. DNA target is unlabeled and detected by detection (secondary) probe synthesized with a fluorophore at 5' end, which transduces the binding event into fluorescence signal. The intensity of fluorescence signal is directly proportional to the amount of target hybridised.

Step 1:
Immobilisation of amino modified full length miRNA195 probe to carboxylic acid surface with EDC linker
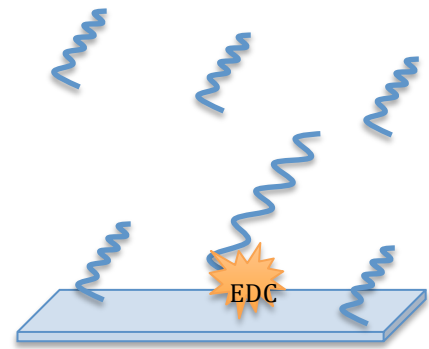
Step 2:
Washing step to reduce non-specific binding and loosely bound DNA probe
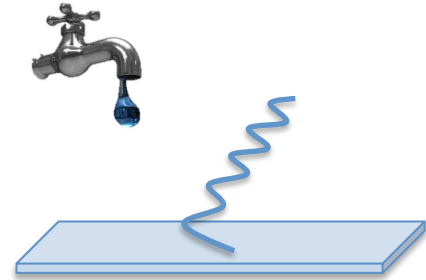
Step 3:
Hybridisation of fluorescently labelled miRNA195 (full length) target to the immobilised DNA probe. Signal obtained if full match occurs.
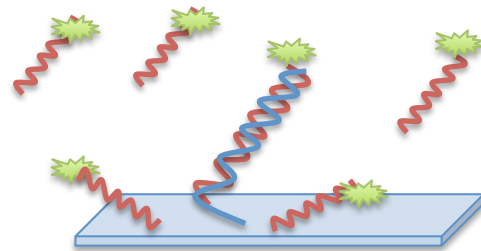
Step 4:
Final **washing** step to reduce non-specific binding of target.
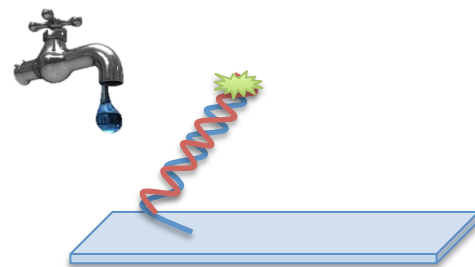
Figure 1.11 Schematic of DNA direct binding assay.

Step 1:
Immobilisation of amino modified half-length miRNA195 capture probe to carboxylic acid surface with EDC linker
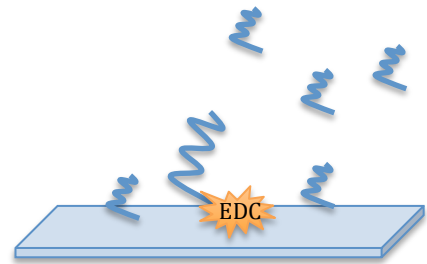
Step 2:
Washing step to reduce non-specific binding and loosely bound DNA probe
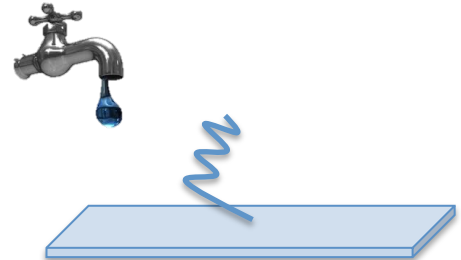
Step 3:
Hybridisation of miRNA195 (full length) target to the immobilised DNA capture probe.
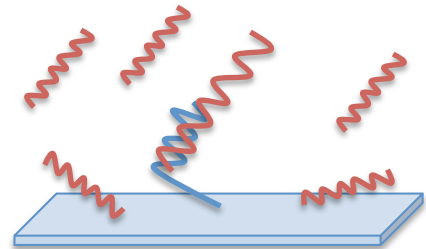
Step 4:
Washing step to reduce non-specific binding of the target
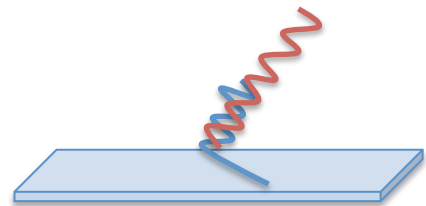
Step 5:
Binding of the remaining half of the DNA probe (detection probe) with labelled fluorescently. Signal obtained if full match occurs.
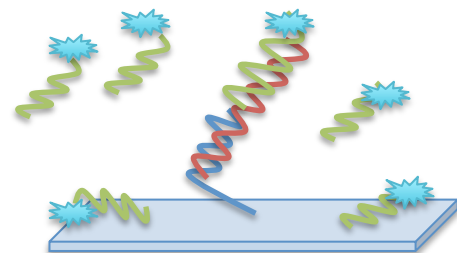
Step 6:
Final **washing** step to reduce non-specific binding of capture probe.
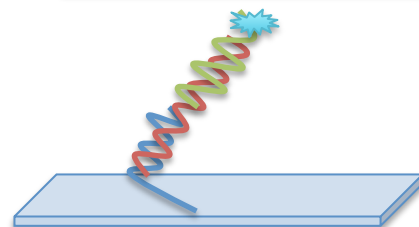
Figure 1.12 Schematic of sandwich DNA binding assay.

1.8 Surface science: importance in biosensor's development

Surface science can be defined as a study of chemical and physical phenomena which takes place at the interface of two phases such as solid-liquid interfaces, liquid – gas interfaces etc. Two main fields are included under the umbrella of surface science:

- surface physics - study of physical changes occurring at interfaces, such as changes of topography upon substrate functionalization. The above changes can be monitored and tested using atomic force microscopy and ellipsometry (thickness changes).

- surface chemistry - study of the chemical changes and reactions at the interfaces. Surface chemistry can also be referred to as surface engineering as it involves modifying the chemical composition of the surface by the introduction of desired elements or functional groups. The above is incorporated in order to produce a specific functional film, which may be utilized as an anchoring platform for biomolecule listed in figure 1.13.
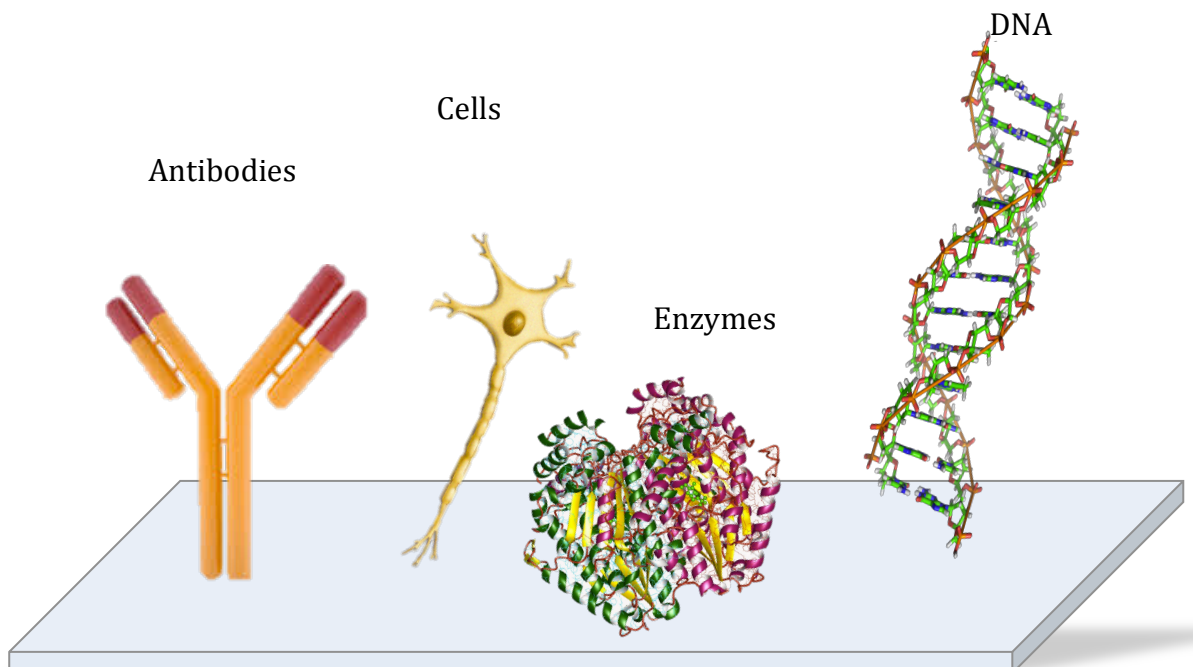
Figure 1.13 Modified supports are anchoring point for biomolecules, such as antibodies, cells, enzymes and DNA in bioassay development.

Surface chemical modifications can improve surface properties in terms of lowering non-specific binding, manipulating surface charge or hydrophobicity of the substrate, which is a paramount factor in microfluidics devices development. Chemical reactions can be measured by real time measurements including label free quartz crystal microbalance or dual polarization interferometry [56]. Fluorescence labelling of the biomolecules and fluorescence scanning is also a popular and reliable method.

Surface science is an interdisciplinary area where properties and processes at interfaces between synthetic materials and biological environments are investigated and bio functional surfaces are fabricated. Surface science touches on a vast array of applications in many research and medical areas, such as:

- medical implants in the human body,

- biosensors and biochips for diagnostics,

- tissue engineering,

- bioelectronics,

- artificial photosynthesis, and

- biomimetic materials [56].

There are major challenges associated with development of surfaces, which are listed in Table 1.6.

Table 1.5 Challenges in development of surfaces for DNA assays

Challenge	Role
Non specific binding	Compromises assay efficiency
Stability of immobilised DNA probe	Surface confined probe should remain stable and active
Limit of detection	Lowest amount of analyte detected
Time	Real time measurement, instant results, prep time
Ease of surface preparation	Bulk production, longevity

Detection elements play a crucial role in analyte recognition in biosensors. Therefore surface chemistry is a key step in immobilisation of biomolecules on the biosensor surface [57]. Major progress in research is necessary to realize selective, high affinity, high- binding-capacity analyte capture methods to push the POC devices performance forward. The ability to effectively control the background response and directly regulate the device limit-of-detection (LOD) is critical, as well as overcoming non-specific adsorption (NSA) of biomolecules, such as protein or nucleic acids onto the surface [11,58,59]. Signal interference and the non-specific adsorption are the biggest concern and challenge in the development of surfaces for biosensors. NSA (non specific absorption) or NSB (non specific binding) is an undesired adsorption of analytes other than target analytes, which is often a case with analysis of complex biological samples such as blood. Even purified matrices still consist of a cocktail of potentially interfering biomolecules, very similar to target analytes of interest. The above will prevent the detection and automatically lower the specificity and accuracy of the test. Moreover, the biggest consequence of NSA, besides altering the biosensor's performance, is the occurrence of "false positive"/"false negative" results; incorrect response to a binding event. Possibly NSB is the biggest issue in biosensor development and why biosensors still are not a robust alternative diagnostic tool in clinical analysis [60].

Glass and silicon were the first materials used to fabricate biosensor platforms. Since then, there has been a veritable explosion of lab-on-a-chip devices fabricated in a wide range of materials, using different fabrication techniques and forming diverse microfluidic systems [61,62].

Surface science plays a major role in an assay development and the next important step is bio-conjugation technique of biomolecules to the solid platform. Immobilisation techniques for assay development are listed and discussed in more details in the next section.

1.9 Immobilisation techniques for assay development

Immobilisation strategies for biomolecules on surfaces to achieve biosensor and biomedical diagnostic functions are of great importance. There are a number of different immobilisation chemistries, which are mainly based on three important mechanisms:

- *physical adsorption* - the simplest immobilisation method, no nucleic acid modifications are required. This method of immobilisation is based on ionic interactions taking place between the negatively charged groups present on the DNA probe and positive charges covering the surface [46,63].

- *covalent immobilisation* - requires chemical modification of the surface when fabricating microarrays [64–67].

- *streptavidin-biotin immobilisation* - highly specific binding of streptavidin and biotin is often used for DNA immobilisation [46,68,69].

As mentioned in table 1.6, minimization of non-specific binding is the biggest challenge in achieving the high sensitivity and selectivity of the assay. Immobilisation has also an effect on the stability of the immobilised probes. Table 1.7 depicts the unresolved challenges involved in the immobilisation techniques.

Table 1.6 Advantages and disadvantages of immobilisation methods of DNA probes on functionalized surfaces [46].

Immobilisation method	Interaction or reaction	Advantages	Drawbacks
Physical Adsorption	Charge-charge interaction or hydrophobic interaction	• Simple • Fast • Direct method (no linker molecules) • Suitable for DNA and RNA	• Desorption by change of ionic strength or pH • Random orientation • Desorption by detergent • Problem of crowding effect and poor reproducibility
Covalent bonding	Chemical bonding	• Good stability • High binding strength	• Use of linker molecules • Slow, irreversible • Problem of crowding effect
Streptavidin – Biotin interactions	Specific Streptavidin – Biotin interactions	• Improved orientation • High specificity and functionality • Well controlled • Reversible	• Expensive, slow • Problem of crowding effect • Use of biocompatible linker • Poor reproducibility

In this work, covalent bonding was used to immobilise DNA probe onto a solid support appropriately functionalised. Table 1.8 lists number of different immobilisation methods used for covalent linkage of biomolecules to the solid supports. Use of carbodiimide as a reagent/linker is most frequently used in covalent reactions, 1-Ethyl-3-(3-dimethylaminopropyl) carbodiimide (EDC) is used in this research work as an activation coupling agent between amino modified DNA probe and carboxylic acid modified surface (highlighted in red in table 1.8).

Table 1.7 Different immobilisation methods used for covalent linkage of biomolecules to the solid supports

Surface function	Interaction or reaction	Advantages	Drawback
Carboxyl (EDC coupling)	Chemical bonding with amine DNA	• Simple method • High surface coverage • Easy coupling reaction	• pH, ionic strength, concentration, reaction time dependant
Aldehyde	Chemical bonding with amine-DNA	• Good stability • High binding strength • Long term use stability • Less random immobilisation	• Long hybridisation time • Limits the absolute signal intensity • High hybridisation temperature
Epoxy	Chemical bonding with hydroxyl, amine and sulfhydryl groups	• Easy protocol for immobilisation • Good stability • High binding strength • Long term use stabilitty	• Reactions between DNA and epoxy are extermely slow • Low immo-bilisation density
Iso-thiocyanate	Chemical bonding amine - DNA	• Well ordered surface • Re-usability • High density DNA/area • Long term use stability	• High non – specific hybridisations • Long hybridisation time
Maleimide	Chemical bonding with sulfhydryl group of DNA	• Faster immobilisation reaction • Good stability • Re-usability • High binding sterngth	• Degradation in aqueous solutions • High non-specific intercations
Mercapto-silane	Chemical bonding DNA-SH	• Good stability • Re-usability • High binding strength • Stable for long term use	• High non specific interaction • High hybridisation temperature

1.10 Description of equipment used in this thesis

During this research study a number of different analytical techniques were applied in order to characterise the developed surfaces and to investigate biomolecule-surface interactions. Below description of the equipment used in this project can be found.

1.10.1 Water contact angle

The determination of solid/vapour and solid/ liquid interfacial tensions is of importance for a wide range of problems in microfluidics systems and plays a major role in development of POC bio-devices. The attractiveness of using contact angles (CA) to estimate the solid/ vapour and solid/liquid interfacial tensions is due to the relative ease with which contact angles can be measured on suitably prepared solid surfaces. In 1805 Young recognized that the possibility of estimation of the solid surface tensions from contact angles relies on a relation between both of them [70]. The photograph of water contact angle (WCA) instrument used is shown in figure 1.14.
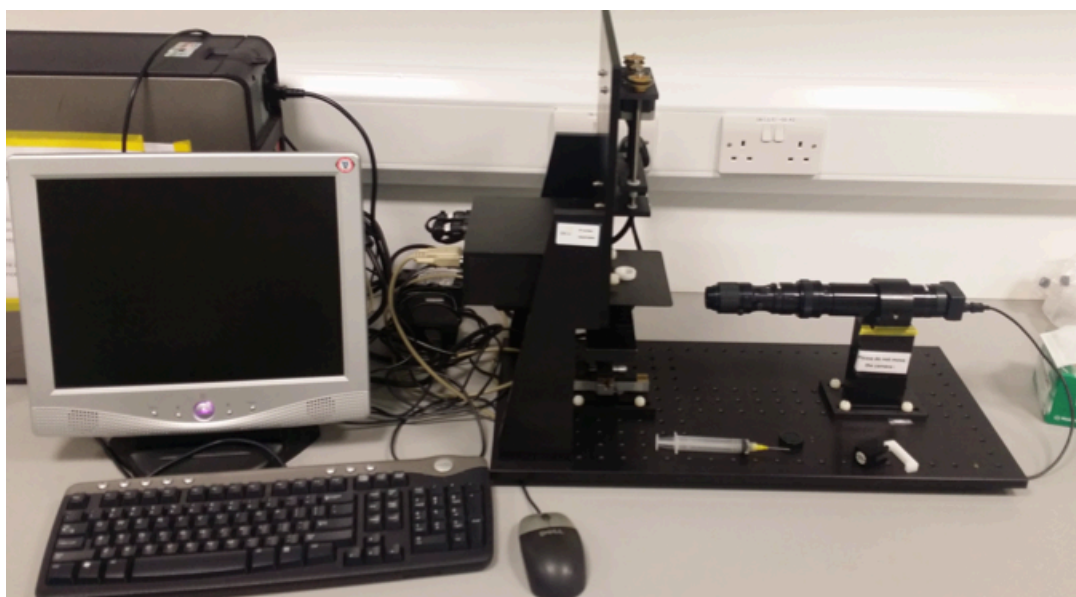
Figure 1.14 Photograph of First Ten Angstroms FTA200 contact-angle analyser set up.

The contact angle of a liquid drop on a solid surface can be defined by the mechanical equilibrium of the drop under the action of three interfacial tensions: solid/vapour, solid/liquid and liquid/vapour, see figure 1.16. The shape of a drop resting on a surface depends on the material properties of the drop, the air (or vapour) around it, and the surface on which it is placed [71,72]. This equilibrium relation is known as Young's equation, figure 1.15

$$\gamma^{sv} = \gamma^{sl} + \gamma^{lv}\cos\theta$$
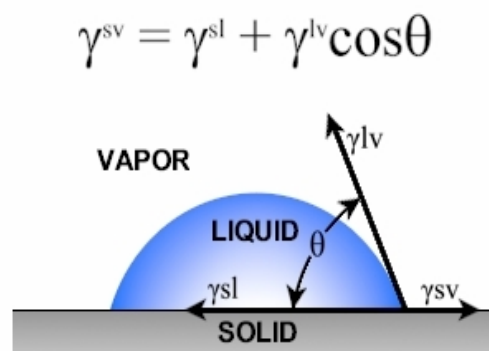
θ is the contact angle

γ^{sl} is the solid/liquid interfacial free energy

γ^{sv} is the solid surface free energy

γ^{lv} is the liquid surface free energy

Figure 1.15 Schematic of a sessile-drop contact angle system [71].

CA is geometrically defined as the angle formed at the interface between a droplet of liquid, and the surface under examination, figure 1.16. Although a relatively simple characterisation method, a surface CA influences a range of properties, such as the functionality of the surface, biological interactions, and flow capabilities. Some benefits of this characterisation technique include its non-destructive nature, as well as its rapid throughput and inexpensive setup costs [71,72]. A wide spectrum of CA values provides a rapid confirmatory test for the functionality of the prepared surfaces. WCA results can be found in chapter 3.
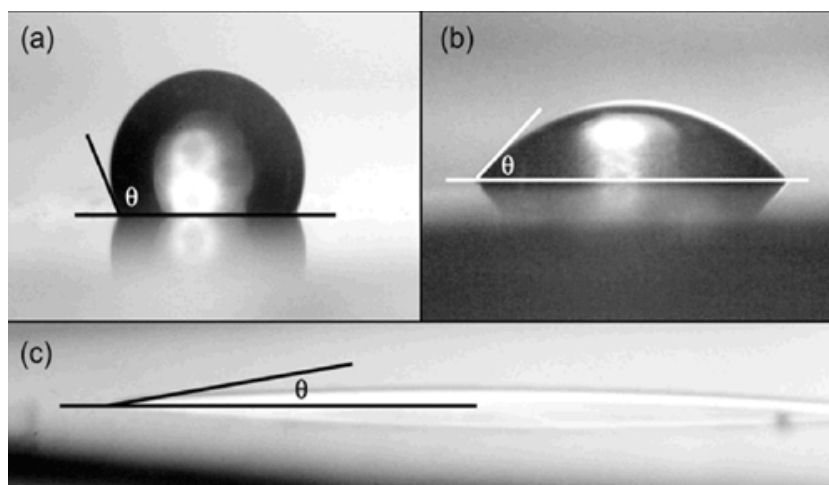
Figure 1.16 Example of droplet on (a) hydrophobic surface, (b) hydrophilic surface and (c) very hydrophilic surface [73].

1.10.2 Ellipsometry

Ellipsometry was developed in the 1960s to provide the sensitivity necessary to measure nanometre-scale layers, and ever since interest in ellipsometry has grown steadily. Today, optical properties of thin organic layers are of high interest in research areas like biomaterials, biosensors, and fabrication of devices using organic layers, interfacing electronics with biological systems. Ellipsometry is an optical technique for the investigation of the dielectric properties (complex refractive index or dielectric function) of thin films. Upon the analysis of the change of polarisation of light, which is reflected off a sample, ellipsometry can yield information about layers that are thinner than the wavelength of the probing light itself. The technology is non-destructive, contactless, and can probe the complex refractive index and thickness of a film [74,75]. Ellipsometric techniques are based on a suitable manipulation of the polarisation state by auxiliary polarising elements and measured sample. The basic Polariser–compensator–sample–analyser (PCSA) configuration of an ellipsometer is shown in figure 1.17, consisting of the following components:

- a light source,
- linear polariser (P),
- retarder (called also compensator, C),
- sample (S),
- linear polariser (called analyser, A),
- detector.

The arm with the source, polariser and retarder prepares a known polarisation state of light incident on the sample. The arm with the analyser and detector is used to detect the change of polarisation produced by the sample. An alternative PSCA scheme results from moving the compensator between the sample and analyser.
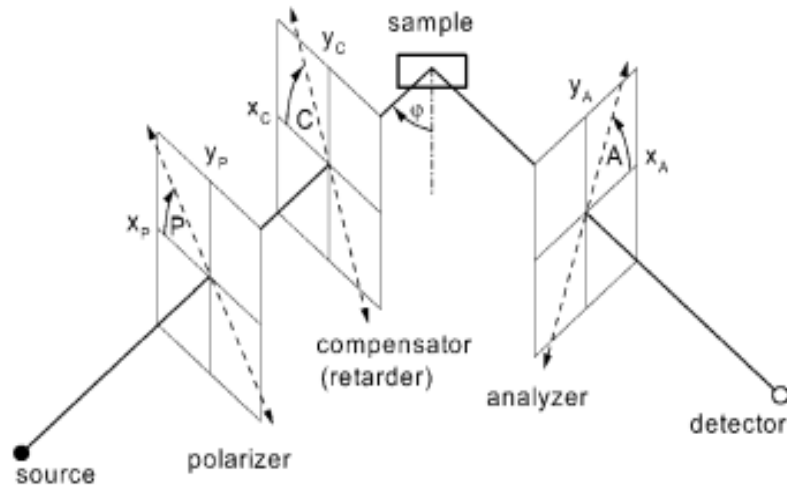
Figure 1.17 Polariser–compensator–sample–analyser (PCSA) configuration of an ellipsometer [75].

In this thesis, ellipsometry was used as a characterisation tool to analyse and determine if the deposition of various surfaces was successful and to determine the thickness of deposited films. Figure 1.18 shows an instrument used in this research. In some cases, variations of the surfaces thickness even by few nanometres could make a significant difference and could have a significant effect on an assay. Ellipsometry technique was used to measure thickness of deposited films on solid supports (silicon) in this work, and the results are presented in chapter 2.

Figure 1.18 Photograph of open environment M-2000UI Ellipsometer set-up.

1.10.3 Atomic Force Microscopy

Atomic force microscopy (AFM) is a useful tool for direct measurements of micro structural parameters and unravelling the intermolecular forces at the nano scale level with atomic-resolution characterisation. AFM has a wide range of applications including: electronics, semi-conductors, materials and manufacturing, polymers, biology and biomaterials [76].

An AFM system typically consists of:

- a micro-machined cantilever probe

- a sharp tip mounted to a piezoelectric (PZT) actuator

- a position-sensitive photo detector for receiving a laser beam ireflected off the end-point of the beam to provide cantilever deflection feedback.
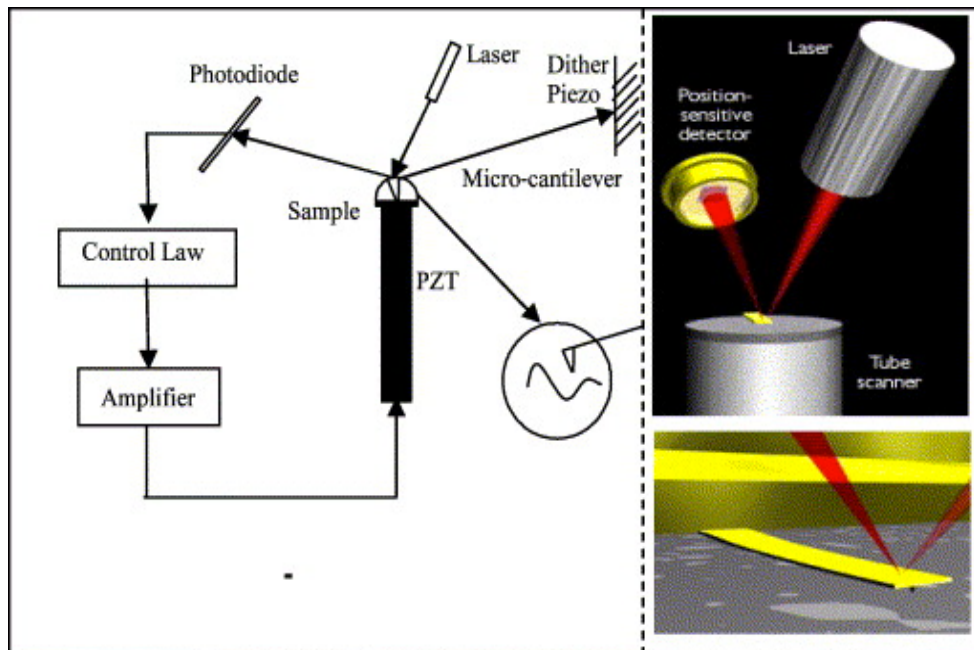
Figure 1.19 Schematic of basic AFM operation (left), real micro-cantilever and components (right) [77].

The main AFM operation principle is to scan the tip over the sample surface with feedback mechanisms that enable the PZT scanners to maintain the tip at a constant force, or constant height above the sample surface. As the tip scans the surface of the sample, moving up and down with the contour of the surface, the laser beam is deflected from the cantilever and provides measurements of the difference in light intensities between the upper and lower photo detectors. Feedback from the photodiode difference signal, through software control from the computer, enables the tip to maintain either a constant force or constant height above the sample, figure 1.19. In the constant force mode, the PZT transducer monitors real time height deviation. In the constant height mode, the deflection force on the sample is recorded [76]. Figure 1.20 shows an instrument used in this research. Results from AFM analysis are presented in chapter 2.
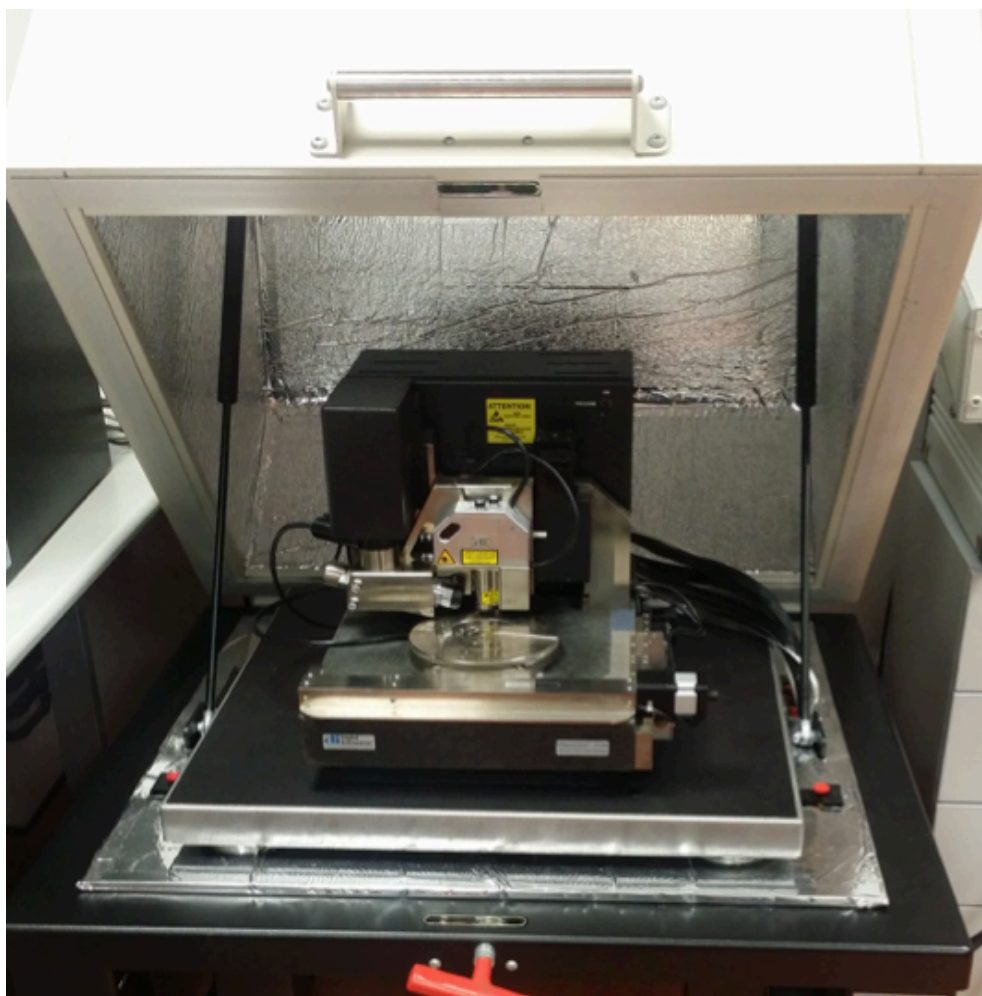
Figure 1.20 Photograph of the Dimension® AFM set up.

1.10.4 Fluorescence spectroscopy

Laser fluorescence scanning is a powerful tool used to detect fluorescently labelled biomolecules on a solid support and to examine molecular interactions. Biologically important interactions that can be analysed, include hybridisation between nucleic acid primers and DNA or RNA targets and bio conjugation between antigen and antibodies [78]. Fluorescence spectroscopy is very often utilised in biological studies using fluorophore that is site-specifically attached to macromolecules [79]. Fluorophore is a component that causes a molecule to absorb energy of a specific wavelength and then re-remit energy at a different but equally specific wavelength, hence they play a central role in fluorescence spectroscopy [80]. These labelled reagents, for example immunological or DNA probes, are added into the reaction mixture where they interact specifically with the analyte of interest in the assay [81]. The amount of fluorescence

signal can be directly correlated with the amount of analyte in the solution/bound to the surface; figure 1.21 represents images from fluorescence scanner analysis. In this thesis fluorescence spectroscopy instrument, figure 1.22, is utilised as a quantitative technique to investigate DNA probe immobilisation, DNA hybridisation and the amount of non-specific binding. Fluorescence intensity analysis is presented in all chapters throughout this thesis.
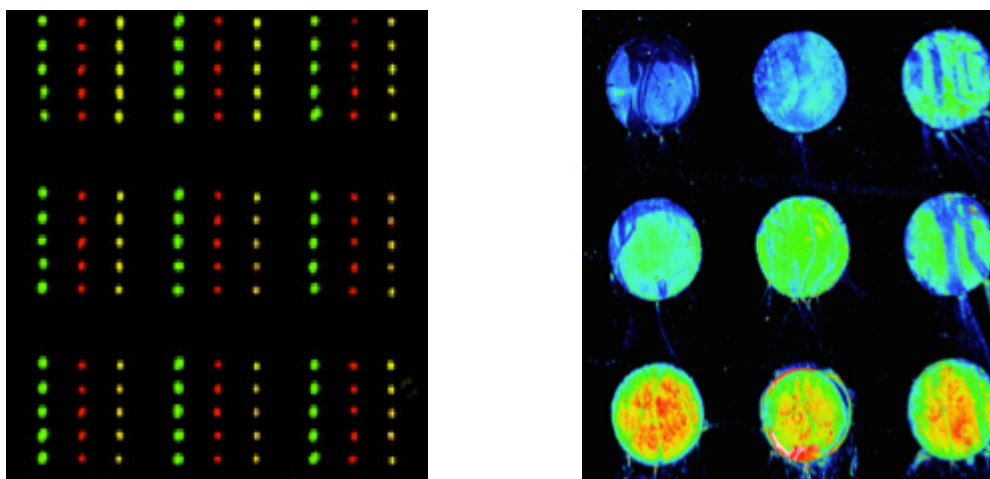
Figure 1.21 Photograph of images from fluorescence scanner analysis. (left) manual spotting, (right) micro-spotting.

Figure 1.22 Photograph of Perkin Elmer Scan array Gx Microarray scanner, fluorescence scanner set

1.10.5 The toluidine blue method (metachromatic staining)

The toluidine blue (TB), also known as tolonium chloride, stain is a way of marking tissue for microscopic examination. TB is an acidophilic metachromatic dye that selectively stains acidic tissue components (sulfates, carboxylates, and phosphate radicals) [82]. TB has an affinity for nucleic acids, and therefore binds to nuclear material of tissues with a high DNA and RNA content. It is used to stain nucleic acids blue and polysaccharides purple and also increases the sharpness of histology slide images. It has wide application in forensic examination [82,83]. TB is a cationic dye that also shows a strong affinity for interaction with carboxylic acid groups under certain conditions. TB is also used in research as a method to determine the number of carboxylic acid groups present on a surface and assumes that each carboxylic acid group binds to one molecule of toluidine blue [84].

In this thesis TB has been used to characterise the functionality of the carboxyl surfaces, as it is extremely specific to binding carboxylic groups, and creates a strong but reversible ionic bond to deprotonated carboxyl's on a surface coated in AA [84]. After rinsing away all of the unbound excess dye, the ionically bound quantity of dye can then be removed using an wash with excess acetic acid, a competing carboxylic acid group to those present on the surface. This solution, containing all of the dye that was bound to a surface, can be tested using a UV-vis spectrometer, as acetic acid does not interfere with UV-vis signals. The result from this shows an analysis of the amount of carboxyl groups present across the entire surface of the substrate.

TB was used to establish whether or not TEOS/AA surfaces were successfully produced by PECVD. Using the TB method of characterisation, a range of samples was tested with TEOS, TEOS/AA coatings, and some plain and oxidised substrate control samples as well as oxidised PMMA included. The experiment was adapted from similar experiments performed in work by Drews et al [84] and Sano et al [85]. UV-Vis data is not definitive, so a calibration curve must be created to compare subsequent experiments. Calibration curves were constructed using standard dilution methods, shown in chapter 2.

1.10.6 Dual Polarization Interferometry

Label-free biosensors offer detection of bimolecular interactions with a number of applications such as drug discovery, biomedical research and environmental safety [86]. Dual polarization interferometry (DPI) is a label free, optical biosensor, also described as an evanescent technique. DPI is an emerging sensitive analytical technique, capable of precise measurements of the thickness and density in a real time of material attached to the surface of an optical sensor chip [87–89]. DPI has seen a large increase in interest by the scientific community over the past decade since the technique was first commercialized in 2000 by Farfield Group, Ltd [88]. DPI measurements of surface adlayer (a layer that has formed on a surface by adsorption) dimensions and densities can be made in real time. The instrument is comprised of:

- an optical assembly, consisting of a helium – neon laser, which emits light at a wavelength of 632.8 nm,

- a means to select plane – polarized light,

- a sensor coructed using two optical waveguides stacked one on top of the other, and

- a camera [90,91].

The instrument accepts a sensor chip (dimensions 24×5.8 mm), which comprises five layers of deposited silicon oxynitride [88].

In principle, DPI utilises a waveguide structure that consists of a stack of dielectric layers with reference and sensing layers separated by a layer of cladding that mimics Young's 2-slit experiment in optics [92]. A top dielectric layer is etched to reveal the sensing layer so that two separate channels can be present on a single sensor chip. Light from a laser is passed through the sandwiched waveguide structure and an interference pattern is detected on the opposing side by a camera. Any changes in refractive index that take place on the sensing layer alter the phase position of the fringes relative to the reference layer and are detected in real time, as shown in figure 1.23.
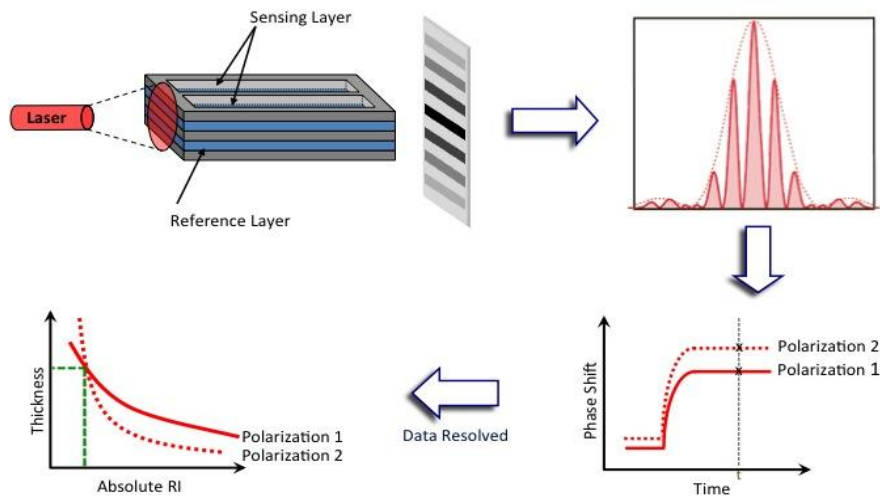
Figure 1.23 Schematic of a DPI sensor chip and the interference pattern produced when light is applied onto the side of a chip [93].

In order to interpret DPI data, Swann *et al.* [93] proposed an elegant matrix by correlating the different parameters (thickness, density, mass coverage) calculated from both the TM and TE responses.

The polarisation of the laser in DPI method rotates to excite two polarisation modes of the waveguides. The depth of evanescent field differs for each polarisation and TM mode is less sensitive to changes taking place in close proximity to the waveguide surface than TE mode. The layer structure can be estimated based on the relative responses. TM mode and TE mode are used to solve Maxwell's equation to find the exact layer condition [89,91], see figure 1.24. The change and difference in the TE and TM modes allows for the determination of thickness, refractive index, density and mass of the adsorbed layers.
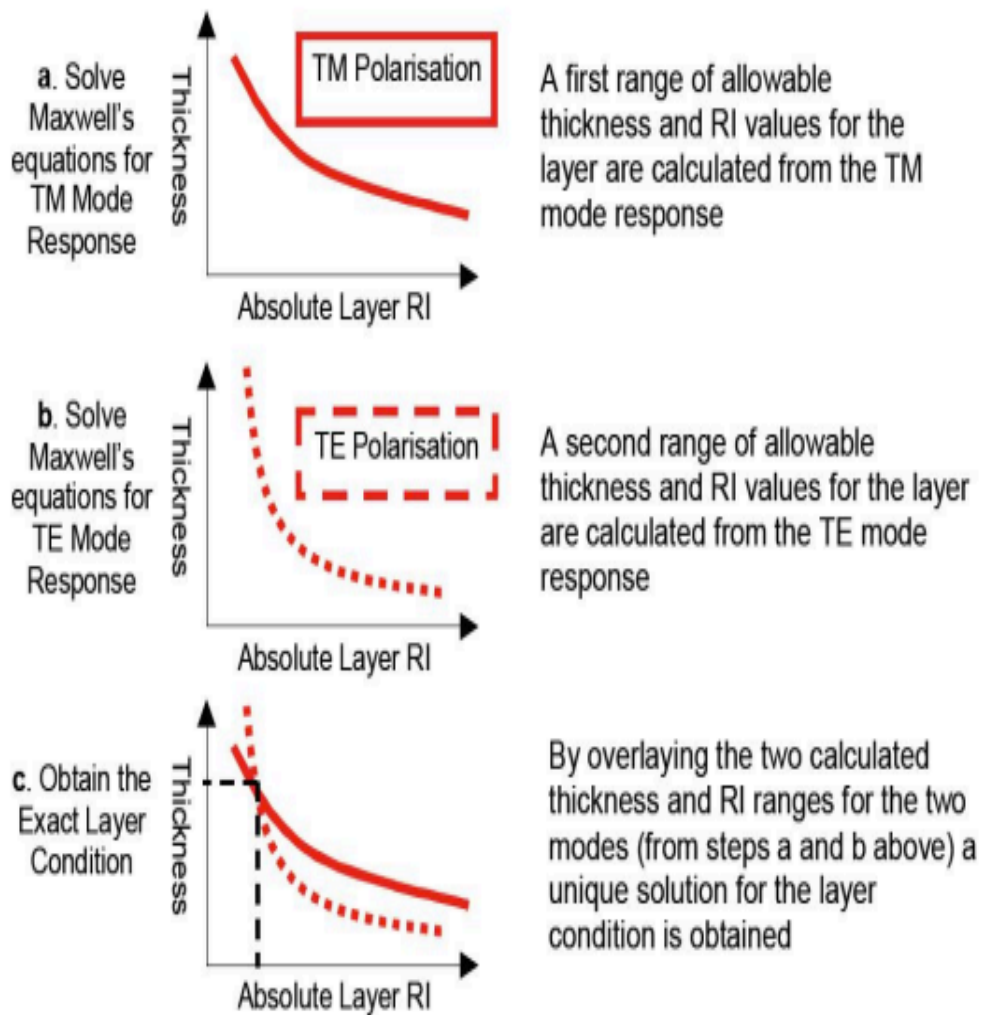
Figure 1.24 Generating an analytical solution using Maxwell's equations for any given point on the dual polarisation response curves.

This type of detailed information can be extremely helpful to the design of surfaces for optical biosensors and for characterizing the conformational changes of macromolecular interactions [93]. DPI is a biosensor that provides real time structural information on bio-layer behaviour and growth at a resolution equal to or higher than current methods.

In this thesis, DPI instrument shown in figure 1.25, was used to determine DNA behaviour on carboxylic acid surfaces prepared on DPI chips and results are presented in chapter 5.

Figure 1.25 Photograph of DPI Farfield set-up.

1.10.7 Quartz Crystal Microbalance

To investigate molecular interactions without the use of reporter labels, it is necessary to couple a molecular recognition element (e.g. an antibody or target receptor) to a transducer that converts a chemical or biological interaction into an electrical signal. The definition of a biosensor can be interpreted as a unique combination of a receptor for molecular recognition and a transducer for transmitting the interaction information into an electrical signal. In turn, a transducer is more specifically defined as a device for converting energy from one form to another for the purpose of measurement of a physical quantity or for information transfer. The use of acoustic waves is one of the most appropriate direct transduction mechanisms, because the parameters that describe the wave propagation (e.g. wave velocity) depend on the properties of the propagating material [94,95].

Quartz crystal microbalance (QCM) instrument, figure 1.26, it is a biosensor that allows label- free and real-time detection of biomolecules in liquid through the change in resonance frequency of a quartz-plate oscillator [96]. Q-Sense instruments also measure dissipation, which provides information about the structure and viscoelasticity of the sensor surface adhering film.

43
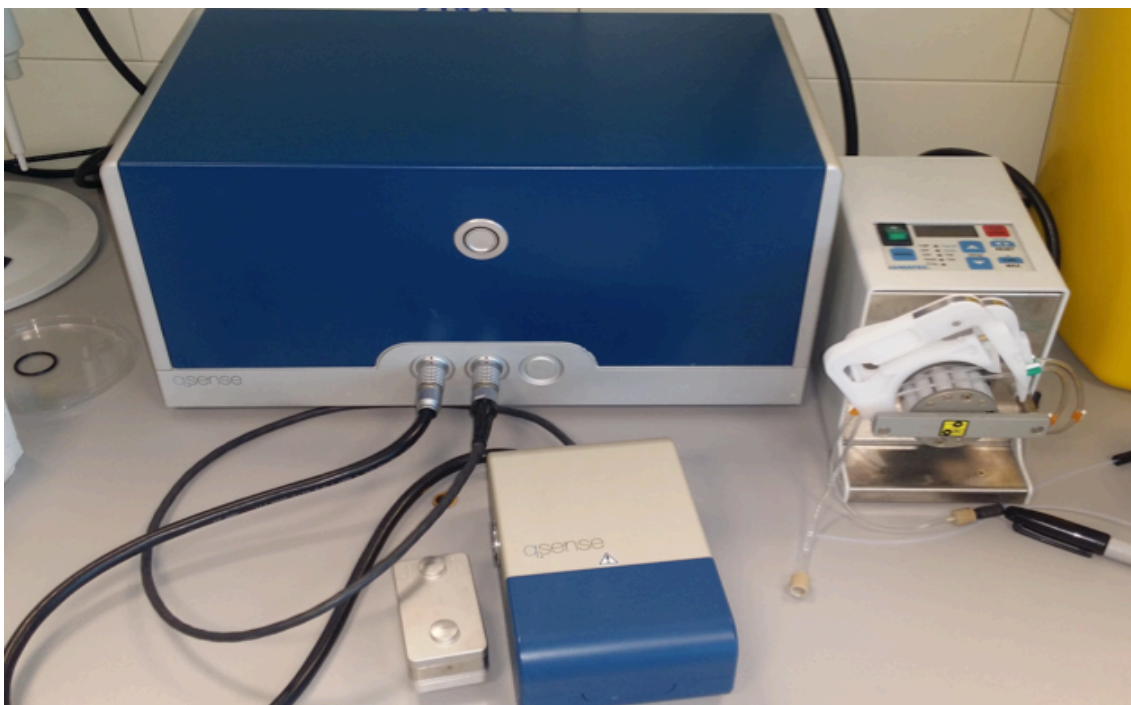
Figure 1.26 Photograph of QCM set up, model: Q sense E1.

A fundamental aspect of QCM is a thickness shear mode (TSM) acoustic wave resonator, in which an AT-cut thin quartz disk (i.e. a disk cut from a quartz mineral at a 35.25° orientation to its optical axis) is sandwiched between two metal electrodes, typically made of gold, figure 1.27. As a result of the piezoelectric nature of the quartz material, the application of an alternating electric field produces a shear (tangential) deformation. Upon deformation, both surfaces move in parallel but opposite directions, being thus motion antinodes, thereby generating acoustic waves that propagate through the bulk of the material across the crystal, in a direction that is perpendicular to the surface, and with wavelengths that are multiple factors of double the thickness of the substrate (tQ) [97].

A very common use of QCM is as a mass sensor, often in determination of thin-layer thickness or in gas sorption studies [98]. It can also be used as a chemical sensor if the surface of the microbalance is pre-covered in a chemically-sensitive layer.
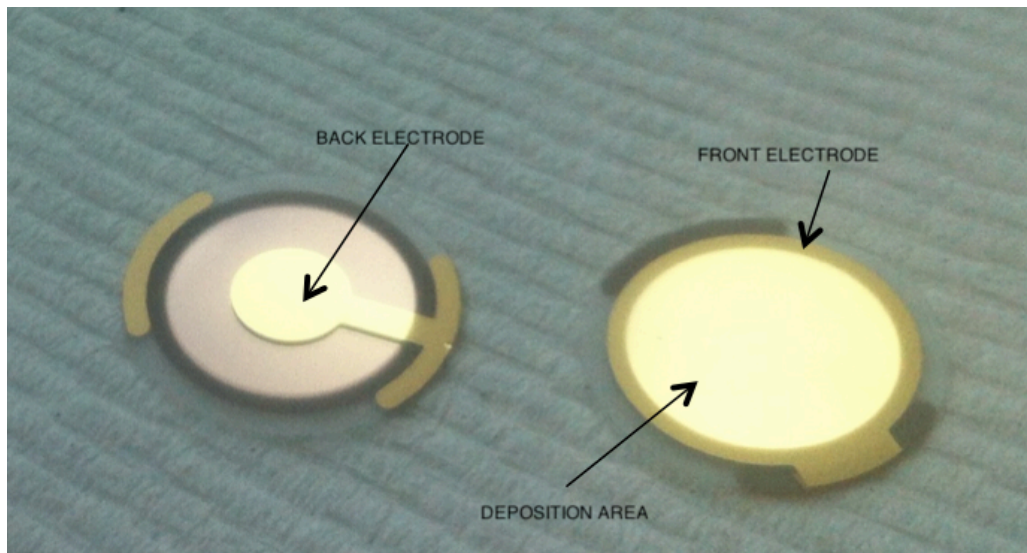
Figure 1.27 Photograph of typical quartz crystal resonators as used for QCM, metalized with gold electrodes (left: back electrode, right: front electrode).

The Sauerbrey equation establishes a linear relationship between resonant frequency and small mass increments (see below) [99].

$$\Delta f = - \frac{2 f_0^{\,2}}{A \sqrt{\rho_q \mu_q}} \Delta m$$

f_0 Resonant frequency (Hz)

Δf Frequency change (Hz)

Δm Mass change (g)

A Piezoelectrically active crystal area (Area between electrodes, cm^2)

ρ_q Density of quartz ($\rho_q = 2.643$ g/cm^3)

μ_q Shear modulus of quartz for AT-cut crystal ($\mu_q = 2.947 \times 10^{11}$ g·cm^{-1}·s^{-2})

The Sauerbrey equation makes the assumption that the mass deposited or the film formed at the surface of the crystal follows the vibration of the crystal and therefore the loaded crystal would simply behave as if it were thicker. The effective wavelength of the crystal is thus increased and consequently its resonant frequency decreases. This model assumes that no energy dissipation occurs and will thus only be valid for thin, rigid and uniform films that have similar acoustic properties as those of the bulk crystal material [99].

Piezoelectric transduction enables a label-free detection of bio-recognition events and typically is used in micro-gravimetric devices, generally known as QCM, in a variety of different applications, such as monitoring and characterisation of (bio) film deposition, detection of specific antigens, biomolecule binding kinetics, cell adhesion, and DNA detection. The QCM is a highly sensitive instrument, which determines the nature of binding interactions in real time within a label free environment [99].

Results from QCM measurements carried out to quantify the amount of ssDNA probe immobilised onto the different surfaces are presented in chapter 4. The total amount of DNA (in nanograms) per unit of 1 cm^2 at a given DNA molecular weight can be calculated according to the Sauerbrey equation [100]. The value of DNA mass (ng/cm^2) can be further converted into the amount of molecules per cm^2 using Avogadro's number and molecular weight of DNA.

1.10.8 Total Internal Reflection Ellipsometry

Total Internal Reflection Ellipsometry (TIRE) combines the assets of both spectroscopic ellipsometry and surface plasmon resonance (SPR) techniques. Therefore, it has a significant advantage due to simultaneous measurements of two ellipsometric parameters, C and D, which are related to the amplitude and phase shift of p- and s-components of polarized light respectively. This gives the possibility to analyse time dependent changes of amplitude C(t) and phase D(t) during the immobilisation of biomolecules on the solid–liquid interfaces and/or interaction of immobilised biomolecules with an analyte present in the solution. Figure 1.28 illustrates the hardware used in this research work.
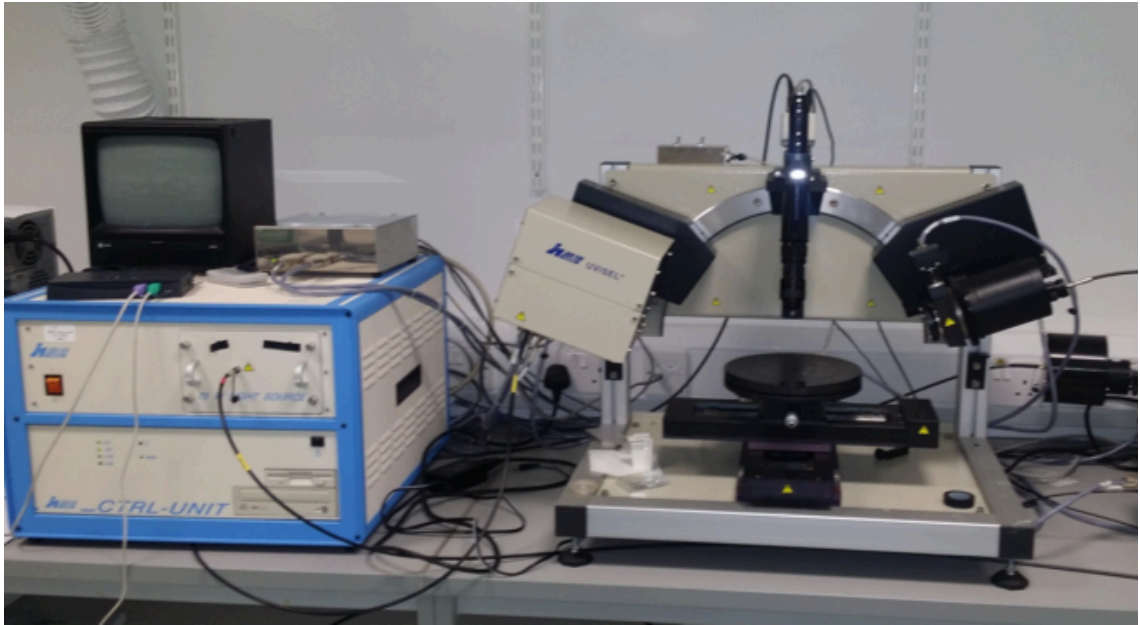
Figure 1.28 Photograph of TIRE setup.

TIRE is a suitable method to obtain a precise refractive index and thickness of the formed layers. For this reason TIRE has the potential to be a powerful tool for in situ monitoring of protein/ DNA adsorption process [101–105]. It utilises 5 main chambers, which can be used to perform 5 separate experiments. The syringe pump is attached to one end, which enables liquid flow at desired speed; the outlet goes out to waste. Prism, see figure 1.29, is in optical contact with the flow cell, which is a glass slide with a thin gold layer (c. 40 nm gold layer).
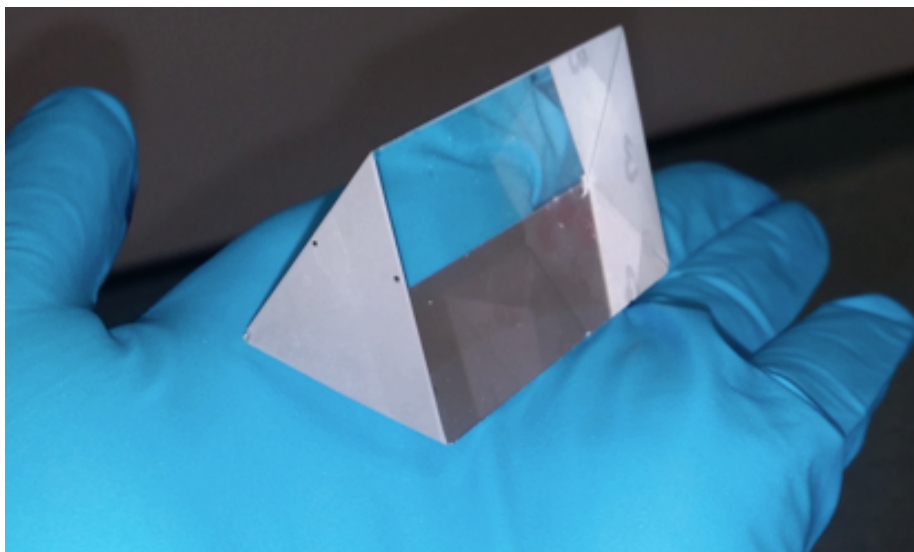
Figure 1.29 BK7 prism used in TIRE set up.

Liquid flowing via chambers in the cell may cause changes in thickness, roughness or other properties of the layer, especially with DNA probes being immobilised to the surface. The optical conditions will change at the interface, which can be monitored as changes in the ellipsometric angles ψ and Δ [101], figure 1.30. Results from the TIRE analysis are presented in chapter 5.
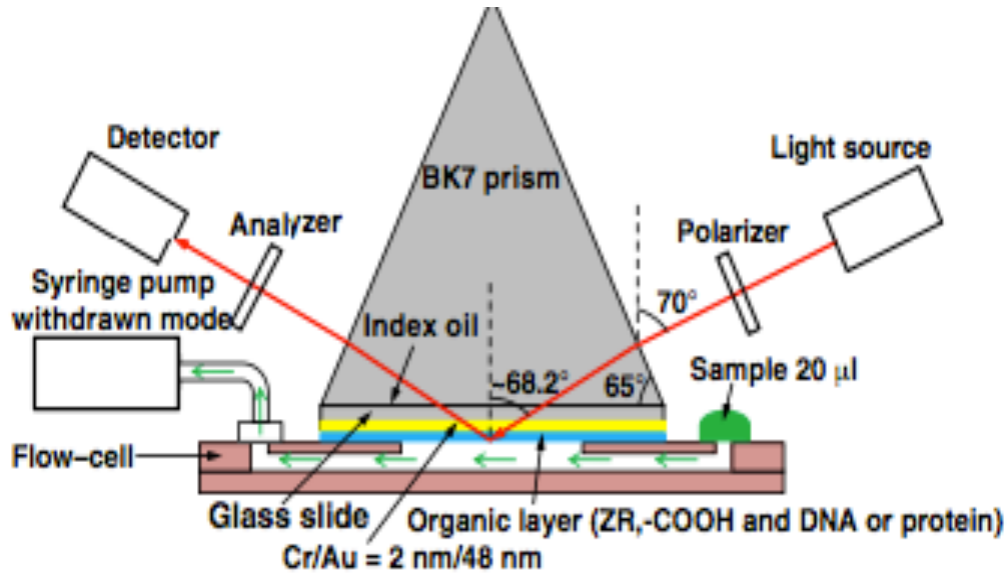
Figure 1.30 Schematic of TIRE experimental setup (not to scale) fitted on a UVISEL spectroscopic ellipsometer and a Harvard apparatus syringe pump [103].

TIRE measures two ellipsometric angles Ψ and Δ, versus wavelengths [101]. These Ψ and Δ values are defined by the ratio ρ of the reflection coefficients Rp and Rs for components of light polarized parallel and perpendicular, respectively, to the plane of incidence following the ellipsometry equation:

$$\rho = \frac{Rp}{Rs} = \tan \psi \exp (i\Delta)$$

$\rho = \dfrac{R_p}{R_S}$ complex quantity; ratio of Rp and Rs

$\tan \psi$ amplitude ratio upon reflection

Δ phase shift (difference)

Ψ and Δ also depend on the angle of incidence (Φ) and wavelengths (λ). The refractive indices and thicknesses of each layer of the reflecting surfaces can be found by fitting the measured Ψ and Δ data to a defined model [101,103].

1.10.9 UV/O$_3$ and oxygen plasma

In this work, UV/O$_3$ and oxygen plasma are techniques used to activate carboxylic acid groups on PMMA spin coated substrates to form ox.PMMA. Figure 1. 31 shows an instrument used for UV/O$_3$ activation of substrates and figure 1.32 shows an instrument used for oxygen plasma activation of substrates. Comparison results of both techniques are presented in chapter 3.
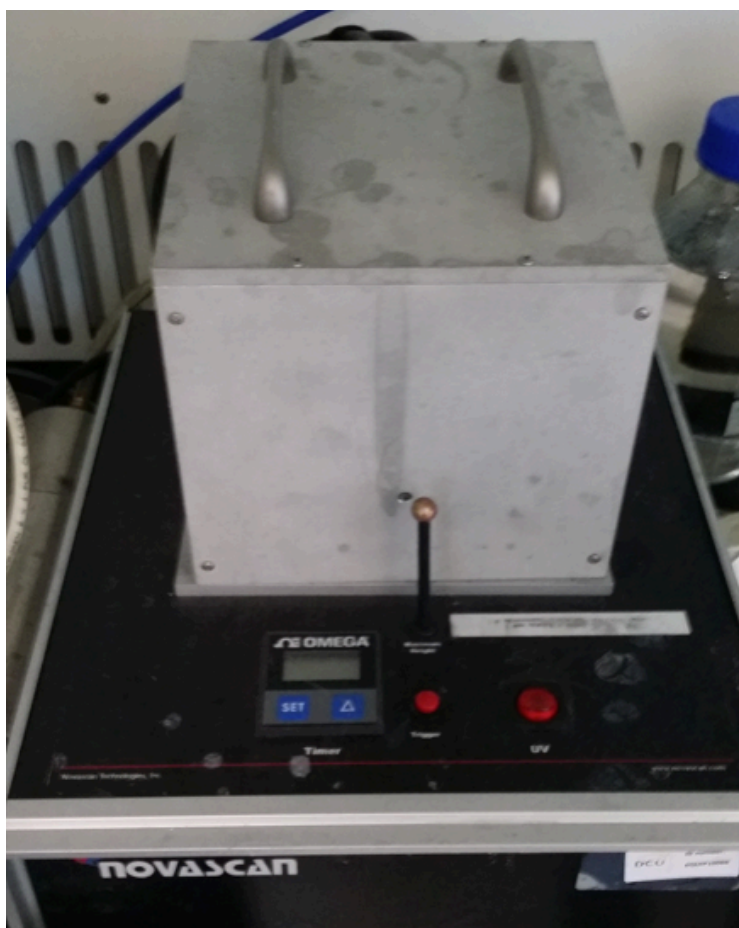
Figure 1.31 Ozone cleaning and activation system - PSD-UV, Novascan Technologies used for activation on PMMA surfaces.

Figure 1.32 Oxford Instruments Plasmalab 100 PECVD system used for direct plasma activation of substrates.

1.10.10 Spin coating

Spin coating can be described as a procedure applied to deposit uniform thin (more than 200 nm) or ultrathin (less than 200 nm) to flat substrates, such as glass, polymes etc [106,107]. A small droplet of material used to coat is usually placed in the centre of the substrate and spin speed is applied, which results in substrate being rotated at high speed. The rotation of the substrate helps spread the coating material by centrifugal forces [108]. Time, concentration of the coating material and rotation speed have an effect on thickness of the spin coated film [3]. Spin coating has wide applications in micro-fabrication of oxide layers using sol-gel precursors and in photolithography to create thin and uniform thicknesses at nano-scale [109]. In this work spin coating is used to produce ultrathin layers of PMMA [3], which are further activated and are used as a functionalised film for bioassays and will be detailed in chapter 2 and 3. Figure 1.33 shows a spin coater used.

Figure 1.33 Photograph of WS-400A-6NPP/LITE spin coater.

The housing of this system is made from a solid co-polymer, which is able to resist solvents and strong acids and bases. Liquids and gases are efficiently controlled, by the special design of the unique internal bowl-shaped chamber with its bottom gutter and clear dome lid. The chamber is electrically interlocked so rotation and dispensing are disabled when opened and latched, and locked until finished with 0 rpm is sensed.

1.10.11 Ultraviolet – visible Spectroscopy

Ultraviolet – visible (UV – vis) Spectroscopy is based on use of light in the visible and adjacent ranges. The perceived colour of the liquid/chemical used is directly affected by the absorption/reflectance in the visible range. Molecules undergo electronic transition in this particular region of the electromagnetic spectrum [110]. UV-vis spectroscopy is applied in analytical chemistry for the quantitative determination of different analytes. In this study UV-vis spectroscopy was used for performance of toluidine blue experiment. Figure 1.34 shows a schematic of UV – vis spectroscopy and figure 1.35

shows the spectrophotometer instrument used. Results from UV – vis spectrometer are presented in.
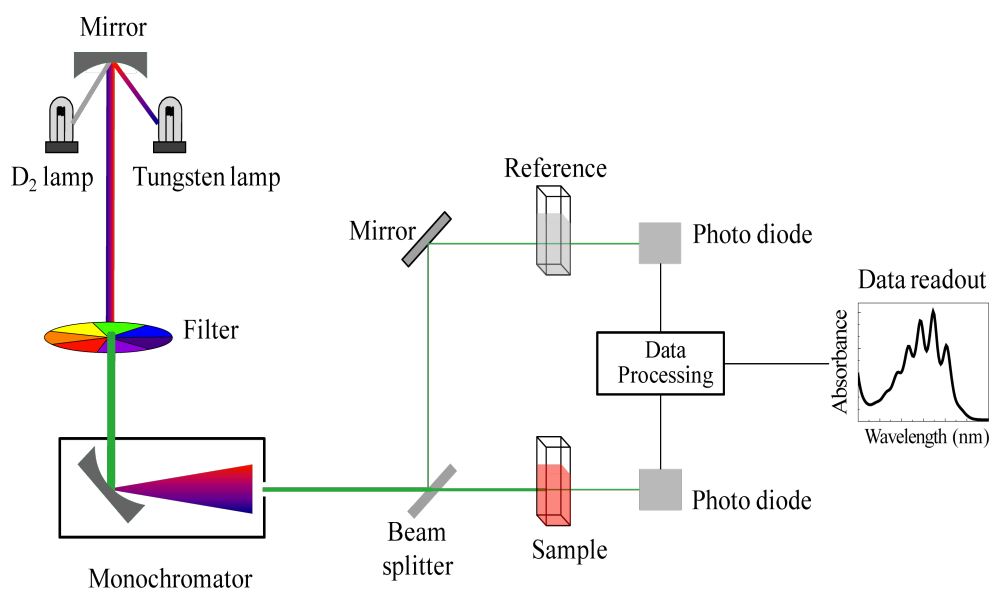
Figure 1.34 Schematic of UV-vis spectrometer.

Figure 1.35 Evolution 60S UV-Visible Spectrophometer instrument used in this research work.

1.11 Thesis objectives

This thesis sought to address a number of different scientific questions.

First, how to fabricate functionalised substrate support to be used in bioassay for the detection of biomolecules, such as breast cancer (BC) specific biomarker *miR195?* Panel of –COOH supports were tested: ox.PMMA, TEOS/AA, mercaptoundecanoic acid self assembly monolayer, succinic anhydride, alkyne modified ox.PMMA surface and APTES as an amino surface.

Second, how can the overall BC assay hybridisation efficiency be improved? Ox.PMMA was used as a support and the use of novel immobilisation technique – click chemistry (CC) was introduced. The specificity of the CC reaction is not temperature depend, while EDC is only specific at higher temperatures.

Third, based on these research findings, can a sandwich assay on modified surface with revised conditions in order to detect BC-specific *miR195* DNA be optimised? Assays were performed on ox.PMMA with incorporation of CC linker to improve assay efficiency; including specificity and sensitivity. CC is more suitable for point-of-care devices, as the CC-enabled assays can be performed at room temperature with greater hybridisation efficiency.

Finally, can an alternative detection method for miRNA for an early BC diagnosis be developed? An attempt was made to use label free method to detect BC specific biomarker, based on quenching phenomenon.

The above are described in distinct chapters and it is believed that they will have an impact on the future research and applications in the biosensor research field.

Chapter 2

2 Development and characterisation of novel functionalised surfaces for DNA biomolecule attachment

2.1 Introduction

This chapter includes description of development and characterisation of panel of newly designed functionalised solid supports, which can further be adapted and suitable for DNA bio-conjugation.

Relationship between solid support and biomolecules attachment are of a paramount importance in biosensor development. The main aim is to develop coating that is:

- robust,

- easy to prepare and

- promotes only specific biomolecule binding.

Here, a panel of –COOH films prepared with different methods, which are further characterised, is explored. A novel ox.PMMA film preparation is introduced, which meets all the above requirements [3]. Advantages of ox.PMMA and additional tests are included in chapter 3.

Numbers of different techniques are available for the synthesis of various functionalised films on solid supports for the purpose of DNA immobilisation for bioassays. Among these, wet chemistry APTES depositions on Zeonor® slides or TEOS/AA slides are the common ones used by researchers. This work explores the fabrication and evaluation of specific surfaces, including carboxylic acid and amino depositions. In this chapter, the recipes and production methods as well as morphological, structural and functional characterisation of deposited films are investigated in detail using a number of different techniques.

Here is the list of developed surfaces:

- Tetraethyl Orthosilicate/Acrylic acid (TEOS/AA)

- APTES

- SAM, MUA on gold and on other substrates

- Succinic Anhydride

- Spin coated (oxidised) PMMA

- Alkyne modified ox.PMMA surface.

The paragraph lists and describes the techniques used in this study including:

- water contact angle,

- ellipsometry

- atomic force microscopy

- the toluidine method (TB method).

Tetraethyl Orthosilicate **(TEOS)** has become popular in the research community as a source of silicon for PECVD systems, especially in the case of SiO_2 thin film depositions. It is mainly used as a crosslinking agent in silicone polymers and as a precursor to silicon dioxide in the semiconductor indstry [111]. TEOS $(Si(OC_2H_5)_4)$, figure 2.1, is a silica (Si) atom with four ethoxy groups attached, which are liable (easily displaced from the Si atom) also called Orthosilicate [112] .
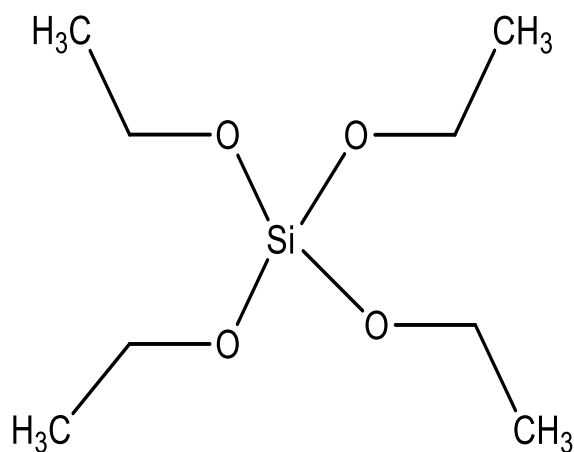
Figure 2.1 Chemical structure of TEOS.

Acrylic acid **(AA)** is an organic compound; consisting of a carboxylic acid terminus and a vinyl group ($CH_2=CHCOOH$), figure 2.2. AA has been used for years in the production of a range of compounds, such as polyacrylates and acrylic esters. AA can be deposited by PECVD and it creates a layer of carboxyl groups (-COOH), which can be activated to interact with the NH_2 amine group present on DNA. The advantage of AA-based carboxyl layers is the ability to remain functional after interaction with water (e.g. unlike epoxy). This characteristic is very favourable for diagnostic devices, which are often subjected to various washing and protein immobilisation stages [113–115].
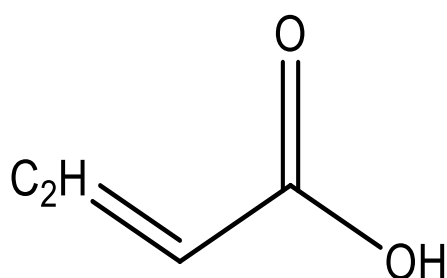
Figure 2.2 Chemical structure of Acrylic Acid.

Films formed as a result of sequential, plasma assisted fragmentation and deposition from vapours of AA and TEOS have very special properties. Some of the properties of TEOS include the ability to adhere to the plastic substrate and also to act as a network building layer for further cross-linking with AA, the sequential plasma deposition

resulting in a film of composition graded from inside to outside. Due to the presence of silanols (Si-OH) a large uptake of water molecules is possible. The above characteristic leads to significant hydration of the layer, which in combination with high total negative charge lowers the non-specific binding of biomolecules. Furthermore, the specific combination of TEOS and AA significantly increases the proportion of carboxyl groups in the layer, above that found from deposition of AA alone. As reported by other member of our group, the deposited layers were found to exhibit low non-specific binding for negatively charged particles and biomolecules and high binding capacity for specific functionalisation [116].

Aminopropyltriethoxysilane **(APTES),** figure 2.3, is chemically stable organosilane, which has been widely adopted in the creation of amino functionalised surfaces for use in biomedical environments, i.e. implants and sensing devices. It is easily covalently bound to prepared surfaces through silanisation, which involves the hydroxyl groups present on the substrate essentially attacking and displacing the alkoxy (ethoxy) groups of the APTES, creating covalently bound –Si-O-Si- matrices [117].
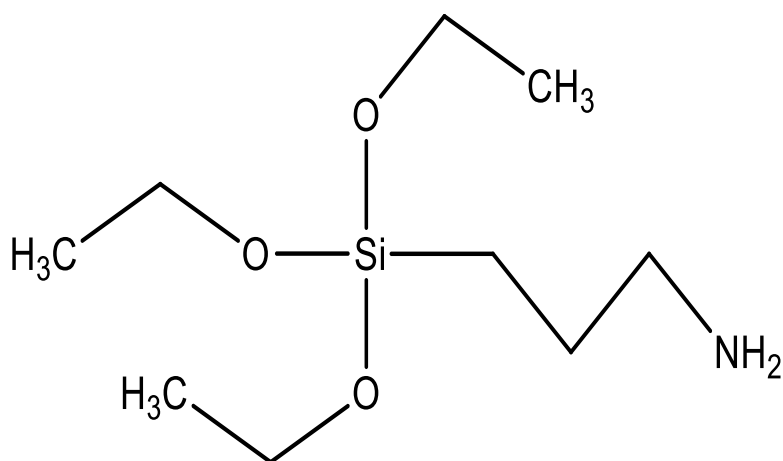
Figure 2.3 Chemical structure of Aminopropyltriethoxysilane (APTES).

Organic self-assembled monolayers **(SAMs)** are of great importance in surface technology since the presence of chemically bound molecules renders the properties of an interface entirely different compared to those that are unmodified. SAMs are typically formed by exposure of solid substrates to amphiphilic molecules with chemical groups that exhibit strong affinities for the substrate. Gold is the most frequently used metal because it does form a stable oxide layer under ambient conditions and potentially provides a reproducible, convenient, and robust method with which to incorporate functionality at the surface in a chemically and physically well-defined way [118].

$$HSCH_2(CH_2)_8CH_2 \overset{O}{\underset{\|}{C}} OH$$
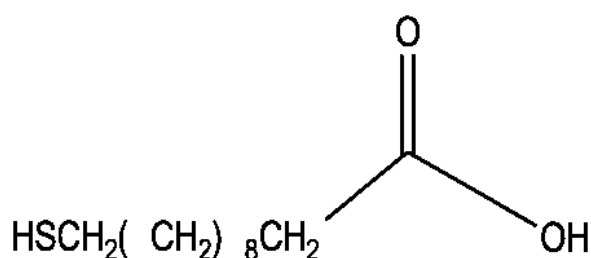
Figure 2.4 Chemical structure of 11-Mercaptoundecanoic acid (MUA).

MUA is a long backbone chain with carboxyl (-COOH) and thiol (-SH) end groups, figure 2.4. The thiolated end binds covalently to gold, forming a monolayer of carboxyl groups, see figure 2.5.

58
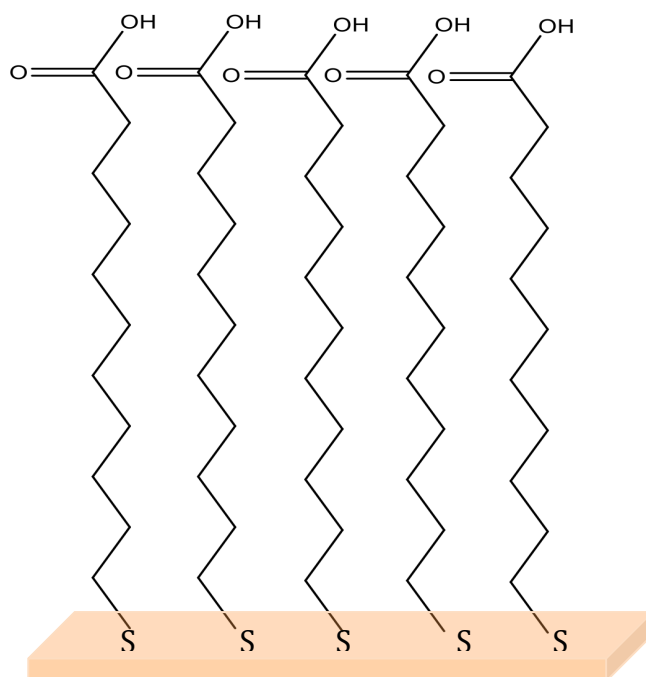
Figure 2.5. Chemical representation of MUA SAM monolayer.

Due to the presence of the thiol end group, MUA naturally binds to gold substrates. In the case of other substrates, cross-linking is required. DPI experiments were performed to investigate DNA behaviour on MUA. The purchased DPI chips are made of silicon oxide rather than gold/ gold-coated and therefore they were required to be modified. The procedure involved the use of sulfo-SIAB, a water-soluble, mid-length (10.6 angstrom) cross-linker for amine to thiol conjugation via sulfo-*N*-hydroxysuccinimide (sulfo-NHS) ester and iodoacetyl reactive groups, figure 2.6.
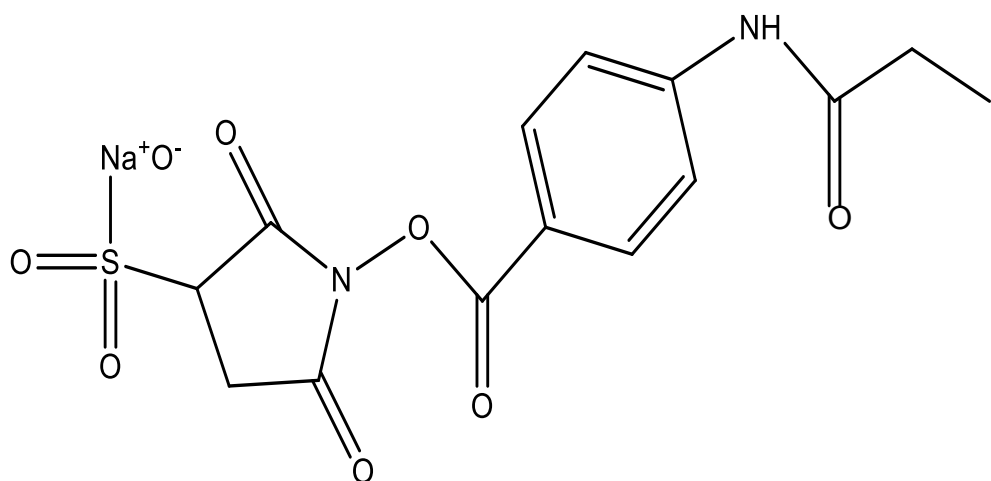
Figure 2.6 Chemical structure of sulfo-SIAB.

Succinic anhydride **(SA)**, also called dihydro-2,5-furandione, is an organic compound with the molecular formula $C_4H_4O_3$, figure 2.7. This colourless solid is the acid anhydride of succinic acid.
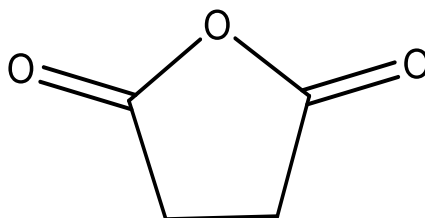
Figure 2.7 Chemical structure of SA.

SA was used as -COOH surface for DNA behaviour investigation. Direct binding of SA to the DPI chip is not straightforward; hence APTES was used as an immobilisation layer.

Spin coating is used widely for depositing thin polymer layers on flat solid substrates [107,108,119–125]. Poly(methyl methacrylate) (PMMA) is a thermoplastic single-copolymer (homopolymer) which has applications in electron beam (EBL) and scanning probe lithography (SPL) as a positive or negative resist (at high enough doses) due mainly to its highest resolution among conventional organic electron beam resists [106]. It is also an attractive material for the fabrication of low-cost micro-total analysis systems (m-TAS) since it possesses excellent optical, thermal, chemical and biocompatible properties [126]. Spin-coated PMMA is utilised as a thin film commonly used as resist films in micro/nanofabrication processes [106]. If the specific and appropriate treatment of its surface is applied, PMMA can be functionalised/modified to enable the covalent attachment of biomolecules for bioassay development [126–128], figure 2.8.

poly(methyl methacrylate)   ox. poly(methyl methacrylate)
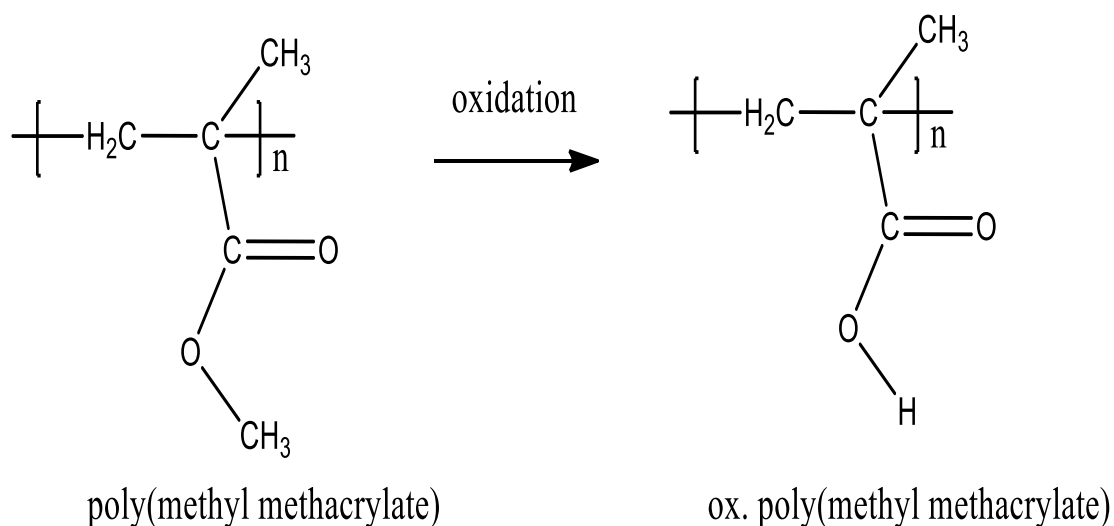
Figure 2.8 Poly(methyl methacrylate) after oxidation to form ox.PMMA.

Further analysis and characterisation of the two chosen films: TEOS/AA and ox. PMMA was carried out, as two of them have the biggest potential to be used in future biosensor development. Both of them proved to have multiple advantages over the state of the art. PMMA can be prepared by wet chemistry and TEOS/AA is prepared by PECVD, both techniques are not time consuming and allow preparation of a large number of samples at once. Both processes allow functionalisation of different substrates, such as plastic or glass, unlike MUA, which requires a gold substrate. AFM analysis was used to compare smoothness and overall topography of both surfaces. Both surfaces proved to be smooth with no significant features. Both surfaces were also tested in terms of robustness against multiple washings. From the above analysis it was determined that ox.PMMA is covalently anchored to the surface, where with TEOS/AA it is not the case. The hypothesis was made, that the surface anchoring method fails and TEOS or AA is being washed away along with the probes attached to it. In order to verify the above, the ox. PMMA surface was tested. Our hypothesis has been confirmed; the signal of DNA probe adsorbed covalently to the surface remains the same regardless of the wash on ox.PMMA, while with TEOS/AA signal of DNA probe adsorbed decreases gradually with each additional wash.

Finally with collaboration with another researcher from our group, the best-known method (BKM) for TEOS/AA deposition by PECVD was determined. For this, the toluidine blue method, complemented by ellipsometry to measure the deposited film thickness and water contact angle instrument to measure the hydrophobicity of film, were used. TB is a dye, which binds specifically to –COOH groups, which was utilised

as an additional technique to characterise some of the substrates. TB test gives an average of –COOH groups on a surface. TB is a suitable qualitative method to confirm the presence or absence of active –COOH groups on the surface. Due to this fact, TB has been used as an additional test to ellipsometry to measure deposited film thickness and water contact angle technique to measure the hydrophobicity of a film in the development of a BKM for TEOS/AA by PECVD. A conclusion has been drawn based on the collective results in this chapter, that ox. PMMA is the most suitable surface and it is further explored in chapter 3.

2.2 Experimental details

In this study, preparation of novel functionalised surfaces to be suitable for DNA assay development is described. Prepared surfaces are being analysed and the results are compared amongst them all. Two the most suitable surfaces are chosen, based on advantages and disadvantages, listed in this chapter.

Additionally a BKM for TEOS/AA depositions by PECVD is being determined.

2.2.1   Materials and instrumentation

PMMA sheets (0.25 mm thick, impact modified, MW ¼ 120 000) were sourced from Goodfellow Cambridge Limited (Huntingdon, England). Zeonor® substrates, injection-molded cyclic olefin polymer (COP) slides (Zeonor® 1060R, 25 mm x 75 mm, 1 mm thick) were sourced from Sigolis (Uppsala, Sweden). Gold-coated standard glass microscope slides (Ti/Au, 5 nm/30 nm, 25 mm x 75 mm, 1.1 mm thick) were sourced from PhasisSarl (Geneva, Switzerland). Universal microscope glass slides were sourced from VWR (Dublin 15, Ireland). PTFE filter (pore size 0.25 μm) (Chroma-filXtra PTFE-20/25 Macherey-Nagel, Duren, Germany) 1-Ethyl-3-(3- dimethylaminopropyl) carbodiimide (EDC), 2-(N-morpholino) ethanesulfonic acid buffer (MES), sodium dodecyl sulfate (SDS), saline-sodium citrate (SSC), 11 Mercaptoundecanoic acid 95 % (MUA), Succinic anhydride ≥ 99 % (GC), Toluidine Blue O and toluene (anhydrous, 99.8 %), Tetraethyl orthosilicate (TEOS/AA) reagent grade 98%, (3 – Aminopropyl)trethoxysilane (≥98%) were purchased from Sigma Aldrich (Arklow,

Ireland). TEOS/AA. Improved Super Cone tips for AFM were purchased from Team Nanotec. Amino-modified oligonucleotide DNA probes (5'-GCC-AAT-ATT-TCT-GTG-CTG-CTA-3') (miR-195 probe, 21-mer) and synthetic oligonucleotide target DNAs (5'-TAG-CAG-CAC-GTA-AAT-ATT-GGCG-3') (miR-16 target, 22-mer) with Cy3 label and without the label and (5'-TAG-CAG-CAC-AGA-AAT-ATT-GGC-3') (miR-195 target, 21-mer) with Cy3 label and without the label were sourced from Eurofins MWG Operon (Ebersberg, Germany). All chemicals were used as received without further purification.

Instrumentation used in support of this work in chapter 2:

- Spin coater
- UV/O_3 and O_2 plasma
- Ellipsometry
- Water contact angle instrument
- AFM
- UV-vis

2.2.2 Preparation of Tetraethyl Orthosilicate/Acrylic acid (TEOS/AA) surface

TEOS/AA was deposited on Zeonor substrate with PECVD by in house technician. Figure 2.9 represents a sequential deposition of TEOS/AA.
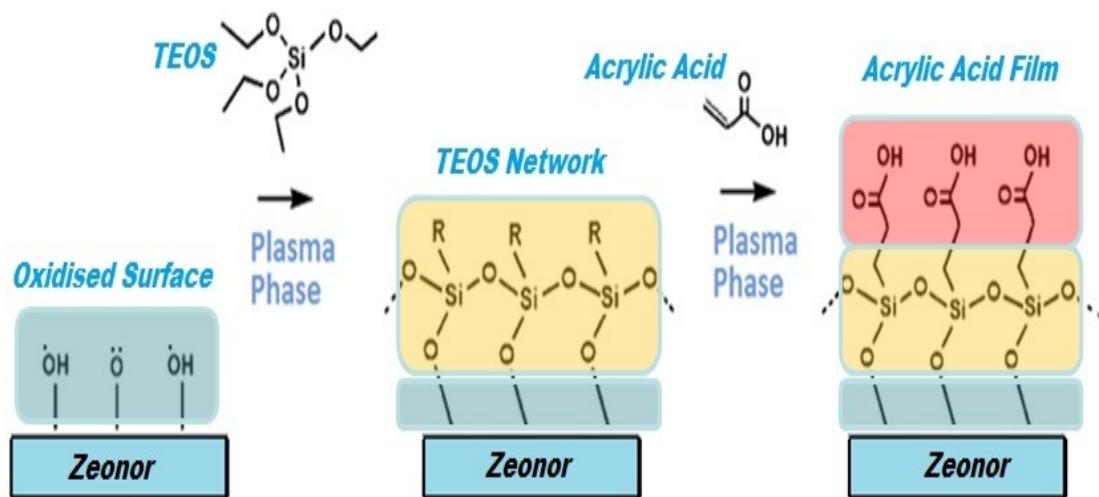
Figure 2.9 Sequential TEOS/AA deposition.

Image taken from Ruairi Monaghan's (DCU) thesis with his permission.

2.2.3   Preparation of 3-Aminopropyltriethoxysilane surface

APTES coatings by the PECVD method are prepared in house, see figure 2.10.
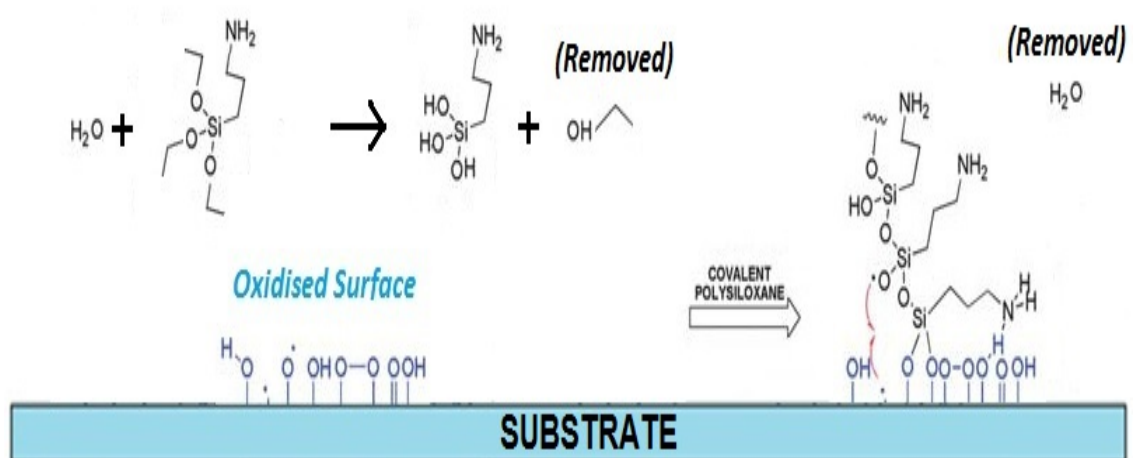
Figure 2.10: Diagram showing the silanization of APTES onto an oxidised polymer.

Image taken from Ruairi Monaghan's (DCU) thesis with his permission.

APTES can also be prepared by wet chemistry. The protocol for chemically depositing APTES is as follows:

- Substrate (glass, Zeonor, silicon) needs to be oxidised - either through oxygen plasma treating or other methods like UV-Ozone treatment
- Dip the freshly oxidized substrates in the deposition solution (92:5:3 mixture of isopropanol/ethanol, DI water, and APTES)
- Store the substrates for 2 hours at room temperature in solution
- Sonicate substrates in isopropanol for 15 minutes twice
- Rinse the substrates with isopropanol
- Bake the substrates in oven for 1 hour at 80°C (substrates may stick to holder during baking so care must be taken)
- Cool the substrates for 30 minutes at room temperature

Coated slides can then be stored as needed.

2.2.4 Preparation of 11-Mercaptoundecanoic acid, self assembled monolayer surfaces

SAM on gold were prepared as follows:

- Incubate gold substrates in freshly prepared thiol solutions (5mM) using ethanol for 12 h.
- After the formation of SAMs, rinse gold substartes with a copious amount of ethanol and DI water,
- Use stream of nitrogen gas to dry substrates.

Water contact angle was used as a confirmation test of the successful depositions and should be around 55°.

2.2.5 Preparation of 11-Mercaptoundecanoic acid (MUA) on substrate other than gold

Use of MUA on substrates other than gold requires introduction of a linker. Protocol of preparing MUA on DPI chips (silicon oxide) is as follows:

- The DPI chips were coated with liquid APTES (see section 2.2.3.)
- DPI chip coated with liquid APTES is submerged in sulfo-SIAB (5 mM) solution prepared with PBS (pH 6.5) for 30 minutes to let amine-to-thiol conjugation
- Substrates then were washed with DI water and dried using stream of nitrogen gas.
- Modified surfaces in this manner were then ready for MUA incubation overnight (see section 2.2.4)
- After formation of the SAM, substrates were rinsed with a copious amount of ethanol and DI water, and finally dried using a stream of nitrogen gas.

2.2.6 Preparation of Succinic Anhydride surfaces

An adapted protocol [129] for SA immobilisation was used, see the protocol:

- Primary amino groups in APTES films were initially converted to carboxyl groups by incubation in THF containing 5 mg/ml SA and 5 % v/v triethylamine (TEA) for 4 hours
- Rinse with DI water.

Figure 2.11 represents SA preparation, including prior liquid APTES functionalisation followed by THF incubation.

Water contact angle was used as a confirmation test of the successful depositions as well as surface characterisation, and should be around 60-65°.
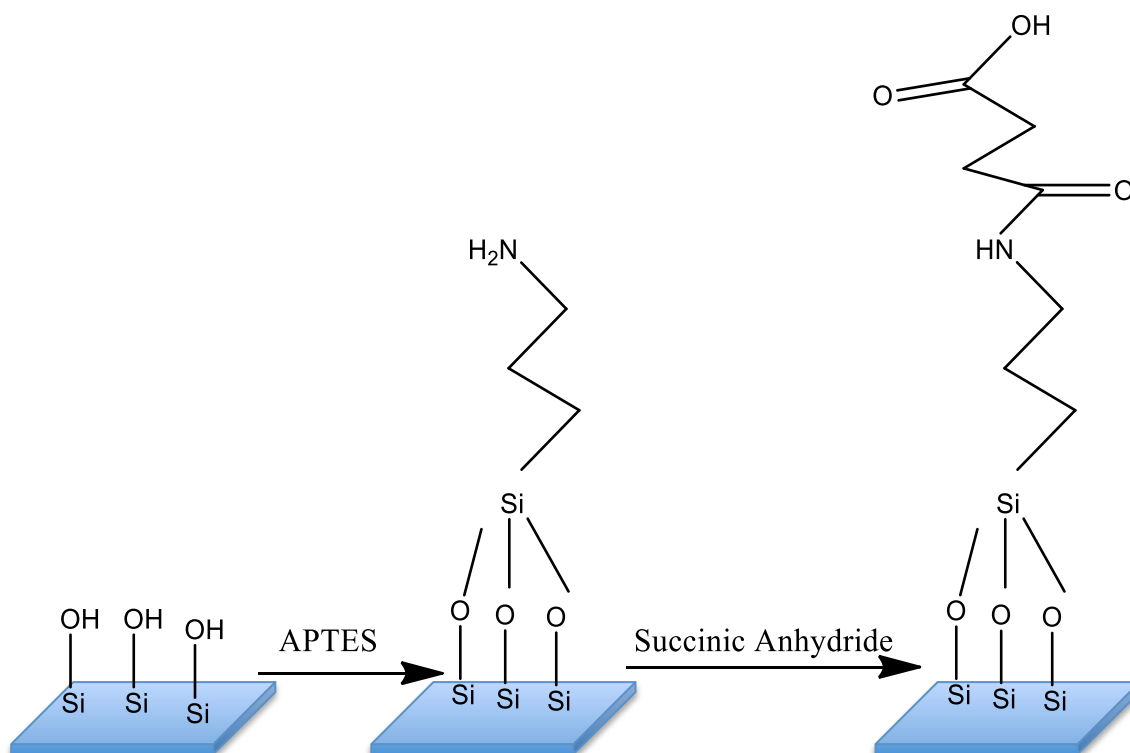
Figure 2.11 SA preparation, including prior liquid APTES functionalisation followed by THF incubation.

2.2.7 Preparation of spin coated poly (methyl methacrylate) surfaces

Protocol for preparations of spin coated PMMA is as follows:

- Take off protection film from the PMMA sheet
- Cut PMMA sheet into small pieces
- Weight out 0.001g, 0.002g, 0.005g of PMMA pieces for 0.1 %, 0.2 or 0.5 % PMMA concentration respectively
- Place into a glass vial with 10 ml of 80 % ethanol or toluene depending on the underlying substrate used (i.e. gold or Zeonor®) to result in 0.1 % PMMA concentration. Toluene dissolve Zeonor substrates, hence 80 % ethanol is recommended
- Use sonicator at 40 ° for 30 minutes to dissolve the PMMA pieces
- Filter dissolved PMMA through a PTFE filter (pore size 0.25 µm) to eliminate precipitates and dust particles. Cleaning of the substrates prior spin coating:
- Fill the tank with 2 % of Micro90 detergent for cleaning step

- Place the slides in a slider holder and submerge them in Micro90

- Sonicate for 30 minutes

- Rinse slides in water

- Fill another tank with isopropanol and submerge slides

- Sonicate for 30 minutes

- Rinse slides in water

- Dry with nitrogen stream

Spin coating of dissolved PMMA protocol:

WS-400A-6NPP/LITE spin coater, Laurell Technologies Corporation, North Wales, USA, figure 1.35, was the system used to spin coat ultra thin films of PMMA on substrates such as: glass, Zeonor®, gold and silicon, throughout this study.

- Place a slide at the centre of spin coater's holder

- Apply vacuum to immobilise the slide

- Place 1 ml of dissolved PMMA solution on the middle of the slide

- Set the settings: 3000rpm, 5 seconds acceleration for 1 minute

- Press start

- Take the slide off and transfer to a holder

The curing process protocol:

- The PMMA films are cured in an oven at 80 °C for 1 h or in the fume hood over night.

Oxidation of spin coated PMMA surfaces with UV/O$_3$:

UV/O$_3$ treatment was performed using a commercial ozone cleaning and activation system (PSD-UV, Novascan Technologies, Ames, IA, USA). According to the manufacturer specifications, at the 50 W power setting, approximately 50 % of the total lamp output power is delivered around the 254 nm peak and 5 % around the 185 nm peak. The optical power was kept constant but the treatment time was varied. A period of 8 minutes of UV/O$_3$ treatment was optimal for spin coated thin PMMA films. When the treatment time was too short, insufficient numbers of carboxylic functionalities were generated, while if the treatment time was too long, the thin PMMA film was etched away [130].

- Place cured PMMA samples (do not touch the interface, pick up by the edge of the slide) onto UV/O$_3$ device

- Initiate oxidation for 4-8 minutes as required

- Remove samples from the device

- Alternatively oxygen plasma can be used to activate the surface (4-8 minutes)

2.2.8 Preparation of alkyne-modified ox. PMMA surface

A novel type of surface has been developed during this study – alkyne functionalised ox. PMMA surface which is suitable for click chemistry DNA conjugation. Protocol is as follow:

- Ox. PMMA (see section 2.2.7) is modified; incubate for 40 minutesat room temperature with 1 % w/v solution of 1-amino-3-butyne with 100 mM EDC in DI water

- Following incubation, 20 minutes washing is applied: 10 minutes in 0.2XSSC + 0.1 %SDS and 10 minutes in 0.2XSSC to remove any residues. The chemical modification of ox. PMMA to Alkyne ox. PMMA surface is shown in figure 2.12.
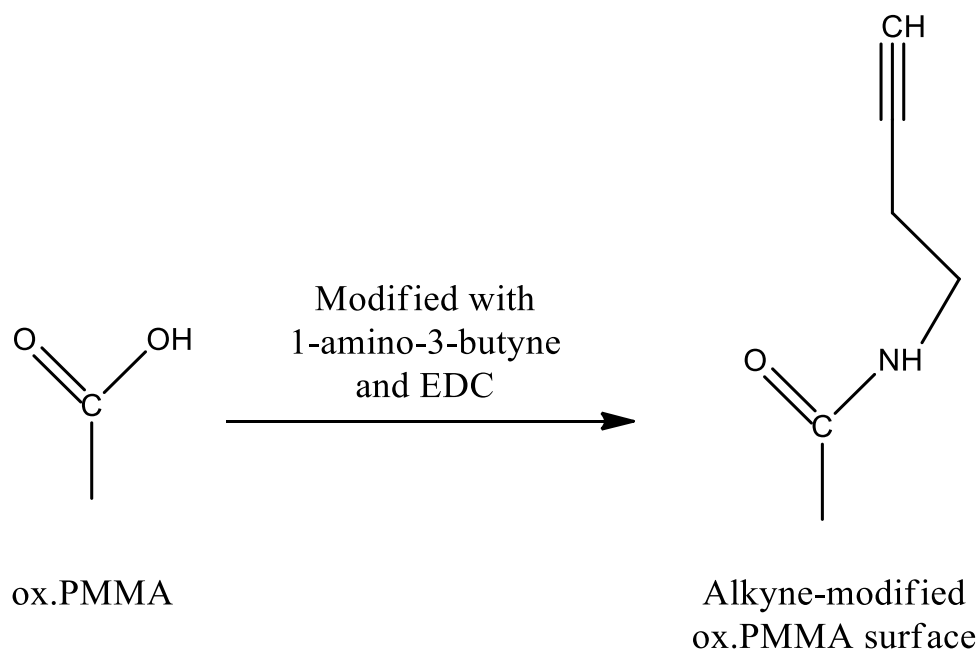
Figure 2.12 Chemical modification of ox. PMMA to Alkyne ox. PMMA surface

2.2.9 TB staining of carboxylic surfaces

Modified protocol [84]

- Using a 0.1mM NaOH solution, create a 0.1mM dilution of toluidine blue (0.0305g per 1L)

- Incubate substrates for 1 hour @ 40°C with 50ml of fresh toluidine blue solution

- Rinse surfaces using fresh 0.1mM NaOH to remove excess dye

- Incubate substrates in Acetic Acid: Water (50:50) solution for 30 minutes @ 40°C

- Solution can be measured using UV-Vis (absorbance 626nm – 635nm). Evolution 60S UV-Visible Spectrophometer, Thermo Scientific, Ireland, was the instrument used in this study. As stated by the manufacturer, this instrument acquires accurate spectra with scan speeds up to 4200 nm/min and its dependent on dual-beam optics in order to achieve superior photometric accuracy during long measurements. The measurements are acquired from the UV to the near-IR.

- Figure 2.13 shows a schematic and principles of the TB reaction.
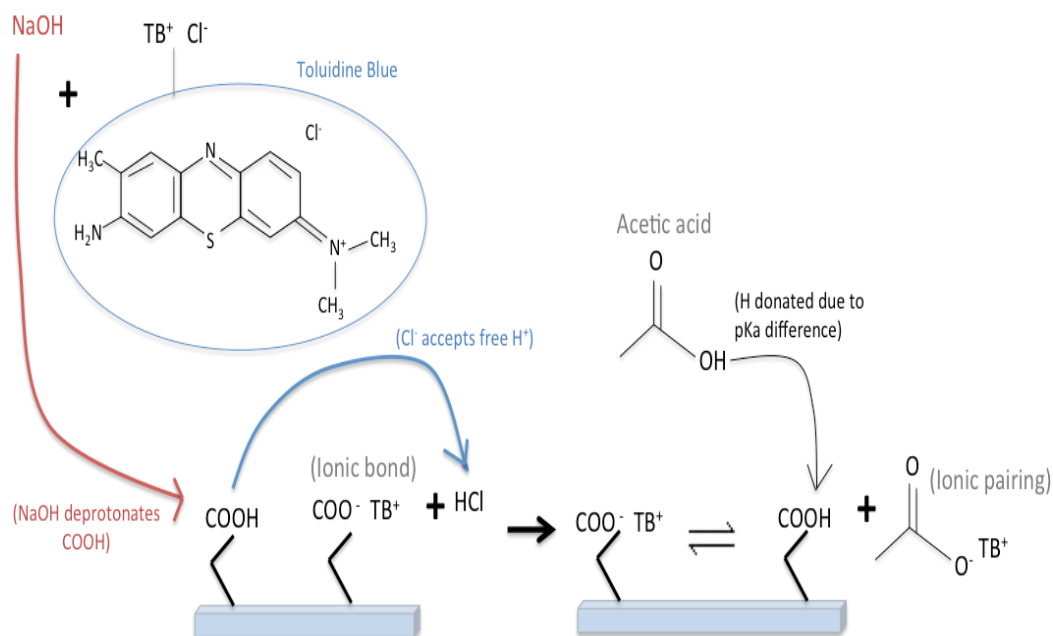
Figure 2.13 Schematic and principles of the TB reaction.

2.2.10 AFM analysis

- Substrate surfaces were examined using an atomic force microscope (AFM) on a Veeco Dimension 3100 instrument.
- The AFM was used in tapping mode using Tap300Al-G tips from Budget Sensors (Sofia, Bulgaria)
- High aspect ratio images were measured using Improved Super Cone tips from Team Nanotec; both tips had a resonant frequency of 300kHz and force constant of 40 Nm^{-1}.
- Images were analysed using WSxM software [131].

2.3 Results and discussion

This section shows results of determination of two most suitable surfaces for further analysis based on advantages and disadvantages while compared with other prepared surfaces. Further and more detailed analysis of the chosen surfaces is included in this paragraph. Additionally TB method is used in determination of the BKM for TEOS/AA.

2.3.1 Determination of two most suitable surfaces for further analysis

A number of different surfaces have been developed during this study. The analysis of all of them would be time consuming; hence the decision was made to choose two most suitable surfaces, which will be used for further analysis. Table 2.1 presents all surfaces developed describing advantages and disadvantages of the preparation process.

Ox.PMMA and TEOS/AA have been chosen as two most suitable surfaces (more advantages while compared with other surfaces). Both techniques are not time consuming and result in ultrathin and uniform carboxylic acid film. Analysis of ox.PMMA and TEOS/AA surfaces are performed in next sections.

Table 2.1 Advantages and disadvantages of the preparation process of various surfaces.

Type of surface	Advantages	Disadvantages
TEOS/ AA *(-COOH)*	• Reproducible • Time efficient • Uniform • Ultra-thin film • High throughput • No limitations to substrates used	• Requires PECVD, which may not be easily accessible
MUA *(-COOH)*	• Inexpensive and accessible reagents • No need for expensive equipment	• Extra step required if surfaces other than gold used • Time consuming • Poor uniformity
SA *(-COOH)*	• Inexpensive and accessible reagents • No need for expensive equipment	• Poor reproducibility • Poor uniformity • Laborious • Time consuming
Ox.PMMA *(-COOH)*	• Ultrathin film • Uniform • Reproducible • Time efficient • Inexpensive reagents • Production in bulk • No limitation to substrates used	• Need access to equipment such as: sonicator and spin coater
APTES (-NH$_2$)	Used as a control	

2.3.2 Analysis of chosen surfaces: PMMA and TEOS/AA

PMMA and TEOS/AA films have been chosen for further analysis, as two of them have the biggest potential to be used in future biosensor development, based on adaptability of production process. Both of them proved to have multiple advantages over other developed surfaces. Ox. PMMA can be prepared by wet chemistry and TEOS/AA is prepared by PECVD, both techniques are not time consuming and allow preparation of a large number of samples at once. Both processes allow functionalization of different substrates, such as plastic or glass, unlike MUA, which requires a gold substrate or an additional step if substrate other than gold is used.

First AFM analysis was used to compare smoothness and overall topography of both surfaces. The aim was to obtain as smooth film, c. less than 8nm. Dimensions of single stranded DNA probes are approx. 8nm x 1.5nm [126], when fully stretched. However probes are not rigid as double helix, but are as flexible as a strand of a hair. That is why the smoothness of the surface is of paramount importance, to prevent DNA strand get buried between peaks and valleys of the rough surface. This could have a negative effect on orientation and availability of the DNA for further hybridisation [100]. Figures 2.14 and 2.15 show AFM images of substrates such as glass, Zeonor® and TEOS/AA washed and unwashed films and plain/ox. PMMA. Glass and Zeonor® were washed prior deposition in a 2 % Micro90 solution in an ultrasonicator for 30 minutes, rinsed with DI water and ultra-sonicated for a further 30 minutes in Isopropanol and blow dried with N_2. This washing is applied to any new substrate samples prior to deposition to avoid any contamination or residues left during fabrication, packaging or transportation. Despite an extensive washing prior AFM analysis, there have been some artefacts observed, see figure 2.14 and 2.15. They could represent some dust particles, as the measurements are not taking in a clean room environment.

73

Substrate-
Washed plain Zeonor®   Unwashed TEOS/AA   Washed TEOS/AA

Substrate-   Plain PMMA on glass   Ox. PMMA on glass
Washed glass only
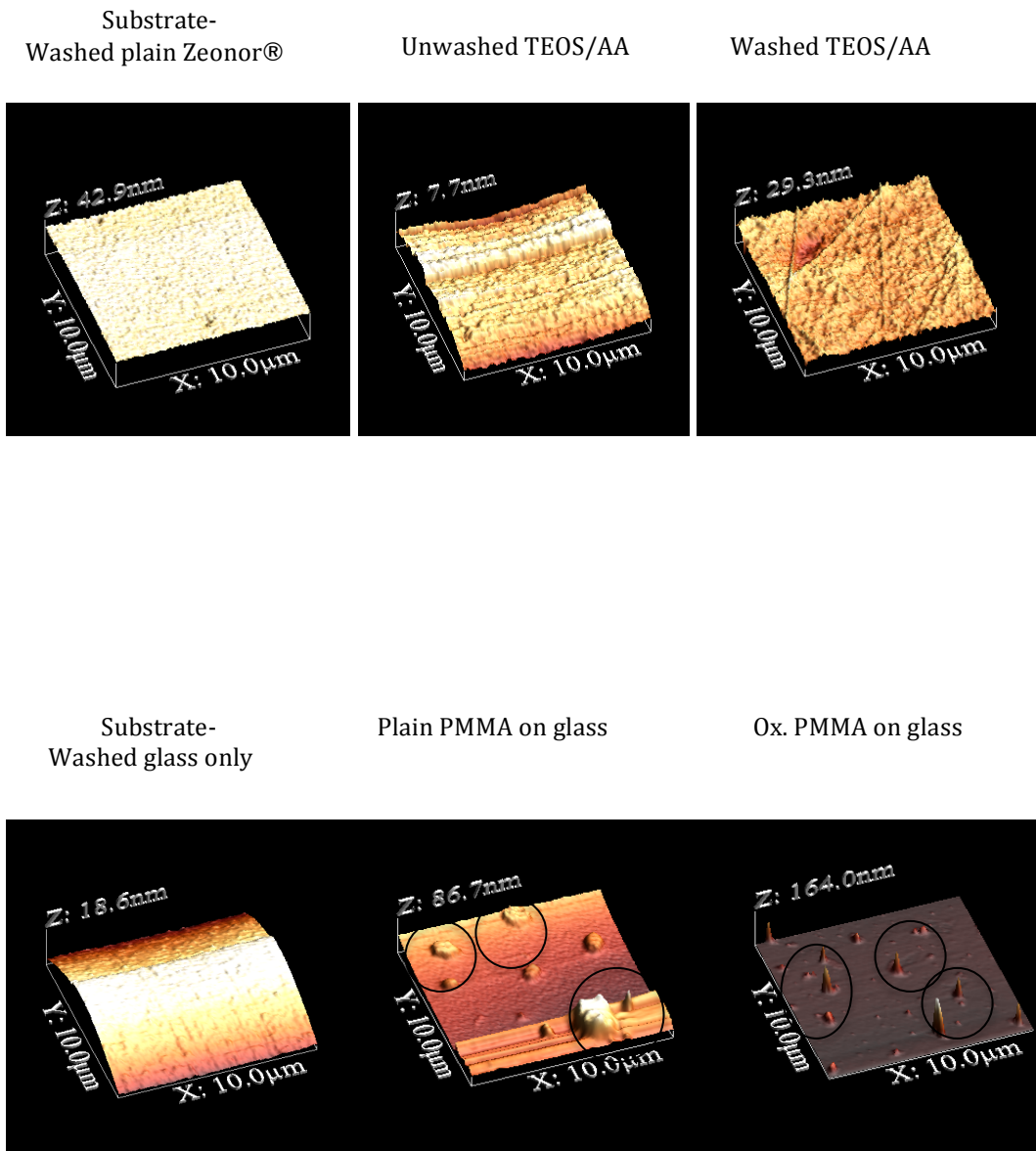
Figure 2.14 AFM analysis of substrates: Zeonor®, glass; and washed and unwashed TEOS/AA on Zeonor® and PMMA and ox.PMMA on glass. Area scanned 10 μm x 10 μm. Circled are the artefacts possibly caused by dust particles.
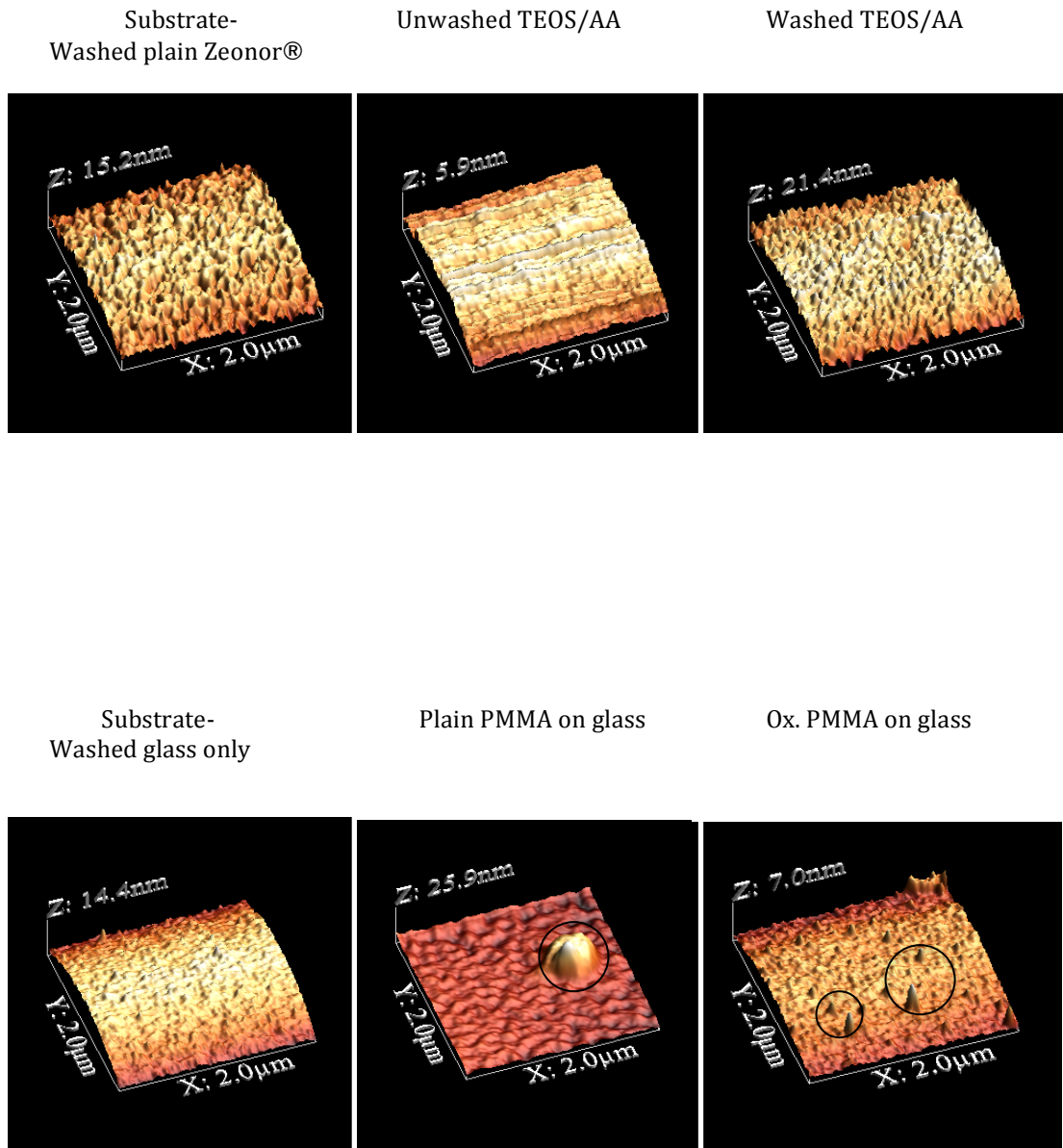
Figure 2.15 AFM analysis of substrates: Zeonor®, glass; and washed and unwashed TEOS/AA on Zeonor® and PMMA and ox.PMMA on glass. Area scanned 2 μm x 2 μm. Circled are the artefacts possibly caused by dust particles.

TEOS/AA washed refers to TEOS/AA washed by rinsing the slide with DI water after deposition processes. TEOS/AA not washed is simply TEOS/AA straight from the PECVD chamber with no further washing or modification. The washing step after TEOS/AA depositions helped to reduce the amount of loosely bound groups, leaving it with intact functionality. It was also noticed that contact with water increases overall roughness, which is possibly associated with film swelling upon contact with liquid. However the increase is insignificant. Figure 2.16 combines revised average roughness for each substrate. There are minimal variations between surfaces; all surfaces results in roughness lower than 1.8 nm. It was confirmed that all surfaces are quite smooth and almost featureless, which makes them ideal for DNA immobilisation. Higher values for average roughness in case of TEOS/AA could also be caused by the underlying substrate – Zeonor®, which as can be seen from figure 2.16, is rougher than glass, which is used for PMMA. Epoxy, commercially available surface, is exceptionally smooth, however it is not smoother than ox. PMMA.
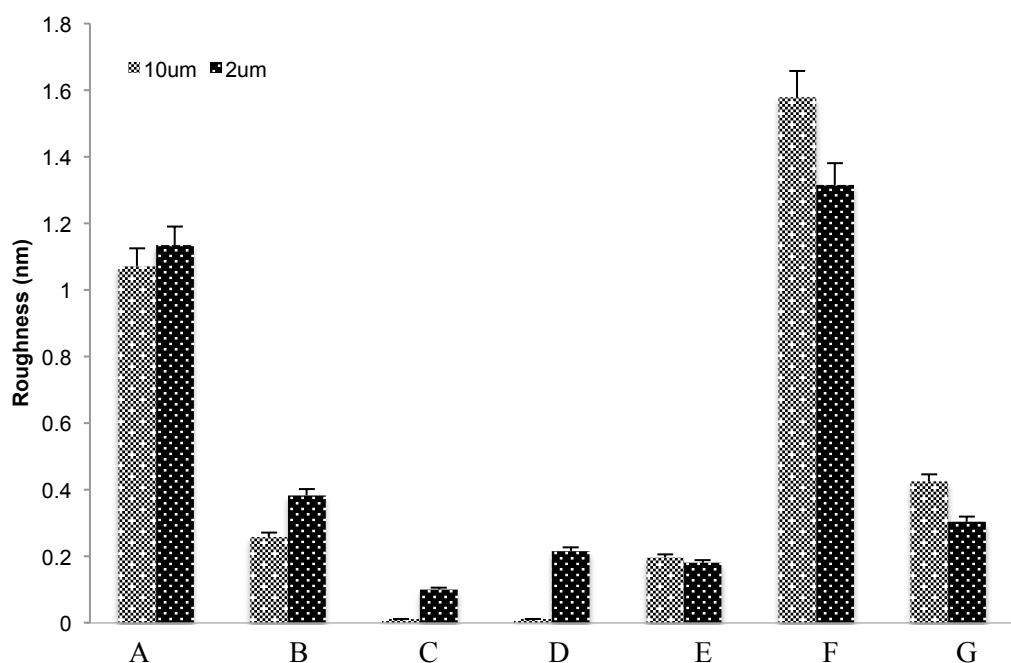
Figure 2.16 Average roughness of various substrates analysed by AFM, n=3. A-washed Zeonor, B-washed glass, C-plain PMMA, D-ox.PMMA, E-unwashed TEOS/AA, F-washed TEOS/AA and G-Epoxy.

Images from AFM of various substrates are presented in figure 2.14 and 2.15. Two different area sizes were scanned: 10 μm and 2 μm. To conclude there are some noticeable features observed, like dust particles, however overall roughness is below 2 nm, which is suitable to be use for DNA experiments.

2.3.3 TEOS/AA and ox. PMMA – surface stability and robustness upon multiple washing

The sensitivity and selectivity of biosensors depend mainly on the quality and robustness of the interface [132]. The surface configuration must stay intact against multiple washes and the immobilisation, that is, the active site must remain accessible and active. The surface has to withstand multiple washes aimed at enhancing sensitivity and selectivity of the assay. Here, TEOS/AA and ox. PMMA are tested against multiple washes in order to establish the stability and robustness of the deposited film.

Amino modified 1 μM DNA probes with fluorophore attached at the other terminus immobilisation with EDC linker was used as a confirmatory test for surface stability. In the presence of EDC, amine groups (on DNA terminal) and carboxylic acid groups (on the surface) bind covalently and the reaction is very specific. Hence DNA probe is immobilised via $-NH_2$ and the slide was then scanned – before wash. The same slide then was subjected to a wash and scanned after each 20 minutes wash. Figure 2.17 represents the results for up to 6 washes for TEOS/AA and figure 2.18 represents the results for up to 6 washes for ox. PMMA.
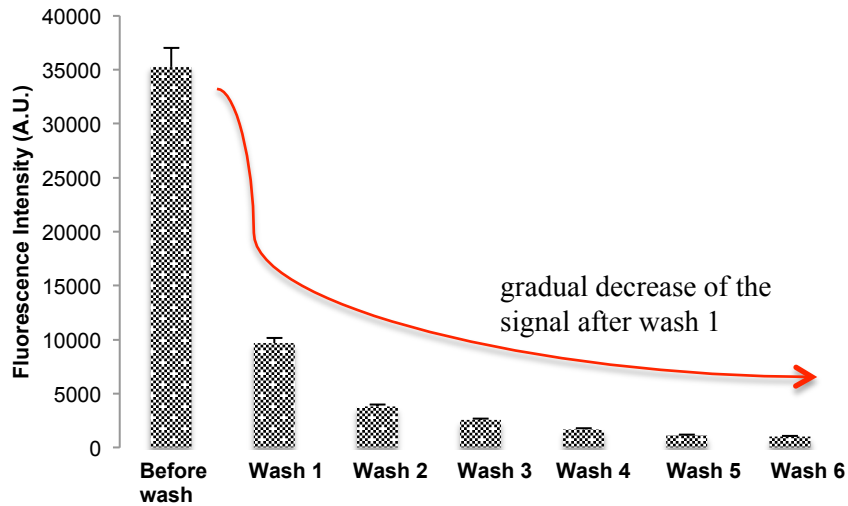
Figure 2.17 1μM DNA probe immobilised onto TEOS/AA, grey bars represent EDC linker in the DNA sample. Fluorescence intensity before (first bar) vs. fluorescence intensity after washes. Each wash = 20 minutes in total, 10 minutes with 2xSSC and 0.1 % SDS followed by 10 minutes with 2xSSC only. Error bars are equal to the standard deviation of three fluorescence intensity measurements, n=3.

Figure 2.18 1μM DNA probe immobilised onto ox.PMMA, bars represent EDC linker in the DNA sample. Fluorescence intensity before (first bar) vs. fluorescence intensity after washes. Each wash = 20 minutes in total, 10 minutes with 2xSSC and 0.1 % SDS followed by 10 minutes with 2xSSC only. Error bars are equal to the standard deviation of three fluorescence intensity measurements, n=3.

Fluorescence intensity is directly proportional to the amount of DNA probe bound to the surface. DNA Fluorescence signal on TEOS/AA deteriorates along with every additional wash, see figure 2.17. The unwashed slide has a high signal of almost 35K A.U., which confirms a lot of non-specifically and loosely bound DNA probe to the surface. The signal decreases by more than a half after wash one. At this stage the DNA probe should be covalently bound, and should stay at this level regardless of washing. However, it is observed that the signal gradually decreases as a function of repeated washing steps. The hypothesis was made, that the surface anchoring method fails and TEOS or AA is being washed away along with the probes attached to it. It also raises a question of the surface chemistry surviving, ie: the film stays intact, however the bond between the DNA molecule and the surface is compromised resulting in DNA being washed away. In order to verify the above, ox. PMMA surface was tested; see figure 2.18. Aminated DNA with fluorophore was immobilised to ox. PMMA surface in the same manner as for TEOS/AA, same wash protocol was also applied. If there were a problem with the linking chemistry (bond between the surface and a DNA molecule), a similar result would be expected, gradual decrease of the signal as a function of bond being disturbed and DNA molecules being washed away. However quite opposite is observed, see figure 2.18; the signal stabilises after the first wash. Our hypothesis has been confirmed; signal of DNA probe adsorbed covalently to the surface remains the same regardless the wash on ox.PMMA. Before wash the signal is high as expected due to the large amount of non-specifically and loosely bound DNA. After the first 20 minutes wash, the signal decreases by almost a half, which is very similar to the decrease observed on TEOS/AA. However unlikely with TEOS/AA surface, DNA probe is covalently attached to the ox.PMMA surface and the signal is maintained at the same level, which confirms the stability of the surface. From the results above, conclusion has been drawn that the TEOS/AA recipe needs more optimization in order to improve its stability and robustness against multiple washing steps and another member of this research group has continued this work. Ox. PMMA has proven to be durable and robust surface, which can withstand multiple washes. Due to findings described above, decision had been made to concentrate on further development and optimisation of ox. PMMA and to use this surface as a platform for DNA experiments and further research, which is explained in more detail in Chapter 3.

2.3.4 Quantification of carboxylic acid groups using TB method on various surfaces

The toluidine blue (TB) test was used in this study in order to verify the amount of the carboxylic acid groups on surfaces such ox.PMMA and TEOS/AA.

In microarray technology the surface density of the immobilised oligonucleotide probe is a paramount parameter. A poor surface coverage will result in a low hybridisation signal and will have a negative effect on the hybridisation rate [100,133]. However, a very high surface density may also not be ideal as it can possibly result in steric interference between the covalently immobilised oligonucleotides, preventing access to the complimentary DNA target strand [134].

In this study TB has been used to characterize the functionality of the carboxyl surfaces and to determine the amount of –COOH functionalised groups/ DNA probe immobilised. TB (used in NaOH solution) is extremely specific to binding carboxylic groups, and creates a strong ionic bond to deprotonated carboxyl's on a surface coated in AA.

Prior to surface testing with the TB method, concentration curves had to be constructed in order to verify the relation between absorbance and the concentration. Figure 2.19 presents range of concentration curves:

A) 0.02 mM – 0.08 mM;

B) 0.002 mM-0.01 mM;

C) 0.8 μM – 2.4 μM.

Due to the wide range of concentrations, three individual graphs were constructed, figure 2.19.

A)

$y = 19.37x + 0.651$
$R^2 = 0.96034$

B)

$y = 34.215x + 0.0011$
$R^2 = 0.94244$

C)

$$y = 0.0565x - 0.0263$$
$$R^2 = 0.98551$$
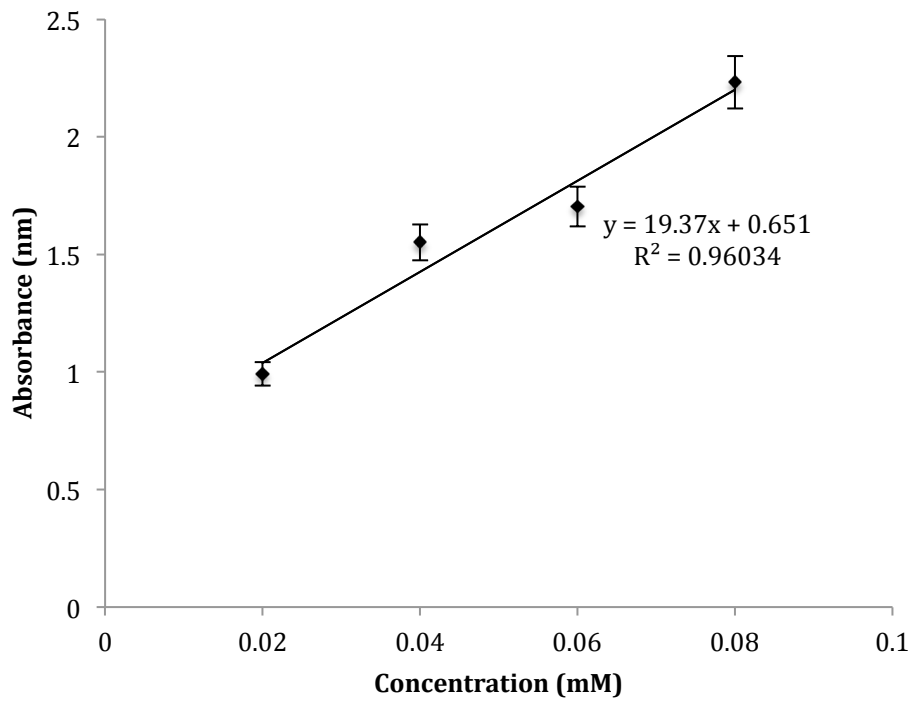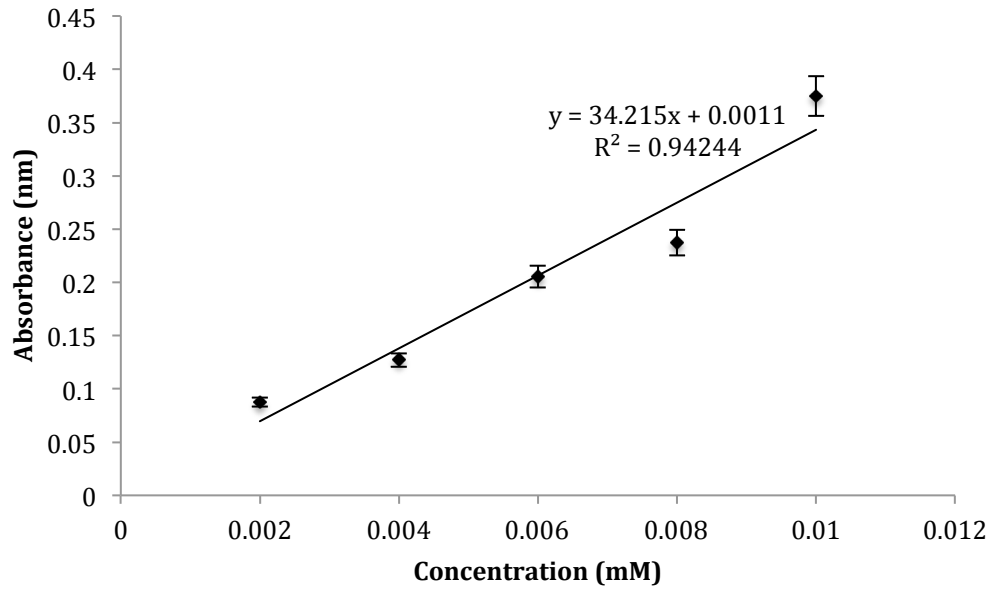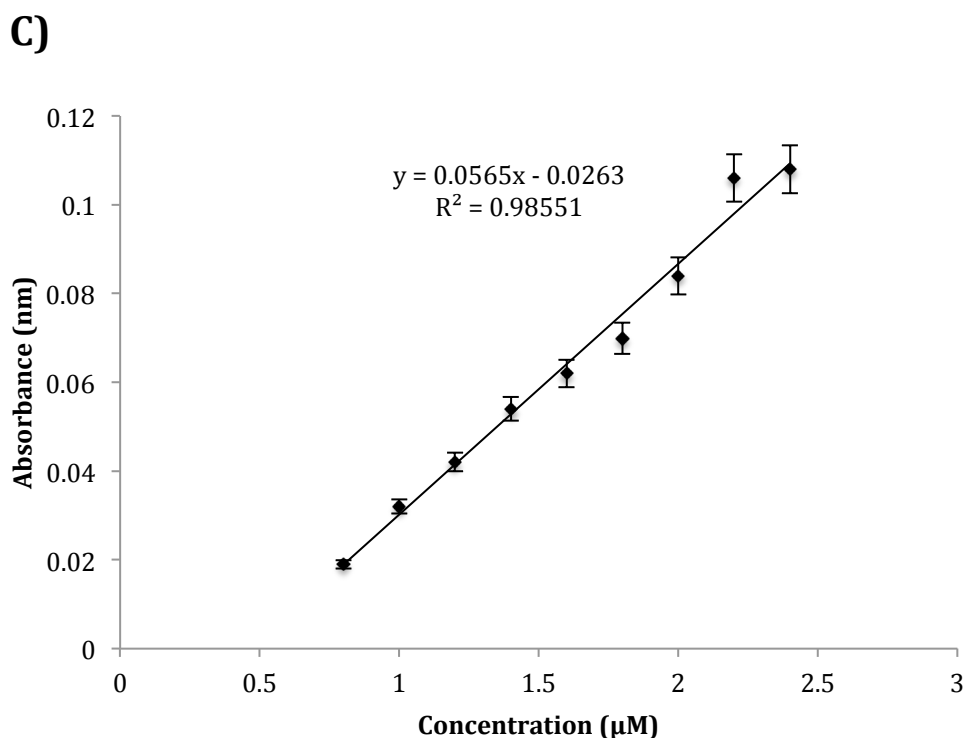
Figure 2.19: Calibration curves at different concentration range: (a) 0.02 mM – 0.09 mM; (b) 0 mM - 0.01 mM; (c) 0 uM – 2.5 uM. Error bars are equal to the standard deviation of three fluorescence intensity measurements, n=3.

TB staining was used to determine the density of carboxylic groups on plain Zeonor® and oxidised (UV/O$_3$ treatment) Zeonor®. Absorbance value was used as an indicator of carboxylic acid density. From the graph in Figure 2.20, the difference in absorbance between non – treated and treated Zeonor® slides is significantly noticeable. A very similar result was observed in treated versus non – treated PMMA substrate, see figure 2.21. The above results were as expected, non – treated PMMA or Zeonor® slides do not have any active carboxylic acid groups. Only upon activation of the above surfaces, chemical modifications occur resulting in active carboxylic groups.
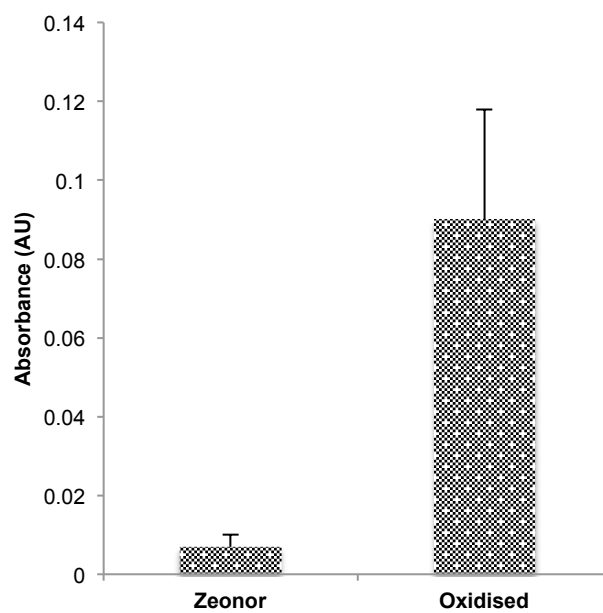
Figure 2.20 TB absorbance on plain Zeonor® vs. oxidised Zeonor®. Error bars are equal to the standard deviation of three fluorescence intensity measurements, n=3.
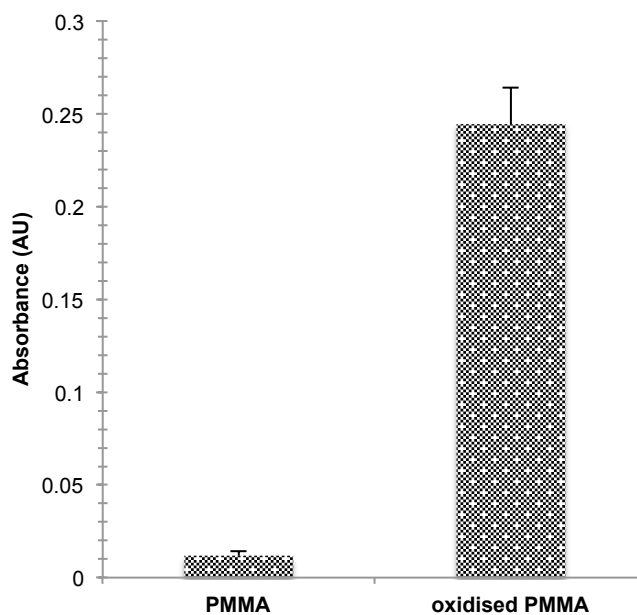
Figure 2.21 TB absorbance on plain PMMA vs. oxidised PMMA. Error bars are equal to the standard deviation of three fluorescence intensity measurements, n=3.

To calculate the amount of molecules per unit area, the equation shown below was used:

$$molecules\ per\ nm^2 = (1{\times}10^{16}\delta - 1.05{\times}10^{14})/\alpha$$

In this instance α represents the area of the coated flat surface of the substrate (nm^2), and δ represents the absorbance of the solution containing the toluidine blue released from the surface, measured by UV-Vis (A.U.). The absorbance values were applied in calculations to obtain the number of carboxylic group molecules per area (cm^2). The table 2.2 shows the number of molecules per cm^2 area for ox. Zeonor®, ox. PMMA, plain Zeonor®, PMMA and SAM MUA on Au. Ox. PMMA shows the highest density of –COOH groups. Ox. Zeonor® and MUA on Au have very similar –COOH group density, and they are approx. 3 times smaller than Ox. PMMA. Plain Zeonor® and PMMA have no –COOH groups, which is expected. Figure 2.22 shows a graphical representation of results shown in Table 2.2.

Table 2.2: Number of molecules per $1cm^2$ on various substrates.

Substrate	Concentration	Number of molecules (per cm^2)
Ox. PMMA	7 µM	$8.94*10^{14}$
Ox. Zeonor®	2.2 µM	$2.814*10^{14}$
Plain Zeonor®	0.007 µM	0
Plain PMMA	0.012 µM	0
MUA on gold	0.9 µM	$2.64*10^{14}$
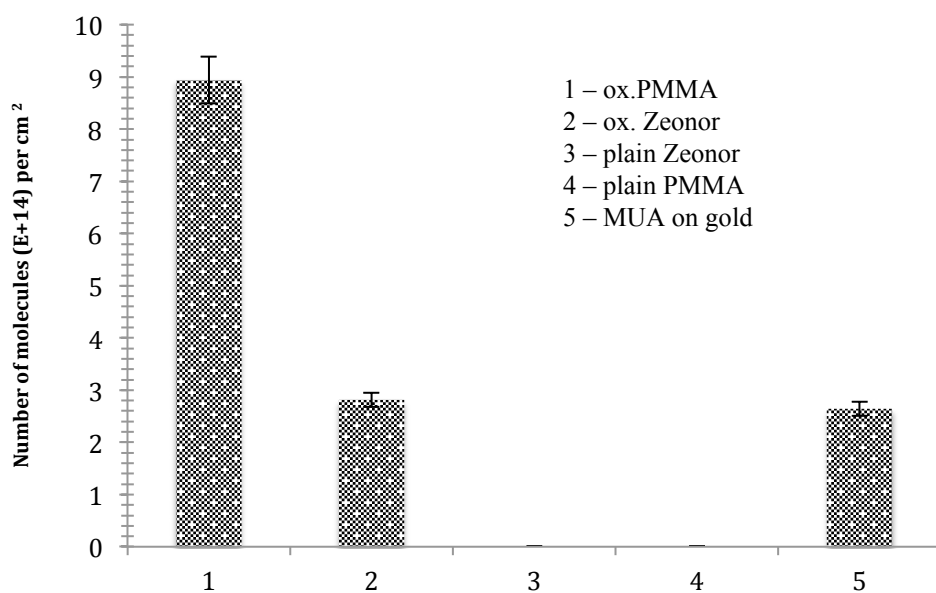
Figure 2.22 Graphical illustration of results shown in the table 2.2. Error bars are equal to the standard deviation of three fluorescence intensity measurements, n=3.

2.3.5 TB method used for the development of the best-known method for TEOS/AA by PECVD.

TB method was also used in developing the best-known method (BKM) for TEOS/AA depositions on glass substrate. Depositions were prepared by in house by PECVD and the deposition performance analysed with the amount of the carboxylic acid groups on the surface determined. TEOS/AA and TEOS-only were prepared in batches of 6 each and AA-only (acrylic acid only) and another TEOS/AA depositions were prepared in batches of 8. Variations between the same depositions are quite significant as seen in figure 2.23. There was a compelling difference in between TEOS/AA depositions itself TA and TAA, which suggests that the current recipe is not robust and it is not uniform throughout the deposition processes. This work was done with collaboration with the fellow research member. TB method was used to analyse surface prepared by other researcher.
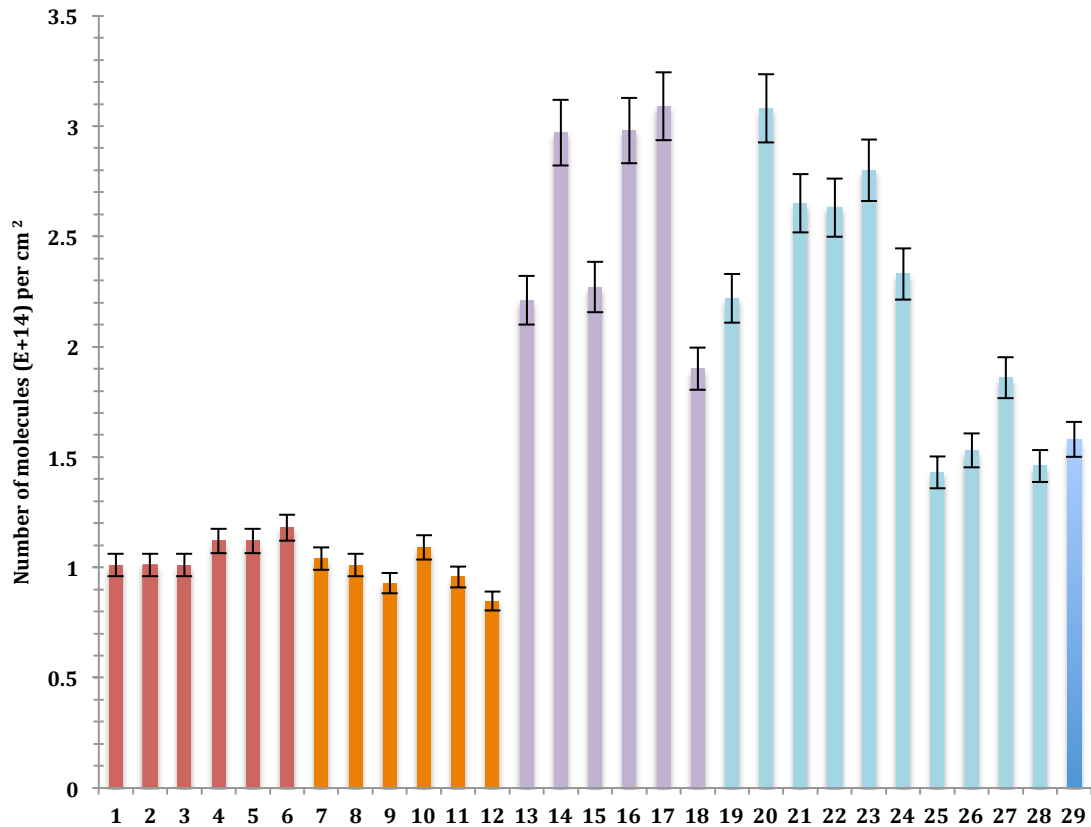
Figure 2.23 Number of molecules (E+14) per cm^2 on TEOS/AA [1-6], TEOS only [7-12], Acrylic acid only [13-18] and another TEOS/AA [19-28]. Error bars are equal to the standard deviation of three fluorescence intensity measurements, n=3.

3 final recipes were developed:

1) 4 minute depositions (2 min Teos + 2 min AA) @ 5 Watts

2) 4 minute depositions (2 min Teos + 2 min AA) @ 15 Watts

3) 4 minute depositions (2 min Teos + 2 min AA) with the TEOS @ 40 Watts and AA @ 5 Watts.
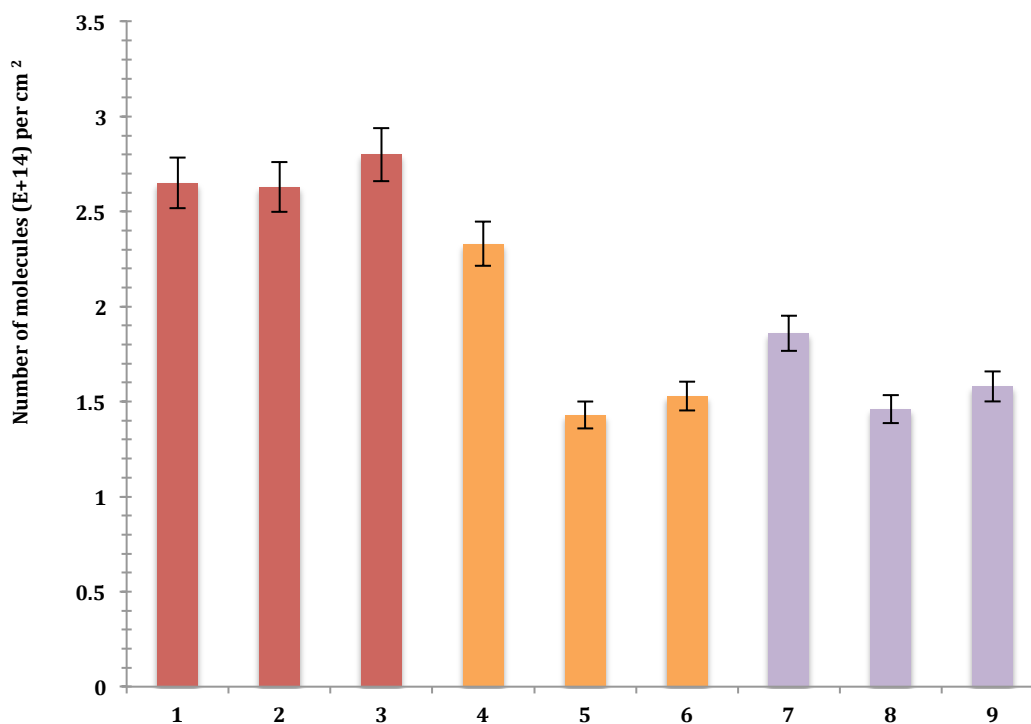
Figure 2.24 Carboxylic acid molecules (E+14) per cm^2 on samples 1-3 are all recipe 1, samples 4-6 are all recipe 2 and samples 7-9 are all recipe 3. Error bars are equal to the standard deviation of three fluorescence intensity measurements, n=3.

Using the TB method all three recipes were characterised, with results of the number of molecules shown in figure 2.23. Recipe 1 is most reproducible and results in uniform depositions with an estimate final number of over 2.50E+14 molecules per cm^2. Recipe 2 varies between 1.50E+14 and 2. 50E+14, which a significant difference. This recipe is not reproducible and will not be utilised in a deposition process. Finally recipe 3 only varied between 1.50E+14 and 2. 00E+14, however the overall number of molecules is lower than the one in recipe 1. Below are additional measurements used to determine the BKM.
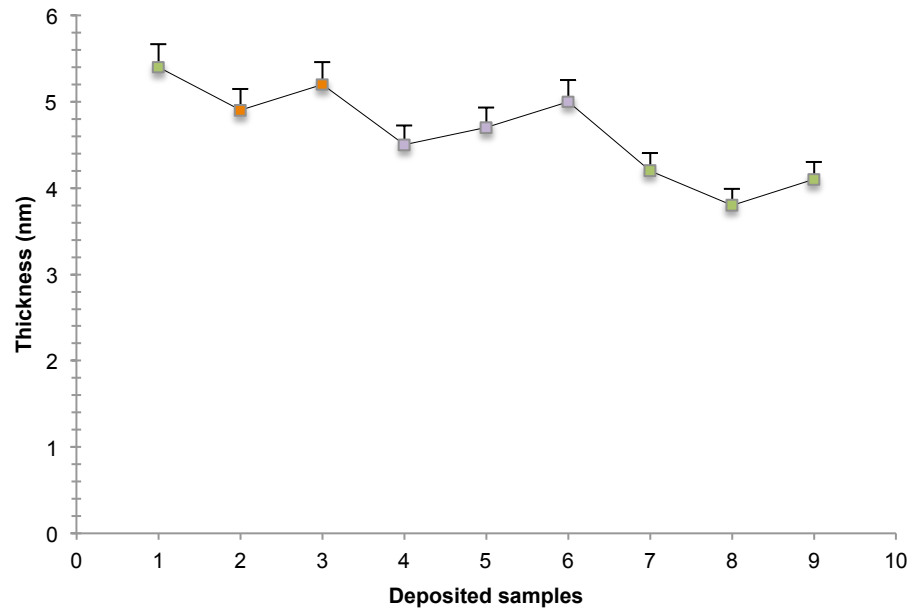
Figure 2.25 Thickness (nm) measurements of samples: 1-3 recipe 1, 4-6 recipe 2 and 7-9 recipe 3. Error bars are equal to the standard deviation of three fluorescence intensity measurements, n=3.
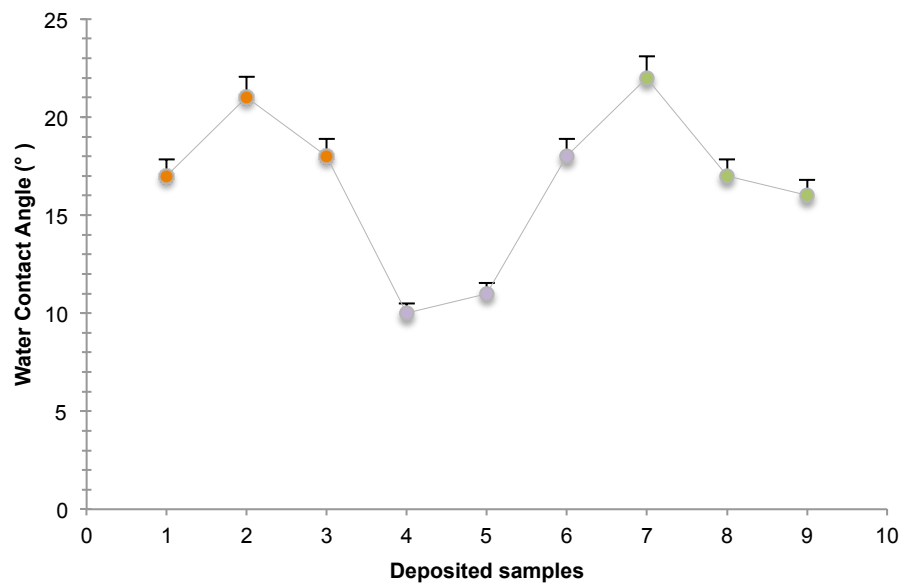
Figure 2.26 Contact angle (°) measurements of samples: 1-3 recipe 1, 4-6 recipe 2 and 7-9 recipe 3. Error bars are equal to the standard deviation of three fluorescence intensity measurements, n=3.

From figures 2.25 and 2.26, contact angle (figure 2.25) values are most consistent for recipe 1 and the thickness (figure 2.26) has only small variations. The average thickness is c. 5 nm and average contact angle is c. 18.6 °. Recipe 2 and 3 have significant variations in water contact angle, which suggests that depositions are not reproducible and the deposition process results in various film composition and coverage. By combining all results, recipe 1 has been chosen as BKM for TEOS/AA depositions at the time.

The TB method was applied to obtain the information about the density of –COOH groups in order to characterise surfaces and obtain TEOS/AA BKM. Although this method is very specific for –COOH groups, it is not suitable for identifying the uniformity of –COOH distribution. The TB test gives an average of –COOH groups on a surface, but it does not explain the distribution of them. For example, Zeonor® slide is –COOH coated and undergoes TB testing. There might be areas on a slide, which are less covered with carboxylic groups and others that can be tightly packed with carboxylic groups. Due to the low sensitivity of the scanner used in the lab, and discrepancies with the equation provided by the calibration curve at low absorbance values, this method of carboxylic acid group quantification was considered not sensitive enough. It did however provide a clear contrast between untreated and treated substrates, displaying the presence of intact carboxylic groups on the surface. As an alternative of toluidine blue experiments, direct DNA immobilisation was suggested to be an accurate method for detection of the presence of carboxylic acid groups.

2.4 Summary and conclusion

Determination of the most suitable carboxylic acid surface for bioassay development was the main aim of this chapter. A panel of different –COOH functionalised films were developed, including novel ox.PMMA film [3], which is explained in more detail in chapter 3. Each one of them was compared in terms of ease of preparation and time required for the preparation. Number of surfaces was investigated; however two most suitable were chosen to be used for further analysis and which have the biggest potential for future bioassay adaptation. TEOS/AA and ox.PMMA proved to have multiple advantages over five other functionalised surfaces described in this work. Both films do not require time-consuming preparation steps and both of them can easily be prepared in larger batches and in advance. The ease of preparation and ability to coat different substrates is another advantage over other substrates. Unlike MUA, which requires a gold under layer, ox.PMMA and TEOS/AA can be easily prepared on plastic platforms (Zeonor) or glass. The smoothness of the surface in bioassay development is of paramount importance, due to the size of the molecules to be immobilised onto it. An extensive AFM analysis was performed and it confirmed that there are minimal variations between two surfaces (TEOS/AA and ox.PMMA); both surfaces resulted in roughness lower than 1.8 nm. The DNA molecule is approx. 3nm x 8 nm, hence roughness of the surface of lower that 2 nm is ideal. DNA will not be positioned or peaks and valleys of the surface topography will not compromise its activity. This analysis confirms that both of them are quite smooth and almost featureless, which makes them ideal for DNA immobilisation.

Another important points in the development a surface for biosensor applications are:

- the quality of the interface

- the robustness of the interface.

The surface film configuration must stay intact against multiple washes and the immobilisation, that is, the active site must remain accessible and active. The surface has to withstand long-time reaction or washes aimed at lowering NSB.

Hence TEOS/AA and ox. PMMA were tested against multiple washes in order to establish the stability and robustness of the deposited film. As a result the TEOS/AA recipe needs more optimisation in order to improve its stability and robustness against multiple washing steps, as it was noticed it washes away after multiple washes. However, ox. PMMA has proven to be a durable and robust surface, which can withstand multiple washes. This leads to the further work described in the next chapter 3 including further development and optimization of ox. PMMA and to use this surface as a platform for DNA experiments and further research.

Finally, toluidine blue test (TB) was employed in order to compare the amount of the carboxylic acid groups on surfaces such ox.PMMA and TEOS/AA. The surface density of −COOH is proportional to the amount of the immobilised oligonucleotide probe. A poor surface coverage will result in a low hybridisation signal and will have a negative effect on the hybridisation efficiency [134]. However, a very high surface density may also not be ideal as it can possibly result in steric interference between the covalently immobilised oligonucleotides, preventing access to the complimentary DNA target strand [134]. Scanning electron microscope (SEM) was used in order to identify the distribution of DNA molecules on the surface. SEM produces images of a sample by scanning it with a focused beam, however after many attempts, images were featureless, hence the distribution of the DNA molecules could not be observed. This could be due system's resolution limitations, as the molecules of ssDNA are in nm range.

Additionally TB method was used in developing of the best-known method (BKM) for TEOS/AA depositions in collaborations with other fellow PhD researcher within our group.

Table 2.3 Summary of chapter 2 – key messages.

CHAPTER 2 – key messages
• TEOS/AA and ox.PMMA proven to be the most suitable films for bioassay development
• ox.PMMA is a more stable film than TEOS/AA in terms of stability against multiple washes
• TEOS/AA requires more optimisation
• Ox. PMMA to be used as a platform for DNA experiments and further research
• Full characterisation of ox.PMMA to be carried out – Chapter 3

Chapter 3

3 Fabrication and characterisation of spin coated ox. PMMA.

3.1 Introduction

Following the results from the previous chapter, ox.PMMA was chosen to be a suitable and promising surface for assay development. Fabrication of ox.PMMA needed to be characterised first and it is fully described in this chapter.

This chapter is based on work which was published in *Journal of Material Chemistry B* [3].

Spin coating PMMA is a relatively well-known process [106,125]. However to date there has been no direct comparison of the different oxidation methods to activate the surface, nor has oxidised spin coated PMMA been used as a platform for DNA hybridisation or immunoassays. In this chapter, a comparison of the stability, functionality and fabrication process of spin coating and surface activating a thin film of PMMA on a variety of underlying substrates is described. Activation by two different methods, UV/O$_3$ and oxygen plasma, is compared, with a focus on the stability of functionalisation over 24 days. Adhesion studies and robustness of binding of immobilised biomolecules to each surface is also reported and a direct comparison to commercially available epoxy and bulk PMMA surface is performed. Finally, three applications of the activated, spin coated PMMA films are demonstrated: (a) fluorescence quenching of dye-labelled molecules bound to thin PMMA layers on gold, (b) a DNA direct binding assay, and (c) a sandwich immunoassay.

Biomedical diagnostics and adjunct therapeutics are generating keen interest and intense activity, particularly in the realm of rapid, self-contained medical systems suitable for use on-chip assay, such as point-of-care (POC) [135]. Synthetic polymers are a promising alternative substrate for biosensors because of their low specific gravity, a selectable range of mechanical and surface properties, and a number of well-established high-volume, low-cost manufacturing techniques [136]. A subset of synthetic polymers also possess excellent optical properties

such as low intrinsic auto-fluorescence and high transparency [137]. Poly (methyl methacrylate) (PMMA) is a particularly attractive material for the fabrication of low-cost micro-total analysis systems (μ-TAS) as it possesses excellent optical, thermal, chemical and biocompatibility properties [126]. PMMA can be used to fabricate microchips with micro-channels by injection moulding, hot embossing/imprinting, [127,138] laser cutting, or laser ablation [139,140]. Pristine PMMA is a relatively inert and moderately hydrophobic material; it does not possess suitable surface chemical functionalities to enable covalent immobilisation of biomolecules. Consequently, without pre-treatment, bio-recognition elements such as oligonucleotides and antibodies can only be non-covalently adsorbed on the methyl ester surface, typically resulting in poor device longevity and/or poor performance.

In chapter 2 it was shown that through appropriate surface treatment, PMMA can be oxidised using methods, such as UV/O$_3$ and O$_2$ plasma, to form a carboxylic acid surface to enable the covalent attachment of biomolecules for bioassay development.

Other procedures for the chemical functionalisation of PMMA involve amination in a *N*-lithioethylenediamine solution followed by the addition of a homo bi-functional cross-linker molecule such as glutaraldehyde to enable attachment of aminated biomolecules, followed by capping of the unreacted aldehyde functional groups with a reducing agent [133,141]. Wet chemistry is also applied to generate reactive functional groups on the surface and base/acid hydrolysis of PMMA can be used to generate carboxylic acid groups [127,141–144]. Alternatively, PMMA can be activated by plasma treatment or UV (e.g. deep UV, vacuum UV) [145–148]. The surface activation by UV/O$_3$ differs significantly from the low-pressure oxygen plasma discharge. Plasma treatment can chemically modify the top few nanometres of a polymer surface without using solvents or generating chemical waste, and with less degradation and roughening of the material than many wet chemical treatments [149,150]. UV/O$_3$ has been extensively used to pre-treat surfaces for fluorescence-based bimolecular detection techniques. Modification of polymers by UV/O$_3$ treatment is also a very attractive method for providing carboxylic functionality as it offers the ability to tailor the depth of surface reactivity by varying the wavelength and thus controlling the absorption coefficient [9,145–147,151–155]. Oxygen plasmas are very effective at oxidising organic substrates such as PMMA. [130,156].

3.2 Experimental details

Different characterisation techniques were used to investigate a newly fabricated PMMA surfaces. Preparation of PMMA included the use of different parameters of spin coater as well as different PMMA concentrations. To activate the surface (PMMA to ox.PMMA) two oxidation techniques were used. DNA assay and immunoassay was used to show the applications of the surface used. Longevity studies were performed to obtain the surface activity as a function of time.

3.2.1   Materials and instrumentation

PMMA sheets (0.25 mm thick, impact modified, MW ¼ 120 000) were sourced from Goodfellow Cambridge Limited(Huntingdon, England). Zeonor® substrates, injection-molded cyclic olefin polymer (COP) slides (Zeonor® 1060R, 25 mm x 75 mm, 1 mm thick) were sourced from Sigolis (Uppsala, Sweden). Gold-coated standard glass microscope slides (Ti/Au, 5 nm/30 nm, 25 mm x 75 mm, 1.1 mm thick) were sourced from PhasisSarl (Geneva, Switzerland). Universal microscope glass slides were sourced from VWR (Dublin 15, Ireland). PTFE filter (pore size 0.25 μm) (Chroma-filXtra PTFE-20/25 Macherey-Nagel, Duren, Germany). 1-Ethyl-3-(3- dimethylaminopropyl) carbodiimide (EDC), 2-(N-morpholino) ethanesulfonic acid buffer (MES), sodium dodecyl sulfate (SDS), saline-sodium citrate (SSC), 11-Mercaptoundecanoic acid 95 % (MUA), Succinic anhydride ≥99 % (GC), were purchased from Sigma Aldrich (Arklow, Ireland). Amino-modified oligonucleotide DNA probes (5'-GCC-AAT-ATT-TCT-GTG-CTG-CTA-3') (miR-195 probe, 21-mer) and synthetic oligonucleotide target DNAs (5'-TAG-CAG-CAC-GTA-AAT-ATT-GGCG-3') (miR-16 target, 22-mer) with Cy3 label and without the label and (5'-TAG-CAG-CAC-AGA-AAT-ATT-GGC-3') (miR-195 target, 21-mer) with Cy3 label and without the label were sourced from Eurofins MWG Operon (Ebersberg, Germany). Human IgG (hIgG), anti-human IgG (α-hIgG), Cy5-labelled anti-human IgG (α-hIgG-Cy5), and Cy3-labelled anti-mouse IgG (α-mIgG-Cy3) were sourced from Biomeda Corp. (Burlingame, California). All chemicals were used as received without further purification.

Instrumentation used in support of this work in chapter 3:

- Spin coater
- UV/O_3 and O_2 plasma
- Ellipsometry
- Water contact angle instrument
- AFM
- Fluorescence scanner

3.2.2 Preparation of spin coated poly (methyl methacrylate) surfaces

Protocol for preparations of spin coated PMMA is as follows:

- Take off protection film from the PMMA sheet
- Cut PMMA sheet into small pieces
- Weight out 0.001 g of PMMA pieces for 0.1 PMMA concentration respectively
- Place into a glass vial with 10 ml of 80 % ethanol to result in 0.1 % PMMA concentration.
- Use sonicator at 40 ° for 30 minutes to dissolve the PMMA pieces
- Filter dissolved PMMA solutions through PTFE filter (pore size 0.25 µm)

Cleaning of the substrates prior spin coating:

- Fill the tank with 2 % of Micro90 detergent for cleaning step
- Place the slides in a slider holder and submerge them in Micro90
- Sonicate for 30 minutes
- Rinse slides in water
- Fill another tank with isopropanol and submerge slides
- Sonicate for 30 minutes
- Rinse slides in water
- Dry with nitrogen stream

Spin coating of dissolved PMMA protocol:

- Place a slide at the centre of spin coater's holder

- Apply vacuum to immobilise the slide

- Place 1 ml of dissolved PMMA solution on the middle of the slide

- Set the settings: 3000 rpm, 5 seconds acceleration for 1 minute

- Press start

- Take the slide off and transfer to a holder

The curing process protocol:

- The PMMA films are cured in an oven at 80 °C for 1 h or in the fume hood over night.

- Figure 3.1 represents a schematic of PMMA preparation.
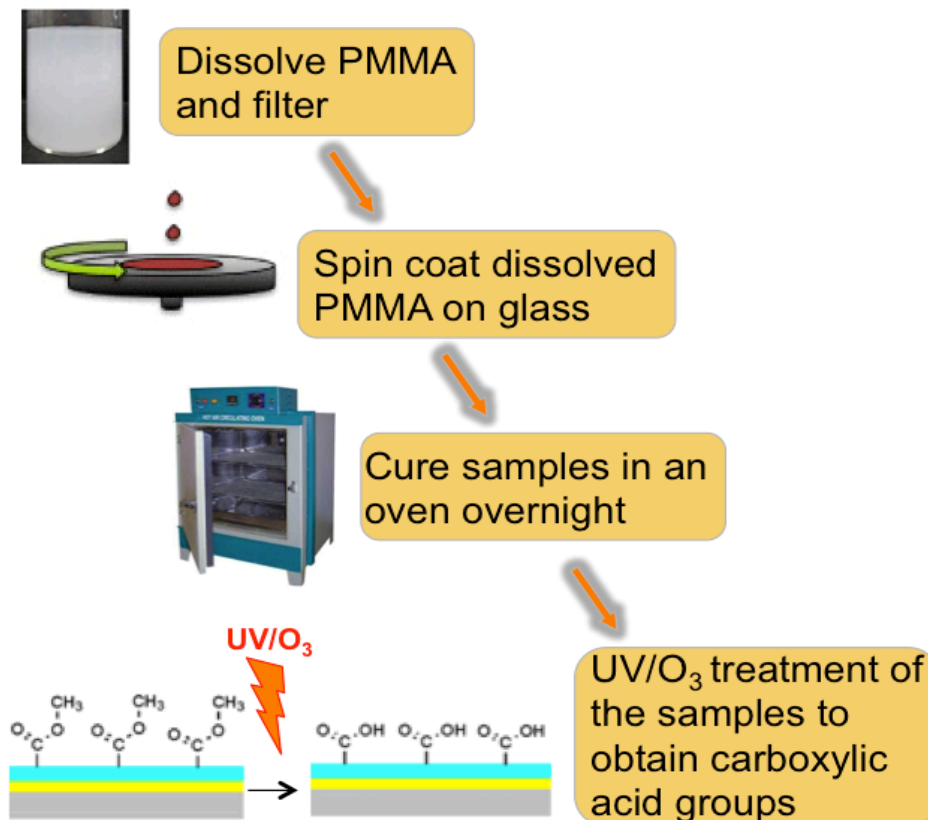
Figure 3.1 Schematic representation of PMMA film fabrication and activation.

Oxidation of spin coated PMMA surfaces with UV/O$_3$:

UV/O$_3$ treatment was performed using a commercial ozone cleaning and activation system (PSD-UV, Novascan Technologies, Ames, IA, USA). According to the manufacturer specifications, at the 50 W power setting, approximately 50 % of the total lamp output power is delivered around the 254 nm peak and 5 % around the 185 nm peak. The optical power was kept constant but the treatment time was varied. A period of 8 minutes of UV/O$_3$ treatment was optimal for spin coated thin PMMA films. When the treatment time was too short, insufficient numbers of carboxylic functionalities were generated, while if the treatment time was too long, the thin PMMA film was etched away [130].

Oxidation of spin coated PMMA surfaces with oxygen plasma:

Direct plasma activation was carried out in an Oxford Instruments Plasmalab 100 PECVD system, figure 1.34, which consists of a parallel-plate reactor with a radio-frequency (13.56 MHz) driven top electrode, which incorporates a showerhead for uniform gas feed into the vacuum chamber. Substrates are supported on a 200-mm-diameter quartz wafer, which is placed on the bottom electrode. This electrode and the chamber walls are electrically grounded. Plasma activation is performed under the following conditions: oxygen gas flow 50 standard cm^3/min (SCCM), pressure 200 mTorr, radio-frequency power 50 W, bottom plate temperature 20 °C, processing time 1 minute.

- Place cured PMMA samples (do not touch the interface, pick up by the edge of the slide) onto UV/O$_3$ device
- Initiate oxidation for 4-8 minutes as required
- Remove samples from the device
- Alternatively oxygen plasma can be used to activate the surface (4-8 minutes).

The coating of PMMA films onto glass slides required an additional step, due to the hydrophobicity of the glass. The water contact angle of glass is very low; hence, the PMMA solution could not gain contact with it during spin coating. In order to modify the hydrophobicity of the glass, the deposition of a silicon oxide layer was applied to ensure adhesion of the PMMA. The silicon oxide was

deposited with a plasma enhanced chemical vapour deposition (PECVD) method using a Plasmalab 100 system. The precursor reagents for this process were oxygen gas and hexamethyldisiloxane (HMDSO). The silicon oxide layer thickness was approximately 30 nm.

3.2.3   DNA washing protocol

Each washing step for DNA described contains three distinct stages; 10 minutes in 0.2XSSC + 0.1 % SDS followed by two 10 minutes washes in 0.2X SSC. After initial immobilisation, slides were washed once (all three stages). The fluorescent signal measured then was taken as the signal from covalently bound DNA (having removed most of the physically bound DNA). Each wash step thereafter contained the three wash stages.

3.2.4   DNA Direct Hybridisation Assay

- Place well template sticker onto modified surface.

Probe immobilisation:
- 1 µM of DNA - micro RNA 195 analogue (miR195) probe in MES and 100 mM EDC was manually spotted onto the ox. PMMA (50 ul) surface
- incubate for 40 minutes at room temperature.
- Remove spotting solution by vacuum
- Wash slides extensively to minimise any NSB and loosely bound DNA molecules
- Dry the slide by centrifugation or stream of nitrogen.

Target hybridisation:
- 0.1 µM DNA target in 2X SSC was spotted manually onto previously immobilised probe
- Incubate for 3 hours in a humidity chamber to avoid evaporation of spotted solution
- Remove the spotting solution by vacuum
- Wash following the wash protocol detailed in section 3.2.3.
- Dry the slide by centrifugation or stream of nitrogen

- Scan using the fluorescence scanner.

3.2.5 Antibody Sandwich Assay

Surface activation:

- Place well template sticker onto modified surface.
- Manually spot 0.01 g EDC + 0.003 g NHS in 500 µL of MES onto the surface
- Incubate for 15 minutes at room temperature
- Remove the spotting solution by vacuum

α-hIgG *immobilisation:*
- Spot manually 10 µg/ml of α-hIgG
- Incubate for 1 hour at 37 °C in a humidity chamber
- Wash with 0.1M PBS/1 % Tween twice and then PBS only.

Blocking:
- 0.1 M ethanolamine was spotted for 10 minutes to allow deactivation of EDC/NHS.
- Rinse with Di H_2O for 1 minute.

Further spotting:
- Spot 4 mg/ml of hIgG solution
- Incubate at 37 °C for 1 hour in a humidity chamber
- Wash with 0.1M PBS/1 % Tween twice and then PBS only
- Spot 20 µg/ml of the α-hIgG-Cy5 solution
- Incubate for an hour at 37 °C
- Washed the substrate with PBS/Tween and PBS only.
- Scan the substrate with the fluorescence scanner.

3.2.6 Longevity studies

- Prepare set of Zeonor® slides as per section 3.2.2.
- The spin coated, oxidised slides were prepared on the first day and stored under vacuum conditions in separate petri dishes until required.
- The measurements of thickness (n=3) and contact angle (n=3) were taken on particular days.

3.2.7 Metal induced fluorescent quenching measurements using fluorescent scanner

- Gold coated glass slide was spin coated with PMMA, using protocol 3.2.2
- $-NH_2$ modified DNA probe (labelled with Cy3 fluorophore) was immobilised to the ox.PMMA surface (3.2.4) as it was used as an indicator of quenching
- 3.2.3 DNA washing protocol was applied
- Slide with immobilised labelled DNA was scanned using fluorescent scanner

3.2.8 Ellipsometry – film thickness measurements

- Thickness of spin coated (ox.)PMMA on slides was measured using ellipsometry
- 3 measurements were taken of the same slide at three different locations and the average was then calculated.

3.2.9 WCA – film hydrophobicity measurements

- Hydrophobicity of the film was measured using water contact angle instrument
- 3 measurements were taken of the same slide at three different locations and the average was then calculated.

3.2.10 AFM analysis

- Substrate surfaces were examined using an atomic force microscope (AFM) on a Veeco Dimension 3100 instrument.
- The AFM was used in tapping mode using Tap300Al-G tips from Budget Sensors (Sofia, Bulgaria)
- High aspect ratio images were measured using Improved Super Cone tips from Team Nanotec; both tips had a resonant frequency of 300kHz and force constant of 40 Nm^{-1}.
- Images were analysed using WSxM software [131].

3.3 Results and discussion

In this chapter section thickness analysis of spin coated PMMA films was carried out and is described. AFM technique was used to investigate (ox.) PMMA film morphology, pre and post the oxidation process. The ability of biomolecules conjugation to ox. PMMA and stability of the film against multiple washes is also detailed. Longevity studies of ox.PMMA for up to 28 days is investigated, as a function of film thickness and water contact angle. Quenching of fluorophore emission experiment is outlined. Finally ox.PMMA film is applied in a DNA and antibody binding experiments respectively.

3.3.1   Thin PMMA spin coated film process – thickness analysis

Toluene was the solute of choice to dissolve PMMA in. However after a while, it was observed that Zeonor® slides become cloudy while exposed to toluene for too long. It was noticed that toluene can dissolve Zeonor®, so a new dissolving solute was suggested – 80 % ethanol [157], which proven to be suitable for Zeonor® and all other substrates (glass, gold and silicon). A test was performed to determine if there any major differences in film thickness and composition between toluene dissolved PMMA and 80 % ethanol dissolved PMMA. Figure 3.2 and figure 3.3 show thickness measured by ellipsometry and water contact angle respectively, both measured before and after oxidation.
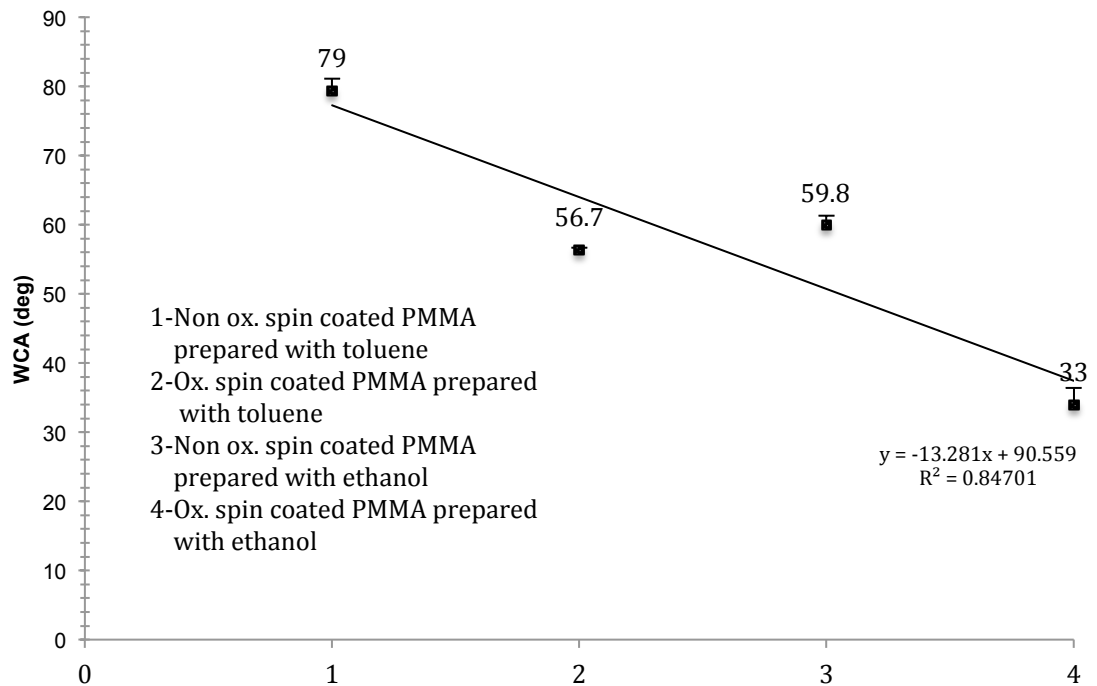
Figure 3.2 Water contact angle (WCA) of spin coated PMMA before and after oxidation, dissolved in two different solutes: ethanol and toluene. Error bars are equal to the standard deviation of three fluorescence intensity measurements, n=3.
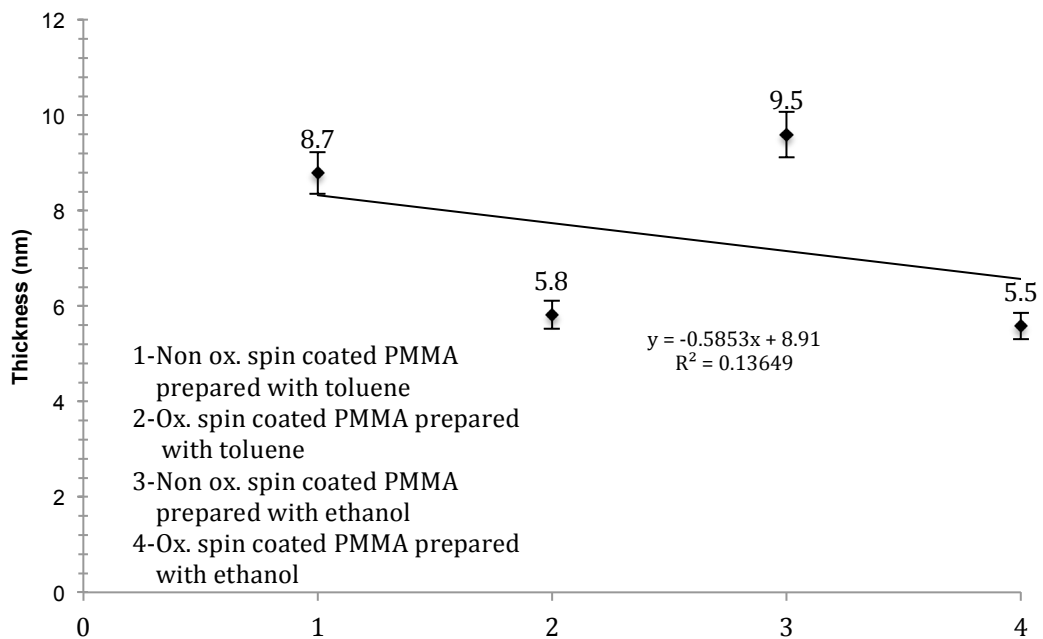
Figure 3.3 Thickness and water contact angle (WCA) of spin coated PMMA before and after oxidation, dissolved in two different solutes: ethanol and toluene. Error bars are equal to the standard deviation of three fluorescence intensity measurements, n=3.

103

As seen in figure 3.2 and 3.3, there were no significant differences in WCA and thickness between two solutes, as expected.

The thicknesses of the films spin coated on glass and silicon substrates at different spin speeds, using solutions with different concentrations of PMMA are presented in figure 3.4. Film thickness of the coating was measured at several locations (edge of the slide and the centre) and the average thickness was obtained. The difference between thicknesses at different locations was less than 1 %, which confirms uniformity of the coating. A number of different protocols were used to produce the thinnest coatings. Not surprisingly, it was found that the lowest concentration (0.1 % w/v) at the highest speed (3000 rpm) resulted in the thinnest film, which measured less than 8 nm.
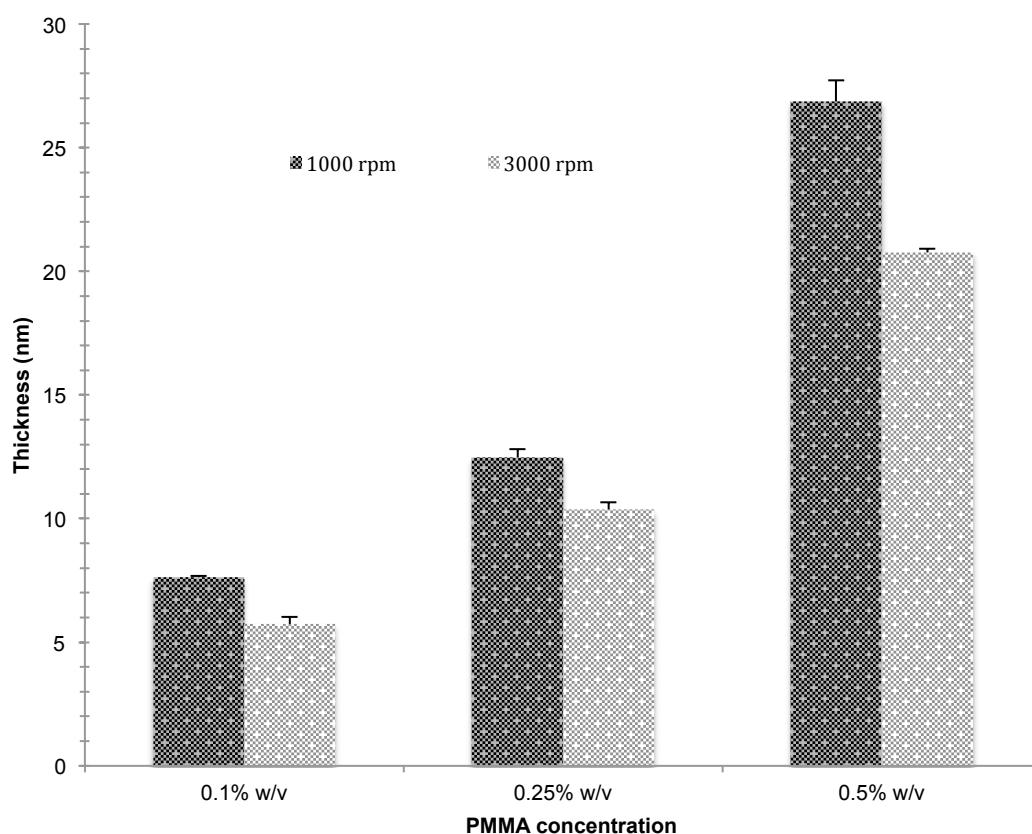
Figure 3.4 PMMA film thickness (nm) as a function of spin coating speed and concentration. Error bars are equal to the standard deviation of three water contact measurements (n=3).

Tight control over the thickness of films that support capture moieties is very important for a particularly sensitive bio analytical method, fluorescent quenching by proximity to a metal surface and surface plasmon resonance (SPR) [155]. In this method, the distance between surface-immobilised biomolecules and an underlying metal layer can be related to the strength of the quenching phenomenon: thicker PMMA spacer films reduce the quenching that occurs when a fluorophore is close to a metallic surface; thinner films increase it [158,159]. Control of the thickness of the layer allows optimisation of the distance between the metallic surface and the fluorophore in order to enhance the change in the fluorescence signal [160,161].

Spin coated PMMA shows good adhesion on all surfaces tested except for glass slides. Good adhesion of PMMA layer was observed on silicon substrates, which typically develop a thin ~2 nm silicon oxide layer on the surface. This result suggested that coating the glass slides with a thin oxide layer might improve adhesion. For this reason, the surface is activated with a thin oxide layer using hexamethyldisiloxane (HMDSO) as a precursor. Adhesion to plastics such as Zeonor®, as well as silicon, does not require any further modifications of the substrate.

3.3.2 Surface morphology of spin coated PMMA films on COP substrates pre- and post-activation by oxidation

Cyclic olefin copolymers (COP), e.g. Zeonor®, are often used in lithography and micro/nanofabrication applications as less-expensive alternatives to silicon substrates, typically as injection-moulded slides, chips, or microfluidic devices. While lacking the ultra-smooth surface characteristic of polished Si wafers, COP surfaces are generally suitable for conducting bioassays [126], with careful control of surface morphology/roughness being advisable to provide reproducible immobilisation of capture moieties and consistent binding of target analytes. Atomic Force Microscopy (AFM) was used to characterise the overall roughness and morphology of the PMMA-film-coated substrates before and after the activating treatment. Uncoated Zeonor® was compared to three types of PMMA-coated Zeonor®: as-deposited PMMA, PMMA oxidised by O_2 plasma, and

PMMA oxidised by UV/O_3. All four surfaces appeared featureless with low average roughness, < 1.4 nm, see figure 3.5.
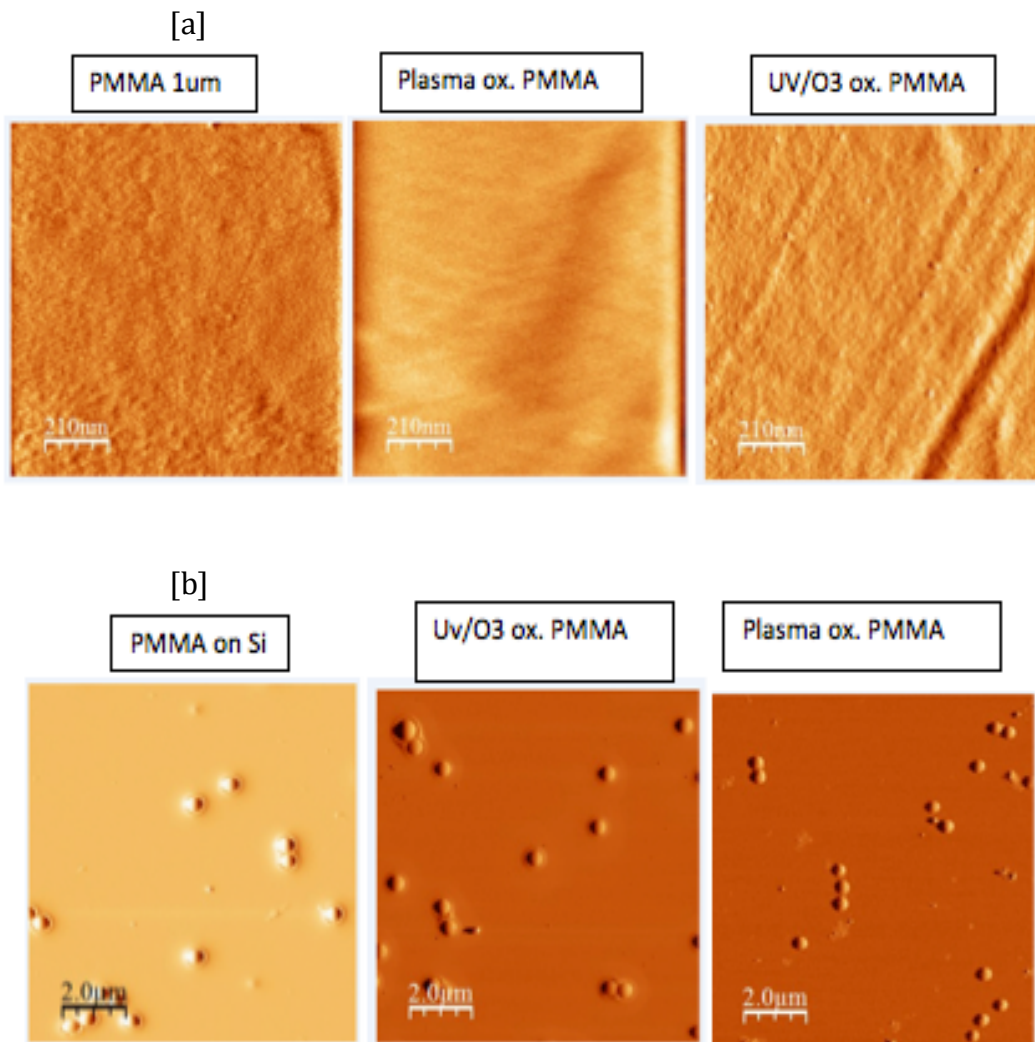
Figure 3.5 (a) AFM results of spin coated PMMA film dissolved in 80 % ethanol on Zeonor®, then oxidised by UV/O_3 and oxidised by plasma *(images from left)*; (b) AFM results of spin coated PMMA film dissolved in toluene on Zeonor®, then oxidised by UV/O_3 and oxidised by plasma *(images from left)*.

It was observed that the deposition of PMMA increases the RMS roughness from ~ 0.6 nm (uncoated Zeonor®) to ~ 1.3 nm (spin coated PMMA); treatment by either UV/O_3 or O_2 plasma oxidation then reduces the roughness to < 1.0 nm. This suggests that both oxidation processes effectively smooth the deposited PMMA layer, presumably by etching away protruding asperities. Etching

involves detachment of loosely bound chemical groups from a top layer and leaving all the finely packed and attached groups to the substrate, resulting in a

smoother layer. In terms of the RMS roughness, plasma oxidised surfaces also have a very similar roughness to surfaces treated with UV/O$_3$. The surface roughening is possibly the result of a difference in the mechanical properties between the oxidised layer near the surface (caused by atomic oxygen or ozone) and the underlying UV radiated substrate (caused by UV lamp or radiation generated at the plasma discharge). To utilise spin coated PMMA films in fabrication methods that include photolithography, and for some optical detection modalities, knowledge of the film thickness and wettability in relation to the spin coating and post-processing parameters is important. These parameters were measured with such applications in mind, and to discover any correlation between film surface morphology, film thickness and wettability.

Ellipsometry is an optical technique and it measures the change of polarization upon reflection, hence the reflective material, silicon, was used here instead of transparent glass or plastic. A thin PMMA film was spin coated from a concentration of 0.1 % w/v PMMA in toluene onto a silicon wafer at 3000 rpm for 1 minute and cured at room temperature under vacuum overnight, followed by in an oven at 90 °C for 120 minutes. Figure 3.6 represents thickness and figure 3.7 represents water contact angle measurements for the as-deposited film (spin coated PMMA) as well as after UV/O$_3$ (Ox. PMMA UV/O$_3$), and oxygen plasma treatment (Ox. PMMA Plasma).
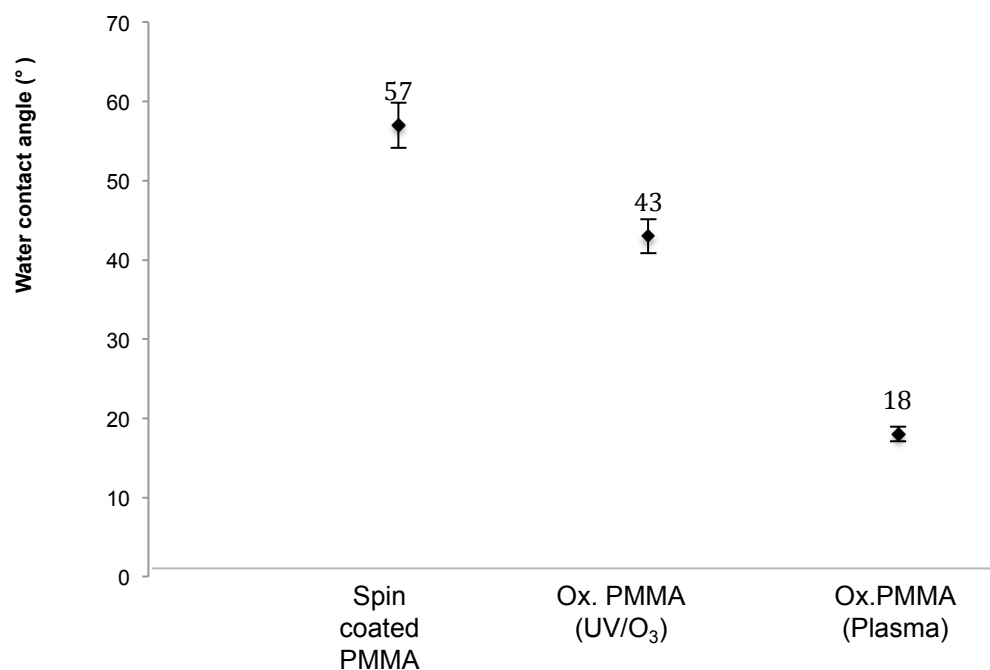
Figure 3.6 Average water contact angle of spin coated PMMA, UV/O$_3$-oxidised PMMA (ox. PMMA) and O$_2$ plasma-oxidised PMMA. Error bars are equal to the standard deviation of three fluorescence intensity measurements, n=3.
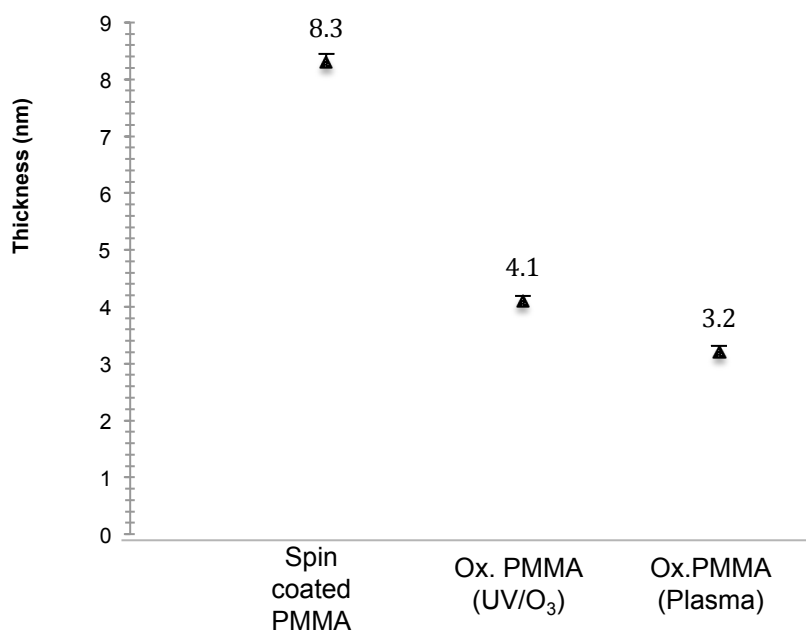
Figure 3.7 Average thickness of spin coated PMMA, UV/O$_3$-oxidised PMMA (ox. PMMA) and O$_2$ plasma-oxidised PMMA. Error bars are equal to the standard deviation of three fluorescence intensity measurements, n=3.

The thickness of the film oxidised by plasma is lower than that oxidised by UV/O$_3$. The water contact angle of the non-oxidised surface was measured at 57°, considerably higher than that of the oxidised surfaces (43° for UV/O$_3$ treated and 18° for plasma treated). This showed that the oxidation did indeed take place. The surface activation by low-pressure oxygen plasma discharge is mainly due to oxygen ion bombardment of the polymer substrate where the energy of the impacting ions, typically greater than 10 eV (230 kcal/mol), is sufficient to break any bond in the polymer. The bombardment is random and the process may involve the scission of polymer chains by cleavage of backbone bonds or the functionalisation of polymer by group removal and/or oxidation of the methyl or methyl-ester group in PMMA [114,130,156]. The data in figure 3.4 is consistent with etching that is more aggressive during plasma oxidation compared to the UV/O$_3$ process, which relies on ester group dissociation and methyl/backbone scissioning and oxidation.

The binding potential of oxidised spin coated PMMA was compared to an oxidised PMMA sheet. Immobilisation procedure was the same for both substrates: ox.PMMA sheet and ox.PMMA spin coated. Figure 3.8 shows that the spin coated PMMA was highly active after 8-minutes of oxidation and bound a substantial amount of DNA probe. On the other hand, 8 minutes oxidation was not enough to activate the PMMA sheet; hence, no DNA bound to the surface. It can therefore be concluded that spin coated oxidised PMMA provided a highly activated surface to which biomolecules could bind, when compared the oxidised PMMA in the bulk. It was suggested that this increased binding results from spin coated films acting as quasi three-dimensional structures in which there is a lack of close-packing between the functional groups when compared to the material in bulk, thus providing increased functionality on the surface [162].
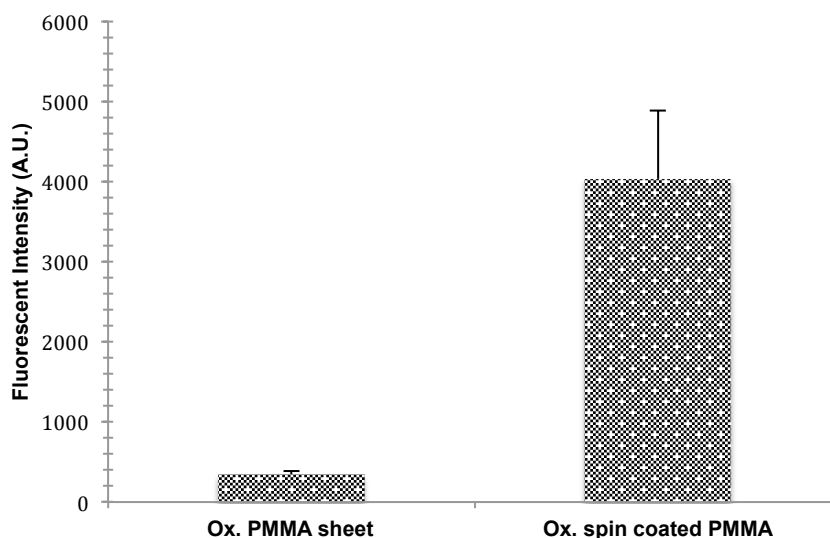
Figure 3.8 Fluorescent intensity of signal from Cy5-labelled DNA probe immobilised to ox. PMMA sheet vs. ox. spin coated PMMA, both treated with UV/O_3 for 8 minutes. Error bars are equal to the standard deviation of three fluorescence intensity measurements, n=3.

3.3.3 Covalent biomolecule immobilisation onto oxidised PMMA spin-coated films

Cy5 dye-labelled, 22-mer DNA probe was used to demonstrate the immobilisation efficacy of the activated PMMA polymer surface. DNA binding was examined for activated PMMA produced by both oxidation processes: UV/O_3 (8 minutes treatment) and oxygen plasma (1-minute treatment) with and without including a covalent linker, EDC. Figure 3.9 shows the results as fluorescence intensity, which is proportional to the quantity of DNA bound to the surface.
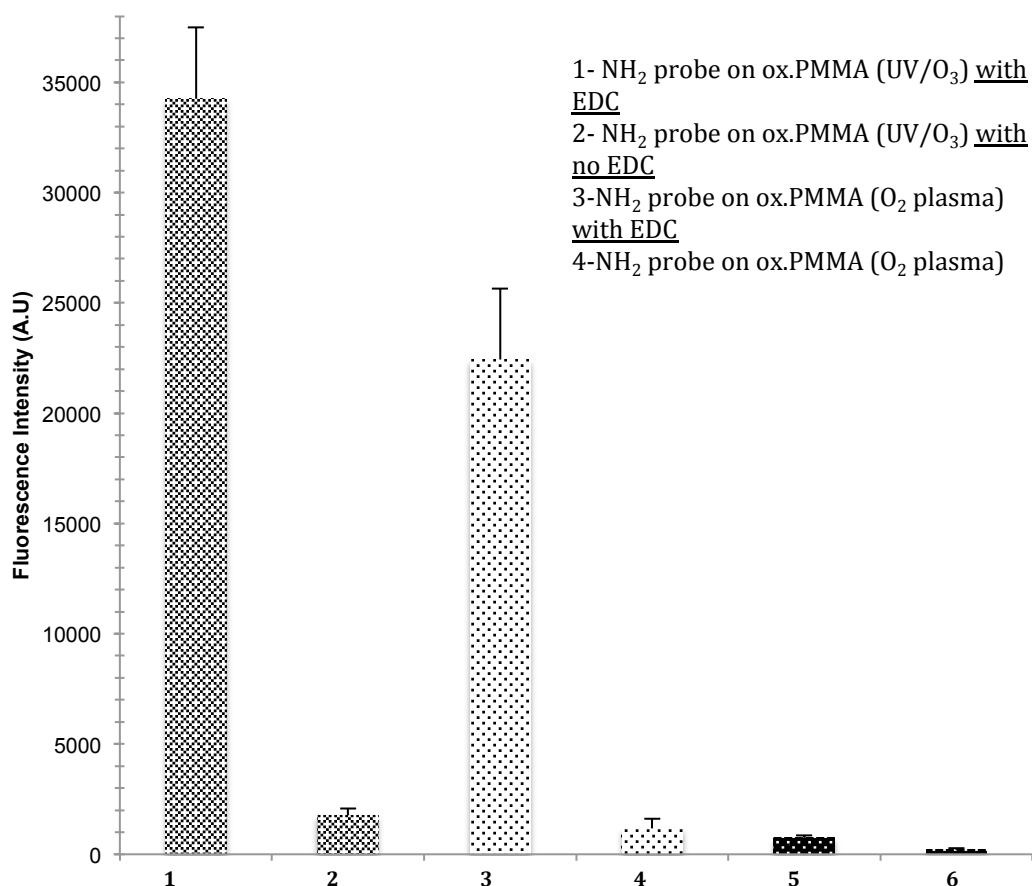
Figure 3.9 Fluorescence intensity (after one wash) of DNA probe immobilised on as deposited and ox. PMMA films (by UV/O_3 and O_2 plasma respectively), with and without EDC covalent linker. Error bars are equal to the standard deviation of three fluorescence intensity measurements, (n=3). Fluorescent intensity was measured at instrument gain of 90.

Non-oxidised PMMA has a minimal DNA probe binding, regardless of the use or lack of the EDC linker. In terms of oxidised PMMA by either UV/O_3 or plasma, the amount of DNA bound with EDC linker is much higher than DNA bound/adsorbed without EDC linker. From these results, it is clear that the binding of the probe to the oxidised PMMA is covalent and requires an EDC linker, with very little physical or non-specific binding occurring.

3.3.4 Stability of the ox. PMMA film upon washing

Chapter 2 reports on the long-term stability of spin-coated films under aqueous conditions. In this chapter adhesion of the oxidised PMMA films to the surface as well as its robustness to multiple washes is tested. In addition to results presented in Chapter 1 contact angle and thickness of deposited film is tested to reassure about stability of ox. PMMA against multiple washes.

The recipe of 0.1 % PMMA spin coated at 3000 rpm for 1 minute, followed by UV/O$_3$ oxidation, results in great adhesion and robustness against multiple washing as seen in figure 3.10 (repeat of figure 2.17).
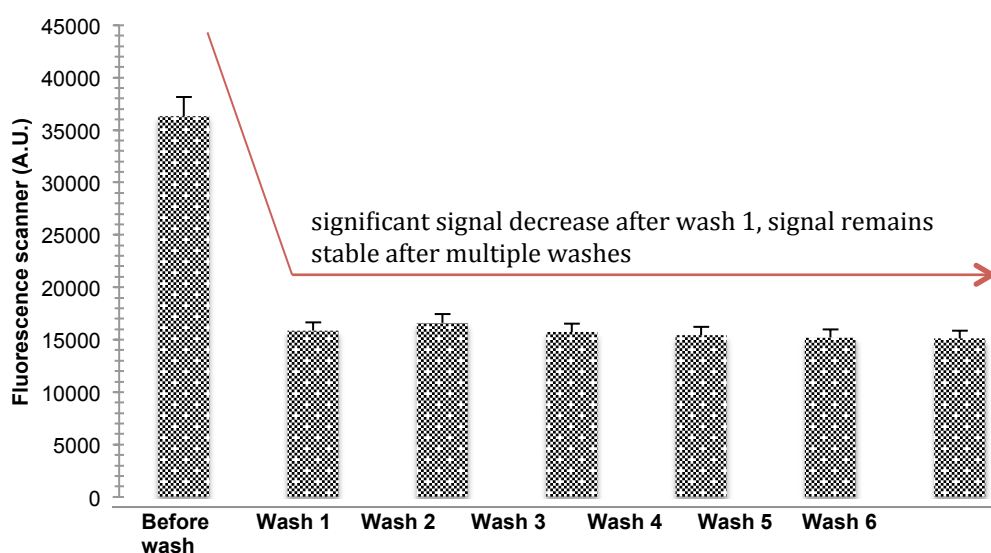
Figure 3.10 1µM DNa probe immobilised onto ox.PMMA, bars represent EDC linker in the DNA sample. Fluorescence intensity before (first bar) vs. fluorescence intensity after washes. Each wash = 20 minutes in total, 10 minutes with 2xSSC and 0.1 % SDS followed by 10 minutes with 2xSSC only. Error bars are equal to the standard deviation of three fluorescence intensity measurements, n=3.

A high fluorescence signal was apparent from the Cy3-labelled DNA before wash, suggesting that there are some physically adsorbed DNA strands on the slide. After the wash, the fluorescence signal decreases by half, indicating removal of non-covalently-bound DNA. The amount of DNA present on the surface stabilises after the first wash regardless of how many further washes were carried out (up to 6 were tested).

Stability of the spin coated PMMA against washing was investigated by additional thickness (ellipsometry) measurements. The thin film had to be spin coated on a reflective material (silicon in this instance). Silicon was spin coated with PMMA and oxidised by UV/O$_3$. The thickness was measured after each wash, see figure 3.11.
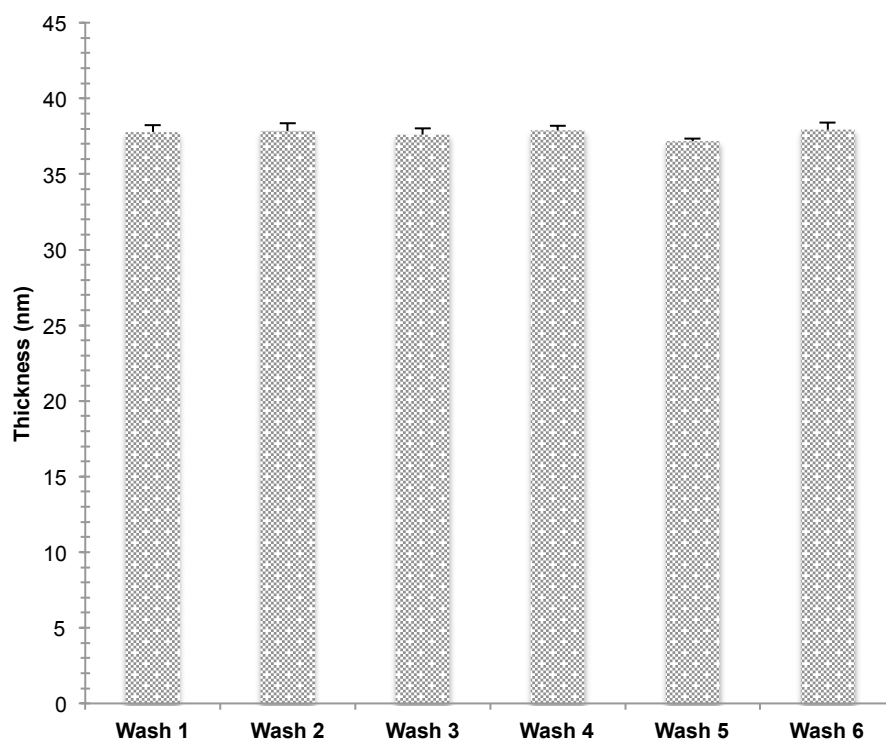
Figure 3.11 Thickness (nm) of ox. spin coated PMMA on silicon substrate after 6 washes, n=3. Each wash: 10 minutes with 0.2XSSC+ 0.01 % SDS followed by 10 minutes with 0.2XSSC. Error bars are equal to the standard deviation of three fluorescence intensity measurements, n=3.

There was no decrease in thickness of PMMA, which would suggest the PMMA film is robust against multiple washing steps. It also confirms good adhesion of the film to the substrate, silicon in this case.

3.3.5 Longevity studies

Longevity studies were carried out for PMMA films oxidised by either UV/O_3 or oxygen plasma. The aim of this study was to determine how long do carboxylic acid groups remain active following the activation process. Activity of the film after the oxidation process is paramount in order to determine storing and shelf life of the prepared films. Figure 3.12 summarises the results of a longevity study over a period of 24 days of the spin-coated film oxidised using UV/O_3.
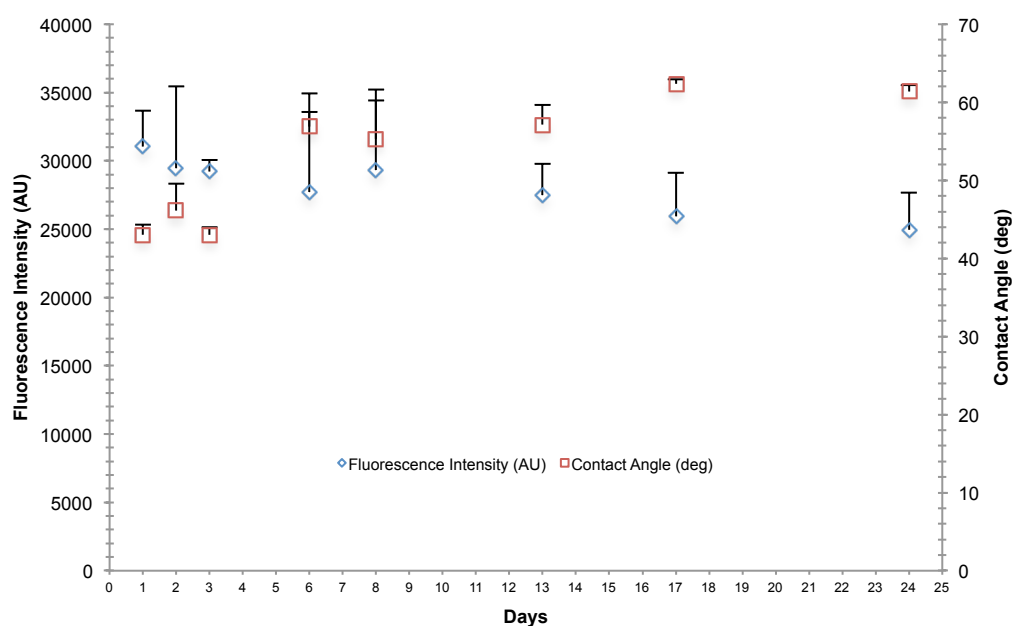
Figure 3.12 Longevity study of PMMA film spin coated and oxidised by UV/O_3 then functionalised by covalent linkage of Cy3-labelled DNA, over a period of 24 days, n=3. Error bars are equal to the standard deviation of three fluorescence intensity measurements. Fluorescent intensity was measured at instrument gain of 90.

Contact angle and fluorescence intensity of newly bound Cy3- labelled DNA were measured on the first three days in a row, followed by every 2nd/ 3rd day until day 24. DNA spotting for fluorescent intensity measurements was made on the same day the slide was tested. In Figure 3.12, slight variations in the fluorescence intensity and contact angle of the bound DNA are observed, which could be caused by variations between each coated slide. The longevity studies were also performed for spin coated PMMA on Zeonor® oxidised with oxygen plasma for 1 minute; the data are shown in figure 3.13.

114
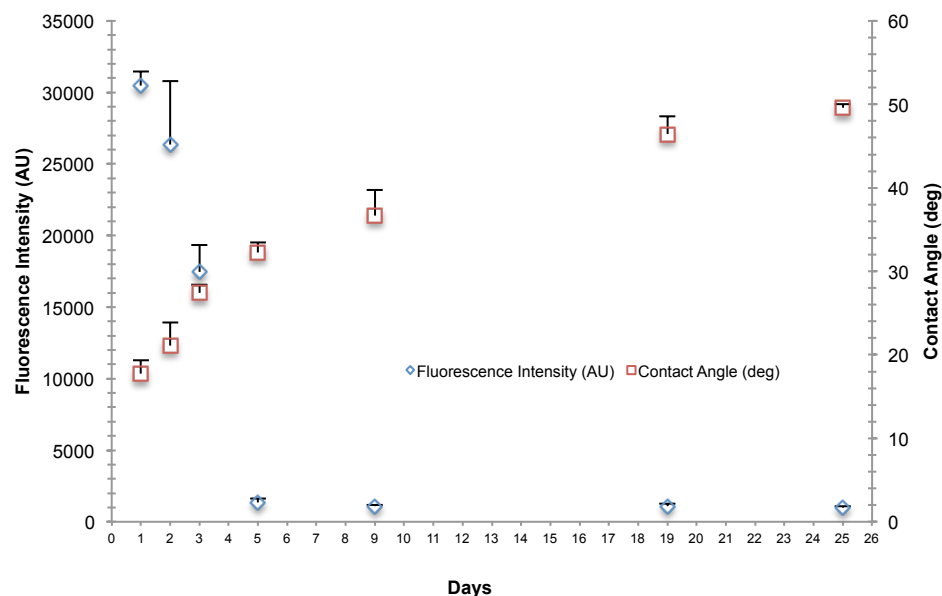
Figure 3.13 Longevity study of PMMA film spin coated and oxidised by O_2 plasma, then functionalised by covalent linkage of Cy3-labelled DNA, over a period of 25 days, n=3. Fluorescence intensity and water contact angle were measured. Error bars are equal to the standard deviation of three fluorescence intensity measurements. Fluorescent intensity was measured at instrument gain of 90.

There was a significant decrease in the fluorescence signal observed in the first 5 days. The intensity of fluorescence decreased after day 5 and remained at this level. The use of EDC linker chemistry in the fluorescence studies, alongside stringent washing protocols confirms to us that the binding occurring is covalent. The results showed that surfaces oxidised by plasma do not remain active for covalent binding for long periods when compared to those oxidised using UV/O_3, which provided strong binding for up to 24 days. A change in the water contact angle for films oxidised by plasma over 25 days indicated that the surface was unstable after oxidation.

Longevity studies indicate that UV/O_3 treated substrates retain their functionality over a longer period than those treated by oxygen plasma. The polymer PMMA absorbs UV radiation with wavelengths below 255 nm [145]. Short wavelength UV radiation (below 255 nm) is typically absorbed on the top layer of the polymer substrate up to a few hundred nanometres; the penetration depth is

115

wavelength dependent [161]. The improved longevity of the UV/O$_3$ treated samples is therefore associated with the modification method where UV radiation penetrates through the entire PMMA film, ~5-30 nm thick. Thus, the UV radiation generates carboxylic groups within the polymer, not limited to the film surface as in the case of plasma treatment. In this manner, the UV/O$_3$ treated sample is not susceptible to functionality changes on the polymer surface after polymer chain diffusion brings bulk material to the surface over prolonged periods. In the case of oxygen-plasma treated samples, only the top polymer layer is modified, but the bottom layer remains unmodified. In addition to the UV radiation, the presence of ozone has to be considered. The effect of ozone or atomic oxygen is localised to the substrate surface, as it cannot penetrate the polymer unlike the UV radiation. Yuan et al. have reported that the combined reaction of VUV and atomic oxygen with PMMA substrate is lower than the sum of individual effects indicating an interfering effect that hinders the mass removal [161].

3.3.6 Quenching of fluorophore emission

As previously described, varying the polymer concentration and spinning speed can control the PMMA film thickness. Thickness control is beneficial to control and optimise the strong quenching that occurs when a fluorophore is close to a metallic surface [146,147,154,155]. Figure 3.14 shows the fluorescence signal on a gold-coated glass substrate with thin and thick layers of spin coated PMMA. The layers measure thicknesses of 5.1 ± 0.2 nm, 11.08 ± 0.22, 15.81 ± 0.39, 26.0 ± 0.5 nm and 38.79 ± 0.44 nm respectively. The difference in the fluorescence intensity of an immobilised probe was significant: the quenched signal for the thinnest gold film was negligible compared to an unquenched signal of the thickest film.
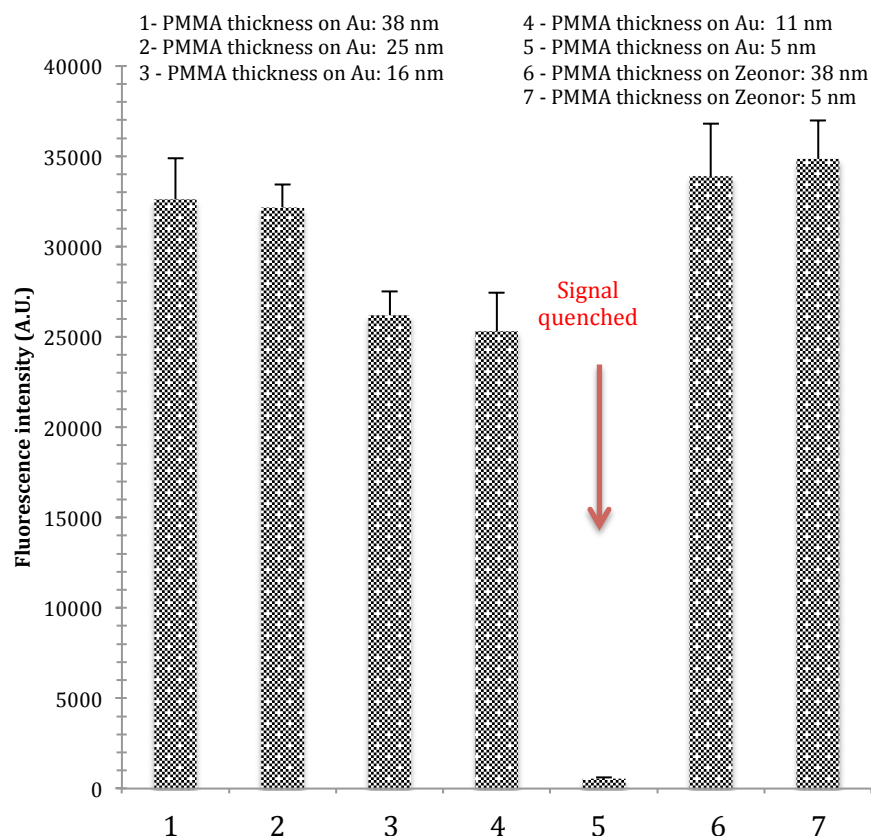
Figure 3.14 Quenching effect on different thicknesses of spin coated PMMA films on gold-coated glass substrates. The thinnest and thickest films of ox. PMMA on Zeonor® (without any gold layer) were used as a control. Error bars are equal to the standard deviation of three fluorescence intensity measurements, n=3.

The same protocol was followed for thick and thin PMMA layers without gold under layers, resulting in similarly large fluorescence signals for both. This control showed that the small signal of DNA bound to the thin PMMA layer on gold was not simply due to a lack of bound DNA.

3.3.7 DNA and antibody-binding experiments

The suitability of spin coated oxidised PMMA for performing both a DNA direct binding and an antibody sandwich assay (α-hIgG/hIgG/α-hIgG-Cy5) was investigated. A schematic diagram of both assays is shown in figure 3.15(a) and 3.15(b).
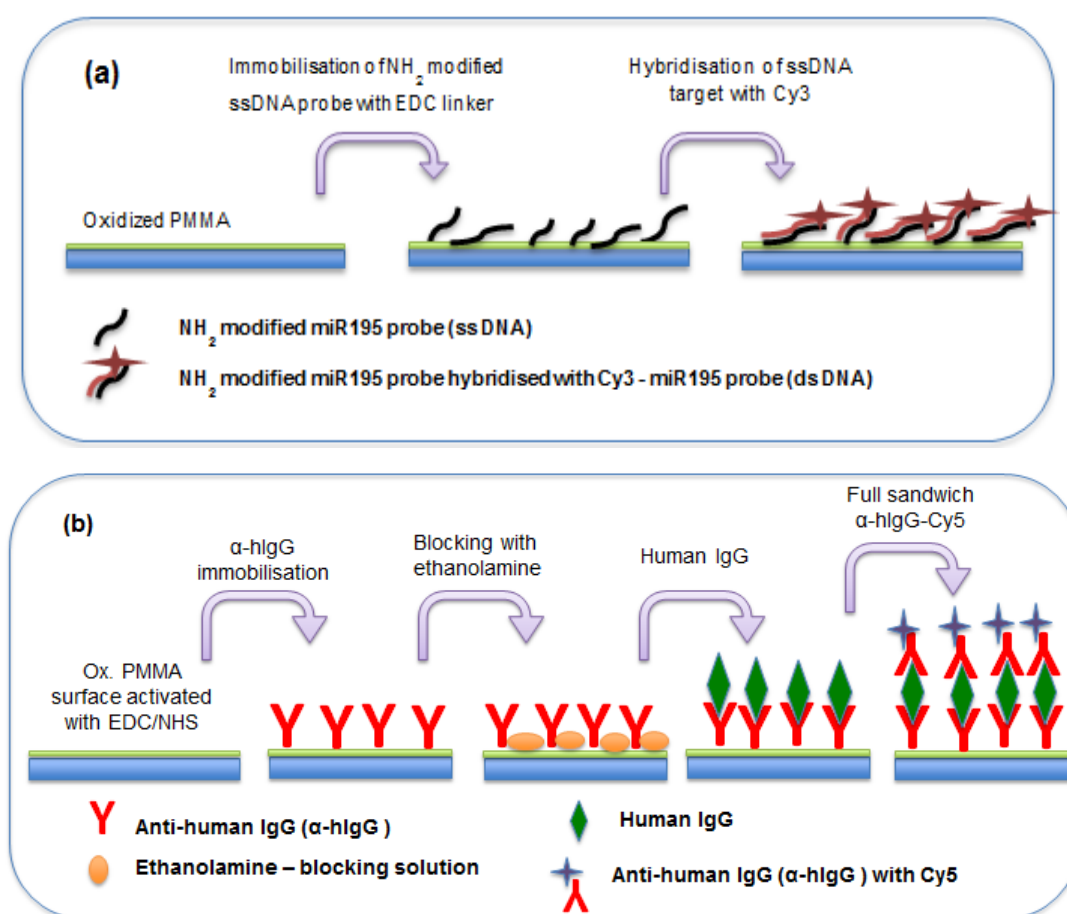
Figure 3.15 (a) Schematic diagram of DNA binding experiment on glass, spin coated with PMMA and oxidised in UV/O$_3$. (b) Schematic diagram of full IgG sandwich binding experiment on a glass, spin coated with PMMA and oxidised in UV/O$_3$.

For the DNA direct hybridisation assay, capture probes were immobilised using EDC linker chemistry and controls were used to examine NSB to the ox. PMMA surface. Results are shown in figure 3.16.
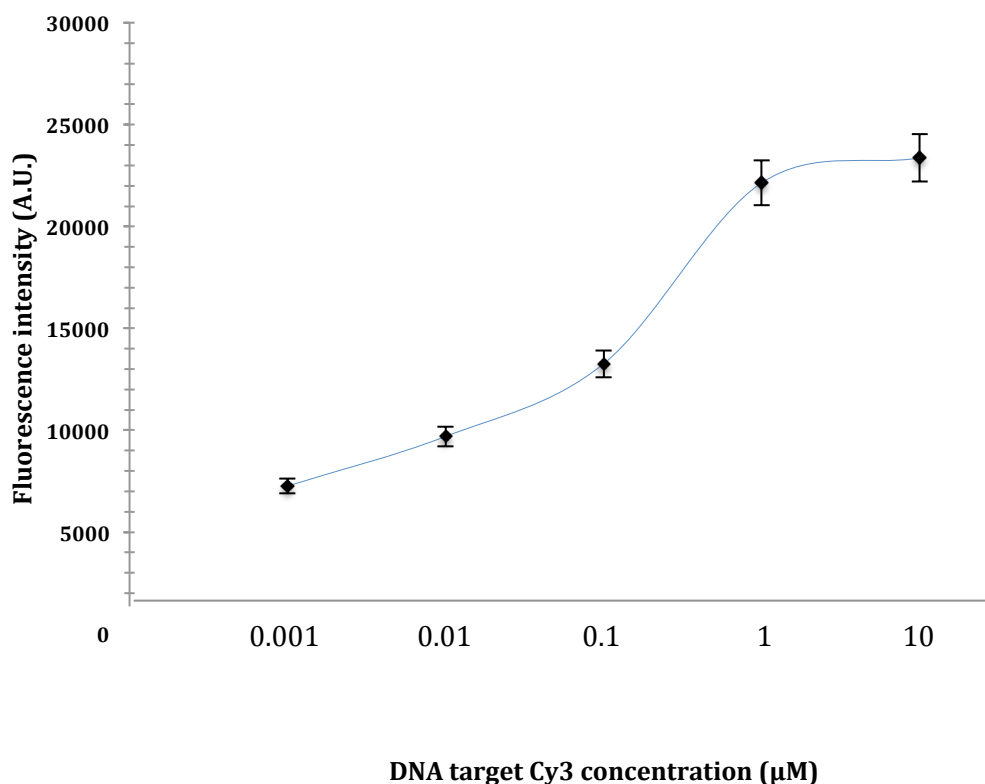
Figure 3.16 Fluorescence intensity of DNA binding experiment with different DNA target concentrations: 0-10 μM on oxidised PMMA. Fluorescent intensity was measured at instrument gain of 70. Error bars are equal to the standard deviation of three fluorescence intensity measurements, n=3.

The DNA oligomers used were amine-modified, enabling the use of EDC directly in the DNA probe solution. The fluorescence signal for the full hybridisation was significantly high, which confirms a successful hybridisation. A number of controls were carried out to determine if the high signal for DNA hybridisation was specific. All controls showed minimal fluorescence intensity. Control 1 (fluorescent intensity = 13.98 ± 4.2) showed minimal binding of aminated probe to the oxidised PMMA in the absence of EDC linker, which confirmed that EDC linker was crucial to obtain covalent DNA probe immobilisation. Control 2 (fluorescent intensity = 91.3 ± 14.3) was used to determine if the target could

bind non-specifically to the surface during the hybridisation step, since there would have been available areas on the surface after probe immobilisation. The fluorescence signal was minimal which proved that the target did not bind to the surface during hybridisation step; hence, the signal obtained for hybridisation was extremely specific. Finally, minimal fluorescence signal in Control 3 (fluorescent intensity = 26.9 ± 3.9) confirmed that the aminated-DNA probe did not bind to non-oxidised PMMA.

For the immobilisation of antibodies to the surface, EDC/NHS was used to activate the surface before adding any protein as carboxylic acid terminal groups on the protein could bind with amino terminal groups on the protein in the presence of EDC, resulting in crosslinking. Controls were used to determine specificity of the experiment. Results are shown in figure 3.17.
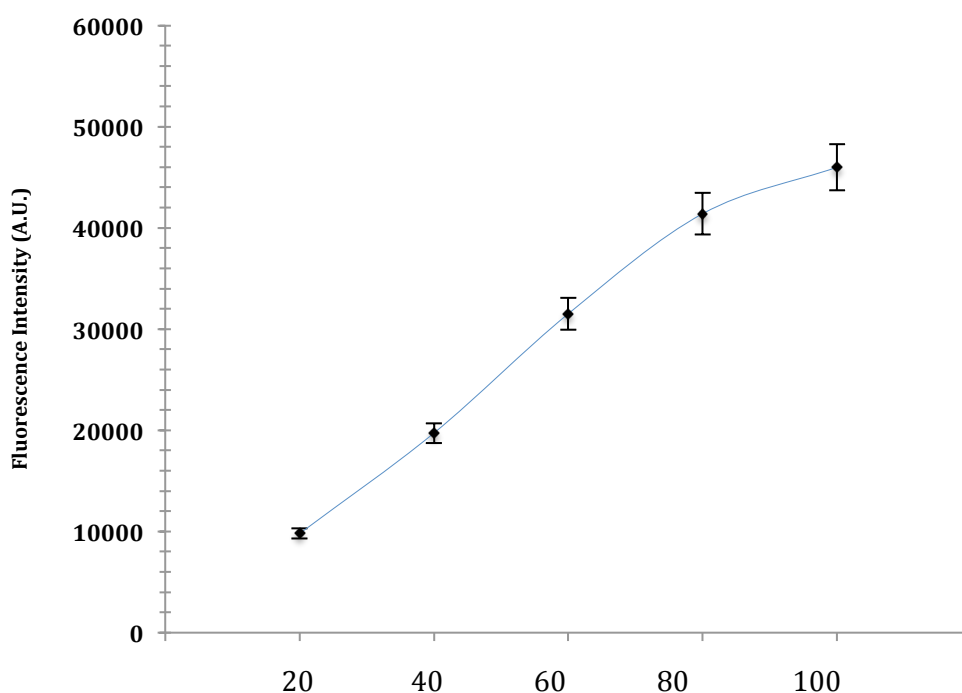
Figure 3.17 Fluorescence intensity of IgG binding experiment with different hIgG concentrations: 0-100 µg/ml on oxidised PMMA. Fluorescent intensity was measured at instrument gain of 70. Error bars are equal to the standard deviation of three fluorescence intensity measurements, n=3.

A full sandwich binding experiment was carried out showing strong and specific binding of hIgG to α-hIgG immobilised on surface, as well as specific binding of the dye-labelled α-hIgG binding to the bound hIgG. The use of Cy3-labelled anti-mouse antibody (α-mIgG-Cy3) in place of the Cy5-labelled α-hIgG as Control1 confirms the specificity of the binding (fluorescent intensity = 409.83 ± 147.84). Low signal in Control 2 (fluorescent intensity = 287 ± 97) confirmed that α-hIgG-Cy5 did not bind non-specifically when the surface was not activated with EDC/NHS. Control 3 (fluorescent intensity = 254 ± 66) confirmed that α-hIgG did not bind to non-oxidised PMMA. This showed that the oxidised PMMA surface was suitable for immobilisation of proteins followed by a low non-specific binding during sandwich binding experiments.

3.3.8   DNA direct binding performance for ox. PMMA and commercially available Epoxy

The binding ability of spin coated ox. PMMA was compared with that of commercially available epoxy slides, see figure 3.18. Different probe concentrations were spotted on the surface (using EDC for PMMA, no EDC is required for epoxy slides), incubated and washed following the standard protocol described in experimental methods section. The slides were then dried and imaged.
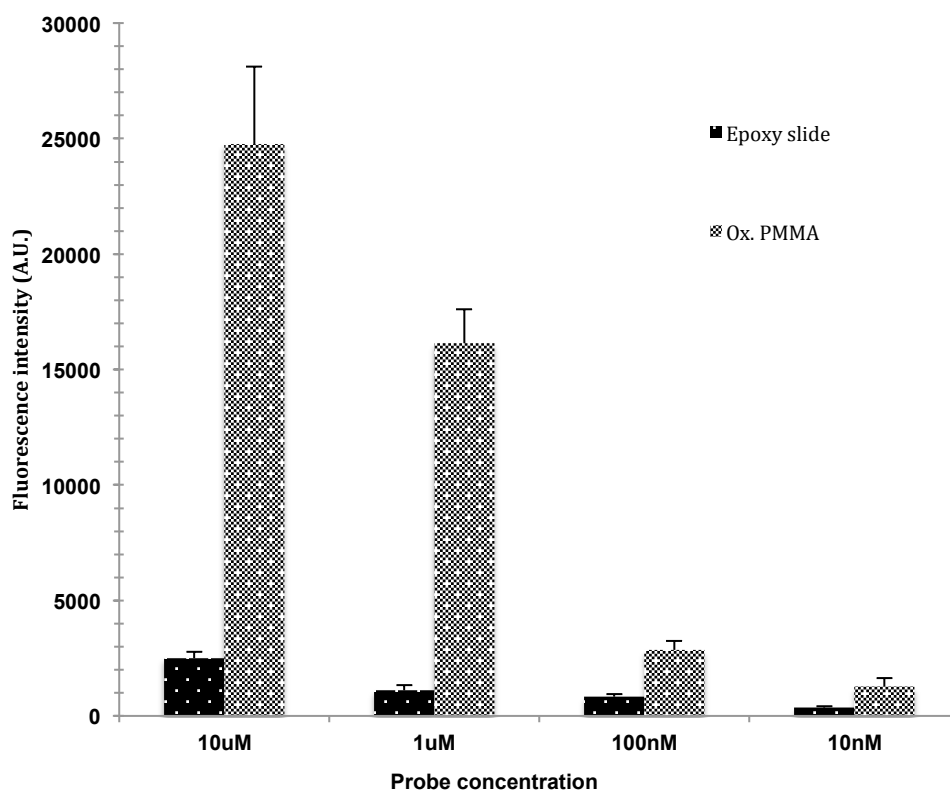
Figure 3.18 Comparison of commercially available Epoxy substrate with the spin coated ox. PMMA. Four different probe concentrations used: 10 μM, 1 μM, 100 nM and 10 nM. Scanned at instrument gain of 70. Error bars are equal to the standard deviation of three fluorescence intensity measurements, n=3.

It can be seen that the ox. PMMA surface binds up to ten times the amount of probe than the commercially available epoxy slides. The difference in probe binding is significant between two surfaces. Increased signal on ox. PMMA is a great advantage in order to enhance the signal and to lower limit of detection. Biomarkers in human's bloodstream are present in extremely low quantities; hence the sensitive detection method/surface is required. The test above confirm, that ox.PMMA is more suitable surface to be used for further research even when compared with the one commercially available.

3.4 Summary and conclusion

A method to prepare a carboxylic acid functional film on different substrates for use in bioassays is reported in this chapter. By varying the condition of the PMMA spin coating process, including PMMA concentration and solvent; thin, smooth and uniform PMMA films are achieved. Tight control over the thickness of films that support capture moieties is very important for a particularly sensitive bio analytical method, fluorescent quenching by proximity to a metal surface. In this method, the distance between surface-immobilised biomolecules and an underlying metal layer can be related to the strength of the quenching phenomenon: thicker PMMA spacer films reduce the quenching that occurs when a fluorophore is close to a metallic surface; thinner films increase it. Spin coated PMMA shows good adhesion on all surfaces tested except for glass slides. The PMMA adhesion onto a glass slide can be improved by coating the glass slides with a thin oxide layer. Hence, it was suggested to pre treat the glass with a thin oxide layer using hexamethyldisiloxane (HMDSO) as a precursor prior PMMA spin coating. Adhesion to plastics such as Zeonor®, as well as silicon, does not require any further modifications of the substrate.

In this chapter PMMA surface activation is investigated. Two different techniques were used to generate carboxylic functionalities, which enable covalent binding of amino modified biomolecules:

- oxygen plasma

- UV/O$_3$.

AFM technique was used to characterise the overall roughness and morphology of the PMMA-film-coated substrates before and after the activating treatment. It was observed that the deposition of PMMA increases the average height, however treatment by either UV/O$_3$ or O$_2$ plasma oxidation then reduces the roughness. This suggests that both oxidation processes effectively smooth the deposited PMMA layer, presumably by etching away protruding asperities. Etching involves detachment of loosely bound chemical groups from a top layer and leaving all the finely packed and attached groups to the substrate, resulting in

a smoother layer. There were no significant differences in average thickness between plasma oxidised surfaces to surfaces treated with UV/O$_3$.

This chapter successfully demonstrates covalent amino modified DNA biomolecule immobilisation onto ox. spin coated PMMA. In this chapter the long-term stability of spin-coated films under aqueous conditions was investigated. In addition to results presented in Chapter 2 contact angle and thickness of deposited film is tested to reassure about stability of ox. PMMA against multiple washes. Longevity studies were presented to compare the stability of the films after the oxidation treatment by UV/O$_3$ and plasma. UV/O$_3$ with comparison to oxygen plasma shows excellent stability of reactivity for a period of up to 24 days. This result could be particularly useful in biosensor applications and confirms that PMMA could be prepared in batches before being employed as a platform. A DNA direct binding assay and IgG immunoassay were successfully demonstrated, confirming the applicability for POC devices and bioassays, specifically showing low non-specific binding. It was shown that by manipulating the spin coated PMMA film thickness on a gold substrate, reduction of the strong quenching or enhancing of the fluorescence signal can be achieved. It can be particularly useful in surface plasmon resonance techniques such as TIRE, where the substrate is gold and the immobilised biomolecule has a fluorophore attached. To avoid quenching of the dye, a thicker film should be applied to increase the distance between metal and fluorophore. The ease of preparation, robustness and plausibly cost effectiveness of PMMA films can possibly find its application in carboxylic acid functionalisation of substrates such as glass, plastic, silicon and many more. The surfaces developed here are currently being used in the development of a point-of-care breast cancer diagnostics assay. Finally the suitability of spin coated ox. PMMA for performing both a DNA direct binding and an antibody sandwich assay (α-hIgG/hIgG/α-hIgG-Cy5) was shown. The overall binding performance was compared between ox.PMMA spin coated films and commercially available Epoxy slide. The difference in probe binding is significant between two surfaces. The ox. PMMA surface binds up to ten times the amount of probe than the commercially available epoxy slides. Increased signal on ox. PMMA is a great advantage in order to enhance the signal and to lower limit of detection. The test above confirm, that ox.PMMA is more suitable surface to be used for further research even when compared with the one commercially available.

Table. 3.1 Summary of chapter 3 – key messages.

CHAPTER 3 – key messages
• Smooth and uniform PMMA film achieved by controlled varying of the process conditions; i.e.: PMMA concentration, spin coating speed and time   •
• Spin coated PMMA shows good adhesion on all surfaces tested
• Minimum NSB demonstrated on ox. PMMA
• Longevity for up to 24 days, films can be prepared and stored
Work published in Journal of Materials Chemistry B – Royal Society of Chemistry

Chapter 4

4 Click chemistry as an immobilisation method to improve oligonucleotide hybridisation efficiency

4.1 Introduction

Following the results from the previous chapter, an improvement of immobilisation technique was required due to DNA BB binding with EDC linker, which had a negative effect on assay efficiency. A novel bio-conjugation method – click chemistry, is proposed; development, optimisation and application of the method are described in this chapter.

This chapter is based on work, which was submitted to be published in *Sensors and Actuators B: Chemical.*

This chapter reports on the conditions under which amino-modified ssDNA immobilisation onto carboxylic acid surfaces using EDC linkers leads to binding at multiple anchoring sites, i.e. BB binding; here the effects of such binding on overall hybridisation efficiency are described. An alternative conjugation method, click chemistry, is shown to improve the quantity and quality of target binding by enabling direct covalent attachment of probe oligonucleotides to the surface without BB binding. EDC and CC approaches are compared in terms of hybridisation efficiency in a direct DNA hybridisation experiment. Work presented in this chapter is directed, ultimately, at improvement of the immobilisation of microRNA (miR) probes onto lab-on-a-chip surfaces for the development of a BC assay; accordingly, our results here use DNA analogues of miR195 (miR195 is stably expressed by breast cancer cells [26–29] and miR16 is an endogenous control to standardize miRNA expression [29]).

Surface arrays of single-stranded DNA (ssDNA) are at the centre of some of the most active areas in biological research as well as practical devices and applications, including point-of-care (POC) devices [163–167]. However, there are still technical hurdles to overcome to make bimolecular diagnostic devices fully robust and reliable.

The improvement of DNA- and protein-based biosensors and microchips often hinges upon the reproducible and effective immobilisation of biomolecules onto solid

substrates [38,168,169], critical to enabling low limits of detection [170]. A well-known approach for producing nucleic acid microarrays is to modify the biomolecule utilised to capture the target of the assay, e.g. a DNA oligomer, with a functional group that allows covalent attachment to a reactive group on the surface [171–173]. For example, oligonucleotides are patterned onto a chemically active surface, using spotting or printing technologies, and immobilised through functional groups on either the 5'- or 3'-oligonucleotide terminus. One class of immobilisation approach uses amine-modified oligonucleotides, which have broad applicability as they can react with carboxylic acid-[174], aldehyde-[175],[176], epoxy-[177],[173] and isothiocyanate-modified surfaces [134]. This amine-modification strategy is just one of several methods for immobilisation of ssDNA probes to surfaces [178], including:

- covalent binding of DNA to self-assembled monolayers of aminosilanes using heterobifunctional cross-linkers [179],

- attachment of thiol-modified oligonucleotides to thiol-functionalised silicon wafers using bi-functional alkyltrichlorosilanes [180],

- tethering of DNA to glass slides via an epoxysilane–amine covalent linkage [181],

- chemo selective coupling of oligonucleotides to alkanethiol SAMs on gold [182], (e) cross-linking to poly-L-lysine-coated surfaces [183], and

- immobilisation of DNA onto solid supports through electrostatic interactions [184].

PMMA is a particularly attractive material for the fabrication of low-cost platforms for POC devices, as described previously in chapter 2 and chapter 3. Pristine PMMA is a relatively inert and moderately hydrophobic material; it does not possess a suitable interfacial chemical structure for covalent surface immobilisation of biomolecules. Consequently, without treatment, bio-recognition moieties such as oligonucleotides and antibodies can only be non-covalently adsorbed on the methyl ester surface, resulting in poor device performance. Previous published work shows that appropriate surface treatment permits PMMA to be functionalised to enable the covalent attachment of biomolecules for bioassay development with little non-specific binding [3]; hence PMMA was selected as the substrate in this work.

Most methods of oligonucleotide immobilisation rely on traditional nucleophilic-electrophilic reactions to achieve coupling of the oligonucleotide to the surface [163,182]. 1-Ethyl-3-(3-dimethylaminopropyl) carbodiimide (EDC) is widely known and the most frequently used carbodiimide [185 - 186]; it reacts with carboxylic acids to form an *O*-acrylisourea intermediate, which subsequently reacts with primary amines to form amide bonds [187]. Attributes of EDC include water solubility, meaning EDC can be directly used with proteins or DNA in aqueous buffer. However, EDC is prone to hydrolysis before and during the coupling reaction, which reduces coupling yields and the half-life of the reagent, as well as making yields irreproducible [188] and promoting the formation of by-products [189–191]. In certain experiments, ethanolamine was used as a surface-blocking agent. This molecule reacts with any activated carboxylic groups remaining on the surface after the DNA immobilisation step [192], figure 4.1, and therefore prevents non-specific binding of target to the surface.
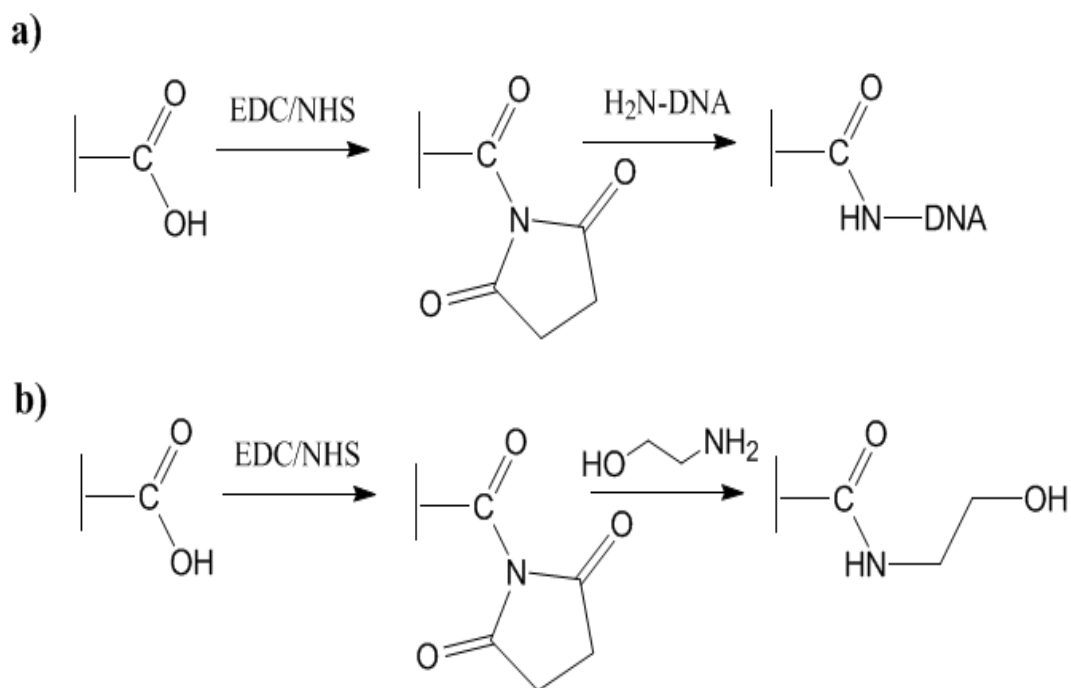
Figure 4.1 a) Covalent coupling of the –NH$_2$ of proteins to a carboxylic acid-terminated surface; b) blocking of unreacted *N*-hydroxysuccinimide esters via ethanolamine.

During this study the evidence of an additional shortcoming of EDC coupling of ssDNA was discovered: EDC could enable amines present on the backbone (BB) of the DNA strand, particularly the primary amines, see figure 4.2, available on adenine, guanine

and cytosine to bind to the carboxylic acid surface alongside the terminal amino group; see figure 4.3. Melting curve analysis was used here to confirm the above hypothesis of EDC drawback. If some of the primary amines normally involved in hydrogen bonding

during hybridisation are therefore unavailable, a smaller number of hydrogen bonds hold the duplex together. At room temperature, mismatches, which also result in smaller numbers of H bonds, do not prevent complementary binding: there is low specificity of hybridisation. At higher temperatures, tolerance to mismatches is comparatively lower and at some "melting temperature", Tm, de-hybridisation occurs. Temperature studies can therefore be used as a means to understand the degree of mismatch (or absent H bonds) in the DNA double helix [193]. Higher temperature hybridisation experiments were carried out to determine the overall binding strength of the DNA hybrid.
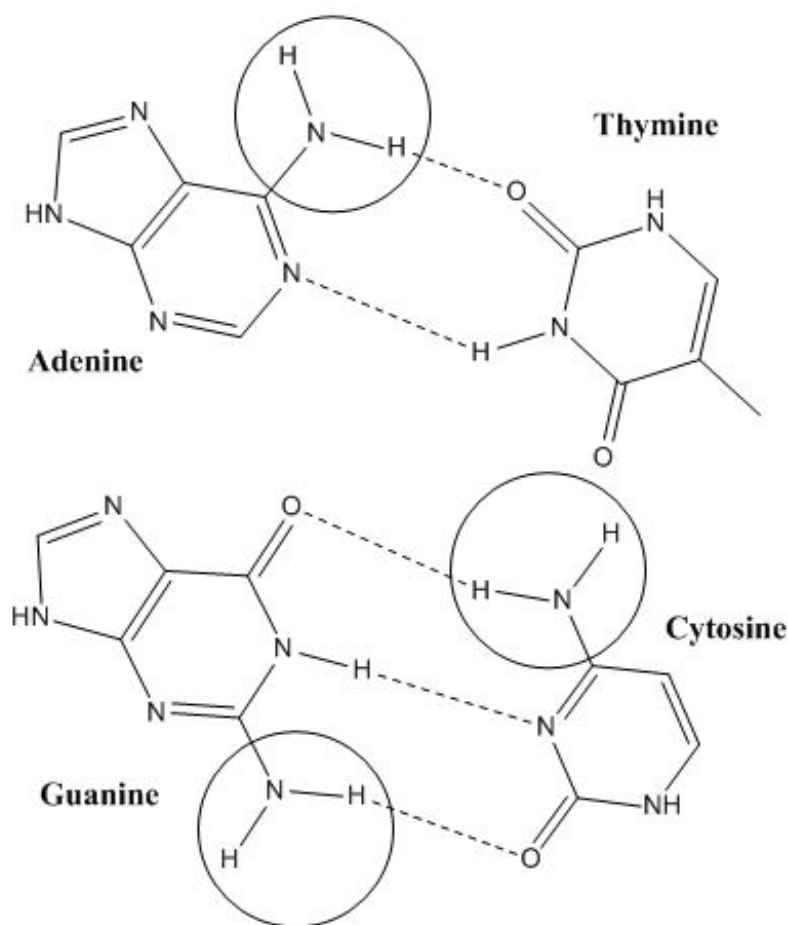
Figure 4.2 Chemical structure of DNA bases; highlighted are bases containing primary amines (adenine, guanine and cytosine).
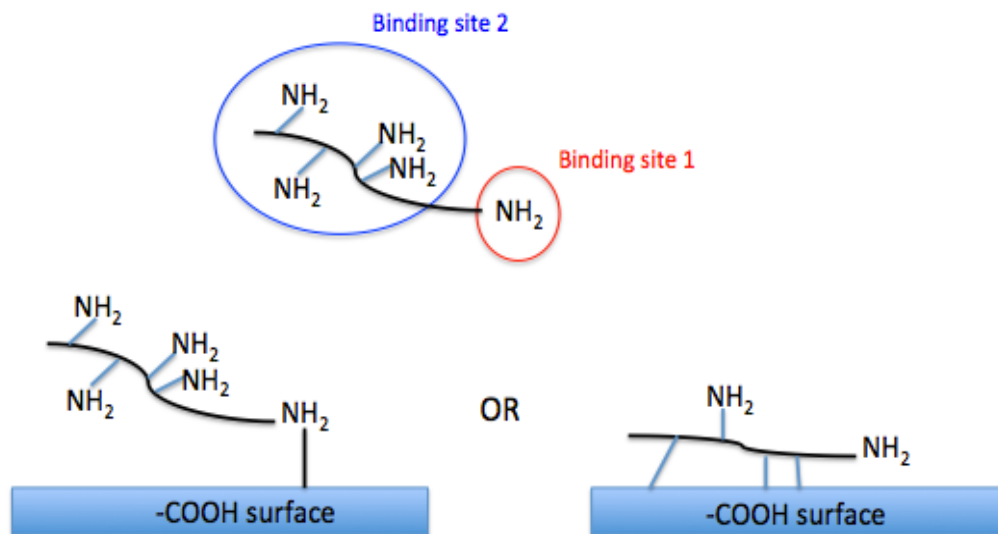
Figure 4.3 Possible ways that amino-modified ssDNA can anchor via EDC to carboxylic acid-functionalised surfaces: Binding site 1 = binding via NH_2-modified terminus; Binding site 2 = binding via BB amines in nucleobases.

In the processes of DNA microarray fabrication, surface activation strategies are widely used to covalently bind probes to surfaces, but technical challenges still plague these methods [194], see table 4.1. Consequently, simple, direct covalent bond formation without by-products would often be preferable.

Table 4.1 Microarray challenges and drawbacks [45,46].

Microarray drawbacks	
Lack of standardisation	Direct comparison of collected data between different reseach groups proofs difficult and inacurate
Inadequate computer based tools	Interpreting microarray experiments is challenging due to the lack of universal bioinformatics models and tools, whicg could enable quick and efficient analysis of the large data sets created within each experiments
Statistical problems	Statistical problems ranging from image analysis to pattern discovery and classification exist.
Insufficient quality	Lack of the way to be able to characterise the quality of microarrays to ensure full functionality
Insufficient sensitivity	Flase results picture due to the poor sensitivity and background noise forces amplification
Lack of reproducibility	Variations between array's coefficients has an negative effect on reproducibility of microarray results
Variability of outcome and fidelity of gene expression data	Application of different bioinformatic protocols to the same microarray making clinical decisions difficult
Effects of probe length	It has shown that for complex diseases a considerable discrepancy exists between the differentially expressed genes identified on oligo arrays arrays and those identified on cDNA microarrays
Cost	Cost associated with design and fabrication of custom microarrays is high but falling. Replication of experiments to minimise statistical variability of results can be also cost prohibitive
Technical challenges	Air bubbles preventing successful spotting

Recent studies have demonstrated that CC is well suited for coupling biomolecules to surfaces [195]. The basic foundations of CC, developed by Sharpless *et al.* [196,197], are now supplemented by several modifications [198]. The best suited of these for microarray construction, arguably, is the Cu(I)-catalysed variant of alkyne–azide cycloaddition (CuAAC) [199], in part because neither azide nor alkyne groups are typically encountered in natural biomolecules: this reaction is highly bio-orthogonal and specific, meaning it is unlikely to interfere with native biochemical (binding) processes [200].

4.2 Experimental details

Click chemistry was applied as an immobilisation technique for DNA bio-conjugation to the solid support (ox.PMMA). Ox.PMMA surface requires further modification to obtain an alkyne modified film and DNA probe is azide modified. Quartz crystal microbalance (QCM) is used in this chapter to quantify the amount of probe bound and compare between CC and EDC linking techniques. Direct and sandwich assays are performed to obtain LOD.

4.2.1   Materials and instrumentation

Poly (methyl methacrylate) sheets (0.25 mm thick, impact modified, MW = 120,000) were purchased from Goodfellow Cambridge Limited (Huntingdon, England). Zeonor® substrates in the form of injection-molded cycloolefin polymer (COP) slides (Zeonor® 1060R, 25 mm × 75 mm, 1 mm thick) were sourced from Sigolis (Uppsala, Sweden). 1-Ethyl-3-(3-dimethylaminopropyl) carbodiimide, ethanol, (95 %) 1-amino-3-butyne (95 %), sodium *L*-ascorbate (≥ 98 %), copper (II) sulfate (≥ 99 %), 4-morpholineethanesulfonic acid sodium salt (MES) hydrate, phosphate-buffered saline (PBS), sodium chloride and trisodium citrate (30M and 300m respectively were used to make saline sodium citrate (SSC), sodium dodecyl sulfate (SDS), and ethanolamine (≥ 99 %), sulphuric acid (H$_2$SO$_4$, 99.999%), hydrogen peroxide solution (H$_2$O$_2$), were all purchased from Sigma Aldrich (Arklow, Ireland). All DNA probes including those pre-labelled with Cy3 and Cy5 (Table 4.2) were purchased from Eurofins MWG Operon (Ebersberg, Germany), except for the azide-miR195 probe (5'/azide/GCCAATATTTCTGTGCTGCTA-3'), which was sourced from

Integrated DNA Technologies (IDT, Leuven, Belgium). All reagents were used as received without further purification.

Instrumentation used in support of this work in chapter 4:

- Spin coater
- UV/O_3 and O_2 plasma
- QCM
- Fluorescence scanner
- AFM

Table 4.2: Oligonucleotides sequences and their abbreviations.

*A = adenine, C = cytosine, G = guanine, T = thymine

DNA sequence	Abbreviation	Abbreviation explained
5'/Amino/GCC AAT ATT TCT GTG CTG CTA-3'	NH_2-mod-P	Amino-modified probe
5'/Amino/GCC AAT ATT TCT GTG CTG CTA(Cy5)-3'	NH_2-mod-P(Cy5)	Cy5-labeled Amino-modified probe
5'GCC AAT ATT TCT GTG CTG CTA-3'	Unmod-P	Unmodified probe
5'GCC AAT ATT TCT GTG CTG CTA(Cy5)-3'	Unmod-P(Cy5)	Cy5-labeled unmodified probe
5'/Amino/GCC AAT ATT TCT GTG CTG CTA(Cy5)-3'	NH_2-mod-P(Cy5)	Cy5-labeled amino-modified probe
5'/Azide/GCC AAT ATT TCT GTG CTG CTA-3'	N_3-mod-P	Azide-modified probe
5'/Azide/GCC AAT ATT TCT GTG CTG CTA(Cy5)-3'	N_3-mod-P(Cy5)	Cy5-labeled Azide-modified probe
5'-(Cy3)TAG CAG CAC GTA AAT ATT GGC G-3'	T(Cy3)	Cy3-labeled DNA target
5'(Cy5)AAA AAA AAA AAA AAA-3'	A chain	Unmodified adenine-only oligonucleotide
5'(Cy5)TTT TTT TTT TTT TTT -3'	T chain	Unmodified thymine-only oligonucleotide
5'(Cy5)ATC GTC GTG-3'	RP(Cy5)	Cy5-labeled reporter probe
5'/Azide/GCC AAT ATT TCT-3'	CP-azide	Capture probe azide
5'/Amino/GCC AAT ATT TCT-3'	CP-amine	Capture probe amine

4.2.2 Preparation of spin coated poly (methyl methacrylate) surfaces

Protocol for preparations of spin coated PMMA is as follows:

- Take off protection film from the PMMA sheet
- Cut PMMA sheet into small pieces
- Weight out 0.001g of PMMA pieces for 0.1 PMMA concentration respectively
- Place into a glass vial with 10 ml of 80 % ethanol to result in 0.1 % PMMA concentration.
- Use sonicator at 40° for 30 minutes to dissolve the PMMA pieces
- Filter dissolved PMMA solutions through PTFE filter (pore size 0.25 µm)

Cleaning of the substrates prior spin coating:

- Fill the tank with 2 % of Micro90 detergent for cleaning step
- Place the slides in a slider holder and submerge them in Micro90
- Sonicate for 30 minutes
- Rinse slides in water
- Fill another tank with isopropanol and submerge slides
- Sonicate for 30 minutes
- Rinse slides in water
- Dry with nitrogen stream

Spin coating of dissolved PMMA protocol:

- Place a slide at the centre of spin coater's holder
- Apply vacuum to immobilise the slide
- Place 1 ml of dissolved PMMA solution on the middle of the slide
- Set the settings: 3000rpm, 5 seconds acceleration for 1 minute
- Press start
- Take the slide off and transfer to a holder

The curing process protocol:

- The PMMA films are cured in an oven at 80 °C for 1 h or in the fume hood over night.

Oxidation of spin coated PMMA surfaces:

- Place cured PMMA samples (do not touch the interface, pick up by the edge of the slide) onto UV/O$_3$ device
- Initiate oxidation for 4-8 minutes as required
- Remove samples from the device
- Alternatively oxygen plasma can be used to activate the surface (4-8 minutes).

The coating of PMMA films onto microscope glass slides required an additional step, due to the hydrophobicity of the glass slides. The water contact angle of glass slides is very low; hence, the PMMA solution could not gain contact with it during spin coating. In order to modify the hydrophobicity of the glass, the deposition of a silicon oxide layer was applied to ensure adhesion of the PMMA. The silicon oxide was deposited with a plasma enhanced chemical vapour deposition (PECVD) method using a Plasmalab 100 system. The precursor reagents for this process were oxygen gas and hexamethyldisiloxane (HMDSO). The silicon oxide layer thickness was approximately 30 nm.

4.2.3   DNA washing protocol

Each washing step for DNA described contains three distinct stages; 10 minutes in 0.2XSSC + 0.1 % SDS followed by two 10 minutes washes in 0.2XSSC. After initial immobilisation, slides were washed once (all three stages). The fluorescent signal measured then was taken as the signal from covalently bound DNA (having removed most of the physically bound DNA). Each wash step thereafter contained the three wash stages.

4.2.4 Alkyne-functionalised oxidised PMMA

A new type of surface suitable for click chemistry-based probe immobilisation was prepared as per protocol:

- ox. PMMA was modified with 1 % solution of 1-amino-3-butyne 100 mM EDC in DiH$_2$O
- incubate for 40 minutes at room temperature. This step allows carboxylic acid groups on the surface (ox. PMMA) to bind to the amino-group end of the molecule, forming an "alkyne-active" layer (-C≡CH).
- Following incubation, 20 minutes washing was applied: 10 minutes in 0.2XSSC + 0.1 % SDS and 10 minutes in 0.2X SSC.

4.2.5 Probe immobilisation with EDC

- Spot manually onto ox.PMMA: 1 μM of probe (NH$_2$-mod-P or unmod-P) in 1000 μL of MES, pH 6.5, with 100 mM EDC
- Incubate for 40 minutes
- Remove spotting solution by vacuum
- Wash the slide extensively: 10 minutes in 0.2XSSC+0.1 % SDS
- Followed by two 10-minute washes in 0.2XSSC
- Dry the slide by centrifugation.

4.2.6 Probe immobilisation with click chemistry

- Modify ox.PMMA as per section 4.2.4.
- Mix 250 μL of 0.5 M of CuSO$_4$ and 2.47 mg of sodium ascorbate together for 10 minutes to produce Cu(I); the solution is orange in colour
- Add 500 μL of 50 % DMSO to this solution
- Add 7.5 μL of 100 μM of N$_3$-mod-P to the solution
- Spot manually the alkyne surface with 50 μL spots
- Incubate for one hour in the humidity chamber
- Remove spotting solution by vacuum
- Wash the slide extensively: 10 minutes in 0.2XSSC+0.1 % SDS

- Followed by two 10-minute washes in 0.2XSSC

- Dry slide by centrifugation or stream of nitrogen.

4.2.7 Ethanolamine blocking and target hybridisation

- Spot 0.1 M ethanolamine (in water) onto a surface
- Incubate for 15 minutes in humidity chamber to deactivate the EDC
- Rinse twice with 0.2X SSC.
- Following blocking step, target can be introduced
- Spot manually 1000 µL of 0.1 µM of T(Cy3) in 2X SSC onto the previously immobilised probe spot
- Incubate for three hours in a humidified chamber to avoid evaporation of the spotted solution
- Remove the spotting solution by vacuum
- Wash the slide extensively: 10 minutes in 0.2XSSC+0.1 % SDS
- Dry slide by centrifugation or stream of nitrogen.

4.2.8 Melting curve analysis

- DNA probes were immobilised onto a slide, as per 4.2.5. and 4.2.6.
- Complimentary target was hybridised, as per 4.2.7
- Melting curve analysis experiments were performed by heating each slide in a humidified oven at a specific temperature
- Each slide generates just one point on the melting curve
- The slides and washing buffers were left in the oven for approximately two hours to make certain that liquid samples on the slide had reached the desired temperature
- After incubation, slides were immediately removed from the oven and washed in heated washing buffers: 10 minutes in 0.2XSSC+0.1 % SDS and 10 minutes 10 minutes in 0.2X SSC only
- Dry slide by centrifugation or stream of nitrogen.
- Slides were immediately analysed by fluorescence readout. The intensity of the fluorescent signal indicates if DNA target melted from its complimentary strand.

137

4.2.9 PIRANHA – cleaning of QCM chips

Piranha solution must be prepared with great care in the designated area.

- Measure 30 ml of Sulfuric acid
- Slowly add 10 ml of 30 % hydrogen peroxide
- Be aware that the solution is extremely exothermic, avoid touching the beaker
- Place QCM chips in a designed Teflon holder
- Leave it for 10 minutes, to allow remove most of the organic matter
- Place QCM chips in a holder onto a beaker with water
- Dispose of PIRANHA solution accordingly
- Dry QCM crystals with stream of nitrogen.

4.2.10 QCM – ssDNA probe quantification

- Spin-coat clean QCM crystals (with PIRANHA, see protocol 4.2.9.) with 0.1 % PMMA, as per protocol 4.2.2 section
- For EDC immobilisation, use MES buffer as a baseline
- Let it run until signal stabilises
- Inject 10 µL of NH_2-mod-P with 990 µL of MES/EDC into a closed circulation
- Allow immobilisation to take place for c. 1 hour or until signal stabilizes
- Wash/inject MES buffer (baseline) to remove excess probe
- Use Saurbrey equation to calculate the final mass of immobilised probe.
- For click chemistry: ox. PMMA was alkyne-modified prior to injection of the probe. During QCM experiments, a 50 % methanol/water buffer was used as a baseline and N_3-mod-P was injected into a closed circulation for 1 hour. The sample was then washed with the baseline buffer to remove excess probe and the mass was calculated.

4.2.11 AFM analysis

- Substrate surfaces were examined using an atomic force microscope (AFM) on a Veeco Dimension 3100 instrument.

- The AFM was used in tapping mode using Tap300Al-G tips from Budget Sensors (Sofia, Bulgaria)
- High aspect ratio images were measured using Improved Super Cone tips from Team Nanotec; both tips had a resonant frequency of 300kHz and force constant of 40 Nm^{-1}.
- Images were analysed using WSxM software [131].

4.3 Results and discussion

In this chapter's section investigation of binding ssDNA to carboxylic acid surfaces via EDC linking chemistry is described. A comparison of probe binding between click chemistry (CC) and EDC is also described in detail. Ethanolamine blocking was introduced as an additional step to prevent NSB. Hybridisation temperature curves were constructed for both: NH$_2$ modified and unmodified probes. Overall hybridisation efficiency of an assay was improved by substituting EDC linking chemistry for CC. Finally direct and sandwich assays were performed to compare the performance efficacy between two immobilisation techniques: CC and EDC.

4.3.1   Binding ssDNA to carboxylic acid surfaces via EDC linking chemistry

The potential binding of DNA through the primary/secondary amines on its backbone (BB) was investigated initially. For this, the binding of A chain, T chain, NH$_2$-mod-P(Cy5), and unmod-P(Cy5) probes with EDC to the ox. PMMA surface was compared. Control experiments, in which no EDC was used, were also carried out. In order to confirm that the ssDNA probe binds covalently, as opposed to being attached by physical absorption [201], an extensive washing protocol was applied, including sodium dodecyl sulphate (SDS). The use of SDS suppresses nuclease activity without disturbing DNA hybridisation [202]. All DNA probes were labelled with Cy5 dye in order to obtain a fluorescence signal, which was directly proportional to the amount of the probe bound covalently to the surface. The fluorescence measurements are presented in figure 4.4.
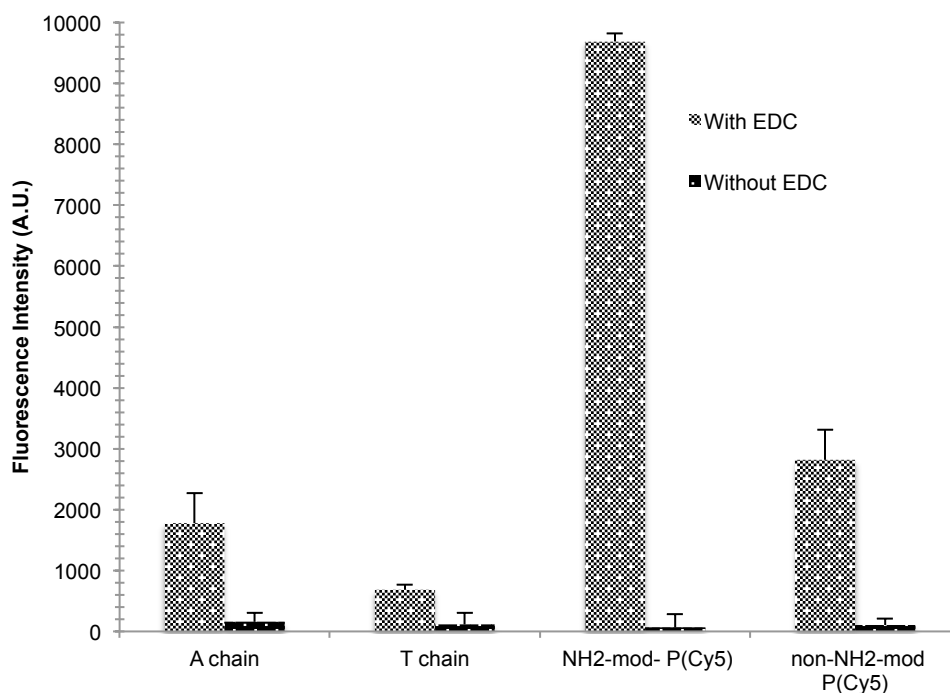
Figure 4.4 A chain, T chain, NH$_2$-mod-P(Cy5), and un-NH$_2$-mod-P(Cy5) immobilisation to ox. PMMA substrates with and without EDC linker. Background fluorescence signal has been subtracted from fluorescence signal. Error bars are equal to the standard deviation of three fluorescence intensity measurements, n=3. Scanned at instrument gain of 60.

In the presence of EDC linker, all the probes investigated bind covalently to the surface, regardless of the terminal modification. In the case of the full-length probes, the difference between fluorescence intensity of the NH$_2$-modified and unmodified DNA probes was just over 30 %. In the case of every probe, there was negligible binding without EDC. If BB binding did occur, then an amino-modified DNA probe would have little or no binding/fluorescence signal, while DNA modified with a terminal amino group would have resulted in a high fluorescence signal. The results in figure 4.4 confirm that the binding is not physical adsorption but rather covalent binding between the carboxylic acid groups on the surface and a nucleophile on the DNA strand.

In the case of the modified probe, the nucleophile expected to react most rapidly is the terminal amino group with which the DNA strand is modified. Possible nucleophiles on the DNA strands that have no amine modification include the primary and secondary amines on the backbone and alcohol/hydroxyl groups on the phosphates. Of the amines that could be involved in binding, primary amines will react at a much faster rate than

secondary amines, which is reflected by the substantial difference in binding between the A chain and T chain probes: thymine does not contain any primary amines, whereas adenine does. It can be seen that where there are no primary amines present, there is significantly less (39 %) binding of the oligomer to the surface. If the hydroxyl groups on the phosphate were primarily responsible for this binding, there would be little difference between the binding ability of the A chain and the T chain.

In the case of the full-length unmodified DNA probe, binding is due to the interaction of the amines on the BB with the EDC-activated surface. Of the bases present in the sequence, 65 % contained primary amines available for interaction with the carboxylic surface (adenine, cytosine and guanine) and there are secondary amines present on thymine, which, although less reactive, could interact with EDC.

In order to investigate this theory, a DNA direct-binding experiment was performed in order to verify whether or not there was an effect on overall hybridisation efficiency. If the probe were immobilised via the amines on the backbone, those bases would be unavailable for hydrogen bonding to form double-stranded DNA with the complementary probe; the hybridisation would not be a 100 % match. In this experiment, probes, bound using EDC, were not labelled with any dye; however, targets were labelled with Cy3 in order to measure the overall hybridisation. Figure 4.5 shows the results in terms of the amount of T(Cy3) hybridised to the immobilised probe, either

NH$_2$-mod-P or unmod-P. The fluorescence signal for NH$_2$-mod-P was over 30 % higher than the fluorescence signal for unmod-P. This indicates that the terminal amine on the modified probe is more readily available for hybridisation and therefore can bind more labelled target. There is also, however, a fairly high signal for the unmodified DNA probe, indicating that the probe is robustly bound to the surface, possibly at multiple locations, e.g. through the amines on the backbone. The probe is also still active and available for hybridisation of the complementary target.
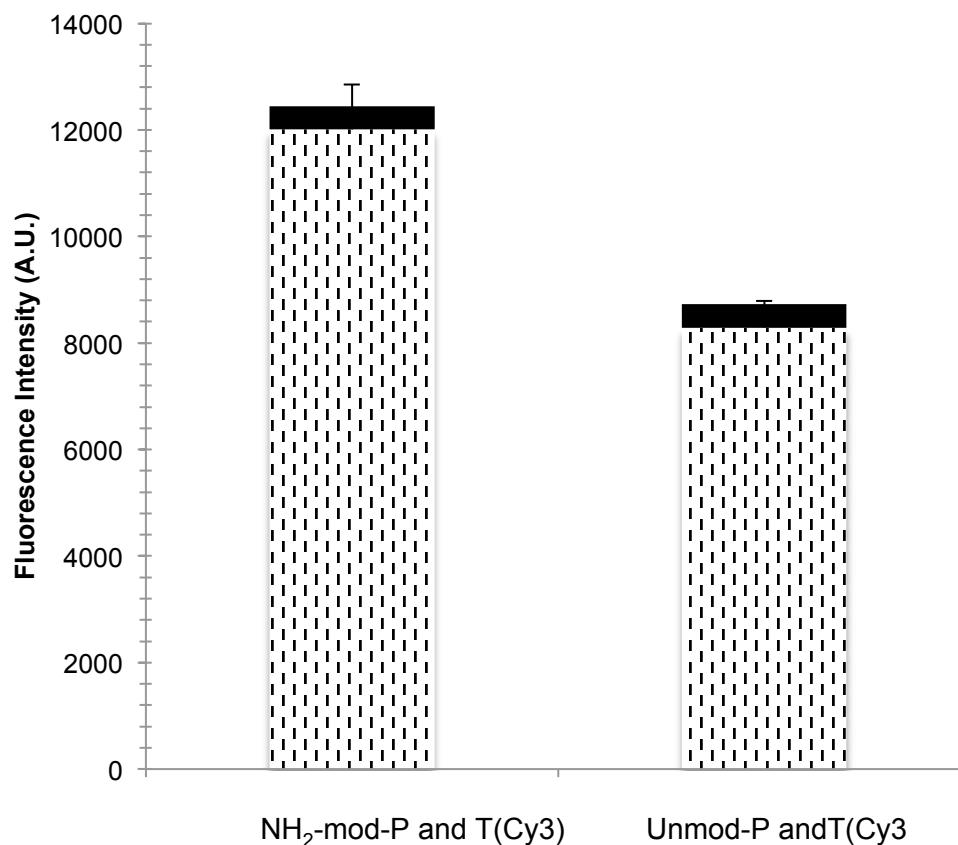
Figure 4.5 Direct binding assay; NH$_2$-mod-P and T(Cy3) and unmod-P and T(Cy3); n=3. The black area at the top of the bar is equivalent to the background signal. Error bars are equal to the standard deviation of fluorescence intensity measurements, n=3.

4.3.2   Probe binding: EDC vs CC

In this paragraph the amount (fluorescence signal) of full-length DNA probe binding via click chemistry and EDC is compared. Figure 4.6 represents binding of DNA probe with Cy5 label only at different concentration range: 10μM-1nM with either CC (black line) or EDC (dotted line).
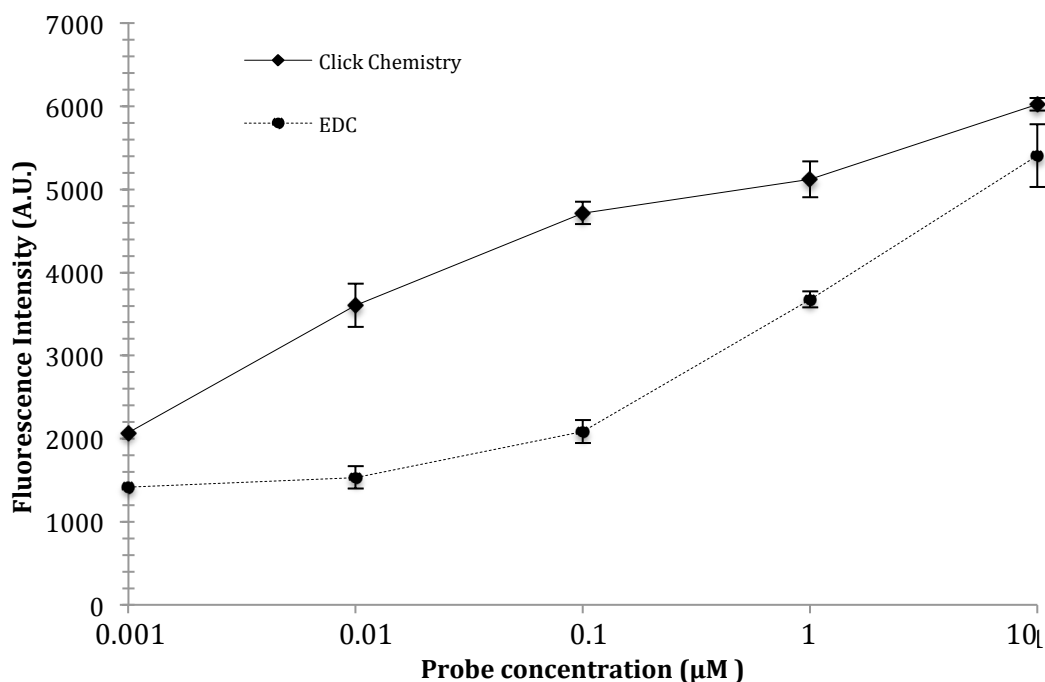
Figure 4.6 N_3-mod-P(Cy5) and NH_2-mod-P(Cy5) immobilised via CC (unbroken line) and EDC (broken line) at range of probe concentrations: 10μM-1nM. Error bars are equal to the standard deviation of fluorescence intensity measurements, n=3.

DNA probe immobilised with EDC linker shows lower binding ability/amount while compared to DNA probe immobilised via CC, figure 4.6. This result supports the hypothesis that the amount of DNA binding via multiple binding sites is lower of that which binds via modified terminus only. Probes bound via CC are not only bound at the higher amount but also are fully available for a complimentary hybridisation.

While probes bound via EDC are immobilised at different points within a strand and are prone to mis-match at room temperature. In order to obtain a specific hybridisation, a higher temperature would need to be applied to prevent mis-matches while EDC in use.

4.3.3 Ethanolamine blocking

Ethanolamine was employed as a block in order to ensure no background binding of the target to the surface, thus maximizing the hybridisation efficiency. Here, fluorescence intensity, which is directly proportional to the amount of DNA bound to blocked and unblocked slides, is compared. NH_2-modified and unmodified probes were immobilised onto ox. PMMA support as previously described. NH_2-mod-P or unmod-P were not

labelled with any dye; T(Cy3) was labelled with Cy3 dye in order to obtain a fluorescence signal for further quantification. Figure 4.7 shows results for blocked versus unblocked NH_2-mod-P (dotted bars) and unmod-P (striped bars) after immobilisation.
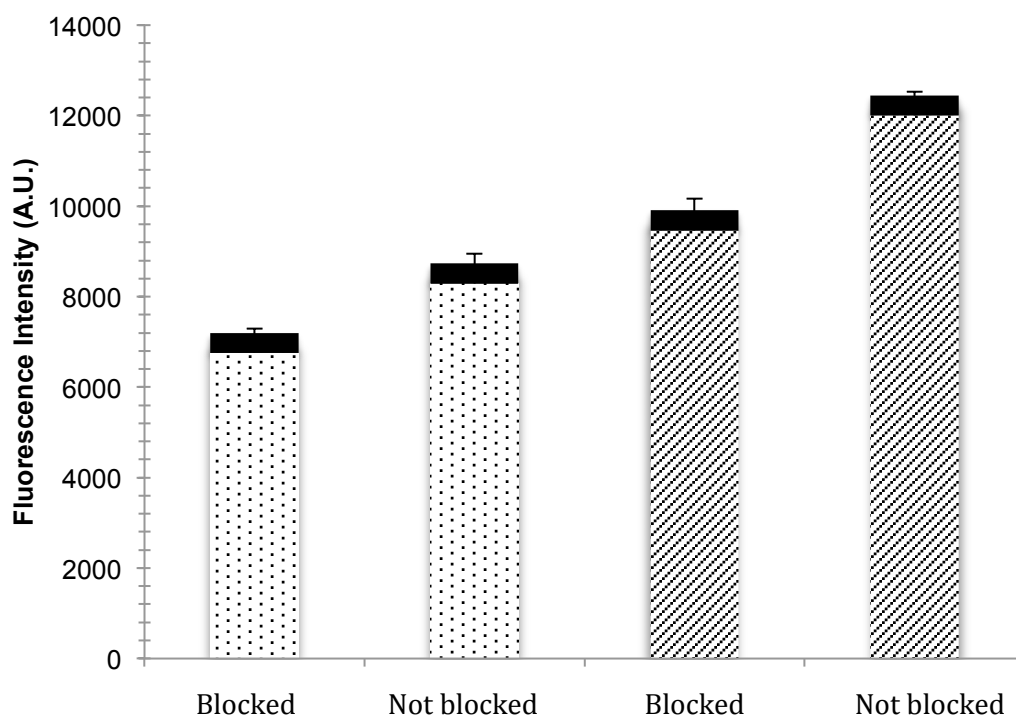
Figure 4.7 Fluorescence signal of T(Cy3) on ethanolamine-blocked prior to hybridisation versus unblocked prior to hybridisation at room temperature. The black area at the top of the bar represents the background signal. Error bars are equal to the standard deviations of three fluorescence intensity measurements, n=3.

Applying ethanolamine as a blocking agent was shown not to make a significant difference in terms of hybridisation efficiency; figure 4.7. There was still a high signal from the unmodified probe regardless of blocking. The kinetics of DNA probe binding to the surface are almost immediate (within seconds), as measured by previous experiments using dual-polarization interferometry and quartz crystal microbalance, figure 4.8; hence it is not entirely surprising that blocking the surface after probe immobilisation was not effective.

Figure 4.9 represents the kinetics of binding of DNA onto the carboxylic acid surface. A quartz crystal microbalance (QCM) measures a mass per unit area by measuring the change in frequency of a quartz crystal resonator [99]. An experiment was carried out using QCM with a gold-coated QCM chip, that has a thin layer of –COOH groups. A solution containing an amino modified probe along with EDC was injected at 500 seconds. Figure 4.8 shows that the binding of the probe to the surface is instantaneous.
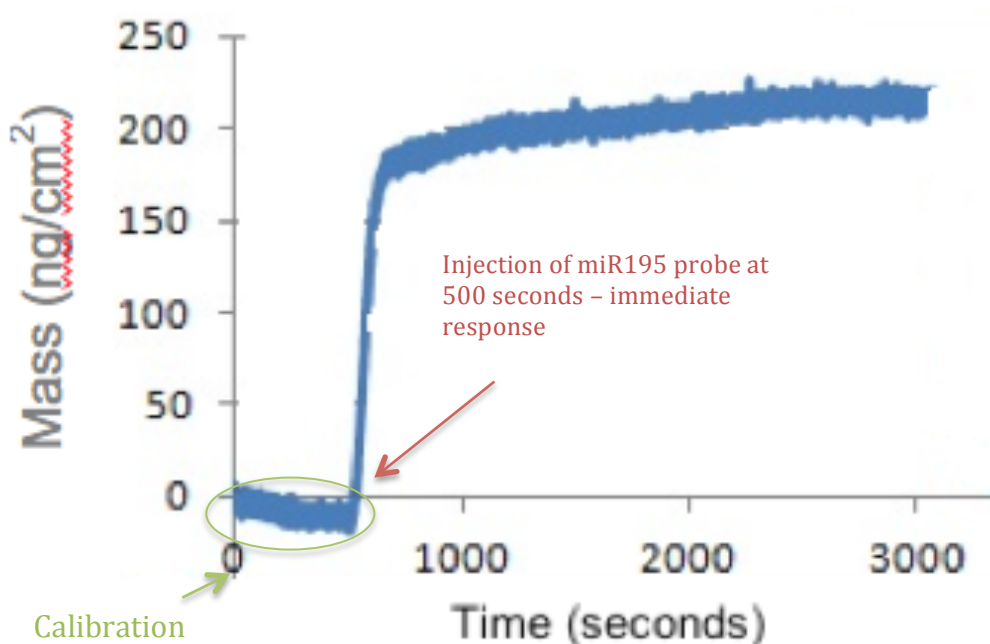
Figure 4.8 DNA kinetics; injection of DNA probe in QCM at 500 seconds.

4.3.4 Hybridisation temperature curves of NH$_2$-modified and unmodified probes

The results presented previously suggest that there is a significant amount of binding of the probe to the surface through its backbone.

Hybridisation was investigated from 20 °C to 62 °C, near the melting temperature of this length of double-stranded DNA molecule with 100 % base matching ($Tm = 64 \pm 4$ °C). This temperature was calculated using the Wallace rule [203], which assigns 2 °C in melting to each A-T pair (2 H bonds) and 4 °C to each G-C pair (3 H bonds).

145

If probes were bound covalently to the surface at multiple points, the bases bound through BB amines would be unavailable to hydrogen bond to the target, causing a decrease in fluorescent signal due to DNA melting below the *Tm* for the fully hybridised double helix. Figure 4.9 shows that at room temperature, there was a high fluorescent signal for the target binding to both the NH_2-modified and un-NH_2-modified probes on the surface; signals for both decrease with each increase in temperature. The loss of signal from the labelled target with temperature increase well below *Tm* indicates significant numbers of missing H bonds between probe and target for both with and without NH_2 modification. While it is challenging to quantify the exact number of nucleobases bound to the surface, each probe strand includes 13 primary amines and 22 secondary amines available for BB binding, plus the primary amine on the terminus in the case of the NH_2-modified probe, which is available for covalent binding. The large and qualitatively similar decrease in the amount of target binding with increasing temperatures well below the *Tm* for both probe types suggests that the terminal amine of the amino-modified probe, while enabling somewhat improved hybridisation, was not the sole binding point.
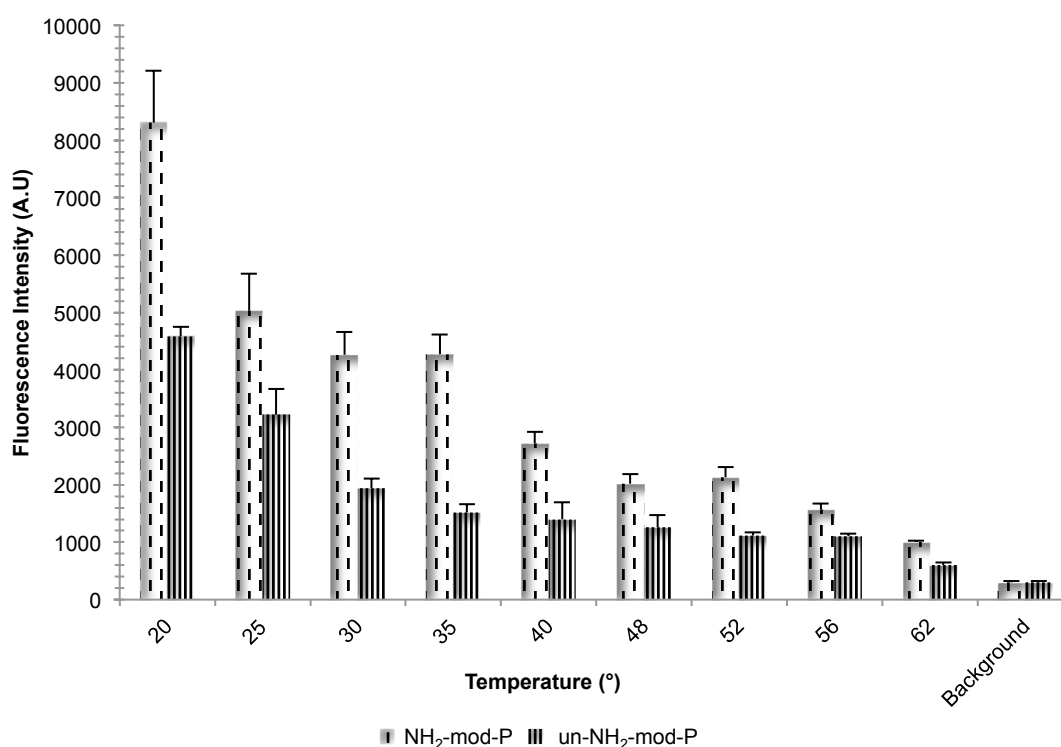
Figure 4.9 Melting curve: fluorescence intensity as a function of temperature. Results are for T(Cy3) hybridised to NH_2-mod-P and unmod-P, plus background signal. Error bars are equal to the standard deviation of three fluorescence intensity measurements, n=3.

146

Control experiments were performed to prove that hybridisation signal was valid, figure 4.10. For Control 1, NH₂-mod-P was spotted onto ox. PMMA in the absence of EDC. For Control 2, T(Cy3) was spotted directly onto ox. PMMA. For Control 3, NH2-mod-P was spotted onto non ox. PMMA in the presence of EDC. All three controls resulted in negligible fluorescent signal, see figure 4.10, demonstrating that, firstly, the EDC linker is required for covalent immobilisation of the DNA probe; secondly, the target does not bind non-specifically to the surface during the hybridisation step; finally, PMMA must be oxidised in order to reliably covalently immobilise aminated biomolecules. For comparison, figure 4.10 also shows the result of the binding of the target T(Cy3) to NH₂-mod-P spotted onto ox. PMMA in the presence of EDC, which produces a readily measured response. It can be concluded, therefore, that the hybridisation signal obtained was specific for the target binding to the DNA probe on the appropriately treated surface.
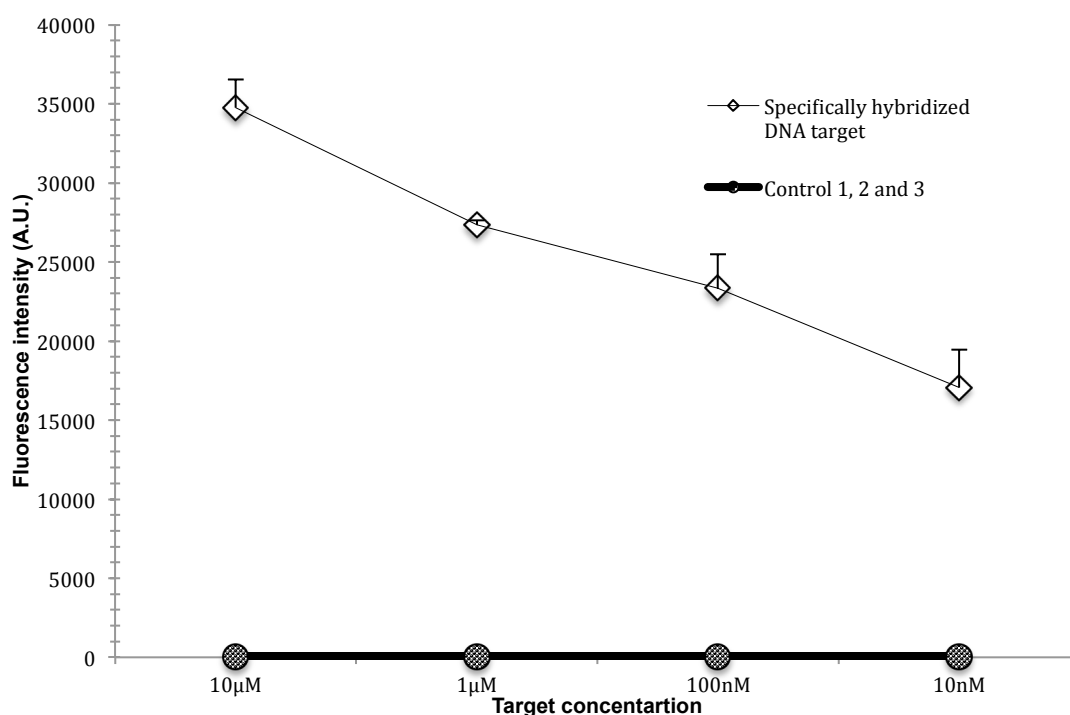
Figure 4.10 Fluorescence Intensity of DNA controls; binding of T(Cy3) to NH2-mod-P spotted onto ox. PMMA in the presence of EDC. Scanned at instrument gain of 80.

When considering whether the unmodified DNA probe covalently bound to the surface in the presence of EDC; F. Everaerts et al. demonstrated that EDC can interact with hydroxyl groups as well as amines [204], i.e., that there was still the possibility that the

DNA strands could be binding to the surface through the hydroxyl groups on the phosphates. However, if this were the case, then the mismatching would not have occurred as described above, as the phosphates would not have been involved in hydrogen bonding between base-pairs, and there would have been no significant melting of the double strand below its *Tm*.

Taken together, the results of figures 4.9 and 4.10 imply that, while EDC linking chemistry is effective in promoting bonding to ox. PMMA, the opportunity for BB binding makes it a less-than-ideal method for immobilisation of ssDNA probe onto carboxylic acid substrates. Therefore click chemistry immobilisation was investigated as an alternative.

4.3.5 Improving hybridisation efficiency using click chemistry

The surface of ox. PMMA was modified in order to create a functional alkyne (-C≡CH) layer so that click chemistry could be used to immobilise azide-modified DNA probes on an (initially) carboxylic acid surface. Water contact angle measurements were used to characterise the alkyne layer and to ensure functionalisation. There is an increase by approx. 15°C from ox. PMMA to the functional alkyne (-C≡CH) layer, figure 4.11. The increased hydrophobicity is consistent with the formation of the alkyne layer.
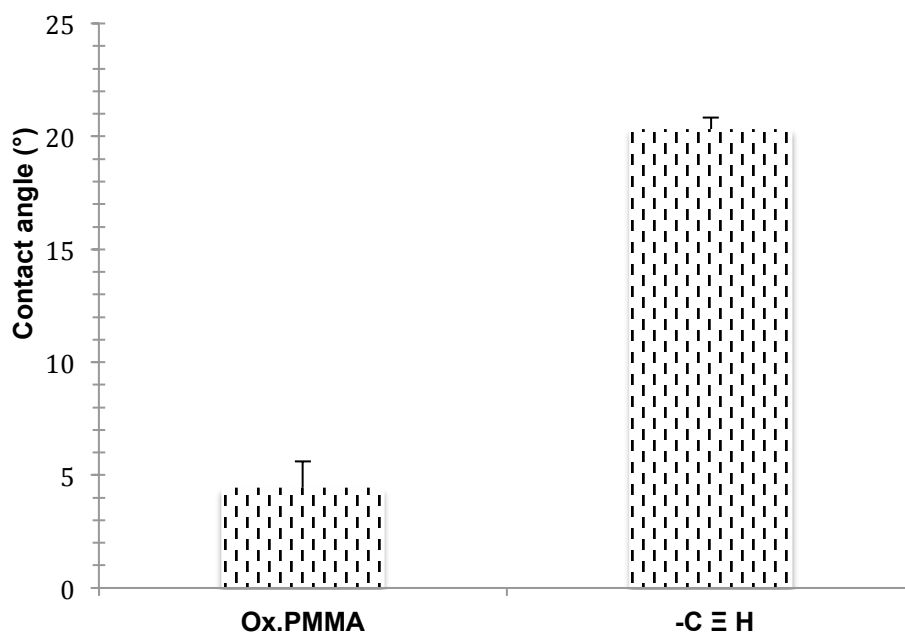
Figure 4.11 Water contact angle (°) of ox. PMMA and further functionalised alkyne surface. Error bars are equal to the standard deviations of three measurements.

148

Figure 4.12 shows height images as seen by AFM of the ox. PMMA surface, alkyne surface and alkyne surface with immobilised probe. The root mean square (RMS) roughness for each surface was calculated to be 1.2 nm, 1.28 nm and 1.33 nm, respectively. These results show that the surfaces are very smooth in general and that roughness increases upon immobilisation of the probe.
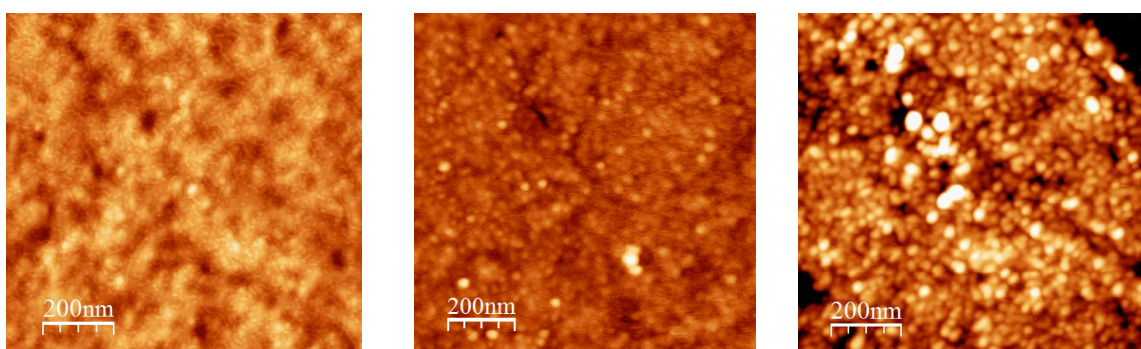
Figure 4.12 Surface topography as measured by AFM of a) prepared ox. PMMA; b) prepared alkyne surface; c) alkyne surface with DNA probe immobilised by click chemistry (10µM, washed three times).

After confirming the smoothness of the surfaces, next step was to proceed to probe immobilisation and hybridisation. To the immobilised probe, Cy3-labelled target (T(Cy3)) was added and hybridisation efficiency at different temperatures was measured. In the case of immobilisation via CC, there are no functional groups available to react with the alkyne on the surface other than the azide in the DNA probe's terminal position. It was hypothesized that this would preclude BB binding and therefore enable hydrogen bonding of all complementary bases for the probe-target pair, hence melting of the DNA double helix would be anticipated to occur at or near the *Tm*.

Figure 4.13 shows the results of conducting the hybridisation at several different temperatures (fluorescence was measured after the surfaces were washed). Despite the temperature increase, the fluorescence signal for the hybridisation remains stable, with the double-stranded helix beginning to melt at temperatures near the *Tm* (64 $^\circ$C, theoretically calculated as described above). The decrease of signal beginning at 60 $^\circ$C could be due to the uncertainty of ± 4 °C in *Tm*, to the energetic range of the melting

process, or to minor fluctuations in the temperature of the oven. The fact that the DNA did not detach or de-hybridise much below *Tm* indicates that the probe was covalently bound via the modified terminus, not via physical adsorption.

Two controls were used to confirm the specificity of binding: in Control 4, T(Cy3) was spotted directly onto ox. PMMA and for Control 5, T(Cy3) was spotted directly onto the alkyne-modified surface. As shown in figure 4.13, there was minimal NSB of the target to either ox. PMMA or alkyne surfaces.
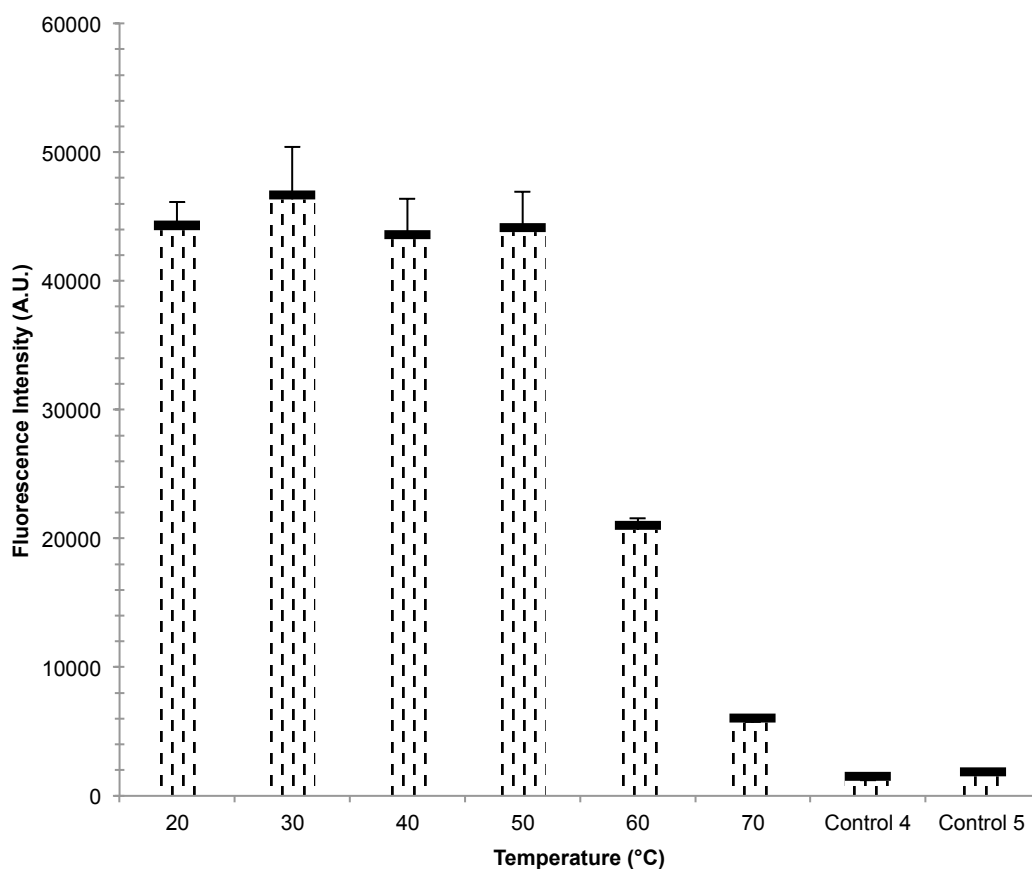
Figure 4.13 Melting curve: fluorescence intensity as a function of temperature. T(Cy3) hybridised to N_3-mod-P, immobilised via click chemistry and washed. Black part at the top of each bar represents the background signal. Error bars are equal to the standard deviation of fluorescence intensity measurements, n=3. Scanned at instrument gain of 90.

It was suspected that the higher efficiency for CC relative to EDC is due to the fact that the DNA probe can only bind via the alkyne-modified end, rather than at multiple points for the EDC linker, making more DNA probes available for hybridisation for CC and also making the hybridisation more specific. This difference in overall hybridisation

150

fluorescence signal can be explained, in effect, as a DNA orientation issue: if the ssDNA probe binds at multiple points along the strand when EDC linking is used, vertical orientation of the DNA on the surface would generally not be achieved, see figure 4.14, limiting the number of strands available for hybridisation on a given surface area of the slide. In the case of CC, single-stranded DNA molecules bind to the surface only via their terminal azide modification, enabling the immobilisation of a higher density of ssDNA and hence more captured target.
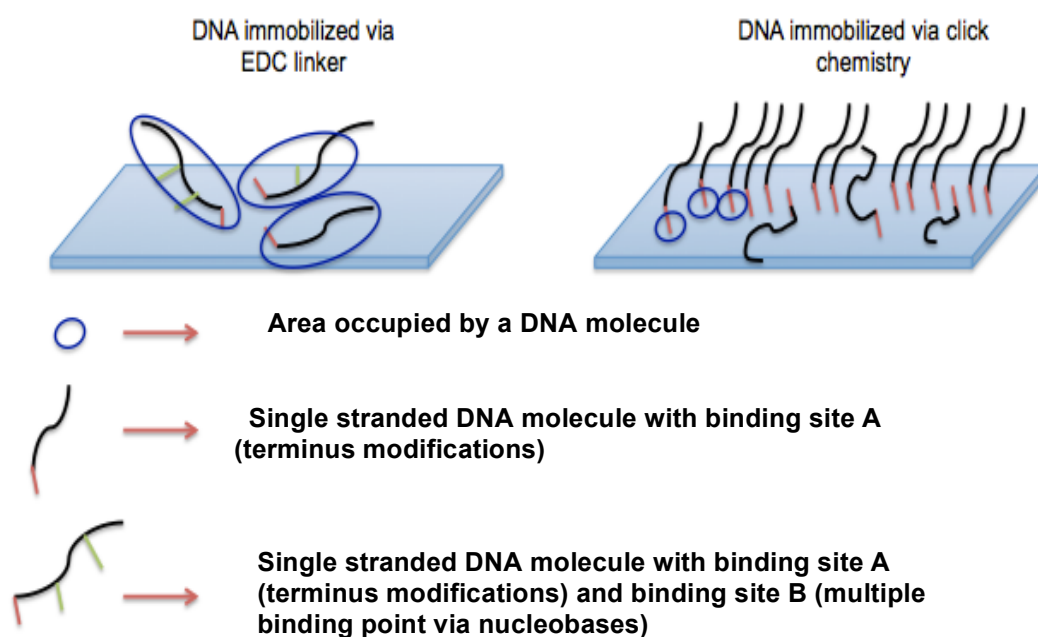
Figure 4.14 Schematic diagram describing single-stranded DNA molecule immobilisation and qualitative details of orientation for EDC and click chemistry immobilisation techniques.

4.3.6 Direct and sandwich DNA binding experiments: EDC versus CC probe immobilisation

The main aim in this paragraph was to compare and determine the most suitable immobilisation method to be used in sandwich nucleic acid assays, which results in good hybridisation efficiency and low limit of detection (LOD). Direct assay was used, as it is easier to perform and contains less steps than sandwich assay. Once all the parameters were established, the use of sandwich assay was next. Both methods are described in detail below.

The hybridisation efficiency as a function of DNA target concentration for both probe immobilisation techniques was measured here, EDC linking and CC, in order to compare hybridisation efficiency as a function of immobilisation technique. Two different types of DNA assays were performed: direct and sandwich. A number of controls were applied in order to ensure that the hybridisation was specific. The first control for EDC immobilisation was used to determine if the NH_2-modified probe binds non-specifically in the absence of EDC linker. For CC, a control was used to determine if the azide-modified probe (CP-azide) could bind in the absence of $CuSO_4$ and sodium ascorbate. The respective control experiments were carried out to determine if target could bind non-specifically to either ox. PMMA or the alkyne-modified surface during hybridisation. Finally, controls experiments were performed to investigate if the aminated or azide-terminated probes bind non-specifically to non-oxidized PMMA. All controls showed negligible fluorescence intensity, confirming the specificity of the experiments.

Experiments were carried out in parallel with the same concentrations of immobilized DNA probe, either CP-amine or CP-azide according to the surface used, and target/ reporter probe mix, T(unlabeled)/RP(Cy5), as described above. Nonetheless, for direct and sandwich assay experiment target hybridisation efficiency was consistently higher for CC-immobilized probes than for EDC-bound probes; as shown in figure 4.15 and 4.16.
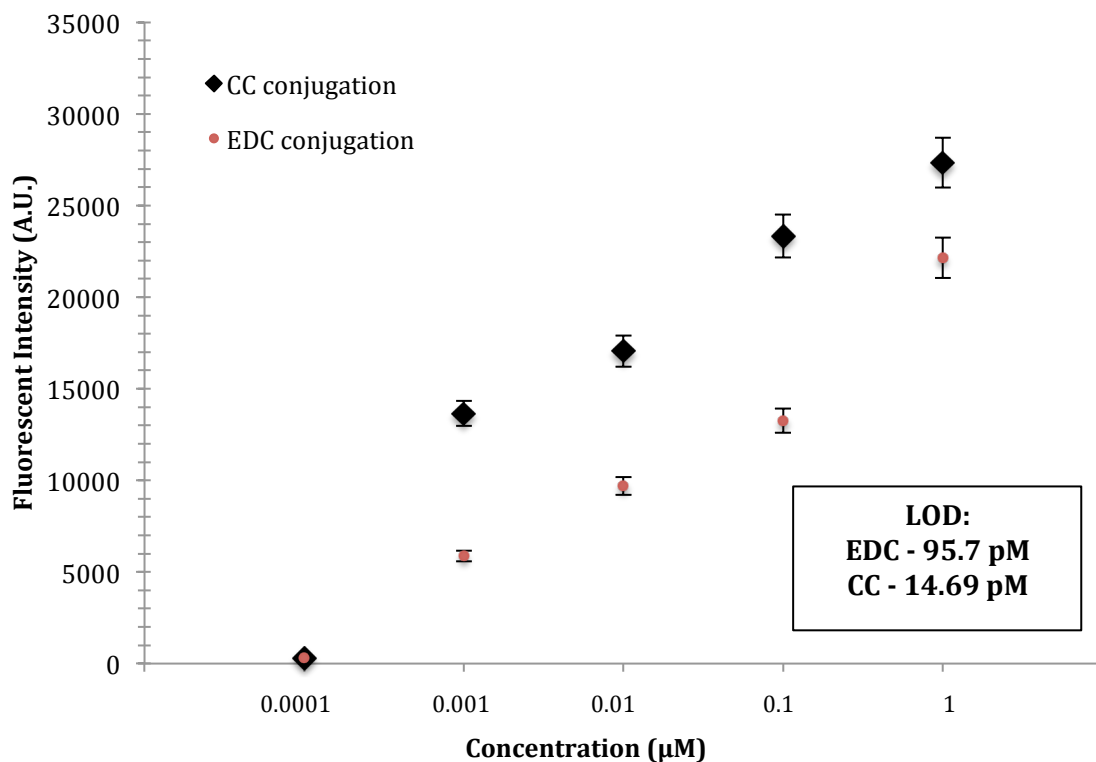
Figure 4.15 Direct DNA binding experiment on DNA probe immobilized by EDC linker chemistry and click chemistry: T(Cy3) was hybridized to NH$_2$-mod-P immobilized via EDC onto –COOH modified surface and to NH$_2$-mod-P immobilized via CC to the alkyne-modified surface. Error bars are equal to the standard deviation of three fluorescence intensity measurements, n=3.
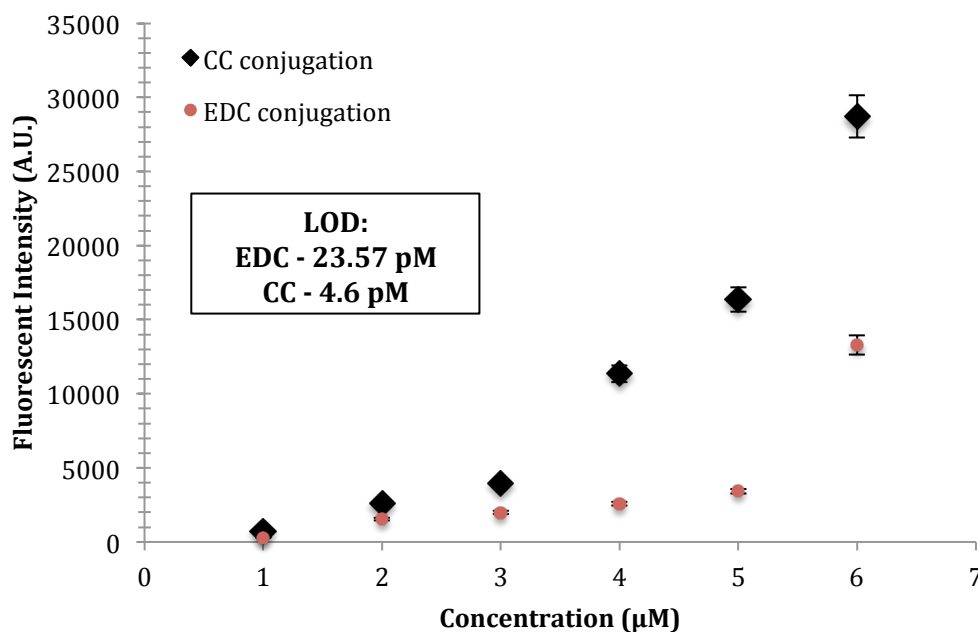
Figure 4.16 Sandwich DNA binding experiment on short DNA probes immobilized by EDC linker and click chemistry: T(Cy3) was hybridized firstly to a reporter probe and then the above was hybridized to the capture probe on the surface. Error bars represent the standard deviations of three fluorescence intensity measurements. Data was fit using a power fit curve. Scanned at instrument gain of 80.

The LOD for all assays was calculated, see the formula below:

$$\textbf{LoB} = \textbf{mean}_{\textbf{blank}} + \textbf{3(SD}_{\textbf{blank}}\textbf{)}$$

LoB is estimated by measuring replicates of a blank sample and calculating the mean result and the standard deviation (SD).

$$\textbf{LoD} = \textbf{LoB} + \textbf{3(SD}_{\textbf{low concentration sample}}\textbf{)}$$

LoD is determined by utilising both the measured LoB and test replicates of a sample known to contain a low concentration of analyte. The mean and SD of the low concentration sample is then calculated according to the formula above [170].

For the direct binding assay, an LOD of 95.7 pM was calculated for the EDC probe assays and 14.69 pM for the CC probes, showing that the CC assay was over six times more sensitive. A similar trend is seen in the sandwich assay where LODs of 23.57 pM for the EDC probes and 4.6 pM for the CC probes were calculated (over 5 times more sensitivity). QCM measurements were performed in order to verify the quantity of probe bound to the ox. PMMA via CC and EDC methods. The QCM results confirmed the above statement, with values of 9.94×10^{11} DNA strands/cm^2 and 217×10^{11} DNA strands/ cm^2 for immobilisation with EDC linker and with CC respectively. The amount of DNA probe bound to ox. PMMA is 20 times more for CC method while compared with EDC linker. The higher efficiency for CC relative to EDC is due to the fact that the DNA probe can only bind via the alkyne-modified end, rather than at multiple points for the EDC linker; if the ssDNA probe binds at multiple points along the strand when EDC linking is used, vertical orientation of the DNA on the surface would generally not be achieved, limiting the number of strands available for hybridisation on a given surface area of the slide. In the case of CC, single-stranded DNA molecules bind to the surface only via their terminal azide modification, enabling the immobilisation of a higher density of ssDNA and hence more captured target. Therefore a conclusion was drawn that the method to immobilise DNA via CC rather than EDC made more DNA probes available for hybridisation and thus the hybridisation more specific.

4.4 Summary and conclusion

An investigation comparing EDC linking and CC as two methods to immobilise single-stranded DNA probes to carboxylic acid surfaces for the purpose of binding complementary ssDNA targets is reported in this chapter. A full description of techniques and protocols in preparation and activation of the functionalised surfaces as well as DNA immobilisation and hybridisation is included. For EDC linking, results are consistent with the binding of DNA probes at least in part through the primary amines on the DNA backbone, a process that decreases the number of -H bonds available to bind target to probe, as confirmed by melting curve analysis. As an alternative to EDC linking chemistry, CC is demonstrated to enable terminus-selective immobilisation of azide-modified probes without interference of any groups on the DNA backbone. To facilitate the CC immobilisation, ox. PMMA was modified with 1-amino-3-butyne to form a functional alkyne-activated surface. The increased amount of DNA probe bound to the surface was observed while compared to the use of EDC linker, by QCM analysis. The assumption has been made that the orientation of immobilised molecule has an effect on the amount of the DNA immobilised. DNA conjugated with EDC linker is immobilised via multiple points on the back bone, which may result in molecule being less flexible and possibly takes up more surface area than a flexible molecule which is attached to the surface via only terminated end (CC conjugated).

 A blocking step was suggested to improve the hybridisation efficiency and to minimize NSB. Ethanolamine was used as a blocking agent and was applied after incubation of probe prior secondary DNA strand being hybridised. However there were no significant difference observed between assays blocked with ethanolamine and one without the blocker.

Finally, direct and sandwich assays have been performed in order to determine LOD. The hybridisation efficiency is compared between the EDC-immobilised DNA and CC-immobilised DNA, with the latter shown to be more specific and more sensitive (i.e. a lower LOD). For the direct binding assay, an LOD of 95.7 pM was calculated for the EDC probe assays and 14.69 pM for the CC probes, showing that the CC assay was over six times more sensitive. A similar trend is seen in the sandwich assay where LODs of 23.57 pM for the EDC probes and 4.6 pM for the CC probes were calculated (over 5 times more sensitivity). This makes CC linker more suitable for point-of-care devices, as the CC-enabled assays can be performed at room temperature with greater hybridisation efficiency and lower LOD can be achieved.

The improvement of immobilisation technique will have a great impact on assay development, as it allows specific immobilisation of DNA onto a carboxylic acid surface at room temperature. EDC linking technique is most commonly used for as a DNA anchoring method [9,100,204,205], hence this finding may be beneficial to other users.

Table 4.3 Summary of chapter 4 – key messages.

CHAPTER 4 – key messages
• EDC linking - DNA probes bind via the primary amines on the DNA backbone
• Click chemistry (CC) suggested as an alternative
• CC – no interference of any groups on the DNA backbone
• Hybridisation efficiency: CC is more specific and more sensitive (i.e. lower limit of detection) than EDC
• CC-enabled assays can be performed at room temperature with greater hybridisation efficiency (while compared to EDC)

Chapter 5

5 DNA orientation investigated on ox.PMMA and other surfaces/films.

5.1 Introduction

This chapter investigates the hypothesis relating to DNA orientation changes on –COOH surfaces; that for single stranded DNA, the phosphate backbone is repelled by the carboxyl groups causing it to face away from the surface up into the buffer. This leaves the bases to face the surface and make favourable non-covalent interactions with functional groups on the surface. Upon hybridisation and formation of the double helix, the negative phosphate groups oriented on the outside of the helical structure cause the double strand DNA to be repelled by the negatively charged surface and stand up, see figure 5.1.
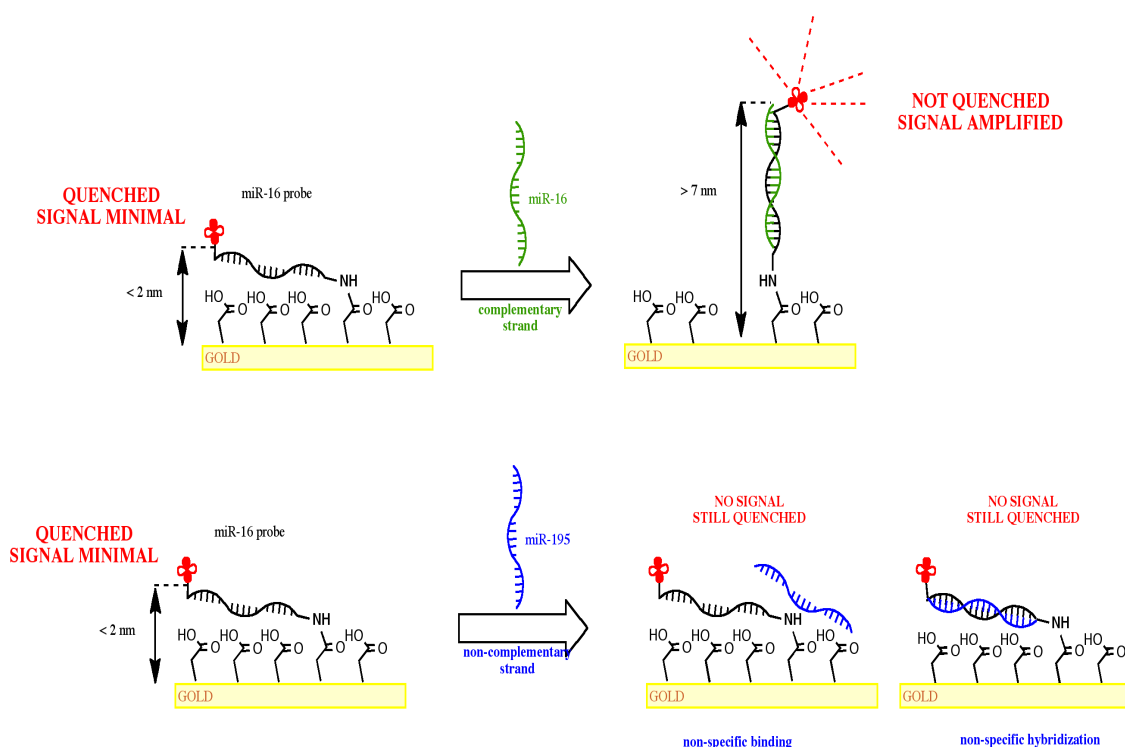
Figure 5.1 DNA orientation change phenomenon.

It was previously observed in this research group that DNA analogues of micro RNA probes change orientation upon hybridisation with a complementary target on TEOS/AA coated surfaces [103]. The phenomenon was described as an orientation change in an oligonucleotide probe upon hybridisation of a matched target as a possible result of the incorporation of a surface coating. The surface was modified using plasma enhanced chemical vapour deposition (PECVD) process comprising of a TEOS adhesion layer followed by a layer of acrylic acid (AA) providing carboxyl group functionality. Covalently immobilised amino-modified oligonucleotides were anchored onto the surface through a covalent bond between their $-NH_2$ and the surface carboxyl groups. Due to the negative charge of the carboxyl groups in buffers with pH above 4.0, it was expected that the negative phosphate backbone of single stranded DNA would be repelled causing the DNA to stand up away from the surface. However, upon immobilisation of ssDNA probes on the TEOS/AA surface, it was observed that the probes were lying down. Upon introduction of the complementary target strand, hybridisation occurred and the orientation of the probes changed to a standing up configuration. This orientation change phenomenon could potentially be developed into a reagent-less measurement platform based on the quenching of a fluorophore when in close proximity (less than 7 nm) to a metal. Oligonucleotide probes would be immobilised at one end and labelled with a fluorophore at the opposite end. The substrate would have a layer of gold underneath the TEOS/AA surface. In the absence of a matched target strand, the probe would be flat down on the surface bringing the fluorophore within a few nm of the Au layer causing emission to be quenched. Upon binding of a complementary target strand, the probe would stand up perpendicular to the surface brining it outside the range of quenching and allowing it to emit a photon. As the orientation change does not occur with non-specific hybridisation (introduction of a mis-matched target), this measurement would provide very high selectivity and sensitivity. In order to explain why this phenomenon happens, assumption has been made that it could be an electrostatic effect.

This chapter describes results relating to the investigation of the orientation of miR16 probe upon hybridisation with miR16 target (referred as a positive control) and miR195 target (referred as a negative control) on various substrates. A number of different surfaces were investigated, including TEOS/AA, MUA, SA, APTES. Techniques used for investigation of DNA orientation on the surfaces were as follows: dual polarization interferometry (DPI), Quartz Crystal Microbalance (QCM) and Total Internal Reflection Ellipsometry (TIRE).

5.2 Experimental details:

Orientation changes of fully hybridised DNA on –COOH functionalised solid supports were investigated in this chapter. To investigate such changes, label free Dual Polarization Interferometry, Quartz Crystal Microbalance and Total Internal Reflection Ellipsometry techniques were employed.

5.2.1 Materials and instrumentation

PMMA sheets (0.25 mm thick, impact modified, MW ¼ 120 000) were sourced from Goodfellow Cambridge Limited(Huntingdon, England). Zeonor® substrates, injection-molded cyclic olefin polymer (COP) slides (Zeonor® 1060R, 25 mm x 75 mm, 1 mm thick) were sourced from Sigolis (Uppsala, Sweden). Gold-coated standard glass microscope slides (Ti/Au, 5 nm/30 nm, 25 mm x 75 mm, 1.1 mm thick) were sourced from PhasisSarl (Geneva, Switzerland). Q-sense QCM crystal/sensors were sourced from Biolin Scientific (Stockholm, Sweden). PTFE filter (pore size 0.25 μm) (Chroma-filXtra PTFE-20/25 Macherey-Nagel, Duren, Germany). 1-Ethyl-3-(3-dimethylaminopropyl) carbodiimide (EDC), 2-(N-morpholino) ethanesulfonic acid buffer (MES), sodium dodecyl sulfate (SDS), saline-sodium citrate (SSC), 11-Mercaptoundecanoic acid 95 % (MUA), Succinic anhydride ≥99 % (GC), and toluene (anhydrous, 99.8 %), Tetraethyl orthosilicate (TEOS/AA) reagent grade 98%, (3 − Aminopropyl)trethoxysilane (≥98%) were purchased from Sigma Aldrich (Arklow, Ireland). Thiol modified DNA, -NH$_2$ modified DNA, DNA target were purchased from Eurofins MWG Operon (Duren, Germany). All chemicals were used as received without further purification.

Instrumentation used in support of this work in chapter 5:

- Spin coater
- UV/O$_3$
- DPI
- QCM
- TIRE

5.2.2 Preparation of spin coated poly (methyl methacrylate) surfaces

Protocol for preparations of spin coated PMMA is as follows:

- Take off protection film from the PMMA sheet
- Cut PMMA sheet into small pieces
- Weight out 0.001 g of PMMA pieces for 0.1 PMMA concentration respectively
- Place into a glass vial with 10 ml of 80 % ethanol to result in 0.1 % PMMA concentration.
- Use sonicator at 40 ° for 30 minutes to dissolve the PMMA pieces
- Filter dissolved PMMA solutions through PTFE filter (pore size 0.25 µm)

Cleaning of the substrates prior spin coating:

- Fill the tank with 2 % of Micro90 detergent for cleaning step
- Place the slides in a slider holder and submerge them in Micro90
- Sonicate for 30 minutes
- Rinse slides in water
- Fill another tank with isopropanol and submerge slides
- Sonicate for 30 minutes
- Rinse slides in water
- Dry with nitrogen stream

Spin coating of dissolved PMMA protocol:

- Place a slide/DPI chip at the centre of spin coater's holder
- Apply vacuum to immobilise the slide
- Place 1 ml of dissolved PMMA solution on the middle of the slide
- Set the settings: 3000 rpm, 5 seconds acceleration for 1 minute
- Press start
- Take the slide off and transfer to a holder

The curing process protocol:

- The PMMA films are cured in an oven at 80 °C for 1 h or in the fume

hood over night.

Oxidation of spin coated PMMA surfaces:

- Place cured PMMA samples (do not touch the interface, pick up by the edge of the slide) onto UV/O$_3$ device
- Initiate oxidation for 4-8 minutes as required
- Remove samples from the device
- Alternatively oxygen plasma can be used to activate the surface (4-8 minutes).

The coating of PMMA films onto glass slides required an additional step, due to the hydrophobicity of the glass. The water contact angle of glass is very low; hence, the PMMA solution could not gain contact with it during spin coating. In order to modify the hydrophobicity of the glass, the deposition of a silicon oxide layer was applied to ensure adhesion of the PMMA. The silicon oxide was deposited with a plasma enhanced chemical vapour deposition (PECVD) method using a Plasmalab 100 system. The precursor reagents for this process were oxygen gas and hexamethyldisiloxane (HMDSO). The silicon oxide layer thickness was approximately 30 nm.

5.2.3   PIRANHA – cleaning of QCM, DPI and gold coated chips

Piranha solution must be prepared with great care in the designated area.
- Measure 30 ml of Sulfuric acid
- Slowly add 10 ml of 30 % hydrogen peroxide
- Be aware that the solution is extremely exothermic, avoid touching the beaker
- Place substrate in a designed Teflon holder
- Leave it for 10 minutes, to allow remove most of the organic matter
- Place substrate in a holder onto a beaker with water
- Dispose of PIRANHA solution accordingly
- Dry substrate with stream of nitrogen.

5.2.4   Preparation of wet chemistry APTES

The protocol for chemically depositing APTES is as follows:

- Substrate (glass, Zeonor, silicon) needs to be oxidised - either through oxygen plasma treating or other methods like UV-Ozone treatment
- Dip the freshly oxidized substrates in the deposition solution (92:5:3 mixture of isopropanol/ethanol, DI water, and APTES)
- Store the substrates for 2 hours at room temperature in solution
- Sonicate substrates in isopropanol for 15 minutes twice
- Rinse the substrates with isopropanol

- Bake the substrates in oven for 1 hour at 80 $^{\circ}$C (substrates may stick to holder during baking so care must be taken)
- Cool the substrates for 30 minutes at room temperature

- Coated slides can then be stored as needed.

5.2.5   Preparation of 11-Mercaptoundecanoic acid, self assembled monolayer surfaces

SAM on gold were prepared as follows:

- Incubate gold substrates in freshly prepared thiol solutions (5mM) using ethanol for 12 h.
- After the formation of SAMs, rinse gold substrates with a copious amount of ethanol and DI water,
- Use stream of nitrogen gas to dry substrates.

Water contact angle was used as a confirmation test of the successful depositions and should be around 55 °.

5.2.6 Preparation of 11-Mercaptoundecanoic acid (MUA) on substrate other than gold

Use of MUA on substrates other than gold requires introduction of a linker. Protocol of preparing MUA on DPI chips (silicon oxide) is as follows:

- The DPI chips were coated with liquid APTES (see section 2.2.3.)
- DPI chip coated with liquid APTES is submerged in sulfo-SIAB (5 mM) solution prepared with PBS (pH 6.5) for 30 mins to let amine-to-thiol conjugation
- Substrates then were washed with DI water and dried using stream of nitrogen gas.
- Modified surfaces in this manner were then ready for MUA incubation overnight (see section 2.2.4)
- After formation of the SAM, substrates were rinsed with a copious amount of ethanol and DI water, and finally dried using a stream of nitrogen gas.

5.2.7 Preparation of Succinic Anhydride surfaces

An adapted protocol [129] for SA immobilisation was used, see the protocol:
- Primary amino groups in APTES films were initially converted to carboxyl groups by incubation in THF containing 5 mg/ml SA and 5 % v/v triethylamine (TEA) for 4 hours
- Rinse with DI water.

5.2.8 QCM – DNA hybridisation protocol

- Spin-coat clean QCM crystals (with PIRANHA, see protocol 5.2.3.) with 0.1 % PMMA, as per protocol 5.2.2 section
- Use MES buffer as a baseline
- Let it run until signal stabilises
- Inject 10 μL of NH$_2$-mod-P with 990 μL of MES/EDC into a closed circulation
- Allow immobilisation to take place for c. 1 hour or until signal stabilises

- Wash/inject MES buffer (baseline) to remove excess probe

- Wait until signal stabilises

- Inject 1 µL miR195 probe with 990 µL of MES into a closed circulation

- Allow hybridisation to take place for c. 1 hour or until signal stabilises

- Wash/inject MES buffer (baseline) to remove excess probe

- Analyse the results

5.2.9 DPI – DNA hybridisation protocol

- Spin-coat clean DPI chip (with PIRANHA, see protocol 5.2.3.) with 0.1 % PMMA, as per protocol 5.2.2 section

- Perform calibration of the instrument first

- Use MES buffer as a baseline

- Let it run until signal stabilises

- Inject 10 µL of NH_2-mod-P with 990 µL of MES/EDC

- Allow immobilisation to take place for c. 30 minutes - 1 hour or until signal stabilises

- Wash/inject MES buffer (baseline) to remove excess probe

- Wait until signal stabilises

- Inject 1 µL miR195 probe with 990 µL of MES

- Allow hybridisation to take place for c. 1 hour or until signal stabilises

- Wash/inject MES buffer (baseline) to remove excess probe

- Analyse the results

5.2.10 TIRE – microfluidic cell assembly

Figure 5.2 represents assembly of microfluidic flow cell in PMMA and pressure sensitive adhesive (PSA) [126].

- (a) top PSA layer containing five reaction microwells (the volume of each microwell is 4.7 µl),

- (b) connecting hole PMMA layer,

- (c) PSA channel layer,

- (d) bottom PMMA layer,
- (e) bonding of top PSA layer and connecting hole PMMA layer,
- (f) bonding of PSA channel layer and bottom PMMA layer,
- (g) complete four-layer microfluidic flow-cell
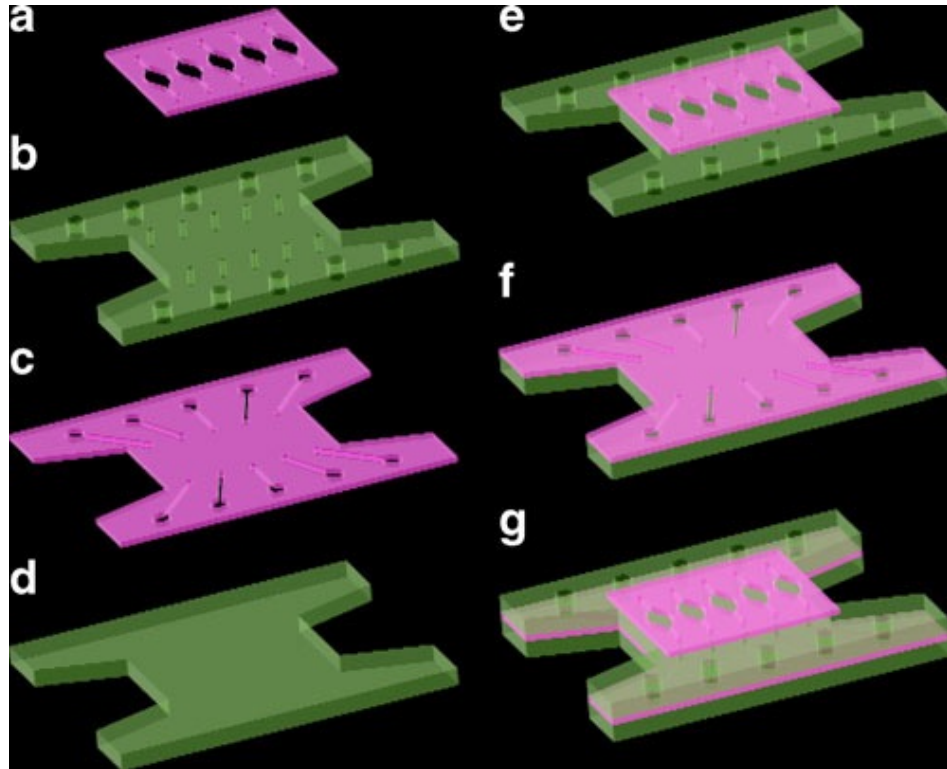
Figure 5.2 Assembly of microfluidic cell [103].

5.2.11 TIRE – DNA hybridisation protocol

- Spin-coat clean gold half slide (with PIRANHA, see protocol 5.2.3.) with 0.1 %
  PMMA, as per protocol 5.2.2 section
- Apply microfluidic cell (as per 5.2.10), make sure there are no air bubbles
- Place the BK7 prism on the top of the sensing substrate with an refractive index
  matching oil and secure by tape, see figure 5.3
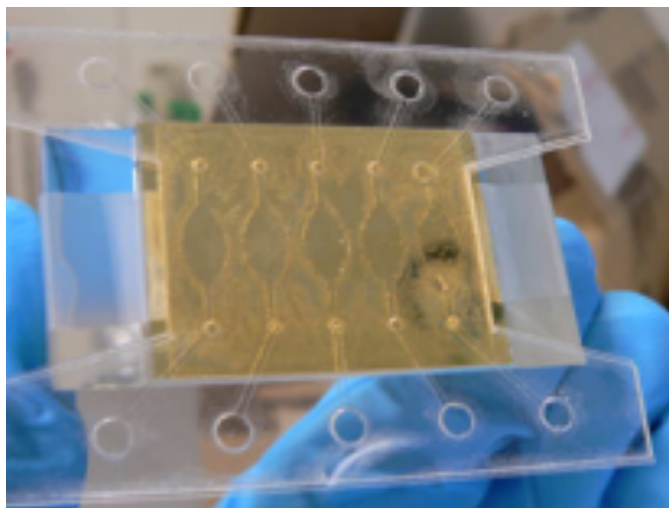
Figure 5.3 Fully assembled microfluidic flow cell and BK7 prism.

- Connect a syringe pump (Harvard Apparatus, Boston, USA) to the outlet of one microwell of the flow cell via polymer tubing and a PDMS connector
- The flow rate was controlled to within 4–5 μl/min.
- Use MES buffer as a baseline
- Let it run until signal stabilises
- Inject 10 μL of NH_2-mod-P with 990 μL of MES/EDC, The volume of analyte should be in excess to the volume of the microwell (4.7 μl) in order to make sure the microwell is always filled with analyte

- Allow immobilisation to take place for c. 30 minutes - 1 hour or until signal stabilises
- Wash/inject MES buffer (baseline) to remove excess probe
- Wait until signal stabilises
- Inject 1 μL miR195 probe with 990 μL of MES
- Allow hybridisation to take place for c. 1 hour or until signal stabilises
- Wash/inject MES buffer (baseline) to remove excess probe
- Analyse the results

166

5.3 Results and discussion

In this chapter's section miRNA (DNA) orientation changes on TEOS/AA surface are described, as well as on other functionalised surfaces, including: self assembly monolayer – Mercaptoundecanoic Acid, Succinic Anhydride, APTES (liquid and PECVD), ox.PMMA and plain gold. Additionally a new technique – Total Internal Reflection Ellipsometry was introduced to determine thickness/orientation changes of DNA.

5.3.1   miRNA (DNA) orientation changes on TEOS/AA

DPI can record thickness changes based on thickness, mass and density changes. The aim here was to determine thicknesses after single stranded probe immobilisation and then the thickness increase after complementary DNA probes hybridisation. Dimensions of single stranded DNA are c. 7/8 nm – 1.5 nm and fully hybridised double helix are c. 7/8 nm – 3 nm.

Table 5.1 DPI measured thickness, mass and density for positive and negative control.

Name	Thickness (nm)	Mass (ng/mm^2)	Density (g/cm^3)
mir16 probe	0.238	0.286	1.201
mir16 target	**8.375**	1.710	0.204
mir16 probe	0.271	0.207	0.761
mir195 target	**1.590**	0.809	0.509

As can be seen in table 5.1, immobilised single stranded probe caused increase of thickness to 0.238 nm along with mass and density increase, suggesting a successful DNA immobilisation to the surface. Upon addition of secondary DNA strand, hybridisation takes place and double helix changes its position to vertical. The full length of 22-mer miRNA (DNA) is approx. 7-8 nm, hence the thickness change from 0.238 nm to 8.375 nm while in standing up position. Mass also increased, however density decreased as expected. Decrease in density can be explained with the analogy that if something is sticking up/standing up density is less than if the same was lying flat.

Based on the result above, further testing was suggested and use of QCM technique was proposed as an alternative method to continue investigation of DNA behaviour on TEOS/AA and other substrates.

QCM measurements give areal mass and dissipation values. Areal mass is defined as an increase of a mass per unit area [100]. Dissipation can be defined as a parameter quantifying the damping in the system, and it is related to the samples viscoelastic properties [100], which can be interpret as thickness. Hybridisation between miR16 DNA probe and miR16 DNA target (complimentary strands) or miR195 DNA probe and miR195 DNA target (complimentary strands) is referred as positive control and hybridisation between (non complimentary probes) miR16 DNA probe and miR195 DNA target or miR195 DNA probe and miR16 DNA target is referred to as negative control in this chapter.
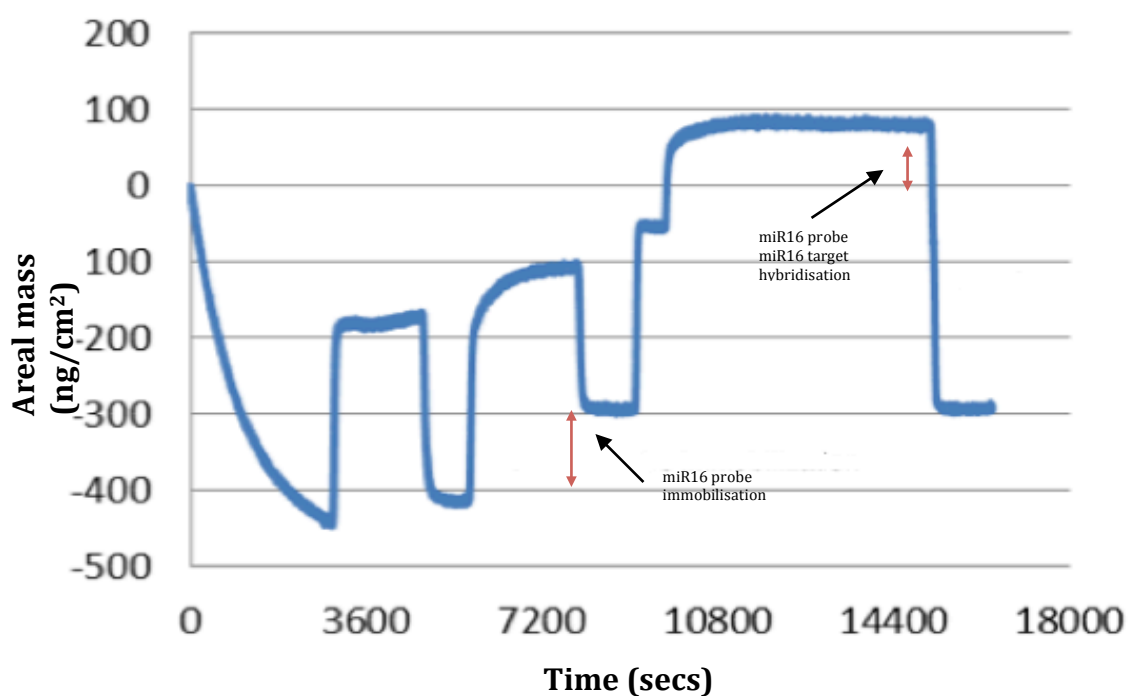
Figure 5.4 Positive control on TEOS/AA, time (secs) vs. areal mass (ng/cm^3), red arrows represent shift between baselines for either immobilisation or hybridisation.
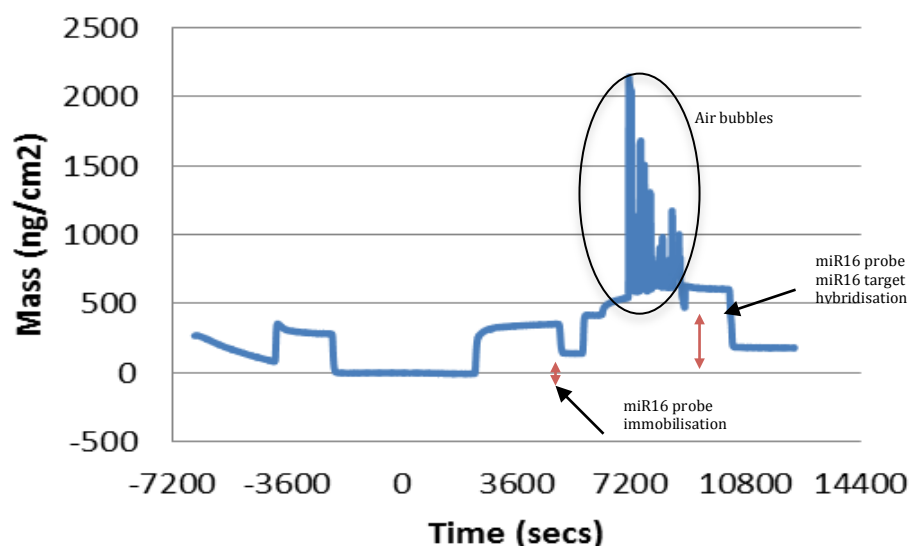
Figure 5.5 Negative control on TEOS/AA, time (secs) vs. areal mass (ng/cm^3), red arrows represent shift between baselines for either immobilisation or hybridisation.

QCM results in figure 5.4 and 5.5 show DNA behaviour for positive and negative control full hybridisation, respectively. A real mass increase is observed by the indication of a significant shift between baselines. However in terms of dissipation or in other words thickness, results are unclear.

The results observed in table 5.1 have proven hard to reproduce despite the multiple repetition and modifications of the experiment conditions. At this point, the explanation was not as clear, so decision has been made to investigate other -COOH functionalised substrates with an alternative technique to observe orientation changes and to continue with the investigation. Films developed and discussed I chapter 2 were applied in this chapter to investigate the relationship between the surface and DNA orientation changes.

5.3.2   miRNA orientation changes on MUA

SAM MUA was used as another type of carboxylic acid surface. It was used to determine if orientation changes occur on other –COOH prepared substrates, as was seen previously on TEOS/AA. QCM, DPI and TIRE were the techniques used for both

positive and negative controls.
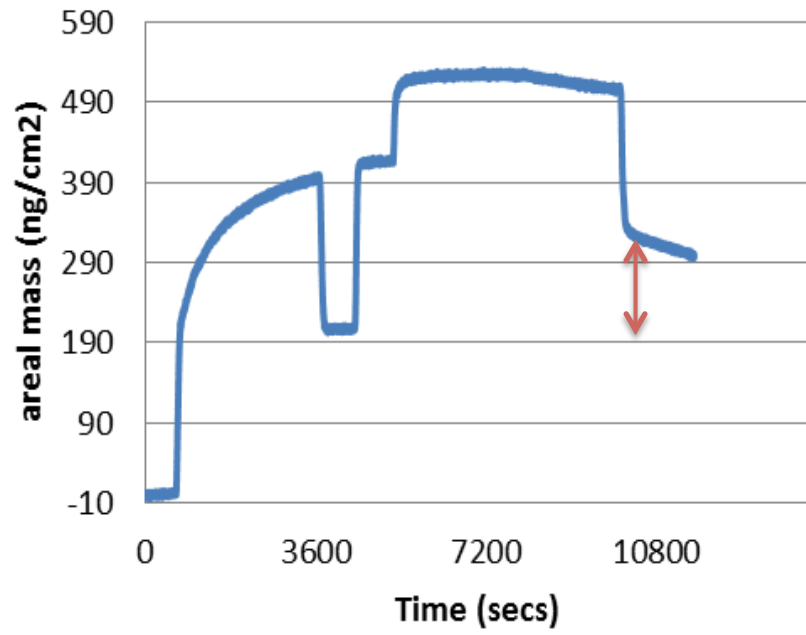
Figure 5.6 Positive control on MUA, time (secs) vs. areal mass (ng/cm^2). Increase in areal mass (red arrow) indicates 50 % hybridisation rate.
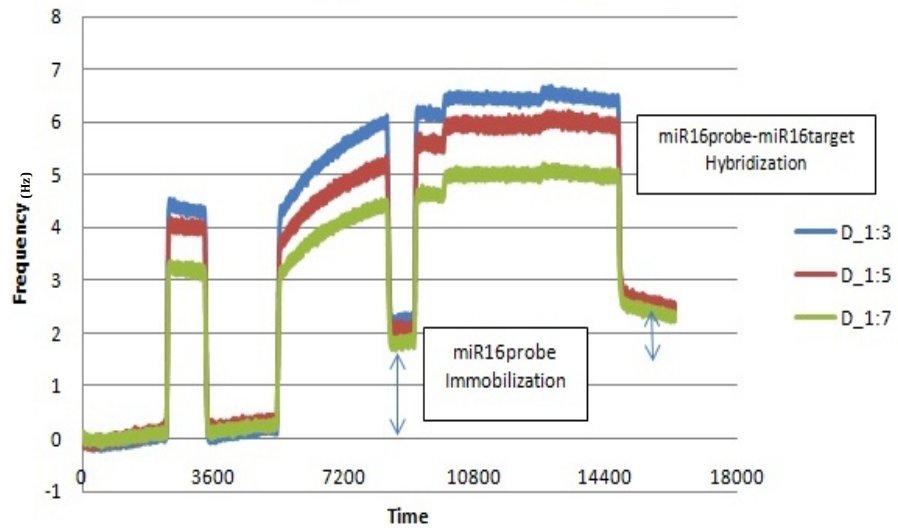
Figure 5.7 Positive control on MUA, dissipation. Small shift in dissipation, DNA film remains rigid.

Table 5.2 Areal mass and dissipation for miR16 probe immobilisation and miR16 probe – miR16 target hybridisation.

Positive control	Areal mass (ng/cm^2)	Dissipation
miR16 probe	206.08 ng/cm^2	$2.07*10^{-6}$
miR16 target	299.53ng/cm^2	$2.3*10^{-6}$

Figure 5.6 represents increase in areal mass from 206.08 ng/cm^2 to 299.53 ng/cm^2, which indicates 50 % hybridisation rate. Only every second probe was hybridised with its complementary target. Figure 5.7 shows a small shift of the dissipation or damping, which is the sum of all energy losses in the system per oscillation cycle. A soft film attached to the quartz crystal gives high dissipation. In contrast, a rigid material gives low dissipation [94], which is a small shift, illustrated in Figure 5.6 and 5.7. From the results summarised in table 5.2, it can be stated that DNA formed double helix in 50 % and dissipation data shows no orientation change upon binding of target on MUA surface. Hybridised DNA on MUA surface is considered to be a rigid film, as not more than $2.00x10^{-6}$ changes in dissipation for every 10 Hz change in frequency was observed.
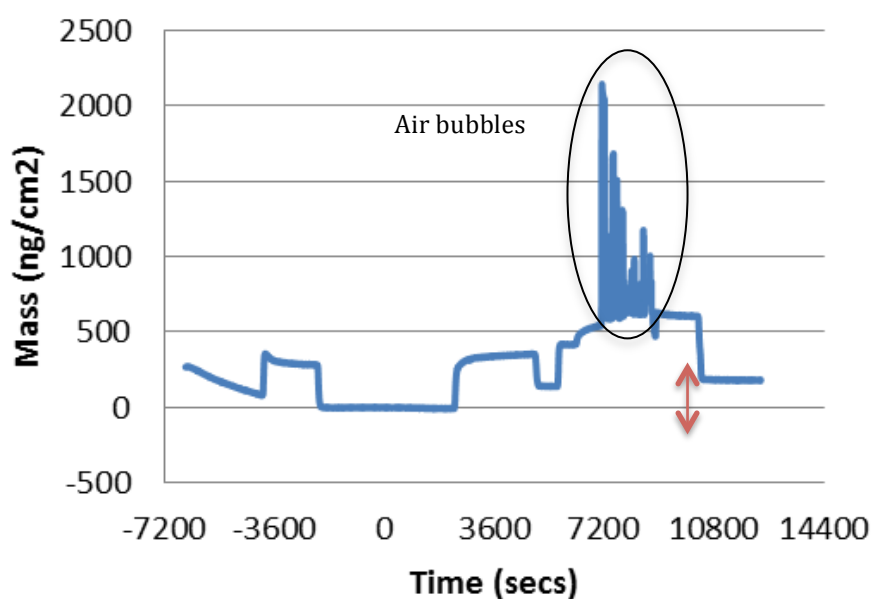
Figure 5.8 Negative control on MUA, time (secs) vs. areal mass (ng/cm^2); Increase in areal mass (red arrow) indicates 23 % hybridisation rate.
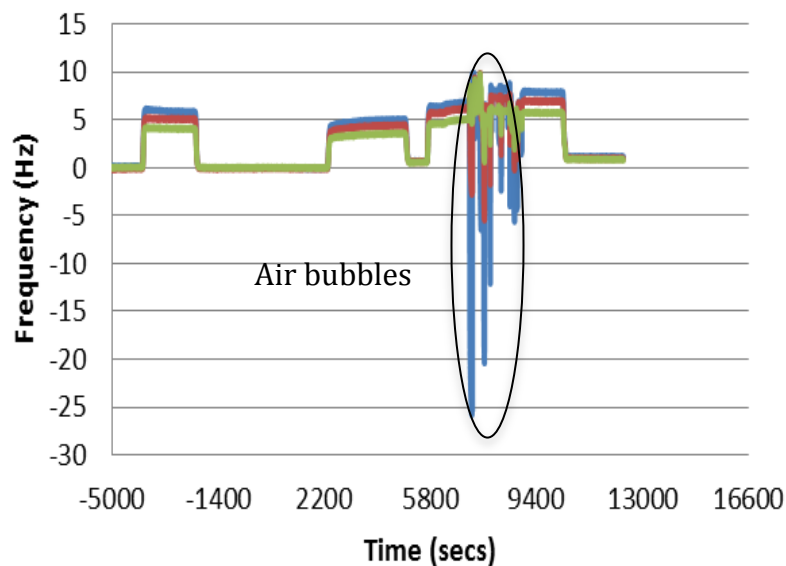
Figure 5.9 Negative control on MUA, dissipation. Small shift in dissipation, DNA film remains rigid.

Table 5.3 Areal mass and dissipation for miR16 probe immobilisation and miR16 probe – miR195 target hybridisation.

Positive control	Areal mass (ng/cm^2)	Dissipation
miR16 probe	139.76 ng/cm^2	$0.64*10^{-6}$
miR195 target	181.25 ng/cm^2	$1.10*10^{-6}$

Figure 5.8 represents increase in areal mass from 139.76 ng/cm^2 to 181.25 ng/cm^2, which indicates 23 % hybridisation rate. It is much lower rate that in case of the positive control, which is expected. Non – specific target can still hybridise but at much lower rate due to its mis - match. Figure 5.9 shows a small shift of the dissipation, which indicates rigidness of the film. In summary, positive control hybridises at a higher rate that negative control, table 5.3. In both cases DNA does not change its orientation upon hybridisation with target on MUA coated substrate.

QCM data can be hard to interpret in terms of thickness measurements. In order to confirm the above results, DPI was used to complement the data. QCM uses gold-coated chips as oppose to DPI, which requires use of specially fabricated silicon oxide chips. Monolayer of MUA can be obtained on gold surface. Since DPI is silicon oxide type of material further linking was required. Combination of wet chemistry (APTES) and sulfo – SIAB linker was applied. The distribution or monolayer of –COOH groups is dependent on uniformity of the first layer, which is liquid APTES.
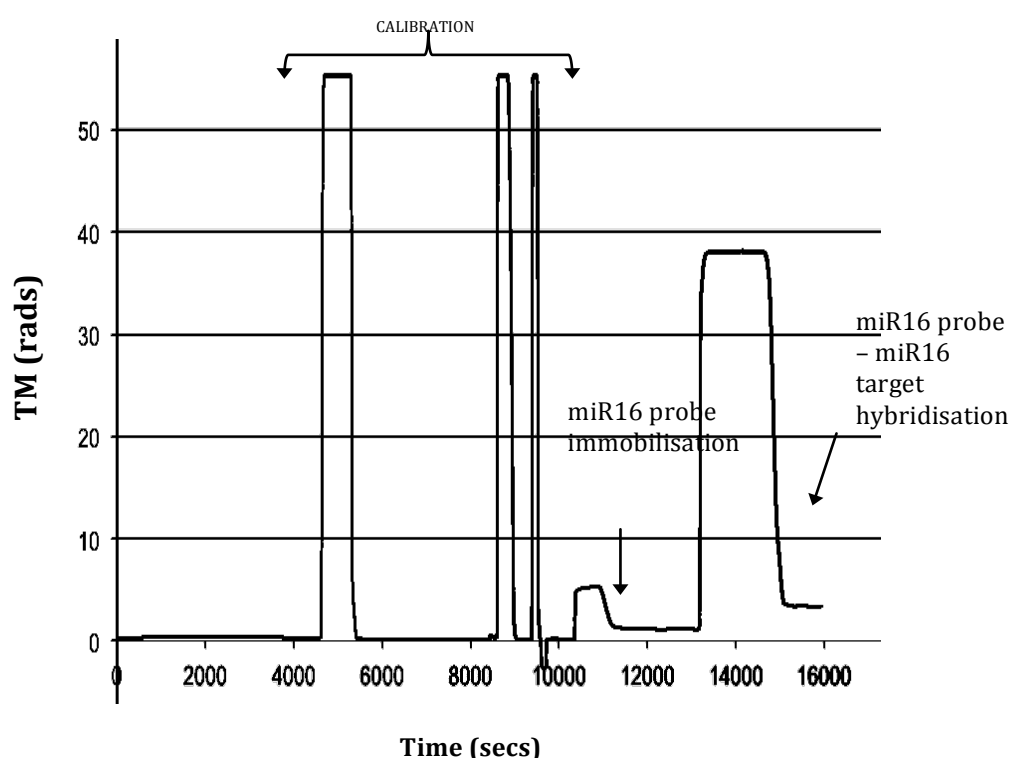
Figure 5.10 Graph represents real time measurement, time (secs) vs. TM (rads) on LA – SS – MUA substrate.

Table 5.4 Changes in thickness (nm), mass (ng/ mm^2) and density (g/cm^3) of probe only and hybridised target.

	Thickness (nm)	Mass (ng/ mm^2)	Density (g/ cm^3)
miR16 probe	0.3934	0.3217	0.8177
mir16 target	2.0728	0.9329	0.4501

From the graph 5.10 and table 5.4, miR16 probe immobilises to the surface, which results in mass increase up to 0.3217 ng/mm^2, thickness increase up to 0.3934 nm and density increase up to 0.8177 g/cm^3. Upon addition of specific target thickness increases to 2.0728 nm and mass increases to 0.9329 ng/mm^2, which indicates successful hybridisation but no orientation changes upon hybridisation. The width of double helix varies between 2-3 nm.
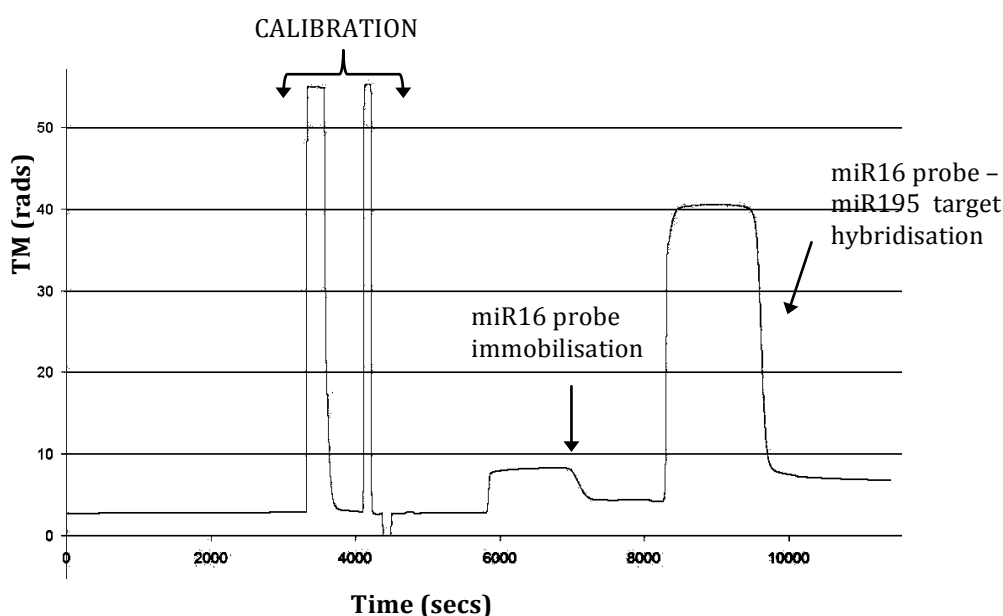
Figure 5.11 Graph represents real time measurement, time (secs) vs. TM (rads)for negative control on LA – SS – MUA substrate.

Table 5.5 **C**hanges in thickness (nm), mass (ng/ mm^2) and density (g/cm^3) of probe only and hybridised target.

	Thickness (nm)	Mass (ng/ mm^2)	Density (g/ cm^3)
miR16 probe	0.7951	0.469	0.5898
mir195 target	2.3268	1.1852	0.5094

From figure 5.11 and table 5.5, miR16 probe immobilises to the surface, which results in mass increase up to 0.469 ng/mm^2, thickness increase up to 0.7951 nm and density increase up to 0.5898 g/cm^3. Upon addition of specific target thickness increases to 2.3268 nm and mass increases to 1.1852 ng/mm^2, which indicates successful hybridisation but no orientation changes upon hybridisation.

DPI measurements confirmed results obtained by QCM technique. DNA does not stand up upon hybridisation with complimentary strand on MUA surface. Studies done by Eva Huang *et al.* show similar results. Her observations were that DNA molecules appear to reside on top of the MUA films with the strands parallel to the underlying gold substrates. In her experiment all the DNA helixes are lying flat on the substrate surface [100].

5.3.3 TIRE analysis

TIRE is a method used to obtain a precise refractive index and thickness of the formed layers. Therefore it was used for determination of DNA orientation changes on MUA surface coatings. Experiment for positive (miR195 probe – miR195 target) and negative control/mismatch (miR195 probe – miR16 target) was performed on TIRE instrument. The four-layer ellipsometric model summarized [103] in table 5.6 was used in the fitting of the measured Ψ and Δ spectra by using DeltaPsi 2 software (HORIBA Jobin Yvon, France) to deduce the thickness of each organic layer added to the gold surface [126]. This model was designed and used previously by fellow researcher in the group.

Table 5.6 Four-layer model used in the fitting of the measured Ψ and Δ spectra [126].

Layer	Materials	Thickness	Refractive index (all fixed)
1	BK7	∞	SCHOTT BK7 data sheet
2	Au	52 nm (fixed)	From Palik [103]
3	Organic layer (Zeonor, COOH, DNA or protein)	Variable	Cauchy: $A + B/l^2 + C/l^4$ A=1.415, B=0.01 nm^2, C=0 [103]
4	Water	∞	From Palik [103]

Ψ and Δ spectra of the complete DNA hybridisation assay are plotted in figure 5.12. The introduction of the capture aminated miR195 ssDNA solution and then the complementary miR195 target ssDNA solution should result in large shifts in both Ψ and Δ spectra from the initial Ψ and Δ spectra of the -COOH surface when the micro-well was filled with the buffer (positive control). The negative control experiment, conducted by incubating the aminated miR195 ssDNA probe solution and then the non-complementary miR16 target ssDNA solution should result in small or no shifts in both Ψ and Δ spectra from the initial Ψ and Δ spectra of the -COOH surface when the micro-well was filled with the buffer (negative control). However, the interpretation of the results proved to be too complicated and inconclusive. No large shifts were observed, which could indicate no orientation changes, but to confirm it correct modelling and results analysis is required.

A decision has been made to continue the study with other characterisation techniques, which had no limitation in terms of understanding and interpreting the data and modelling issues.
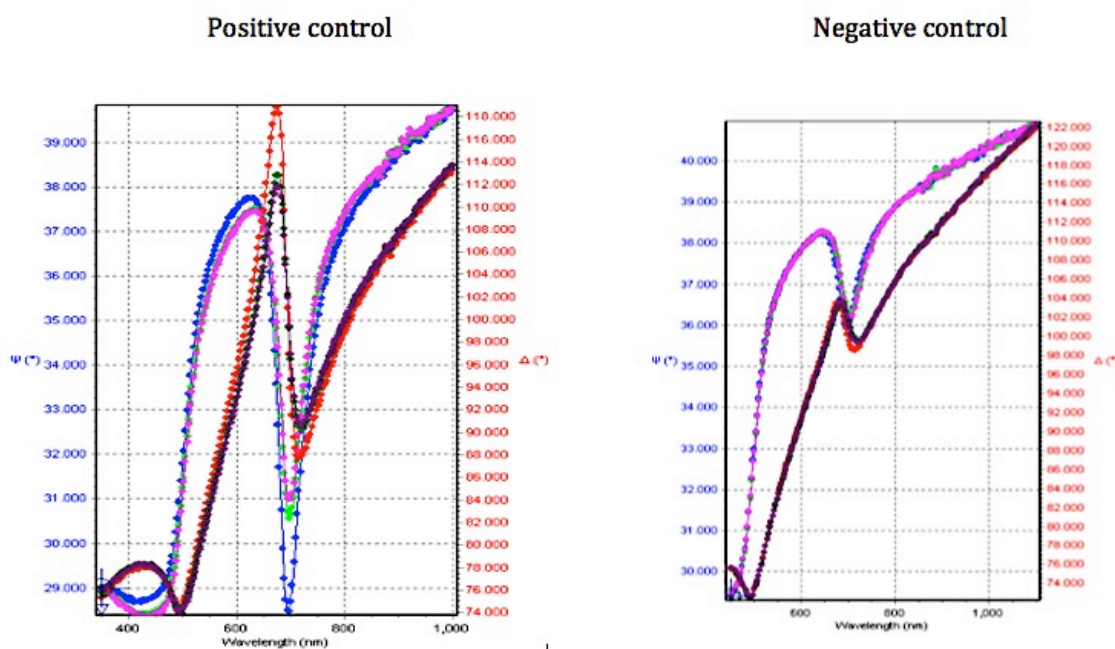
Figure 5.12 TIRE data: (left) positive control, (right) negative control.

5.3.4 DNA orientation changes on Succinic Anhydride

Since it was observed that DNA does not change its orientation on MUA, another surface was tested – SA. SA is hydrolysed amino surface to produce carboxylic acid negatively charged surface and as oppose to MUA it is not monolayer. The uniformity of the surface depends on the coverage of the wet chemistry – APTES. Both positive (miR195 probe – miR195 target hybridisation) and negative controls (miR195 probe – miR16 target hybridisation) were performed and results are shown in figure 5.13.
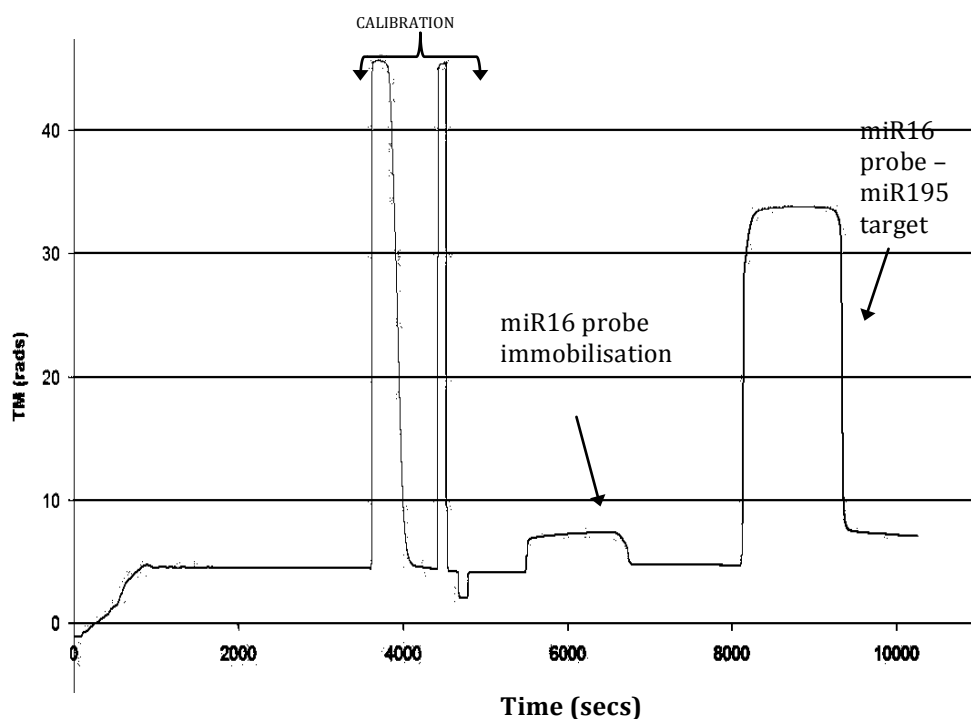
Figure 5.13 Graph represents real time measurement, time (secs) vs. TM (rads) for positive control on SA substrate.

Table 5.7 Changes in thickness (nm), mass (ng/ mm^2) and density (g/cm^3) of probe only and hybridised target

	Thickness (nm)	Mass (ng/ mm^2)	Density (g/ cm^3)
miR16 probe	0.3797	0.1814	0.4777
miR16 target	2.8493	0.9661	0.3391

As seen in figure 5.13 and table 5.7, the successful DNA single probe immobilisation was observed, which is represented in thickness increase up to 0.3797 nm and mass increase up to 0.1814 ng/mm ^{2}. Hybridisation also took place as represented by increase thickness from 0.3797 nm to 2.8493 nm and mass increase from 0.1814 ng/mm ^{2} to 0.9661 ng/mm ^{2}. The results on SA surface are comparable with measurements on LA – SS – MUA substrate and can be interpreted that DNA does not stand up upon hybridisation with complimentary strand.
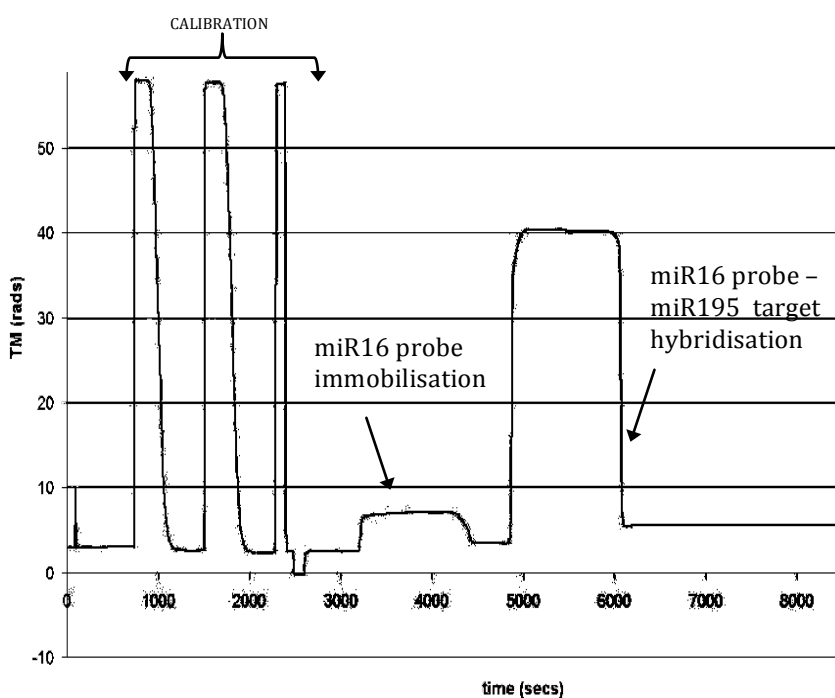
Figure 5.14 Graph represents real time measurement, time (secs) vs. TM (rads) for negative control on SA substrate.

Table 5.8 Table shows changes in thickness (nm), mass (ng/ mm^2) and density (g/cm^3) of probe only and hybridised target.

	Thickness (nm)	Mass (ng/ mm^2)	Density (g/ cm^3)
miR16 probe	0.4742	0.2734	0.5766
mir195 target	5.5492	0.8315	0.1498

The successful DNA single probe immobilisation that is represented in thickness increase up to 0.4742 nm and mass increase up to 0.2734 ng/mm^2 is seen in figure 5.14 and table 5.8. After addition of secondary non –complimentary strand thickness increased up to 5.5492 nm, which would indicate about orientation change. However the assumption has been made that this substantial thickness increase is caused by a large amount of non – specific binding. Secondary strand is probably very attracted to immobilised strand by its electrostatic charge. This result wasn't as expected, but it was repeated and results were reproducible. In order to minimize NSB harsher washing step is required. Mass increase was comparable to the other negative control experiments and it went up to 0.8315 ng/mm^2. Density decrease was substantial, which could possibly indicate that DNA is standing up, but it is more probable that secondary strands are stacked up one on top of another being attracted by probe's charge, see figure 5.15. Thickness changes calculations on DPI are based on average of thickness throughout measured area.
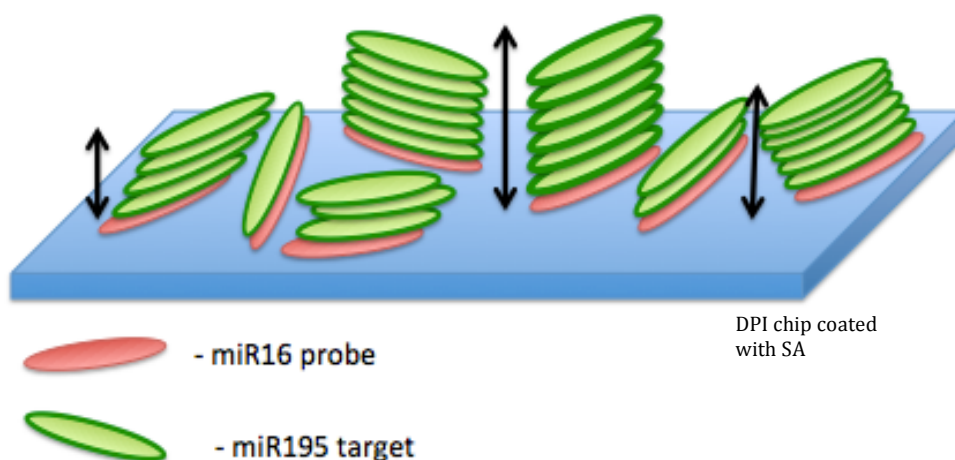
Figure 5.15 DNA ''towers'', miR195 targets stacked up on miR16 probe on SA substrate.

5.3.5 DNA orientation changes on liquid APTES

APTES depositions were prepared by wet chemistry and results in positively charged – NH$_2$ coverage. This surface was used in order to see DNA behaviour on positively charged surface as oppose to the negatively charged carboxylic acid coated surfaces. In order to adhere DNA probe covalently onto the surface, addition of a homo bi-functional cross-linker molecule such as glutaraldehyde to enable attachment of aminated biomolecules is required. An experiment with no glutaraldehyde linker was performed in order to see the binding strength and DNA attraction to the surface (non covalently). Results are presented in figure 5.16 and table 5.9.
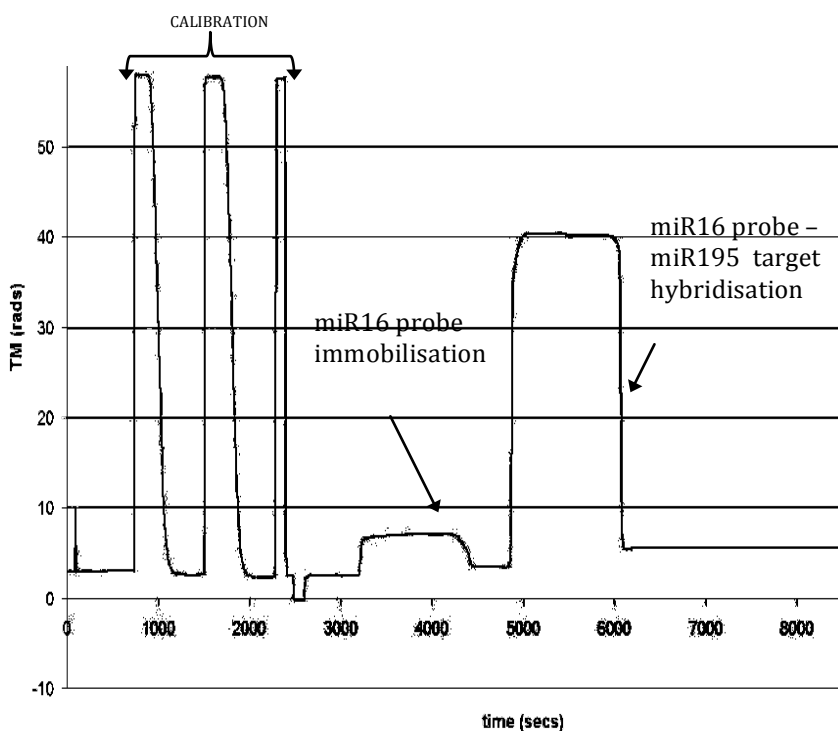
Figure 5.16 graph represents real time measurement, time (secs) vs. TM (rads) for positive control on liquid APTES substrate.

Table 5.9 **T**able shows changes in thickness (nm), mass (ng/ mm^2) and density (g/cm^3) of probe only and hybridised target.

	Thickness (nm)	Mass (ng/ mm^2)	Density (g/ cm^3)
miR16 probe	0.2684	0.1814	0.6758
miR16 target	2.5367	0.2354	0.0928

DNA probe is immobilised in the same manner on positively charged surface as on negatively charged surface. The values increase for thickness and mass on APTES were comparable with thickness and mass increase on MUA. Upon hybridisation with complementary strand, DNA is still lying flat. This means that not every ''tower'' of probe – secondary targets has thickness of 5.5492 nm. Some of the ''towers'' may be higher and/or shorter giving a final thickness average of approx. 5.5 nm. This assumption was based solely on mass changes. It was observed that the mass increase is at the same rate as for negative control on previously described surfaces, which indicates not every probe was stacked up with the same amount of targets.

5.3.6 DNA orientation changes on plain gold

QCM chips are coated with gold. The experiment was carried out to investigate DNA orientation on plain gold chip without any functionalised coatings. In order to immobilise DNA probe onto a bare gold surface anchoring point is required. The DNA probe had to be modified with a -thiol end to be able to covalently adhered to the surface.
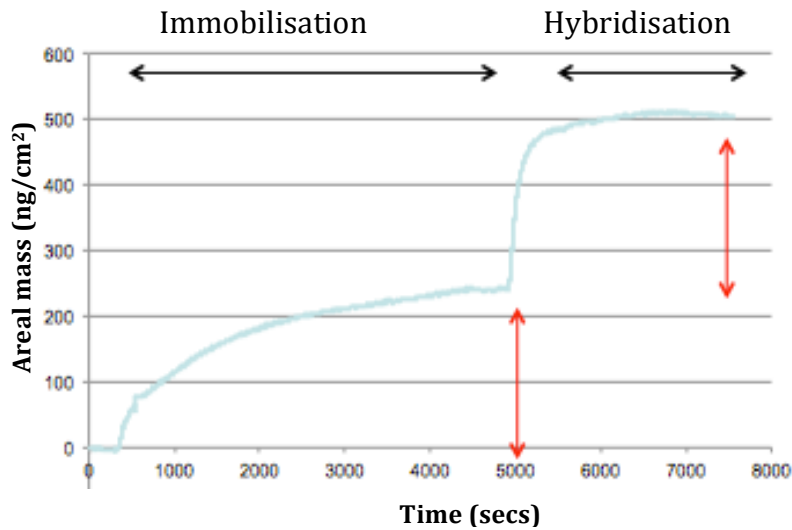
Figure 5.17 Positive control on bare gold, significant shift means successful immobilisation.
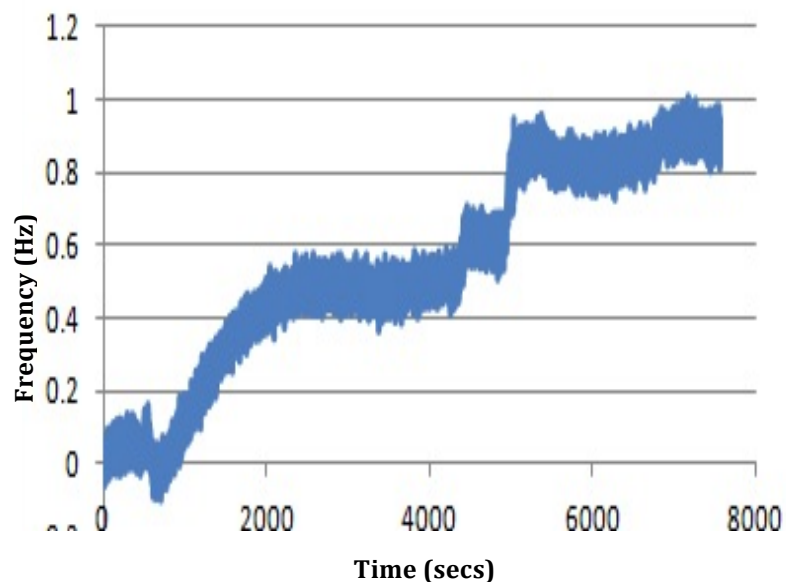
Figure 5.18 Positive control on bare gold, dissipation. Not significant shift, DNA film remains rigid.

Table 5.10 **A**real mass and dissipation for miR16 probe immobilisation and miR16 probe – miR16 target hybridisation.

	Areal mass (ng/cm^2)	Dissipation
miR16 probe - SH	240 ng/cm^2	$0.5*10^{-6}$
miR195 target	500 ng/cm^2	$0.9*10^{-6}$

From figure 5.17 it can be clearly seen that thiolated DNA probe was successfully immobilised onto the bare gold surface. Hybridisation also took place based on areal mass decrease from approx. 240 ng/cm^2 to 500 ng/cm^2, table 5.10, which indicates that almost every single stranded probe was hybridised with its complimentary target. In terms of dissipation, or in other words rigidness of the film, the shift from immobilised probe to hybridised target is not significant, see figure 5.18. Hence, the assumption that DNA is not standing up on bare gold surface.

5.3.7 DNA orientation changes on ox. PMMA

Ox. PMMA was another suggested carboxylic acid negatively charged surface. N. Le *et al*. observed a large increase in thickness corresponding to 6.5 nm for the hybrid helix micro RNA of complementary strands [126]. The following experimentation was performed to confirm the above the results. DNA analogues of micro RNA were used instead; positive and negative controls on PMMA prepared surfaces are presented below.

Table 5.11 Positive control on PMMA; thickness, mass and density changes.

	Thickness (nm)	Mass (ng/ mm^2)	Density (g/ cm^3)
miR16 probe	0.3569	0.1334	0.3737
miR16 target	2.1842	1.2449	0.5699

Table 5.12 Negative control on PMMA; thickness, mass and density changes.

	Thickness (nm)	Mass (ng/ mm^2)	Density (g/ cm^3)
miR16 probe	0.3279	0.2323	0.7085
miR195 target	3.3326	1.2259	0.3679

Positive and negative control on ox.PMMA were performed multiple times and results were reproducible. DNA probe immobilisation was comparable with other surfaces in terms of thickness changes. There were no orientation changes observed upon hybridisation with specific nor non - specific control, see table 5.11 and 5.12. Hybridisation took place in both cases, positive and negative control.

5.4 Summary and conclusion

There was an extensive investigation carried out in order to assess the DNA orientation changes phenomenon. An attempt was made to replicate and understand the previous results [103], which sparked the idea of the DNA standing up upon hybridisation with the complimentary strand. In order to understand it, the decision was made to employ other carboxylic acid group surfaces and compare the results. Also a control, APTES, was used to see if surface charge has an effect on the mentioned phenomenon.

Despite previous observations by N. Le *et al* in this research group [103], results proven to be hard to replicate and the orientation changes recorded by DPI were not observed. However, N. Le prepared his surface coatings on a different tool using a different plasma process configuration, resulting in a different interaction between the plasma and the substrate. Consequently, the nature of the surface chemistry will be different. This could possibly cause the difficulty in repeating the results. The assumption has been made that the amount and distribution of carboxylic acid groups can differ in the functionalised surfaces and can possibly have an effect on the DNA orientation changes.

Additionally QCM is not most suitable technique for thickness/height measurement, as referred to Jiri Janata, Principles of Chemical sensors: *''(…) a limitation arises from the operation of these [QCM] devices in a liquid phase. In such media the output signal of the sensor is affected not only by the incremental mass due to the above reaction, but also by frictional effects at the sensor – liquid interface that affect the energy loss. Water is the required environment for most biological reactions, so it follows that the biological means of achieving chemical selectivity are not generally suitable for this type of sensor* [98] *''.* To summarise the above statement, QCM technique is not suited to determine the DNA molecule orientation, as it relies too much on assumptions.

Table 5.13   Summary of chapter 5 – key messages

CHAPTER 5 – key messages
• Despite the extensive investigation, results were inconclusive

• Possible difficulty in repeating the results:
  • Le *et al* prepared his surface coatings on a different tool using a different plasma process configuration, resulting in a different interaction between the plasma and the substrate.
  • Consequently, the nature of the surface chemistry was different
  • A decision has been made to focus on development of surfaces

6 Major findings and future directions

6.1 Major findings

Work in this thesis was focused on the improvement and development of functionalised films and immobilisation method for bio-conjugation of the biomolecules to solid supports with future application as biosensors. Point-of-care (POC) devices are valuable tools in diagnostics field. However they possess a number of limitations including non-specific binding as well as sensitivity and fabrication challenges. Hence, new formats for POC platforms are required in order to improve overall performance of the devices. Two major findings are described below.

Chapter 3 includes investigation of the use of surface treatments to oxidise PMMA to form a carboxylic acid surfaces in order to enable the covalent attachment of biomolecules, such as DNA or protein. Synthetic polymers are a promising alternative substrate for biosensors because of their low specific gravity, a selectable range of mechanical and surface properties, and a number of well-established high-volume, low-cost manufacturing techniques [58,162]. Amine functionalised surfaces [194,201] and self assembly monolayers [163,179] are also techniques used for development of microarrays and biosensors. Although spin coating PMMA is a relatively well-known process [126], to date there has been no direct comparison of the different oxidation methods to activate the surface, nor has oxidised spin coated PMMA been used as a platform for DNA hybridisation or immunoassays. This thesis addressed the above and tested stability, functionality and fabrication process of both spin coating and oxidation methods to produce robust films [3]. Hence, the major finding is work published to show the superiority of ox. PMMA while compared to other films such as self-assembly monolayers or films prepared by PECVD.

Chapter 4 examines the immobilisation of amino-modified single-stranded DNA onto carboxylic acid surfaces using EDC linkers, which leads to binding at multiple anchoring sites. Orientation of single stranded DNA has the effects on DNA probe distribution and availability for further hybridisation [100]. An alternative conjugation method was proposed; click chemistry, which shows to improve the quantity and quality of target binding and lowering limit of detection (LOD) of hybridisation. The CC immobilisation technique is another major finding during this work (submitted to be

published) , and proves to be a great improvement to currently used immobilisation methods including EDC chemistry [9,205] or thiol-ene chemistry [175].

To summarise, listed below are two major findings as a result of work carried out:

- a suitable and novel surface has been developed for biomolecules bio-conjugation, in application for microarray and further application of biosensors [3]
- a new and improved approach of DNA probe immobilisation to the ox.PMMA surface has been developed to improve assay LOD, sensitivity and specificity (paper submitted to be published).

6.2 Future directions

The ultimate goal would be a development of fully automated DNA sensor for the purpose of early disease diagnosis, ie: breast cancer, from a blood sample. The sensitivity (low LOD) and specificity (low NSB) of the test would be of the paramount importance. It would also be beneficial to adapt the platform, so that multiple biomarkers could be detected in selective manner at low concentration levels. This chapter lists few ideas, which could be incorporated in the future.

After successful development of functionalised surface and DNA immobilisation method suitable for DNA sandwich assay (miR-195), the next step would be to test DNA analogues of biomarkers other than miR-195 in order to expand applicability of the assay design. For instance studies done by other research groups have shown that miRNA-451 (miR-451) is widely deregulated in human breast cancer [206,207] and plays a critical role in tumorigenesis and tumour progression [208]. MiR-451 has the potential in cancer diagnosis, prognosis, and treatment. Research done by Dan Li *et al.* implies that both miR-195 and miR-497 play important inhibitory roles in breast cancer malignancy and may be the potential therapeutic and diagnostic targets [28]. Another work published by Luo Q. *et al* reports that MicroRNA-195-5p is a potential diagnostic and therapeutic target for breast cancer. Mir-195-5p may act as a tumour suppressor in BC [27].

Next step in this study would be to use possibly miR-451 DNA analogues with sandwich assay on developed substrates during this PhD work to determine the ability of target detection. After full assay optimisation, DNA analogues should be replaced with micro RNA and LOD of target detection should be determined.

As mentioned in the paragraph above, a full assay optimisation with miRNA would be the next step. The difference between DNA analogues and miRNA is in its bases; DNA base thymine is replaced by uracil in RNA structure. No assays optimisation with miRNA were performed, hence full adaptation of the novel surface and immobilisation the miRNA capture probe would be required. The environment and handling of miRNA for assays would have to be more sterile and strict, as miRNA are not as robust as DNA; they are sensitive to RNase which is a type of nuclease that catalyses the degradation of RNA into smaller components, consequently denaturing the molecule.

The assay would need to be tested for NSB for miRNA. Other RNAs structurally similar to the one tested should be included, ie: Mir-16 - a housekeeping miRNA in human's body, also used as an endogenous control to standardise miRNA expression [4] does not significantly differ from mir-195 sequence. Hence to avoid false positive results, the biosensor must be able to distinguish between similar sequences of micro RNAs even at very low concentration levels. Currently, minimum NSB with DNA was obtained, however this needs to be tested for other molecules and their binding. The comparison of LOD for DNA and miRNA would be beneficial for the device development. This process would need to result in improving LOD to the range of pico-molar (denoting one trillionth, a factor of 10^{-12}), as the biomarkers are present in blood at the above range.

Following the goals achieved above, next step would be to use clinical samples, whole blood. For this type of BC sensor, blood sample is ideal as obtaining it is neither too invasive nor complicated. However whole blood has a number of other molecules, which may interfere and compromise sensors selectivity and sensitivity. Therefore the sample needs to be purified and RNA needs to be extracted. Ideally the assay would be transferred onto a chip and microfluidic systems would have to be incorporated. Technologies involving microfluidic lab-on-a-chip have many advantages over other techniques, including ability to automate and reduce the time-to-result of bio analytical assays, and ultimately make them more accessible at the point of need. There is a large

range of on-chip detection techniques, however there are only few microfluidic devices for nucleic acid testing integrating sample preparation with detection [209,210].

Work done by the fellow researcher reports for the first time rotationally controlled extraction of total RNA from cell homogenate through novel, solvent-dependent routing on a centrifugal microfluidic platform. This method allows for sample to be prepared and analysed on a single microfluidic chip/device [211,212]. This technique could be used with the functionalised films developed in this study and further optimised in terms of hydrophobicity, which is important for the flow of the liquid. At the moment the hydrophobicity of the ox. PMMA is not too high and not too low, which may be an advantage, but this would have to be further tested.

PMMA could be easily adapted for incorporation into a disk like device, due to its ease of preparation and fabrication. With the click chemistry immobilisation technique the whole assay can be performed at room temperature with specific and accurate results. Therefore no heating device would be necessary, which makes the device design easier and does not require incorporation of complicated and expensive heating elements.

The ability to detect BC at an early stage with the help of biomarkers is of a huge interest in order to reduce mortality, because BC as most of the cancers detected an early stage is more curable than metastatic disease. Therefore biomarkers predicting the occurrence of metastatis in the patient are extremely important. In some cases a panel of biomarkers is required in order to predict a result. Hence, incorporation of few channels into the device developed here and the ability to perform multiple tests simultaneously would be ideal. For instance the combination of three independent biomarkers: urokinase – dependent plasminogen activator system (uPA), the plasminogen activator inhibitor (PAI) and the Thomsen-Friedenreich (TF) antigen applied for an early diagnosis. Other combination of other three independent biomarkers which found its application as a potential panel of biomarkers for the prediction of metastatic disease include: Mammaglobin, osteopontin, snail, twist, Zeb-1, fibroblast growth factor receptors (FGFR), phosphatase and tensin homolog (PTEN) and sirtuins (SIRT) [20]. The DNA assay format may not necessary fit the purpose of the detection for the above molecules. However the novel surface and immobilisation technique may prove useful in the device adaptation.

Bibliography

[1]   WHO, WHO | Breast cancer: prevention and control, Breast Cancer Prev. Control. (2013). available online: http://www.who.int/cancer/detection/breastcancer/en/index1.html

[2]   K. Polyak, Heterogeneity in breast cancer., J. Clin. Invest. 121 (2011) 3786–3788. doi:10.1172/JCI60534.

[3]   M. Rowinska, S.M. Kelleher, F. Soberon, A.J. Ricco, S. Daniels, Fabrication and characterisation of spin coated oxidised PMMA to provide a robust surface for on-chip assays, J. Mater. Chem. B. (2014) 135 - 143. doi:10.1039/C4TB01748J.

[4]   H.M. Heneghan, N. Miller, R. Kelly, J. Newell, M.J. Kerin, Systemic miRNA-195 differentiates breast cancer from other malignancies and is a potential biomarker for detecting noninvasive and early stage disease., Oncologist. 15 (2010) 673–682. doi:10.1634/theoncologist.2010-0103.

[5]   N.C. Registry, Breast Cancer incidence, mortality, treatment and survival in Ireland: 1994-2009, Breast Cancer Incid. Mortality, Treat. Surviv. Irel. 1994-2009. (2012) 4–37. Available online: http://www.ncri.ie/sites/ncri/files/pubs/BreastCancerIncidenceMortalityTreatmen tandSurvivalinIreland1994-2009.pdf

[6]   J. V Lacey, A.R. Kreimer, S.S. Buys, P.M. Marcus, S.-C. Chang, M.F. Leitzmann, RN Hoover, PC Prorok, CD Berg, P Hartge, Breast cancer epidemiology according to recognized breast cancer risk factors in the Prostate, Lung, Colorectal and Ovarian (PLCO) Cancer Screening Trial Cohort., BMC Cancer. 9 (2009) 84 - 96. doi:10.1186/1471-2407-9-84.

[7]   R. A. Smith, IARC Publications - Breast Cancer Screening - IARC Handbook of Cancer Prevention Volume 7, IARC Handbooks Cancer Prev. (2003) 17–57. Available online: http://www.iarc.fr/en/publications/pdfs-online/prev/handbook7/

[8]   G. Danaei, S. Vander Hoorn, A.D. Lopez, C.J.L. Murray, M. Ezzati, Causes of cancer in the world: comparative risk assessment of nine behavioural and environmental risk factors., Lancet. 366 (2005) 1784–1793. doi:10.1016/S0140-6736(05)67725-2.

[9]   S.A. Soper, M. Hashimoto, C. Situma, M.C. Murphy, R.L. McCarley, Y.-W. Cheng, F. Barany, Fabrication of DNA microarrays onto polymer substrates using UV modification protocols with integration into microfluidic platforms for the sensing of low-abundant DNA point mutations., Methods. 37 (2005) 103–113. doi:10.1016/j.ymeth.2005.07.004.

[10]   R.J. Meagher, A. V. Hatch, R.F. Renzi, A.K. Singh, An integrated microfluidic platform for sensitive and rapid detection of biological toxins., Lab Chip. 8 (2008) 2046–2053. doi:10.1039/b815152k.

[11]   V. Gubala, L.F. Harris, A.J. Ricco, M.X. Tan, D.E. Williams, Point of care diagnostics: status and future., Anal. Chem. 84 (2012) 487–515. doi:10.1021/ac2030199.

[12]   P. St-Louis, Status of point-of-care testing: promise, realities, and possibilities., Clin. Biochem. 33 (2000) 427–440.

[13]   J.W. Winkelman, D.R. Wybenga, M.J. Tanasijevic, The fiscal consequences of

central vs distributed testing of glucose., Clin. Chem. 40 (1994) 1628–1630.

[14] H.M. Solomon, R.E. Mullins, P. Lyden, P. Thompson, S. Hudoff, The diagnostic accuracy of bedside and laboratory coagulation: procedures used to monitor the anticoagulation status of patients treated with heparin., Am. J. Clin. Pathol. 109 (1998) 371–378.

[15] P. von Lode, Point-of-care immunotesting: approaching the analytical performance of central laboratory methods., Clin. Biochem. 38 (2005) 591–606. doi:10.1016/j.clinbiochem.2005.03.008.

[16] M.T. Weigel, M. Dowsett, Current and emerging biomarkers in breast cancer: prognosis and prediction., Endocr. Relat. Cancer. 17 (2010) 245–262. doi:10.1677/ERC-10-0136.

[17] L. Chung, K. Moore, L. Phillips, F.M. Boyle, D.J. Marsh, R.C. Baxter, Novel serum protein biomarker panel revealed by mass spectrometry and its prognostic value in breast cancer., Breast Cancer Res. 16 (2014) 63 - 71. doi:10.1186/bcr3676.

[18] K.D. Cole, H.-J. He, L. Wang, Breast cancer biomarker measurements and standards., Proteomics. Clin. Appl. 7 (2013) 17–29. doi:10.1002/prca.201200075.

[19] M. Brooks, Breast cancer screening and biomarkers., Methods Mol. Biol. 472 (2009) 307–321. doi:10.1007/978-1-60327-492-0_13.

[20] M.J.B.S. Brunna dos A. Pultz, F. Andrés Cordero da Luz, P. R. de Faria, A. P. Lima Oliveira, R. A. de Araújo, Far beyond the usual biomarkers in breast cancer: A Review., J Cancer. (2014) 559–571.

[21] S. Taplin, L. Abraham, W.E. Barlow, J.J. Fenton, E.A. Berns, P.A. Carney, Cutter GR, Sickles EA, Carl D, Elmore JG., Mammography facility characteristics associated with interpretive accuracy of screening mammography., J. Natl. Cancer Inst. 100 (2008) 876–887. doi:10.1093/jnci/djn172.

[22] J.S. Mandelblatt, K.A. Cronin, S. Bailey, D.A. Berry, H.J. de Koning, G. Draisma, H. Huang, S. J. Lee, M. Munsell, S. K. Plevritis, P. Ravdin, C. B. Schechter, B. Sigal, M. A. Stoto, N. K. Stout, N. T. van Ravesteyn, J. Venier, M. Zelen, , E. J. Feuer, Effects of mammography screening under different screening schedules: model estimates of potential benefits and harms., Ann. Intern. Med. 151 (2009) 738–747. doi:10.7326/0003-4819-151-10-200911170-00010.

[23] T.M. Svahn, D.P. Chakraborty, D. Ikeda, S. Zackrisson, Y. Do, S. Mattsson, I. Andersson, Breast tomosynthesis and digital mammography: a comparison of diagnostic accuracy., Br. J. Radiol. 85 (2012) 1074–1082. doi:10.1259/bjr/53282892.

[24] L. Chung, R.C. Baxter, Breast cancer biomarkers: proteomic discovery and translation to clinically relevant assays., Expert Rev. Proteomics. 9 (2012) 599–614. doi:10.1586/epr.12.62.

[25] L. Harris, H. Fritsche, R. Mennel, L. Norton, P. Ravdin, S. Taube, MR Somerfield, DF Haynes, RC Jr. Bast, American Society of Clinical Oncology 2007 update of recommendations for the use of tumor markers in breast cancer., J. Clin. Oncol. 25 (2007) 5287–5312. doi:10.1200/JCO.2007.14.2364.

[26] G. Yang, D. Wu, J. Zhu, O. Jiang, Q. Shi, J. Tian, Y. Weng, Upregulation of

miR-195 increases the sensitivity of breast cancer cells to Adriamycin treatment through inhibition of Raf-1., Oncol. Rep. 30 (2013) 877–889. doi:10.3892/or.2013.2532.

[27] Q. Luo, C. Wei, X. Li, J. Li, L. Chen, Y. Huang, H. Song, D. Li, L. Fang, MicroRNA-195-5p is a potential diagnostic and therapeutic target for breast cancer., Oncol. Rep. 31 (2014) 1096–1102. doi:10.3892/or.2014.2971.

[28] D. Li, Y. Zhao, C. Liu, X. Chen, Y. Qi, Y. Jiang, Zou C, Zhang X, Liu S, Wang X, Zhao D, Sun Q, Zeng Z, Dress A, Lin MC, Kung HF, Rui H, Liu LZ, Mao F, Jiang BH, Lai L., Analysis of MiR-195 and MiR-497 expression, regulation and role in breast cancer., Clin. Cancer Res. 17 (2011) 1722–1730. doi:10.1158/1078-0432.CCR-10-1800.

[29] H.M. Heneghan, N. Miller, M.J. Kerin, MiRNAs as biomarkers and therapeutic targets in cancer., Curr. Opin. Pharmacol. 10 (2010) 543–550. doi:10.1016/j.coph.2010.05.010.

[30] H.M. Heneghan, N. Miller, A.J. Lowery, K.J. Sweeney, J. Newell, M.J. Kerin, Circulating microRNAs as novel minimally invasive biomarkers for breast cancer., Ann. Surg. 251 (2010) 499–505. doi:10.1097/SLA.0b013e3181cc939f.

[31] H.M. Muller, A. Widschwendter, H. Fiegl, L. Ivarsson, G. Goebel, E. Perkmann, Marth C, Widschwendter M., DNA Methylation in Serum of Breast Cancer Patients: An Independent Prognostic Marker, Cancer Res. 63 (2003) 7641–7645.

[32] M.J. Fackler, Z. Lopez Bujanda, C. Umbricht, W.W. Teo, S. Cho, Z. Zhang, K. Visvanathan, S. Jeter, P. Argani, C. Wang, J.P. Lyman, M. de Brot, J.N. Ingle, J. Boughley, K. McGuire, T.A. King, L.A. Carey, L. Cope, A.C. Wolff, S. Sukumar, Novel methylated biomarkers and a robust assay to detect circulating tumor DNA in metastatic breast cancer., Cancer Res. 74 (2014) 2160–2170. doi:10.1158/0008-5472.CAN-13-3392.

[33] F. Mar-Aguilar, J.A. Mendoza-Ramírez, I. Malagón-Santiago, P.K. Espino-Silva, S.K. Santuario-Facio, P. Ruiz-Flores, Rodríguez-Padilla C, Reséndez-Pérez D., Serum circulating microRNA profiling for identification of potential breast cancer biomarkers., Dis. Markers. 34 (2013) 163–169. doi:10.3233/DMA-120957.

[34] S.A. Eccles, D.R. Welch, Metastasis: recent discoveries and novel treatment strategies., Lancet. 369 (2007) 1742–1757. doi:10.1016/S0140-6736(07)60781-60788.

[35] K. Tjensvoll, K.N. Svendsen, J.M. Reuben, S. Oltedal, B. Gilje, R. Smaaland, Nordgård O., miRNA expression profiling for identification of potential breast cancer biomarkers., Biomarkers. 17 (2012) 463–470. doi:10.3109/1354750X.2012.686061.

[36] M. V Iorio, M. Ferracin, C.-G. Liu, A. Veronese, R. Spizzo, S. Sabbioni, Magri E, Pedriali M, Fabbri M, Campiglio M, Ménard S, Palazzo JP, Rosenberg A, Musiani P,Volinia S, Nenci I, Calin GA, Querzoli P, Negrini M, Croce CM., MicroRNA gene expression deregulation in human breast cancer., Cancer Res. 65 (2005) 7065–7070. doi:10.1158/0008-5472.CAN-05-1783.

[37] H. Zhang, S.-B. Su, Q.-M. Zhou, Y.-Y. Lu, Differential expression profiles of microRNAs between breast cancer cells and mammary epithelial cells, 28 (2009)

493–499.

[38]   F. S. Ligles, J. W. Hazzard, J. P. Golden, C. A. Rowe, Novel Approaches in Biosensors and Rapid Diagnostic Assays, Springer, (2001) 7 - 15.

[39]   J.D. Newman, A.P.F. Turner, Home blood glucose biosensors: a commercial perspective., Biosens. Bioelectron. 20 (2005) 2435–2453. doi:10.1016/j.bios.2004.11.012.

[40]   A.P.F. Turner, Biosensors: sense and sensibility., Chem. Soc. Rev. 42 (2013) 3184–3196. doi:10.1039/c3cs35528d.

[41]   S.A. Soper, K. Brown, A. Ellington, B. Frazier, G. Garcia-Manero, V. Gau, Gutman SI, Hayes DF, Korte B, Landers JL, Larson D, Ligler F, Majumdar A, Mascini M,Nolte D, Rosenzweig Z, Wang J, Wilson D., Point-of-care biosensor systems for cancer diagnostics/prognostics., Biosens. Bioelectron. 21 (2006) 1932–1942. doi:10.1016/j.bios.2006.01.006.

[42]   B.D. Malhotra, R. Singhal, A. Chaubey, S.K. Sharma, A. Kumar, Recent trends in biosensors, Curr. Appl. Phys. 5 (2005) 92–97. doi:10.1016/j.cap.2004.06.021.

[43]   S. Lahiff, M. Glennon, J. Lyng, T. Smith, N. Shilton, M. Maher, Real-time polymerase chain reaction detection of bovine DNA in meat and bone meal samples., J. Food Prot. 65 (2002) 1158–1165.

[44]   Q. Han, E. M. Bradshaw, B. Nilsson, D.A. Hafler, J. C. Love, Lab-on-a-chip., Lab chip, 10 (2010) 1391-1400 doi: 10.1039/B926849A

[45]   M.B. Miller, Y.-W. Tang, Basic Concepts of Microarrays and Potential Applications in Clinical Microbiology, Clin. Microbiol. Rev. 22 (2009) 611–633. doi:10.1128/CMR.00019-09.

[46]   S.B. Nimse, K. Song, M.D. Sonawane, D.R. Sayyed, T. Kim, Immobilization techniques for microarray: challenges and applications., Sensors (Basel). 14 (2014) 22208–22229. doi:10.3390/s141222208.

[47]   M. Campàs, I. Katakis, DNA biochip arraying, detection and amplification strategies., TrAC Trends Anal. Chem. 23 (2004) 49–62. doi:10.1016/S0165-9936(04)00104-9.

[48]   N.S. Green, S.M. Dolan, T.H. Murray, Newborn screening: complexities in universal genetic testing., Am. J. Public Health. 96 (2006) 1955–1959. doi:10.2105/AJPH.2005.070300.

[49]   A.M. Comeau, R.B. Parad, H.L. Dorkin, M. Dovey, R. Gerstle, K. Haver, A. Lapey, B. P. O'Sullivan, D. A. Waltz, R. G. Zwerdling, R. B. Eaton, Population-based newborn screening for genetic disorders when multiple mutation DNA testing is incorporated: a cystic fibrosis newborn screening model demonstrating increased sensitivity but more carrier detections., Pediatrics. 113 (2004) 1573–81.

[50]   V.-T. Nguyen, S.B. Nimse, K.-S. Song, J. Kim, V.-T. Ta, H.W. Sung, T.Kim, HPAI 9G DNAChip: discrimination of highly pathogenic influenza virus genes., Chem. Commun. (Camb). 48 (2012) 4582–4584. doi:10.1039/c2cc30709j.

[51]   P. Wu, D.G. Castner, D.W. Grainger, Diagnostic devices as biomaterials: a review of nucleic acid and protein microarray surface performance issues., J. Biomater. Sci. Polym. Ed. 19 (2008) 725–753. doi:10.1163/156856208784522092.

[52]   Y.A. Jakubek, D.J. Cutler, A model of binding on DNA microarrays:

understanding the combined effect of probe synthesis failure, cross-hybridization, DNA fragmentation and other experimental details of affymetrix arrays. BMC Genomics. 13 (2012) 201-213. doi:10.1186/1471-2164-13-737.

[53] G.J. Kost, MD, PhD, Z. Tang, MD, D.G. Shelby, MT, R.F. Louie, Point-of-Care Testing: Millennium Technology for Critical Care, Lab. Med. 31 (2000) 402–408. doi:10.1309/0Y5F-B7NP-5Y67-GW7T.

[54] C. Labarca, K. Paigen, A simple, rapid, and sensitive DNA assay procedure, Anal. Biochem. 102 (1980) 344–352. doi:10.1016/0003-2697(80)90165-7.

[55] S.P. Tsai, A. Wong, E. Mai, P. Chan, G. Mausisa, M. Vasser, P. Jhurani, M. H. Jakobsen, W. T. Wong, and J.P. Stephan., Nucleic acid capture assay, a new method for direct quantitation of nucleic acids., Nucleic Acids Res. 31 (2003) 15 - 31. doi: 10.1093/nar/gng025

[56] B. Kasemo, Biological surface science, Surf. Sci. 500 (2002) 656–677. doi:10.1016/S0039-6028(01)01809-X.

[57] A.K. Trilling, J. Beekwilder, H. Zuilhof, Antibody orientation on biosensor surfaces: a minireview., Analyst. 138 (2013) 1619–1627. doi:10.1039/c2an36787d.

[58] P. Jonkheijm, D. Weinrich, H. Schröder, C.M. Niemeyer, H. Waldmann, Chemical strategies for generating protein biochips., Angew. Chem. Int. Ed. Engl. 47 (2008) 9618–9647. doi:10.1002/anie.200801711.

[59] P.-C. Lin, D. Weinrich, H. Waldmann, Protein Biochips: Oriented Surface Immobilization of Proteins, Macromol. Chem. Phys. 211 (2010) 136–144. doi:10.1002/macp.200900539.

[60] S.P. Pankaj Vadgama, Detection Challenges in Clinical Diagnostics, Royal Society of Chemistry. (2013) 35-64 doi:10.1039/9781849737302-00035

[61] L. Gervais, N. de Rooij, E. Delamarche, Microfluidic chips for point-of-care immunodiagnostics., Adv. Mater. 23 (2011) 151–176. doi:10.1002/adma.201100464.

[62] P. Abgrall, A.-M. Gué, Lab-on-chip technologies: making a microfluidic network and coupling it into a complete microsystem—a review, J. Micromechanics Microengineering. 17 (2007) 15–49. doi:10.1088/0960-1317/17/5/R01.

[63] S. V Lemeshko, T. Powdrill, Y.Y. Belosludtsev, M. Hogan, Oligonucleotides form a duplex with non-helical properties on a positively charged surface., Nucleic Acids Res. 29 (2001) 3051–3058.

[64] T.-Y. Lee, Y.-B. Shim, Direct DNA Hybridization Detection Based on the Oligonucleotide-Functionalized Conductive Polymer, Anal. Chem. 73 (2001) 5629–5632. doi:10.1021/ac015572w.

[65] T. de Lumley-Woodyear, C.N. Campbell, A. Heller, Direct Enzyme-Amplified Electrical Recognition of a 30-Base Model Oligonucleotide, J. Am. Chem. Soc. 118 (1996) 5504–5505. doi:10.1021/ja960490o.

[66] S.G. Wang, R. Wang, P.J. Sellin, Q. Zhang, DNA biosensors based on self-assembled carbon nanotubes., Biochem. Biophys. Res. Commun. 325 (2004) 1433–1437. doi:10.1016/j.bbrc.2004.10.188.

[67] V. Pavlov, Y. Xiao, R. Gill, A. Dishon, M. Kotler, I. Willner, Amplified Chemiluminescence Surface Detection of DNA and Telomerase Activity Using

Catalytic Nucleic Acid Labels, Anal. Chem. 76 (2004) 2152–2156. doi:10.1021/ac035219l.

[68]   S. Pan, L. Rothberg, Chemical control of electrode functionalization for detection of DNA hybridization by electrochemical impedance spectroscopy., Langmuir. 21 (2005) 1022–1027. doi:10.1021/la048083a.

[69]   A. Dupont-Filliard, A. Roget, T. Livache, M. Billon, Reversible oligonucleotide immobilisation based on biotinylated polypyrrole film, Anal. Chim. Acta. 449 (2001) 45–50. doi:10.1016/S0003-2670(01)01339-3.

[70]   Dekker Encyclopedia of Nanoscience and Nanotechnology, Volume 5, CRC Press, (2004) 3331 - 3344. doi: 10.1081/E-ENN 120013841

[71]   D.Y. Kwok, A.W. Neumann, Contact angle measurement and contact angle interpretation, Adv. Colloid Interface Sci. 81 (1999) 167–249. doi:10.1016/S0001-8686(98)00087-6.

[72]   R. Tadmor, Line energy and the relation between advancing, receding, and young contact angles., Langmuir. 20 (2004) 7659–7664. doi:10.1021/la049410h.

[73]   A.L. Sumner, E.J. Menke, Y. Dubowski, J.T. Newberg, R.M. Penner, J.C. Hemminger, L. M. Wingen, T. Brauers and B. J. Finlayson-Pitts, The nature of water on surfaces of laboratory systems and implications for heterogeneous chemistry in the troposphere., Phys. Chem. Chem. Phys. 6 (2004) 604 - 613. doi:10.1039/b308125g.

[74]   C.B. J. A. Woollam, B. Johs, C. Herzinger, J. Hilfiker, R. Synowicki, Overview of Variable Angle Spectroscopic Ellipsometry (VASE), Part I: Basic Theory and Typical Applications., Part I Basic Theory Typ. Appl. (1999) 3–28.

[75]   H.G.Tompkins, E.A. Irene, Handbook of ellipsometry, (2005) 1–13.

[76]   N. Jalili, K. Laxminarayana, A review of atomic force microscopy imaging systems: application to molecular metrology and biological sciences., Mechatronics. 14 (2004) 907–945. doi:10.1016/j.mechatronics.2004.04.005.

[77]   K.-H. Park, H.-J. Yoon, S.-J. Kim, G.-J. Lee, H.-K. Park, Y.-G. Park, Surface roughness analysis of ceramic bracket slots using atomic force microscope, Korean J. Orthod. 40 (2010) 294 - 303. doi:10.4041/kjod.2010.40.5.294.

[78]   R. Rigler, Fluorescence correlations, single molecule detection and large number screening applications in biotechnology., J. Biotechnol. 41 (1995) 177–186. doi:10.1016/0168-1656(95)00054-T.

[79]   S. Weiss, Fluorescence Spectroscopy of Single Biomolecules, Science. 283 (1999) 1676–1683. doi:10.1126/science.283.5408.1676.

[80]   J.E. M. Sauer, J. Hofkens, Handbook of fluorescence Spectroscopy and Imaging, (2011) 15–57. Available online: http://www.wiley-vch.de/books/sample/3527316698_c01.pdf

[81]   E.P. Diamandis, T.K. Christopoulos, Europium Chelate Labels in Time-Resolved Fluorescence Immunoassays and DNA Hybridization Assays., Anal. Chem. 62 (1990) 1149–1157. doi:10.1021/ac00221a716.

[82]   G. Sridharan, A.A. Shankar, Toluidine blue: A review of its chemistry and clinical utility., J. Oral Maxillofac. Pathol. 16 (2012) 251–255. doi:10.4103/0973-029X.99081.

[83]   W.S.S. Jonathan S. Olshaker, M. Christine Jackson, Forensic emergency

medicine /, (2007) 150 - 174.

[84] J. Drews, H. Launay, C.M. Hansen, K. West, S. Hvilsted, P. Kingshott, K. Almdal, Hydrolysis and stability of thin pulsed plasma polymerised maleic anhydride coatings., Appl. Surf. Sci. 254 (2008) 4720–4725. doi:10.1016/j.apsusc.2008.01.085.

[85] S. Sano, K. Kato, Y. Ikada, Introduction of functional groups onto the surface of polyethylene for protein immobilization, Biomaterials. 14 (1993) 817–822.

[86] H.N. Daghestani, B.W. Day, Theory and applications of surface plasmon resonance, resonant mirror, resonant waveguide grating, and dual polarization interferometry biosensors., Sensors (Basel). 10 (2010) 9630–9646. doi:10.3390/s101109630.

[87] A. Boudjemline, D.T. Clarke, N.J. Freeman, J.M. Nicholson, G.R. Jones, Early stages of protein crystallization as revealed by emerging optical waveguide technology., J. Appl. Crystallogr. 41 (2008) 523–530. doi:10.1107/S0021889808005098.

[88] G.H. Cross, A.A. Reeves, S. Brand, J.F. Popplewell, L.L. Peel, M.J. Swann, N.J. Freeman, A new quantitative optical biosensor for protein characterisation., Biosens. Bioelectron. 19 (2003) 383–390.

[89] P.D. Coffey, M.J. Swann, T.A. Waigh, F. Schedin, J.R. Lu, Multiple path length dual polarization interferometry., Opt. Express. 17 (2009) 10959 - 10969. doi:10.1364/OE.17.010959.

[90] H. Berney, K. Oliver, Dual polarization interferometry size and density characterisation of DNA immobilisation and hybridisation., Biosens. Bioelectron. 21 (2005) 618–626. doi:10.1016/j.bios.2004.12.024.

[91] M.J. Swann, L.L. Peel, S. Carrington, N.J. Freeman, Dual-polarization interferometry: an analytical technique to measure changes in protein structure in real time, to determine the stoichiometry of binding events, and to differentiate between specific and nonspecific interactions., Anal. Biochem. 329 (2004) 190–198. doi:10.1016/j.ab.2004.02.019.

[92] G.H. Cross, A. Reeves, S. Brand, M.J. Swann, L.L. Peel, N.J. Freeman, J.R Lu, The metrics of surface adsorbed small molecules on the Young's fringe dual-slab waveguide interferometer., J. Phys. D. Appl. Phys. 37 (2004) 74–80. doi:10.1088/0022-3727/37/1/012.

[93] M. Swann, N. Freeman, S. Carrington, G. Roman, P. Barrett, Quantifying structural changes and stoichiometry of protein interactions using size and density profiling, Lett. Pept. Sci. 10 (2003) 487–494. doi:10.1007/BF02442580.

[94] M.A. Cooper, V.T. Singleton, A survey of the 2001 to 2005 quartz crystal microbalance biosensor literature: applications of acoustic physics to the analysis of biomolecular interactions., J. Mol. Recognit. (2007) 154–184. doi:10.1002/jmr.826.

[95] D. Johannsmann, The Quartz Crystal Microbalance in Soft Matter Research: Fundamentals and Modeling, Springer, (2014) 343- 358.

[96] H. Ogi, H. Nagai, H. Naga, Y. Fukunishi, M. Hirao, M. Nishiyama, 170-MHz electrodeless quartz crystal microbalance biosensor: capability and limitation of higher frequency measurement., Anal. Chem. 81 (2009) 8068–8073.

doi:10.1021/ac901267b.

[97] G.N.M. Ferreira, A.-C. da-Silva, B. Tomé, Acoustic wave biosensors: physical models and biological applications of quartz crystal microbalance., Trends Biotechnol. 27 (2009) 689–697. doi:10.1016/j.tibtech.2009.09.003.

[98] J. Janata, Principles of Chemical Sensors, Chapter 4 Mass sensors, (2009) 63-98. doi:10.1007/b136378.

[99] G. Sauerbrey, The Use of Quartz Crystal Oscillators for Weighing Thin Layers and for Microweighing Applications. Z. Physik 155 (1959) 206-22.

[100] E. Huang, F. Zhou, L. Deng, Studies of Surface Coverage and Orientation of DNA Molecules Immobilized onto Preformed Alkanethiol Self-Assembled Monolayers, Langmuir. 16 (2000) 3272–3280. doi:10.1021/la9910834.

[101] H. Arwin, M. Poksinski, K. Johansen, Total Internal Reflection Ellipsometry: Principles and Applications., Appl. Opt. 43 (2004) 3028 - 3036. doi:10.1364/AO.43.003028.

[102] T.E. Tiwald, D.W. Thompson, J.A. Woollam, S. V. Pepper, Determination of the mid-IR optical constants of water and lubricants using IR ellipsometry combined with an ATR cell., Thin Solid Films. 313-314 (1998) 718–721. doi:10.1016/S0040-6090(97)00984-X.

[103] N.C.H. Le, V. Gubala, R.P. Gandhiraman, C. Coyle, S. Daniels, D.E. Williams, Total internal reflection ellipsometry as a label-free assessment method for optimization of the reactive surface of bioassay devices based on a functionalized cycloolefin polymer., Anal. Bioanal. Chem. 398 (2010) 1927–1936. doi:10.1007/s00216-010-4099-4.

[104] I. Baleviciute, Z. Balevicius, A. Makaraviciute, A. Ramanaviciene, A. Ramanavicius, Study of antibody/antigen binding kinetics by total internal reflection ellipsometry., Biosens. Bioelectron. 39 (2013) 170–176. doi:10.1016/j.bios.2012.07.017.

[105] A. Nabok, A. Tsargorodskaya, M.K. Mustafa, I. Székács, N.F. Starodub, A. Székács, Detection of low molecular weight toxins using an optical phase method of ellipsometry., Sensors Actuators B Chem. 154 (2011) 232–237. doi:10.1016/j.snb.2010.02.005.

[106] N.G. Semaltianos, Spin-coated PMMA films., Microelectronics J. 38 (2007) 754–761. doi:10.1016/j.mejo.2007.04.019.

[107] C.J. Lawrence, Spin coating with slow evaporation., Phys. Fluids A Fluid Dyn. 2 (1990) 453 - 456. doi:10.1063/1.857823.

[108] C.J. Lawrence, The mechanics of spin coating of polymer films., Phys. Fluids. 31 (1988) 2786 - 2797. doi:10.1063/1.866986.

[109] D.A.H. Hanaor, G. Triani, C.C. Sorrell, Morphology and photocatalytic activity of highly oriented mixed phase titanium dioxide thin films., Surf. Coatings Technol. 205 (2011) 3658–3664. doi:10.1016/j.surfcoat.2011.01.007.

[110] H. Förster, UV/VIS Spectroscopy, (n.d.) 337–426. doi:10.1007/b94239.

[111] J. Foggiato, Chemical Vapor Deposition of Silicon Dioxide Films,. (n.d.) 111–148.

[112] D.A. Bulla, N. Morimoto, Deposition of thick TEOS PECVD silicon oxide layers for integrated optical waveguide applications., Thin Solid Films. 334 (1998) 60–

64. doi:10.1016/S0040-6090(98)01117-1.

[113] L. Detomaso, R. Gristina, G.S. Senesi, R. d'Agostino, P. Favia, Stable plasma-deposited acrylic acid surfaces for cell culture applications., Biomaterials. 26 (2005) 3831–3841. doi:10.1016/j.biomaterials.2004.10.011.

[114] C. Vilani, D.E. Weibel, R.R.M. Zamora, A.C. Habert, C.A. Achete, Study of the influence of the acrylic acid plasma parameters on silicon and polyurethane substrates using XPS and AFM., Appl. Surf. Sci. 254 (2007) 131–134. doi:10.1016/j.apsusc.2007.07.060.

[115] S. Swaraj, U. Oran, A. Lippitz, J.F. Friedrich, W.E.S. Unger, Study of influence of external plasma parameters on plasma polymerised films prepared from organic molecules (acrylic acid, allyl alcohol, allyl amine) using XPS and NEXAFS., Surf. Coatings Technol. 200 (2005) 494–497. doi:10.1016/j.surfcoat.2005.01.083.

[116] C. Coyle, R.P. Gandiraman, V. Gubala, N.C.H. Le, C.C. O'Mahony, C. Doyle, J. Bryony, P. Swift, S. Daniels, D. E. Williams, Tetraethyl Orthosilicate and Acrylic Acid Forming Robust Carboxylic Functionalities on Plastic Surfaces for Biodiagnostics., Plasma Process. Polym. 9 (2012) 28–36. doi:10.1002/ppap.201100070.

[117] E.J. Szili, S. Kumar, R.S.C. Smart, N.H. Voelcker, Generation of a stable surface concentration of amino groups on silica coated onto titanium substrates by the plasma enhanced chemical vapour deposition method., Appl. Surf. Sci. 255 (2009) 6846–6850. doi:10.1016/j.apsusc.2009.02.092.

[118] Y. Zheng, B. Pathem, J. Hohman, P. Weiss, Functional Supramolecular Assemblies: First Glimpses and Upcoming Challenges, Beilstein-Institut Proc. Funct. Nanosci. (2011), 13 - 36.

[119] D. Meyerhofer, Characteristics of resist films produced by spinning, J. Appl. Phys. 49 (1978) 3993 - 4001. doi:10.1063/1.325357.

[120] S.W.J. Kuan, Ultrathin polymer films for microlithography., J. Vac. Sci. Technol. B Microelectron. Nanom. Struct. 6 (1988) 2274 - 2291. doi:10.1116/1.584069.

[121] L.L. Spangler, J.M. Torkelson, J.S. Royal, Influence of solvent and molecular weight on thickness and surface topography of spin-coated polymer films., Polym. Eng. Sci. 30 (1990) 644–653. doi:10.1002/pen.760301104.

[122] D.E. Bornside, R.A. Brown, P.W. Ackmann, J.R. Frank, A.A. Tryba, F.T. Geyling, The effects of gas phase convection on mass transfer in spin coating, J. Appl. Phys. 73 (1993) 585 - 594. doi:10.1063/1.353368.

[123] D.E. Bornside, Spin Coating of a PMMA/Chlorobenzene Solution, J. Electrochem. Soc. 138 (1991) 317 - 329. doi:10.1149/1.2085563.

[124] D.E. Bornside, C.W. Macosko, L.E. Scriven, Spin coating: One-dimensional model, J. Appl. Phys. 66 (1989) 5185 - 5199. doi:10.1063/1.343754.

[125] C.B. Walsh, E.I. Franses, Ultrathin PMMA films spin-coated from toluene solutions, Thin Solid Films. 429 (2003) 71–76. doi:10.1016/S0040-6090(03)00031-2.

[126] N.C.H. Le, V. Gubala, E. Clancy, T. Barry, T.J. Smith, D.E. Williams, Ultrathin and smooth poly(methyl methacrylate) (PMMA) films for label-free biomolecule detection with total internal reflection ellipsometry (TIRE)., Biosens.

Bioelectron. 36 (2012) 250–256. doi:10.1016/j.bios.2012.04.032.

[127] L. Brown, T. Koerner, J.H. Horton, R.D. Oleschuk, Fabrication and characterization of poly(methylmethacrylate) microfluidic devices bonded using surface modifications and solvents., Lab Chip. 6 (2006) 66–73. doi:10.1039/b512179e.

[128] S. A. Soper, A. C. Henry, B. Vaidya, M. Galloway, M. Wabuyele, R. L. McCarley, Surface modification of polymer - based microfluidic devices., Analytica Chimica Acta, 1 (2002) 87 - 99. doi:10.1016/S0003-2670(02)00356-2

[129] J. Kim, B. State, Chemical Modifications of Amino-Terminated Organic Films on Silicon Substrates and Controlled Protein Immobilization by FTIR and Ellipsometry, (2012) 26 - 57.

[130] N. Vourdas, A.G. Boudouvis, E. Gogolides, Plasma etch rate measurements of thin PMMA films and correlation with the glass transition temperature, J. Phys. Conf. Ser. 10 (2005) 405–408. doi:10.1088/1742-6596/10/1/099.

[131] I. Horcas, R. Fernández, J.M. Gómez-Rodríguez, J. Colchero, J. Gómez-Herrero, A.M. Baro, WSXM: a software for scanning probe microscopy and a tool for nanotechnology., Rev. Sci. Instrum. 78 (2007) 13705 - 13721. doi:10.1063/1.2432410.

[132] M. Zourob, ed., Recognition Receptors in Biosensors, Springer New York, New York, NY, (2010) 47 - 134. doi:10.1007/978-1-4419-0919-0.

[133] F. Fixe, M. Dufva, P. Telleman, C.B. V Christensen, One-step immobilization of aminated and thiolated DNA onto poly(methylmethacrylate) (PMMA) substrates., Lab Chip. 4 (2004) 191–195. doi:10.1039/b316616c.

[134] Z. Guo, R.A. Guilfoyle, A.J. Thiel, R. Wang, L.M. Smith, Direct fluorescence analysis of genetic polymorphisms by hybridization with oligonucleotide arrays on glass supports., Nucleic Acids Res. 22 (1994) 5456–5465.

[135] G.A. Diaz-Quijada, R. Peytavi, A. Nantel, E. Roy, M.G. Bergeron, M.M. Dumoulin, T. Veres, Surface modification of thermoplastics--towards the plastic biochip for high throughput screening devices., Lab Chip. 7 (2007) 856–862. doi:10.1039/b700322f.

[136] Y. Li, Z. Wang, L.M.L. Ou, H.-Z. Yu, DNA detection on plastic: surface activation protocol to convert polycarbonate substrates to biochip platforms., Anal. Chem. 79 (2007) 426–433. doi:10.1021/ac061134j.

[137] Y.H. Tennico, M.T. Koesdjojo, S. Kondo, D.T. Mandrell, V.T. Remcho, Surface modification-assisted bonding of polymer-based microfluidic devices, Sensors Actuators B Chem. 143 (2010) 799–804. doi:10.1016/j.snb.2009.10.001.

[138] Y. Wang, B. Vaidya, H.D. Farquar, W. Stryjewski, R.P. Hammer, R.L. McCarley, S. A. Soper, Microarrays Assembled in Microfluidic Chips Fabricated from Poly(methyl methacrylate) for the Detection of Low-Abundant DNA Mutations, Anal. Chem. 75 (2003) 1130–1140. doi:10.1021/ac020683w.

[139] A. Zribi, J. Fortin, Functional Thin Films and Nanostructures for Sensors Synthesis Physics and Applications - Anis Zribi, Jeffrey Fortin - eBooks & Audio Books, Intergrated Anal. Syst. (2009) 11–67.

[140] L. Yao, B. Liu, T. Chen, S. Liu, T. Zuo, Micro flow-through PCR in a PMMA

chip fabricated by KrF excimer laser., Biomed. Microdevices. 7 (2005) 253–257. doi:10.1007/s10544-005-3999-0.

[141] F. Fixe, M. Dufva, P. Telleman, C.B. V Christensen, Functionalization of poly(methyl methacrylate) (PMMA) as a substrate for DNA microarrays., Nucleic Acids Res. 32 (2004) 9 - 29. doi:10.1093/nar/gng157.

[142] K. Holmberg, H. Hydén, Methods of immobilization of proteins to polymethylmethacrylate., Prep. Biochem. 15 (1985) 309–319. doi:10.1080/00327488508062448.

[143] M. Tanahashi, T. Yao, T. Kokubo, M. Minoda, T. Miyamoto, T. Nakamura, T. Yamamuro, Apatite coated on organic polymers by biomimetic process: improvement in its adhesion to substrate by NaOH treatment., J. Appl. Biomater. 5 (1994) 339–347. doi:10.1002/jab.770050409.

[144] H.K. Varma, K. Sreenivasan, Y. Yokogawa, A. Hosumi, In vitro calcium phosphate growth over surface modified PMMA film., Biomaterials. 24 (2003) 297–303.

[145] D.C. Miller, J.D. Carloni, D.K. Johnson, J.W. Pankow, E.L. Gjersing, B. To, C. E. Packard, C. E. Kennedy, S. R. Kurtz. An investigation of the changes in poly(methyl methacrylate) specimens after exposure to ultra-violet light, heat, and humidity, Sol. Energy Mater. Sol. Cells. 111 (2013) 165–180. doi:10.1016/j.solmat.2012.05.043.

[146] P. Anger, P. Bharadwaj, L. Novotny, Enhancement and Quenching of Single-Molecule Fluorescence, Phys. Rev. Lett. 96 (2006) 113002 - 113025. doi:10.1103/PhysRevLett.96.113002.

[147] G. Schneider, G. Decher, N. Nerambourg, R. Praho, M.H. V Werts, M. Blanchard-Desce, Distance-dependent fluorescence quenching on gold nanoparticles ensheathed with layer-by-layer assembled polyelectrolytes., Nano Lett. 6 (2006) 530–536. doi:10.1021/nl052441s.

[148] E.Gonzalez, M.D. Barankin, P.C. Guschl, R.F. Hicks, Surface Activation of Poly(methyl methacrylate) via Remote Atmospheric Pressure Plasma, Plasma Process. Polym. 7 (2009) 482–493. doi:10.1002/ppap.200900113.

[149] A. Dinklage, T. Klinger, G. Marx, L. Schweikhard, Plasma Physics: Confinement, Transport And Collective Effects, Springer (India) Pvt. Limited, (2007) 1 - 20.

[150] J.M. Lane, D.J. Hourston, Surface treatments of polyolefins, Prog. Org. Coatings. 21 (1993) 269–284. doi:10.1016/0033-0655(93)80044-B.

[151] C.-M. Chan, T.-M. Ko, H. Hiraoka, Polymer surface modification by plasmas and photons, Surf. Sci. Rep. 24 (1996) 1–54. doi:10.1016/0167-5729(96)80003-3.

[152] J.M. Goddard, J.H. Hotchkiss, Polymer surface modification for the attachment of bioactive compounds, Prog. Polym. Sci. 32 (2007) 698–725. doi:10.1016/j.progpolymsci.2007.04.002.

[153] S. Yoshimura, Y. Tsukazaki, M. Kiuchi, S. Sugimoto, S. Hamaguchi, Sputtering yields and surface modification of poly(methyl methacrylate) (PMMA) by low-energy $Ar +/ CF+3$ ion bombardment with vacuum ultraviolet (VUV) photon

irradiation, J. Phys. D. Appl. Phys. 45 (2012) 505201 - 505210. doi:10.1088/0022-3727/45/50/505201.

[154] J. Zhang, J.R. Lakowicz, Metal-enhanced fluorescence of an organic fluorophore using gold particles, Opt. Express. 15 (2007) 2598 - 2612. doi:10.1364/OE.15.002598.

[155] T. Mangeat, A. Berthier, C. Elie-Caille, M. Perrin, W. Boireau, C. Pieralli, B. Wacogne, Gold/Silica biochips: Applications to Surface Plasmon Resonance and fluorescence quenching, Laser Phys. 19 (2009) 252–258. doi:10.1134/S1054660X09020170.

[156] M. Zeuner, J. Meichsner, H.-U. Poll, Oxidative decomposition of polymethylmethacrylate (PMMA) in plasma etching, Plasma Sources Sci. Technol. 4 (1995) 406–415. doi:10.1088/0963-0252/4/3/010.

[157] R. Hoogenboom, C.R. Becer, C. Guerrero-Sanchez, S. Hoeppener, U.S. Schubert, Solubility and Thermoresponsiveness of PMMA in Alcohol-Water Solvent Mixtures, Aust. J. Chem. 63 (2010) 1173 - 1193. doi:10.1071/CH10083.

[158] M. Abouelezz, Studies on the photodegradation of Poly(Methyl Methacrylate), (1978) 78 - 89. Vol NBSIR 78 - 1463.

[159] J.O. Choi, Degradation of poly(methylmethacrylate) by deep ultraviolet, x-ray, electron beam, and proton beam irradiations, J. Vac. Sci. Technol. B Microelectron. Nanom. Struct. 6 (1988) 2286 - 2299. doi:10.1116/1.584071.

[160] H. Shinohara, T. Kasahara, S. Shoji, J. Mizuno, Studies on low-temperature direct bonding of VUV/O 3 -, VUV- and O 2 plasma-pre-treated poly-methylmethacrylate, J. Micromechanics Microengineering. 21 (2011) 85028 - 85039. doi:10.1088/0960-1317/21/8/085028.

[161] H. Yuan, D.R. Killelea, S. Tepavcevic, S.I. Kelber, S.J. Sibener, Interfacial chemistry of poly(methyl methacrylate) arising from exposure to vacuum-ultraviolet light and atomic oxygen., J. Phys. Chem. A. 115 (2011) 3736–3745. doi:10.1021/jp1061368.

[162] C.L. Feng, Z. Zhang, R. Förch, W. Knoll, G.J. Vancso, H. Schönherr, Reactive thin polymer films as platforms for the immobilization of biomolecules., Biomacromolecules. 6 (2005) 3243–3251. doi:10.1021/bm050247u.

[163] N.K. Devaraj, G.P. Miller, W. Ebina, B. Kakaradov, J.P. Collman, E.T. Kool, C.E. Chidsey, Chemoselective covalent coupling of oligonucleotide probes to self-assembled monolayers., J. Am. Chem. Soc. 127 (2005) 8600–8611. doi:10.1021/ja051462l.

[164] S. V Tillib, A.D. Mirzabekov, Advances in the analysis of DNA sequence variations using oligonucleotide microchip technology., Curr. Opin. Biotechnol. 12 (2001) 53–58.

[165] M.W. Kanan, M.M. Rozenman, K. Sakurai, T.M. Snyder, D.R. Liu, Reaction discovery enabled by DNA-templated synthesis and in vitro selection., Nature. 431 (2004) 545–549. doi:10.1038/nature02920.

[166] D. Issadore, R.M. Westervelt, eds., Point-of-Care Diagnostics on a Chip, Springer Berlin Heidelberg, Berlin, Heidelberg, 2013. doi:10.1007/978-3-642-29268-2.

[167] C.A. Borrebaeck, Antibodies in diagnostics - from immunoassays to protein

chips., Immunol. Today. 21 (2000) 379–382.

[168] A.C. Pease, D. Solas, E.J. Sullivan, M.T. Cronin, C.P. Holmes, S.P. Fodor, Light-generated oligonucleotide arrays for rapid DNA sequence analysis., Proc. Natl. Acad. Sci. U. S. A. 91 (1994) 5022–5026.

[169] R.J. Lipshutz, D. Morris, M. Chee, E. Hubbell, M.J. Kozal, N. Shah, N. Shen, R. Yang, S.P.A Fodor, Using oligonucleotide probe arrays to access genetic diversity., Biotechniques. 19 (1995) 442–447.

[170] D.A. Armbruster, T. Pry, Limit of blank, limit of detection and limit of quantitation., Clin. Biochem. Rev. 29 Suppl 1 (2008) S49–52.

[171] M.C. Pirrung, How to Make a DNA Chip, Angew. Chemie Int. Ed. 41 (2002) 1276–1289. doi:10.1002/1521-3773(20020415)

[172] L. R. Middendorf, P. G. Humphrey, N. Narayanan and S. C. Roemer, Essentials of Genomics and Bioinformatics , John Wiley & Sons, (2008) 165 - 185.

[173] D. Peelen, L.M. Smith, Immobilization of amine-modified oligonucleotides on aldehyde-terminated alkanethiol monolayers on gold., Langmuir. 21 (2005) 266–271. doi:10.1021/la048166r.

[174] J. Lahiri, L. Isaacs, J. Tien, G.M. Whitesides, A Strategy for the Generation of Surfaces Presenting Ligands for Studies of Binding Based on an Active Ester as a Common Reactive Intermediate: A Surface Plasmon Resonance Study, Anal. Chem. 71 (1999) 777–790. doi:10.1021/ac980959t.

[175] N. Gupta, B.F. Lin, L.M. Campos, M.D. Dimitriou, S.T. Hikita, N.D. Treat, M. V. Tirrell, D. O. Clegg, E. J. Kramer, C. J. Hawker, A versatile approach to high-throughput microarrays using thiol-ene chemistry., Nat. Chem. 2 (2010) 138–145. doi:10.1038/nchem.478.

[176] M. Schena, D. Shalon, R. Heller, A. Chai, P.O. Brown, R.W. Davis, Parallel human genome analysis: microarray-based expression monitoring of 1000 genes., Proc. Natl. Acad. Sci. U. S. A. 93 (1996) 10614–10619.

[177] J.B. Lamture, K.L. Beattie, B.E. Burke, M.D. Eggers, D.J. Ehrlich, R. Fowler, M. A. Hollis, B. B. Kosicki, R. K. Reich, and S. R. Smith, Direct detection of nucleic acid hybridization on the surface of a charge coupled device., Nucleic Acids Res. 22 (1994) 2121–2125.

[178] R. Voicu, R. Boukherroub, V. Bartzoka, T. Ward, J.T.C. Wojtyk, D.D.M. Wayner, Formation, characterization, and chemistry of undecanoic acid-terminated silicon surfaces: patterning and immobilization of DNA., Langmuir. 20 (2004) 11713–11720. doi:10.1021/la047886v.

[179] L.A. Chrisey, G.U. Lee, C.E. O'Ferrall, Covalent attachment of synthetic DNA to self-assembled monolayer films., Nucleic Acids Res. 24 (1996) 3031–3039.

[180] M.E. McGovern, M. Thompson, Pentafluorinated Probes for the X-ray Photoelectron Spectroscopic Study of Immobilized Bifunctional Silanes, Anal. Chem. 72 (2000) 128–134. doi:10.1021/ac9909352.

[181] W.G. Beattie, L. Meng, S.L. Turner, R.S. Varma, D.D. Dao, K.L. Beattie, Hybridization of DNA targets to glass-tethered oligonucleotide probes., Mol. Biotechnol. 4 (1995) 213–225. doi:10.1007/BF02779015.

[182] M. Boncheva, L. Scheibler, P. Lincoln, H. Vogel, B. Åkerman, Design of Oligonucleotide Arrays at Interfaces, Langmuir. 15 (1999) 4317–4320.

doi:10.1021/la981702t.

[183] M. Schena, D. Shalon, R.W. Davis, P.O. Brown, Quantitative monitoring of gene expression patterns with a complementary DNA microarray., Science. 270 (1995) 467–70.

[184] S.A. Hussain, P.K. Paul, D. Dey, D. Bhattacharjee, S. Sinha, Immobilization of single strand DNA on solid substrate, Chem. Phys. Lett. 450 (2007) 49–54. doi:10.1016/j.cplett.2007.10.075.

[185] G.T. Hermanson, Bioconjugate Techniques, Elsevier, (1996) 259 - 273. doi:10.1016/B978-012342335-1/50004-X.

[186] M.K. Walsh, X. Wang, B.C. Weimer, Optimizing the immobilization of single-stranded DNA onto glass beads., J. Biochem. Biophys. Methods. 47 (2001) 221–231.

[187] Y. Wang, H.-H. Lai, M. Bachman, C.E. Sims, G.P. Li, N.L. Allbritton, Covalent micropatterning of poly(dimethylsiloxane) by photografting through a mask., Anal. Chem. 77 (2005) 7539–7546. doi:10.1021/ac0509915.

[188] P. Gong, D.W. Grainger, Comparison of DNA immobilization efficiency on new and regenerated commercial amine-reactive polymer microarray surfaces, Surf. Sci. 570 (2004) 67–77. doi:10.1016/j.susc.2004.06.181.

[189] R. Bischoff, J.M. Coull, F.E. Regnier, Introduction of 5′-terminal functional groups into synthetic oligonucleotides for selective immobilization, Anal. Biochem. 164 (1987) 336–344. doi:10.1016/0003-2697(87)90502-1.

[190] N. Zammatteo, L. Jeanmart, S. Hamels, S. Courtois, P. Louette, L. Hevesi, et al., Comparison between different strategies of covalent attachment of DNA to glass surfaces to build DNA microarrays., Anal. Biochem. 280 (2000) 143–150. doi:10.1006/abio.2000.4515.

[191] B. Joos, H. Kuster, R. Cone, Covalent attachment of hybridizable oligonucleotides to glass supports., Anal. Biochem. 247 (1997) 96–101. doi:10.1006/abio.1997.2017.

[192] F. Frederix, K. Bonroy, G. Reekmans, W. Laureyn, A. Campitelli, M.A. Abramov, W. Dehaen, G. Maes , Reduced nonspecific adsorption on covalently immobilized protein surfaces using poly(ethylene oxide) containing blocking agents., J. Biochem. Biophys. Methods. 58 (2004) 67–74.

[193] J.H. Fisher, J.F. Gusella, C.H. Scoggin, Molecular hybridization under conditions of high stringency permits cloned DNA segments containing reiterated DNA sequences to be assigned to specific chromosomal locations., Proc. Natl. Acad. Sci. U. S. A. 81 (1984) 520–524.

[194] S.P. Pack, N.K. Kamisetty, M. Nonogawa, K.C. Devarayapalli, K. Ohtani, K. Yamada, Y. Yoshida, T. Kodaki, K. Makino, Direct immobilization of DNA oligomers onto the amine-functionalized glass surface for DNA microarray fabrication through the activation-free reaction of oxanine., Nucleic Acids Res. 35 (2007) 110 - 128. doi:10.1093/nar/gkm619.

[195] J.-C. Meng, G. Siuzdak, M.G. Finn, Affinity mass spectrometry from a tailored porous silicon surface., Chem. Commun. (Camb). (2004) 2108–2109. doi:10.1039/b408200a.

[196] J.-F. Lutz, 1,3-dipolar cycloadditions of azides and alkynes: a universal ligation

tool in polymer and materials science., Angew. Chem. Int. Ed. Engl. 46 (2007) 1018–1025. doi:10.1002/anie.200604050.

[197] H.C. Kolb, M.G. Finn, K.B. Sharpless, Click Chemistry: Diverse Chemical Function from a Few Good Reactions., Angew. Chem. Int. Ed. Engl. 40 (2001) 2004–2021.

[198] H.C. Kolb, K.B. Sharpless, The growing impact of click chemistry on drug discovery., Drug Discov. Today. 8 (2003) 1128–1137.

[199] A.H. El-Sagheer, T. Brown, Click chemistry with DNA., Chem. Soc. Rev. 39 (2010) 1388–1405. doi:10.1039/b901971p.

[200] B. Uszczyńska, T. Ratajczak, E. Frydrych, H. Maciejewski, M. Figlerowicz, W.T. Markiewicz, M.K. Chmielewski, Application of click chemistry to the production of DNA microarrays., Lab Chip. 12 (2012) 1151–1156. doi:10.1039/c2lc21096g.

[201] R. Jafari, F. Arefi-Khonsari, M. Tatoulian, D. Le Clerre, L. Talini, F. Richard, Development of oligonucleotide microarray involving plasma polymerized acrylic acid, Thin Solid Films. 517 (2009) 5763–5768. doi:10.1016/j.tsf.2009.03.217.

[202] E. Graugnard, A. Cox, J. Lee, C. Jorcyk, B. Yurke, W.L. Hughes, Kinetics of DNA and RNA Hybridization in Serum and Serum-SDS., IEEE Trans. Nanotechnol. 9 (2010) 603–609. doi:10.1109/TNANO.2010.2053380.

[203] R.B. Wallace, J. Shaffer, R.F. Murphy, J. Bonner, T. Hirose, K. Itakura, J. Remackle, Hybridization of synthetic oligodeoxyribonucleotides to phi chi 174 DNA: the effect of single base pair mismatch., Nucleic Acids Res. 6 (1979) 3543–3557.

[204] F. Everaerts, M. Torrianni, M. Hendriks, J. Feijen, Biomechanical properties of carbodiimide crosslinked collagen: influence of the formation of ester crosslinks., J. Biomed. Mater. Res. A. 85 (2008) 547–555. doi:10.1002/jbm.a.31524.

[205] Z. Grabarek, J. Gergely, Zero-length crosslinking procedure with the use of active esters, Anal. Biochem. 185 (1990) 131–135. doi:10.1016/0003-2697(90)90267-D.

[206] O. Kovalchuk, J. Filkowski, J. Meservy, Y. Ilnytskyy, V.P. Tryndyak, V.F. Chekhun, I. P. Pogribny, Involvement of microRNA-451 in resistance of the MCF-7 breast cancer cells to chemotherapeutic drug doxorubicin., Mol. Cancer Ther. 7 (2008) 2152–2159. doi:10.1158/1535-7163.MCT-08-0021.

[207] A. Bergamaschi, B.S. Katzenellenbogen, Tamoxifen downregulation of miR-451 increases 14-3-3ζ and promotes breast cancer cell survival and endocrine resistance., Oncogene. 31 (2012) 39–47. doi:10.1038/onc.2011.223.

[208] X. Pan, R. Wang, Z.-X. Wang, The potential role of miR-451 in cancer diagnosis, prognosis, and therapy., Mol. Cancer Ther. 12 (2013) 1153–1162. doi:10.1158/1535-7163.MCT-12-0802.

[209] A.M. Foudeh, T. Fatanat Didar, T. Veres, M. Tabrizian, Microfluidic designs and techniques using lab-on-a-chip devices for pathogen detection for point-of-care diagnostics., Lab Chip. 12 (2012) 3249–3266. doi:10.1039/c2lc40630f.

[210] S.E. McCalla, A. Tripathi, Microfluidic reactors for diagnostics applications., Annu. Rev. Biomed. Eng. 13 (2011) 321–343. doi:10.1146/annurev-bioeng-

070909-105312.

[211] J. Gaughran, N. Dimov, E. Clancy, T. Barry, T.J. Smith, J. Ducree, Multi-stage, solvent-controlled routing for automated on-disc extraction of total RNA from breast cancer cell line homogenate, Transducers Eurosensors XXVII 17th Int. Conf. Solid-State Sensors, Actuators Microsystems (TRANSDUCERS EUROSENSORS XXVII), IEEE, (2013) 305–308. doi:10.1109/Transducers.2013.6626763.

[212] N. Dimov, E. Clancy, J. Gaughran, D. Boyle, D. Mc Auley, M.T. Glynn, Róisín M. Dwyer, H. Coughlan, T. Barry, L. M. Barrett, T. J. Smith, J. Ducrée, Solvent-selective routing for centrifugally automated solid-phase purification of RNA, Microfluid. Nanofluidics. 18 (2014) 859–871. doi:10.1007/s10404-014-1477-9.

APPENDIX

List of publications

1. "Fabrication and characterisation of spin coated oxidised PMMA to provide a robust surface for on-chip assays"

    Milena Rowinska, Susan M. Kelleher, Felipe Soberon, Anthony J. Ricco and Stephen Daniels

    Published in J. Mater. Chem. B 10/2014

2. "Click chemistry as an immobilisation method to improve oligonucleotide hybridisation efficiency for nucleic acid assays"

    Milena McKenna, Felipe Soberon, Antonio J. Ricco, Stephen Daniels and Susan M. Kelleher

    Published in Sensors and Actuators B: Chemical, Ms. Ref. No.: SNB-D-16-00573R3

3. "Soft interfaces as antibody supports: modulation of antigen capture signal in immunoassays by alteration of surface chemistry"

    Peter Akers, Nam Cao Hoai Le, Andrew Nelson, **Milena McKenna**, Christy O'Mahony, Duncan McGillivray, Vladimir Gubala, David E. Williams

    Manuscript submitted to Langmuir

4. "Tuneable carboxylic acid surfaces for biomedical applications prepared using plasma enhanced chemical vapour deposition"

    Ruairi Monaghan, **Milena McKenna**, Shauna Flynn, Aidan Cowley, Felipe Soberon, Stephen Daniels and Susan Kelleher

    Manuscript under preparation

5. "Aqua-art: demonstration of PECVD process applied to adjust/alter hydrophobicity of the surfaces"

    Milena McKenna, Shauna Flynn, Ruairi Monaghan, Aoife MacCormack, Susan Kelleher, Stephen Daniels

    Manuscript under preparation to be submitted to Journal of Chemical Education

Conferences

1. "Improved DNA Immobilisation and Binding Efficiency on Novel Carboxylic
    Acid Surfaces"
    M. Rowinska, S. Kelleher, F. Sobernon, A. Ricco and S. Daniels
    *5th International Conference on Nanotechnology and Biosensors (ICNB
    2014)Barcelona; December 2014*
    (Oral presentation)
    Winner of the best conference presentation

2. "Smart Surfaces for Point-of-Care Diagnostic Devices"
    M. Rowinska, R. Monaghan, S. Kelleher, C. Charlton O'Mahony, R.P.
    Gandhiraman, N.C.H. Le, D.E. Williams, S. Daniels
    Nanoweek, CRANN Institute, Dublin, July 2012
    (Poster presentation)

3. "Vertical or Horizontal? Surface Engineering and Consequences on Selective
    DNA Orientation Changes Upon Hybridisation to its Target "
    V. Gubala, C. Charlton O'Mahony, E. Clancy, **M. Rowinska**, D.E. Williams,
    Europtrode, Barcelona, Spain, April 2012
    (Oral presentation)

4. DNA probe orientation on tailor-made carboxylic acid surfaces
    M. Rowinska, N.C.H. Le, V. Gubala, S. Kelleher and S. Daniels;
    Lab-on-a-chip European Congress; Barcelona; March 2013
    (Poster presentation)

Presentations

1. "Smart Surfaces for Point-of-Care Diagnostic Devices"

   Milena Rowinska, Ruairi Monaghan, Susan Kelleher, Christy Charlton O'MahonyRam Prasad Gandhiraman, Nam Cao Hoai Le, David E. Williams and Stephen Daniels.

   Becton, Dickinson and Company (BD) site visit,

   Biomedical Diagnostic Institute, September 2012

   (Poster presentation)

2. "Can we save 100,007 lives?"

   Milena Rowinska

   Thesis in Three,

   Smock Alley Theatre Dublin, October 2012

   (Oral presentation)

3. "DNA Orientation Changes Upon Perfect Match Hybridisation on PECVD Coated Functional Surfaces"

   Milena Rowinska, Gowri Manickam, Ruairi Monaghan, Ram Prasad Gandhiraman, Vladimir Gubala, Eoin Clancy, David E. Williams, Stephen Daniels, Christy Charlton.

   Academic Advisory Board/Industrial Advisory Board,

   Biomedical Diagnostic Institute, November 2012

   (Poster presentation)

4. "I pink it can be cured"

   Milena Rowinska

   Finalist of Tell It Straight Competition,

   Dublin City University, March 2013

   (Video submission)

5. "DNA probe orientation on tailor-made carboxylic acid surfaces"

    Milena Rowinska, Nam Cao Hoai Le, Vladimir Gubala, Susan Kelleher

    and Stephen Daniels.

    Science Foundation Ireland mid term review

    Biomedical Diagnostic Institute, June 2013

    (Poster presentation)

6. "Improved DNA Immobilisation and Binding Efficiency on Novel Carboxylic

    Acid Surfaces"

    Milena Rowinska, Susan Kelleher, Felipe Soberon, Tony Ricco and Stephen

    Daniels.

    Industrial Advisory Board (IAB)

    Biomedical Diagnostic Institute, November 2014

    (Poster presentation)

7. "Improved DNA immobilisation strategy - DNA binding   interactions on

    carboxylic acid modified supports"

    Milena Rowinska, Susan Kelleher, Felipe Soberon, Tony Ricco and Stephen

    Daniels.

    Scientific Advisory Board (SAB)

    Biomedical Diagnostic Institute, February 2015

    (Poster presentation)

Research abroad

NASA Ames Research Centre, California, USA
Jessica Koehne's research group, *November 2013*

I received extensive training on AFM instrument used in aqueous environment.
Moreover I had an opportunity to test novel AFM tips with carbon nanotube grown at
the bottom of the tip for sensitivity improvement. Additionally I was collaborating with
Dr. Ram Prasad, previous BDI researcher, testing paper samples, which could
potentially be used as biosensor's platform.